

**STUDY OF THE TOXICITY,
IMMUNOLOGICAL AND GENE
EXPRESSION EFFECTS OF COBALT IONS
AND WEAR DEBRIS DERIVED FROM
METAL-ON-METAL HIP IMPLANTS**

by

OLGA MARIA POSADA ESTEFAN

2013

THIS THESIS IS SUBMITTED IN PARTIAL FULFILMENT
FOR THE DEGREE OF
**DOCTOR OF PHILOSOPHY IN
BIOMEDICAL ENGINEERING**

DEPARTMENT OF BIOMEDICAL ENGINEERING
WOLFSON CENTRE
106 ROTTENROW
UNIVERSITY OF STRATHCLYDE
GLASGOW G4 0NW

Acknowledgments

What a journey this has been... So here I am 3 years and 300 pages later full of gratitude towards all the people that helped me get through what so far has been the hardest challenge in my life.

I would like to begin by expressing my sincere gratitude to Prof. Helen Grant for her continuous support throughout my PhD. Her guidance, encouragement, and commitment to this project. I could not have asked for a better supervisor. I am incredibly grateful to Dr. Rothwelle Tate and his never ending knowledge of molecular biology. Always finding time to help me and guide me whether I had an academic or a personal difficulty.

I would also like to thank Mr. Dominic Meek and Sister Helen Murray for arranging the delivery of the samples and collating patient data as well as their support and advice.

In addition, I would like to express thanks to Mrs Catherine Henderson, Mr. Brian Cartlidge, and Mrs Denise Gilmour for their technical support and advice. Especially, I am extremely grateful to Mrs Catherine Henderson. She is the heart and soul of the lab, and it would not have been the same without her. I am also immensely appreciative of the help Denise Gilmour provided in relation to the metal ion analysis.

I am enormously grateful to all my friends, the ones from way back and the ones I have meet during this journey, for being there when I needed them. I am also tremendously thankful to my other half and soul mate who always believed in me. In particular, his patience, encouragement and continuous support. In addition, I am very grateful to Ian and Jean Hamilton who became my family nearly from the beginning and have been so generous and kind to me.

Finally, I would not be here without my family. My parents whose love, hard work, sacrifices, words of wisdom, endless support and faith in me have allowed me to pursue my dreams and achieve my goals. My brother who in his own way has also been so caring and supportive, and whose scenery texts always put a smile on my face. There are no words that can express my infinite love and gratitude towards them.

Abstract

Joint replacements have been used for over 30 years with considerable success as treatment for bone diseases. As a surgical alternative to metal on metal (MoM) total hip replacement, hip resurfacing was developed using Cobalt-Chromium (CoCr) alloys. However, debris particles are generated by wear at the articulating CoCr surfaces. The nanoparticles and ions produced disseminate throughout the body and interact with different cell types.

In order to evaluate the effects of CoCr particles and ions released from MoM implants, U937 cells and primary human lymphocytes were exposed *in vitro* to artificially produced wear debris derived from an ASRTM MoM hip resurfacing. MoM implants release both Cr and Co ions into patients' circulation, with the latter ion being more mobile, and disseminating more widely in the body. U937 cells were treated with Co ions before being exposed to wear debris to investigate the scenario of patients undergoing revision surgery or receiving a second implant. In addition to this, metal ion levels were measured in clinical whole blood samples of patients with MoM hip implants and the relationship between those levels and the expression of key genes involved in the process of bone remodelling was explored.

The findings from this study demonstrated that exposure to high concentrations of CoCr wear debris led to decrease in U937 cell viability after 120h but increased cell proliferation of primary human lymphocytes. Moreover, assessment of apoptosis revealed that metal debris, but not low concentrations of Co ions (0.1 μ M), induced apoptosis in both U937 cells and primary human lymphocytes. Additionally, results showed that whereas cytokine production by U937 cells is affected by both metal debris and metal ions, it is mainly affected by metal debris in primary human lymphocytes.

Changes in human general toxicology-related gene expression in response CoCr wear and Co ions exposure was also evaluated in U937 cells. Real time PCR analysis indicated that CoCr particles were more effective as an inducer of changes

in gene expression when cells were pre-treated with Co ions. Together, results seemed to suggest that the toxicity of Co ions in macrophages could be related to nitric oxide metabolic processes and apoptosis and to IL-2 production modulation in lymphocytes.

ICP-MS analysis of culture medium from cells exposed to increasing concentration of CoCr wear debris demonstrated increasing Co and Cr ion levels representing the corrosion process of the metal debris. Since metal wear debris corrodes under physiological conditions, the ions released may play an important role in the cellular response at the peri-implant tissues.

Finally, whole blood Co and Cr ion levels from patients with MoM implants were also analysed by ICP-MS. The ion levels measured were elevated compared to patients without implants, and one patient had levels that were just above the 7µg/l (7ppb) threshold recommended by the Medicines and Healthcare products Regulatory Agency (MHRA) for Co+Cr in the circulation. A correlation between the ion levels measured and gene expression changes could not be established, due to the low number of patients available for this study.

Results from this investigation showed that metal debris tends to be more toxic and has a greater influence on gene expression in the presence of Co ion pre-treatment. This could have great health implications as it potentially means that patients undergoing revision surgery or receiving a second implant may be at higher risk of adverse tissue response and implant failure.

List of abbreviations

7-AAD	7-Aminoactinomycin D
ANOVA	Analysis of variance
AO	Acridine orange
AP1	Activator protein 1
APC	Antigen presenting cells
ARMD	Adverse reactions to metal debris
ASR	Articular surface replacement
ASTM	American Society for Testing and Materials
BAG1	BCL2-associated athanogene
BCL2	B-cell CLL/lymphoma 2
BHR	Birmingham Hip Resurfacing
BrdU	Bromodeoxyuridine
BSA	Bovine serum albumin
cDNA	Complementary DNA
CCR	Chemokine receptor
CHIT1	Chitinase
CHOP	C/EBP homologous protein
CoC	Ceramic-on-Ceramic
CoCl ₂	Cobalt chloride
CoCr	Cobalt-Chromium alloy
CoP	Ceramic-on-Polyethylene
CPTi	Commercially pure titanium
Cq	Quantification cycle
Ct	Threshold cycle
DC	Dendritic cell
DECR1	2,4-dienoyl CoA reductase 1, mitochondrial
DMSO	Dimethyl Sulfoxide
DNA	Deoxyribonucleic acid
DNase	Deoxyribonuclease
dsDNA	double-stranded DNA
DTH	Delayed-type hypersensitivity
E	Efficiency
EDS	Energy Dispersive Spectroscopy
EDTA	Ethylenediaminetetraacetic acid
ELISA	Enzyme-linked immunosorbent assay
ER	Endoplasmic reticulum
FACS	Fluorescence-activated cell sorting
FCS	Foetal Calf Serum
FE-SEM	Field Emission Scanning Electron Microscope
FITC	Fluorescein isothiocyanate
FOS	FBJ murine osteosarcoma viral oncogene homolog
FPGS	Folylpolyglutamate synthase
FRET	Fluorescence-resonance energy transfer
GC	Guanine-cytosine

G-CSF	Granulocyte colony-stimulating factor
GM-CSF	Granulocyte-macrophage colony-stimulating factor
GRP78	Glucose-regulated-protein-78
GSEA	Gene Set Enrichment Analysis
HEPES	Hydroxyethyl piperazineethanesulfonic acid
hMSC	Human mesenchymal stem cell
HO-1	Heme oxygenase-1
HRP	Horseradish peroxidase
ICP-MS	Inductively coupled plasma mass spectrometry
IFN γ	Interferon gamma
IL-1	Interleukin-1
IL-1 β	Interleukin-1 β
IL-2	Interleukin-2
IL-4	Interleukin-4
IL-6	Interleukin-6
IL-8	Interleukin-8
IL-10	Interleukin-10
IL-13	Interleukin-13
ISTD	Internal standard
LPS	Lipopolysaccharide
LTA	Lymphotoxin alpha
MHC	Major histocompatibility complex
MHRA	Medicines and Healthcare Regulatory Agency
MIQE	Minimum Information for Publication of Quantitative Real-Time PCR Experiments
MLH1	MutL homolog 1
MMR	Mismatch repair
MoM	Metal-on-Metal
MoP	Metal-on-Polyethylene
MSC	Mesenchymal stem cell
NF κ B	Nuclear factor kappa-light-chain-enhancer of activated B cells
mRNA	Messenger RNA
miRNA	microRNA
MTT	3-(4,5-Dimethylthiazol-2-yl)-2,5-diphenyltetrazolium bromide
NaPi	Sodium Phosphate buffer
NJR	National Joint Registry
NK	Natural killer
NOS2	Inducible nitric oxide synthase 2
NR	Neutral red
OA	Osteoarthritis
OPG	Tumor necrosis factor receptor superfamily, member 11b
4-PBA	4-phenylbutyric acid
PAGE	Polyacrylamide gel electrophoresis
PAMP	Pathogen-associated molecular patterns
PARP	Poly-ADP-Ribose-Polymerase

PBMC	Peripheral blood mononuclear cell
PBS	Phosphate buffered saline
PCR	Polymerase chain reaction
PGE ₂	Prostaglandin E ₂
PI	Propidium Iodide
PMA	Phorbol 12-myristate 13-acetate
PMN	Polymorphonuclear neutrophils
PMMA	Polymethylmethacrylate
PPIB	Peptidylprolyl isomerase B (cyclophilin B)
PS	Phospholipid phosphatidylserine
qPCR	Quantitative real-time polymerase chain reaction
RANK	Tumor necrosis factor receptor superfamily, member 11a, NFκB activator
RANKL	Tumor necrosis factor (ligand) superfamily, member 11
RBC	Red blood cell
RNA	Ribonucleic acid
RNase	Ribonuclease
ROS	Reactive oxygen species
RQ	Relative quantitative
RQI	RNA quality indicator
rRNA	Ribosomal RNA
RT	Reverse transcriptase
RT-	Minus reverse transcriptase
RT-PCR	Reverse transcribed polymerase chain reaction
SDS	Sodium dodecyl sulfate
SEM	Scanning Electron Microscope
SEM	Standard error of mean
TBE	Tris-Borate-EDTA
TBS	Tris Buffered Saline
TCR	T-cell receptor
TEMED	N,N,N',N'-Tetramethylethylenediamine
TGF	Transforming growth factor
Th	Helper T-lymphocyte
THA	Total hip arthroplasty
THR	Total hip replacement
TJR	Total joint replacement
TLR	Toll like receptor
TMB	3,3',5,5'-Tetramethylbenzidine
TNFα	Tumor necrosis factor alpha
TPA	12-O-tetradecanoylphorbol-13-acetate
TTBS	Tween Tris Buffered Saline
TRAP1	TNF receptor-associated protein 1
Tris	Tris(hydroxymethyl)aminomethane
TUNEL	Terminal deoxynucleotidyl transferase dUTP nick end labeling
UHMWPE	Ultra-high-molecular-weight polyethylene
UV	Ultraviolet

VD3
WBC
XBP1

1, 25-dihydroxyvitamin D3
White blood cell
X-box binding protein 1

List of tables

Table 1.1. Predicted revision rates for males and females with total hip metal-on-metal articulations by age and head size..	5
Table 1.2. Elemental compositions (% weight) of metal alloys used in orthopaedic implants.	10
Table 1.3. Metal ion levels measured in body fluids from patients with MoM hip replacements.	22
Table 1.4. Typical Concentrations of Metal in Human Body Fluids and in Human Tissue with and Without MoM Total Joint Replacements.....	22
Table 1.5. Studies of the effects of wear debris and ions derived from various materials on U937 cells.	32
Table 1.6. Pro-inflammatory cytokines.	36
Table 2.1. Monoclonal antibodies and isotype controls used to assess CD11c ⁺ DC activation	46
Table 2.2. ICP-MS standards.	53
Table 2.3. Protein standards.	56
Table 2.4. Reagents for casting gels.	57
Table 2.5 Primer sequences, melting temperatures (T _m) as calculated by GeneRunner and amplicon size.	65
Table 2.6. PCR thermal cycling conditions	66
Table 2.7. Preparation of solubilisation matrix solution.....	68
Table 2.8. TaqMan gene expression assays.....	71
Table 3.1. Mean number of viable resting U937 cells as recorded by Confocal Laser Scanning Microscopy following staining with Acridine Orange and Propidium Iodide.	100
Table 3.2. Mean number of viable activated U937 cells as recorded by Confocal Laser Scanning Microscopy following staining with Acridine Orange and Propidium Iodide.	105
Table 3.3. Summary of main results from Chapter 3.....	113
Table 4.1. Metal ions in RPMI-1640 in the presence and absence of metal wear debris.	139
Table 4.2. Metal ions released from different concentrations of wear metal debris.....	140
Table 4.3. Cellular ion up-take.....	143
Table 4.4. GPR results derived from resting U937 cells treated with 2.5mg/1x10 ⁶ cells wear debris and 0.1µM Co for 120h.....	148

Table 4.5. Genes chosen for further expression analysis.	150
Table 4.6. Ranking of the reference genes candidates.	161
Table 4.7. Primer set efficiencies.	163
Table 6.1. RNA quality indicator (RQI) numbers obtained with archived samples stored with no RNA stabiliser.....	200
Table 6.2. RNA quality indicator (RQI) numbers.	201
Table 6.3. RNA quality indicator (RQI) numbers.	202
Table 6.4. Metal ion levels in whole blood from patients with metal-on-metal hip implants.	207
Table 6.5. Effect of RNA quality on reference gene Cqs.	209
Table 6.6. RQI values of whole blood samples from patients and controls (healthy volunteers).	210
Table 6.7. RefFinder ranking order of the four candidate reference genes.	211
Table 6.8. Fold variations of target genes.	212
Table 6.9. RANKL/OPG ratios. RANKL/OPG ratios were calculated for each patient and controls.	214
Table 7.1. Indications for hip revision procedures in 2011 (National Joint Registry, 2012).	221
Table 7.2. Revision rates after primary hip replacement (%) for up to 7 years.	221
Table A.1. MIQE checklist.	253

List of figures

Figure 1.1. Illustration of a normal hip joint.	2
Figure 1.2. Illustration of a diseased hip joint	3
Figure 1.3. Kinds of hip replacements.....	4
Figure 1.4. Schematic illustrating chromium uptake.	13
Figure 1.5. Schematic of the transition from blood-borne monocyte to biomaterial adherent monocyte/macrophage at the tissue/implant material interface.	25
Figure 1.6. Schematic diagram of the debris-induced inflammation process.	37
Figure 2.1 Isolation of peripheral mononuclear cells from buffy coat.....	43
Figure 2.2. Transfer cassettes.	58
Figure 2.3. Key criteria delineating essential technical information required for the assessment of a RT-qPCR experiment.	60
Figure 2.4. Overview of total RNA isolation from U937 cells.	62
Figure 3.1 Carl Zeiss Axio Imager Microscope images of U937 cells..	76
Figure 3.2. Nikon Microscope images of U937 cells (20X)..	78
Figure 3.3. Presence of U937 cells after 24, 48, 72, 96 and 120h exposure to PMA, measured by MTT.....	79
Figure 3.4. Fixed Ost-5 cells and latex beads (40X).....	80
Figure 3.5. Fixed activated U937 cells and latex beads (40X).	80
Figure 3.6. Images of planes at various depths within a 5h activated U937 cell sample (40X).	81
Figure 3.7. Scanning Electron Microscopy images of simulator generated wear debris from an ASR hip implant.....	83
Figure 3.8. Scanning Electron Microscopy images of wear debris from the implant retrieved from a patient undergoing revision surgery.....	83
Figure 3.9. Energy Dispersive X-ray Spectroscopy of simulator generated wear debris from an ASR hip implant.....	84
Figure 3.10. Energy Dispersive X-ray Spectroscopy of sample from a patient undergoing revision surgery.....	84
Figure 3.11. Composition of simulator generated CoCr wear debris from an ASR hip implant and infiltrate from a patient undergoing revision surgery, analysed by EDS.	85
Figure 3.12. Activation of CD11c+ dendritic cells (DCs).	86
Figure 3.13. Resting U937 cell viability after 24, 48 and 120h of exposure to 0.05mg/1x10 ⁶ cells, 0.1mg/1x10 ⁶ cells and 0.2mg/1x10 ⁶ cells wear debris.	87

Figure 3.14 Resting and resting Co pre-treated U937 cell viability after 24, 48 and 120h of exposure to 0.05mg/1x10 ⁶ cells, 0.1mg/1x10 ⁶ cells and 0.2mg/1x10 ⁶ cells wear debris.	89
Figure 3.15 Cell viability at 24 and 120h measured by Neutral Red and MTT.	91
Figure 3.16 Activated U937 cell viability after 24, 48 and 120h of exposure to 0.05mg/1x10 ⁶ cells, 0.1mg/1x10 ⁶ cells, and 0.2mg/1x10 ⁶ cells wear debris.	92
Figure 3.17 Activated and activated Co pre-treated U937 cell viability after 24, 48, and 120h of exposure to 0.05mg/1x10 ⁶ cells, 0.1mg/1x10 ⁶ cells and 0.2mg/1x10 ⁶ cells wear debris.	94
Figure 3.18 Cell viability at 24 and 120h measured by Neutral Red and MTT.	96
Figure 3.19 Fluorescence microscopy images (40X) following PI (Dead cells, red)/AO (Live cells, green) staining of resting U937 and Co pre-treated resting U937 cells exposed to 0.05mg/1x10 ⁶ cells, 0.1mg/1x10 ⁶ cells, and 0.2mg/1x10 ⁶ cells wear debris for 24, 48 and 120h.	99
Figure 3.20. Fluorescence microscopy images (40X) following PI (Dead cells, red)/AO (Live cells, green) staining of resting U937 and Co pre-treated resting U937 cells exposed to 5mg debris/1x10 ⁶ cells, 0.1µM Co and 5mg debris/1x10 ⁶ cells + 0.1µM Co.	100
Figure 3.21. Fluorescence microscopy images (40X) following PI (Dead cells, red)/AO (Live cells, green) staining of activated U937 and Co pre-treated activated U937 cells exposed to 0.05mg/1x10 ⁶ cells, 0.1mg/1x10 ⁶ cells and 0.2mg/1x10 ⁶ cells wear debris for 24, 48 and 120h.	103
Figure 3.22. Fluorescence microscopy images (40X) of activated U937 and Co pre-treated activated U937 cells exposed to 5mg debris/1x10 ⁶ cells, 0.1µM Co and 5mg debris/1x10 ⁶ cells + 0.1µM Co.	104
Figure 3.23 Resting U937 cell proliferation at 24h measured by BrdU.	106
Figure 3.24 Activated U937 cell proliferation at 24h measured by BrdU.	107
Figure 3.25. Cytokine secretion levels of resting and Co pre-treated resting U937 cells at 24 and 120h of exposure to 5mg debris/1x10 ⁶ cells, 0.1µM Co and 5mg debris/1x10 ⁶ cells + 0.1µM Co.	109
Figure 3.26. Cytokine secretion levels of activated and Co pre-treated activated U937 cells at 24 and 120h of exposure to 5mg debris/1x10 ⁶ cells, 0.1µM Co and 5mg debris/1x10 ⁶ cells + 0.1µM Co.	111
Figure 3.27. Cup angular position <i>in vivo</i> and in the simulator.	116
Figure 4.1. ICP-MS Internal standard (ISTD) recovery.	134
Figure 4.2. ICP-MS Internal standard (ISTD) recovery.	135
Figure 4.3. ICP-MS internal standard recovery of the candidates Sc, Rh, In. Red dotted line marks acceptable range limits for internal standard recovery.	137

Figure 4.4. ISTD recovery from ICP-MS analysis of culture medium samples.....	138
Figure 4.5. Metal ion concentrations in culture medium from resting U937 cells.).....	141
Figure 4.6. Metal ion concentrations in culture medium from activated U937 cells..	142
Figure 4.7. Early apoptosis, late apoptosis and necrosis of resting U937 and Co pre-treated resting U937 cells measured by FACS.....	145
Figure 4.8. Detection of PARP and PARP fragments by western blot as indication of early apoptosis of resting U937 and Co pre-treated resting U937 cells.....	146
Figure 4.9. Schematic overview of a biological process perturbation.	149
Figure 4.10. Melting curve analysis. Curves showing peaks of specific product at >78°C and some non-specific product at lower temperatures.	153
Figure 4.11. Horizontal gel electrophoresis of PCR amplification products from untreated resting U937 cells (control).....	155
Figure 4.12. Horizontal gel electrophoresis of PCR amplification products from resting and Co pre-treated resting U937 cells exposed to 2.5mg debris/1x10 ⁶ cells for 120h.....	156
Figure 4.13. Horizontal gel electrophoresis of PCR amplification products from resting and Co pre-treated resting U937 cells exposed to 0.1µM Co for 120h.	157
Figure 4.14. Horizontal gel electrophoresis of PCR amplification products from resting and Co pre-treated resting U937 cells exposed to 2.5mg debris/1x10 ⁶ cells+0.1µM Co for 120h. U937 ⁻). The fourth lane is the cDNA _{U937} reaction and the fifth is the cDNA _{PreCoU937} reaction.	158
Figure 4.15. qPCR amplification plot. The grey square indicates the exponential region, where the threshold for C _q value determination is set.	161
Figure 4.16. RefFinder results. Comprehensive gene stability integrates the four commonly used approaches to compare and rank the tested candidate reference genes calculating the geometric mean of their weights for the overall final ranking.	162
Figure 4.17. Gene fold change assuming 100% primer efficiency.	166
Figure 4.18. Gene fold change corrected to primer efficiency.....	168
Figure 5.1. Cell number (NR) and metabolic activity (MTT) of human lymphocytes.....	179
Figure 5.2. Proliferation of human lymphocytes measured by BrdU assay.	180
Figure 5.3. Cytokine production by human lymphocytes.....	181
Figure 5.4. Apoptosis.	183
Figure 6.1. RQI calculation.	192
Figure 6.2. Electropherograms from freeze/thaw cycles. Ladder, RNA standard.....	203
Figure 6.3. ICP-MS Internal standard (ISTD) recovery. um. Standards: 0, 0.1, 1, 10, 100, 500, and 1000ppb (0, 0.1, 1, 10, 100, 500, and 1000µg/l).....	205

Figure 6.4. ICP-MS internal standard recovery of the candidates Sc, Rh, In.....	206
Figure 6.5. RefFinder results.....	211
Figure 6.6. Fold variations of target genes.....	213
Figure 6.7. Scatter plots of RANKL/OPG ratios.....	214
Figure 6.8 OPG/RANK/RANKL molecular and cellular mechanisms of action.....	217
Figure 7.1. Total hip articulation trends 2010/2011.....	230

Table of Contents

Acknowledgments.....	II
Abstract	IV
List of abbreviations.....	VI
List of tables X	
List of figures	XII
Table of Contents	XVI
1. INTRODUCTION	1
1.1 The hip joint.....	1
1.2 Hip replacements	3
1.2.1 Implant bearing surfaces.....	6
1.3 Immune response	23
1.3.1 Monocytes and macrophages.....	24
1.3.2 Lymphocytes.....	33
1.3.3 Cytokines	34
1.4 Osteolysis and Aseptic loosening	34
1.5 Aims of the present study	38
2. GENERAL METHODS	39
2.1 Cells	39
2.1.1 Culturing of U937 cells.....	39
2.1.2 Activation of U937 cells	40
2.1.3 Assessment of activated U937 phagocytosis activity.....	41
2.1.4 Isolation of primary human lymphocytes	43
2.1.5 Isolation of primary murine dendritic cells (DCs).....	44
2.1.6 Preparation of metal ion solutions	44

2.1.7	Preparation of metal wear debris	45
2.1.8	Assessing sterility of treated wear debris	45
2.1.9	Surface antigen staining of cells for flow cytometry	46
2.1.10	Characterisation of wear debris derived from a metal-on-metal hip resurfacing	47
2.1.11	Exposure of U937 cells to wear debris and metal ions	47
2.1.12	Exposure of lymphocytes to wear debris and metal ions.....	48
2.1.13	MTT assay for cell viability.....	48
2.1.14	Neutral red assay for cell viability	49
2.1.15	Analysis of cell morphology and viability via microscopy	50
2.1.16	Cell proliferation assay	50
2.1.17	ELISA	51
2.1.18	ICP-MS Analysis of metal ion concentrations	52
2.1.19	Flow cytometry analysis of apoptosis.....	54
2.1.20	Western blot analysis of apoptosis.....	55
2.1.21	Minimum Information for Publication of Quantitative Real-Time PCR Experiments (MIQE)	59
2.1.22	Isolation of total RNA.....	60
2.1.23	cDNA synthesis	62
2.1.24	StellARray TM gene expression array.....	63
2.1.25	Primer design and efficiency determination	64
2.1.26	SYBR Green quantitative real-time PCR	65
2.1.27	Horizontal gel electrophoresis	66
2.2	Analysis of blood samples	67
2.2.1	Storing clinical blood samples.....	67
2.2.2	ICP-MS Analysis of metal ions	67

2.2.3	Isolation of total RNA that includes the small RNA fraction.....	68
2.2.4	cDNA synthesis	70
2.2.5	Stability of RNA after up to 10 Freeze/Thaw Cycles of storage	70
2.2.6	Taqman quantitative real-time PCR	70
2.2.7	Effects of RNA integrity on qRT-PCR results	71
3.	EFFECTS OF COBALT IONS AND WEAR METAL DEBRIS DERIVED FROM A HIP RESURFACING ON U937 CELLS <i>IN</i> <i>VITRO</i>	73
3.1	Introduction.....	73
3.2	Aims.....	74
3.3	Results.....	74
3.3.1	Activation of U937 cells with PMA	74
3.3.2	Activated U937 phagocytosis activity	79
3.3.3	Characterisation of CoCr wear debris.....	82
3.3.4	Sterility of CoCr wear debris to be used in cell culture experiments ...	85
3.3.5	Effects of metal debris and ions on cell viability measured by MTT and NR.....	86
3.3.6	Effects of metal debris and ions on cell morphology assessed with fluorescence microscopy.....	96
3.3.7	Effects of metal debris and ions on U937 proliferation as measured by BrdU.....	105
3.3.8	Effects of metal debris and ions on cytokine release measured by ELISA	107
3.3.9	Summary of major findings	112
3.4	Discussion	114
4.	CORRELATION BETWEEN GENE EXPRESSION, APOPTOSIS AND METAL ION LEVELS ON U937 CELLS <i>IN VITRO</i>	123

4.1	Introduction.....	123
4.2	Aims.....	132
4.3	Results.....	132
4.3.1	Protocol development for ICP-MS analysis of culture medium.....	132
4.3.2	Metal ions release into cell culture medium	139
4.3.3	Cellular metal ion up-take.....	143
4.3.4	Apoptosis analysis of U937 cells following exposure to CoCr wear debris and Co ions.....	143
4.3.4.1	Flow cytometry of resting U937 cells following 24 and 48h exposure to CoCr wear debris and Co ions	144
4.3.5	Gene expression analysis of resting U937 cells following 120h exposure to CoCr wear debris and Co ions.....	147
4.4	Discussion.....	169
5.	EFFECTS OF COBALT IONS AND WEAR METAL DEBRIS DERIVED FROM A HIP RESURFACING ON FRESHLY ISOLATED HUMAN LYMPHOCYTES <i>IN VITRO</i>	175
5.1	Introduction.....	175
5.2	Aim	178
5.3	Results.....	178
5.3.1	Effects of metal debris and ions on human primary lymphocyte cell viability as measured by MTT and NR.....	178
5.3.2	Effects of metal debris and ions on human primary lymphocyte cell proliferation assessed with BrdU	179
5.3.3	Effects of metal debris and ions on cytokine release by human primary lymphocyte cells measured by ELISA.....	180
5.3.4	Effects of metal debris and ions on human primary lymphocyte cell apoptosis assessed by flow cytometry	182
5.4	Discussion.....	183

6.	CORRELATION BETWEEN GENE EXPRESSION AND METAL ION LEVELS IN CLINICAL BLOOD SAMPLES.....	188
6.1	Introduction.....	188
6.1.1	RNA stability in clinical blood samples	188
7.1.1	Brief review of gene expression studies <i>in vivo</i> related to osteolysis and joint implant failure	195
6.2	Aims.....	199
6.3	Results.....	199
6.3.1	Whole blood sample storage and RNA isolation from samples with the RiboPure Blood kit	199
6.3.2	RNA stability during freeze/thaw cycles	201
6.3.3	Whole blood metal ion levels	203
6.3.4	Effects of RNA integrity on qRT-PCR results	207
6.3.5	Whole blood gene expression analysis	209
6.4	Discussion.....	215
7.	SUMMARY AND FUTURE WORK	221
7.1	Summary of thesis results	221
7.1.1	Effects of cobalt ions and wear metal debris derived from a hip resurfacing on U937 cells <i>in vitro</i>	222
7.1.2	Correlation between gene expression, apoptosis, and metal ion levels on U937 cells <i>in vitro</i>	223
7.1.3	Effects of cobalt ions and wear metal debris derived from a hip resurfacing on freshly isolated human lymphocytes <i>in vitro</i>	224
7.1.4	Correlation between gene expression and metal ions levels in clinical blood samples	225
7.2	Main findings.....	227
7.3	Limitations of these studies	227

7.4	Future work.....	230
7.4.1	Inflammatory response triggering mechanisms	230
7.4.2	Revision surgery patients.....	231
7.4.3	Metal-on-Metal Implants: Epigenetic effects	232
7.4.4	Implications of this research to the health and quality of life of patients with MOM	233
APPENDIX		236
Appendix 1. Sodium Phosphate buffer (NaPi) composition.....		236
Appendix 2. Fluorescence microscopy images of resting and activated U937 cells exposed to varying concentrations of metal wear debris.		236
2.1.	Fluorescence microscopy images (40X) following PI (Dead cells, red)/AO (Live cells, green) staining of resting U937 and Co pre-treated resting U937 cells exposed to 0.05mg/1x10 ⁶ cells, 0.1mg/1x10 ⁶ cells, and 0.2mg/1x10 ⁶ cells wear debris for 24 and 120h.....	236
2.2	Fluorescence microscopy images (40X) following PI (Dead cells, red)/AO (Live cells, green) staining of resting U937 and Co pre-treated resting U937 cells exposed to 5mg debris/1x10 ⁶ cells, 0.1µM Co and 5mg debris/1x10 ⁶ cells + 0.1µM Co	240
2.3	Fluorescence microscopy images (40X) following PI (Dead cells, red)/AO (Live cells, green) staining of activated U937 and Co pre-treated activated U937 cells exposed to 0.05mg/1x10 ⁶ cells, 0.1mg/1x10 ⁶ cells and 0.2mg/1x10 ⁶ cells wear debris for 24, 48 and 120h.	243
2.4	Fluorescence microscopy images (40X) of activated U937 and Co pre-treated activated U937 cells exposed to 5mg debris/1x10 ⁶ cells, 0.1µM Co and 5mg debris/1x10 ⁶ cells + 0.1µM Co.	247
Appendix 3. MIQE check list.....		250
PUBLICATIONS		254
REFERENCES.....		255

1. INTRODUCTION

The present work will focus on the toxicity, immunological and gene expression effects of cobalt ions and wear debris produced by a metal-on-metal hip resurfacing device. This section gives an introductory overview of the hip joint and hip replacements as a commonly used option to treat hip diseases. Special attention will be given to metal-on-metal devices as the long term consequences to being exposed to metal wear particles and ions are still not fully understood.

1.1 The hip joint

The hip joint, scientifically referred to as the acetabulofemoral joint, is the joint between the femur and acetabulum of the pelvis and its primary function is to support the weight of the body in both static (e.g. standing) and dynamic (e.g. walking or running) postures. It allows flexion and extension, adduction and abduction, circumduction, and rotation. The hip is a ball-and-socket synovial joint (Figure 1.1). A round, cup-shaped structure on the acetabulum, forms the socket for the hip joint. The rounded head of the femur forms the ball of the joint. Hyaline cartilage lines both the acetabulum and the head of the femur, providing a smooth surface for the moving bones to glide past each other. Hyaline cartilage also acts as a flexible shock absorber to prevent the collision of the bones during movement. Between the layers of hyaline cartilage, synovial membranes secrete watery synovial fluid to lubricate the joint capsule (Navarro-Zarza et al., 2012, Field and Rajakulendran, 2011).

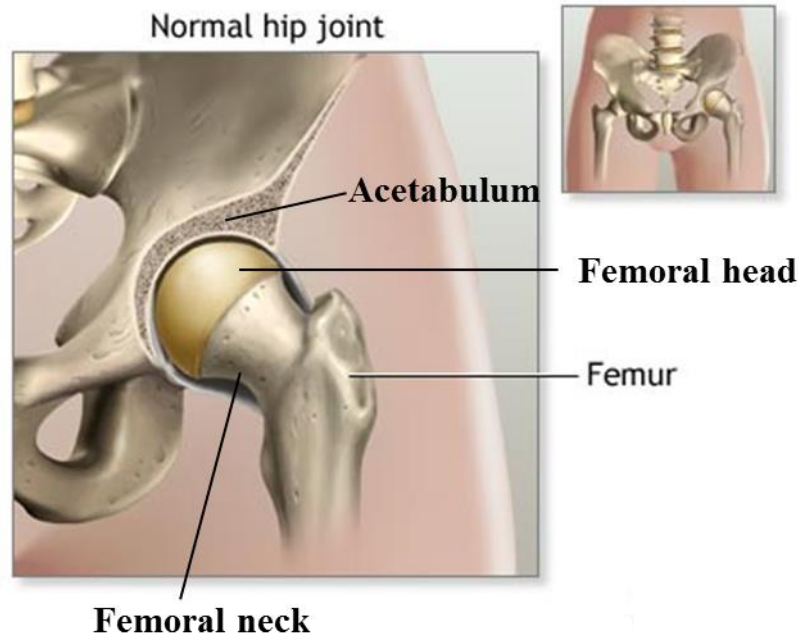


Figure 1.1. Illustration of a normal hip joint (adapted from http://www.pennmedicine.org/encyclopedia/em_PrintPresentation.aspx?gcid=100006&ptid=3).

There are several conditions which can lead to chronic hip pain and disability including fracture, inflammatory conditions, synovial abnormalities and tumours (Mengiardi et al., 2007). Arthritis is a form of joint disorder that involves inflammation of one or more joints. Even though there are over 100 types, osteoarthritis (OA) is the most common form of arthritis, a leading cause of disability, and the most common cause for hip replacement surgeries (Sanders et al., 2004). OA begins asymptotically in the 20s and 30s, with symptoms beginning in the 40s through 60s, and becoming more common by the 70s (Shelton, 2013). In OA, cartilage covering the end of the bones becomes weaker when the normal process of cartilage remodelling becomes altered (Figure 1.2). Without the protection of the cartilage, the bones begin to rub against each other and the resulting friction leads to pain and stiffness (Desrochers et al., 2013).

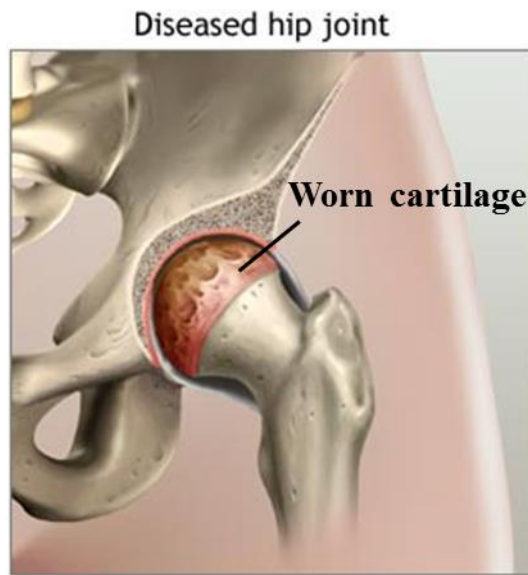


Figure 1.2. Illustration of a diseased hip joint (adapted from http://www.pennmedicine.org/encyclopedia/em_PrintPresentation.aspx?gclid=100006&ptid=3).

1.2 Hip replacements

Prosthetic replacement of human joints is one of the most promising methods in treating post-traumatic and degenerative joint diseases (Rosenberg et al., 2006). Phillip Wiles is credited with performing the first hip arthroplasty in 1938. It was a metal-on-metal total hip made of stainless steel. Its failure was due to loosening and this implant is regarded as the precedent of the modern genre (Learmonth et al., 2007). However, the orthopaedic surgeon Sir John Charnley is considered the father of the modern total hip arthroplasty (THA) (Knight et al., 2011, Gomez and Morcuende, 2005). Charnley introduced the concept of low friction arthroplasty using high-density polyethylene as a bearing material as well as fixing components to bone with acrylic cement (Knight et al., 2011).

Total hip arthroplasty (Figure 1.3) is an orthopaedic procedure that involves the surgical excision of the head and proximal neck of the femur and removal of the acetabular cartilage and subchondral bone. An artificial canal is created in the proximal medullary region of the femur and a femoral prosthesis, composed of a stem and head, is inserted into the femoral medullary canal. An acetabular

component with an articulating surface is inserted proximally into the enlarged acetabular space. Finally, these total hip arthroplasty components must be fixed firmly to the bone (Siopack and Jergesen, 1995). According to the latest report from the Centers for Disease Control, 230,000 THA surgeries were performed in the United States alone in 2007 (CDC, 2010) and the demand for THA is expected to grow by 172% by 2030 (Kurtz et al., 2007). Considering that the median estimated cost of primary hip replacement per patient has been reported to be £5084 (£4588-£5812) in the UK (Fordham et al., 2012) and \$12846 (\$12715-\$13470) in the United States (Antoniou et al., 2004), the increase in THA surgeries can have a financial impact on the healthcare systems.

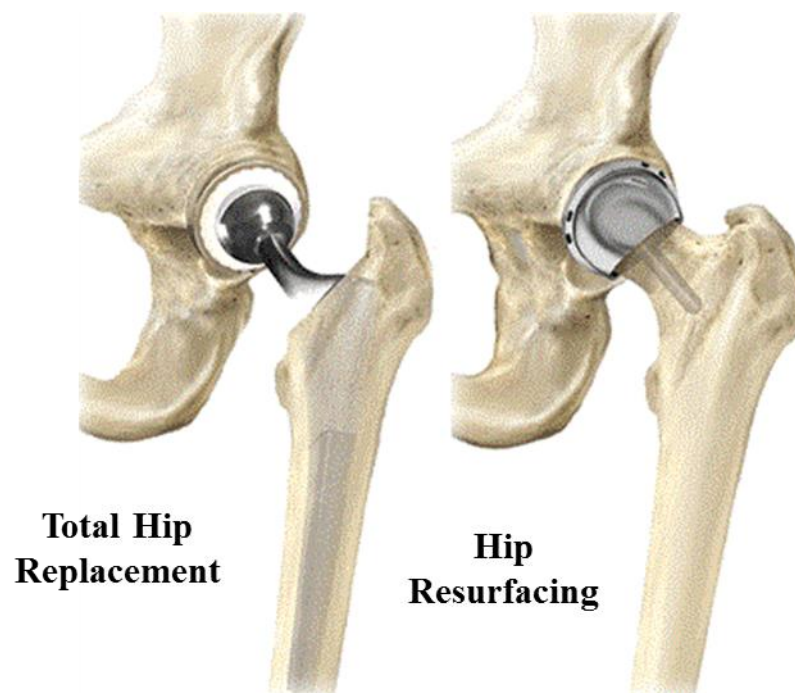


Figure 1.3. Kinds of hip replacements. (adapted from <http://www.orthopaedicspecialistsct.com/hipResurfacing.asp>)

THA is a surgery that serves as the standard treatment of hip disease (Jiang *et al.*, 2011). However, there are limitations with THA and it has been reported to fail in younger patients (Table 1.1) with more active lifestyles (Karas, 2012, Siverling et al., 2012). Total hip replacements may fail for a variety of reasons including fracture of the implant, aseptic loosening, infection, wear, and dislocation (Malchau et al., 2002). Additionally, as shown in Table 1.1, the rate of failure tends to be greater in

females perhaps due to differences in hip anatomy. Developments in THA have been directed at the reduction of the rate of failure while accommodating the high-activity profile of younger patients (Learmonth et al., 2007).

Age	Head size	Year 1	Year 3	Year 5	Year 7
Males					
55	28mm	0.73%	1.89%	3.30%	4.59%
55	36mm	0.86%	2.22%	3.86%	5.38%
55	46mm	1.04%	2.70%	4.70%	6.54%
55	48mm	1.09%	2.81%	4.89%	6.79%
55	50mm	1.13%	2.93%	5.09%	7.06%
55	52mm	1.18%	3.05%	5.29%	7.34%
70	28mm	0.66%	1.70%	2.94%	4.07%
70	36mm	0.78%	1.99%	3.44%	4.76%
70	46mm	0.95%	2.43%	4.19%	5.79%
70	48mm	0.99%	2.53%	4.36%	6.03%
70	50mm	1.03%	2.63%	4.54%	6.26%
70	52mm	1.07%	2.74%	4.72%	6.51%
Females					
55	28mm	0.98%	2.71%	4.82%	7.25%
55	36mm	1.14%	3.14%	5.58%	8.38%
55	42mm	1.28%	3.51%	6.23%	9.34%
55	44mm	1.33%	3.64%	6.46%	9.68%
55	46mm	1.38%	3.78%	6.70%	10.03%
70	28mm	0.73%	2.01%	3.56%	5.34%
70	36mm	0.85%	2.33%	4.13%	6.18%
70	42mm	0.95%	2.61%	4.61%	6.90%
70	44mm	0.99%	2.71%	4.79%	7.15%
70	46mm	1.03%	2.81%	4.97%	7.42%

Table 1.1. Predicted revision rates for males and females with total hip metal-on-metal articulations by age and head size. Percentages are based on 9,445 male and 9,234 female uncemented total hip metal-on-metal cases between April 2003 and September 2011 (National Joint Registry, 2012).

Improvements in surgical techniques, prosthetic designs, and instrumentation have allowed the development of hip resurfacing (HR, Figure 1.3) as a surgical alternative for younger and more active individuals (Siverling et al., 2012). Several advantages of resurfacing over standard THA have been suggested. It conserves bone on the femoral side, allows more range of motion, a more normal gait pattern, increased activity levels and ease of revision (Quesada et al., 2008, Jiang et al., 2011, Shimmin et al., 2008).

However, specific risks associated with HR surgery include metal ion dispersion from the metal device into the tissues surrounding the implant and blood stream, femoral fracture, and femoral component loosening (Nunley et al., 2009, Siverling et al., 2012, Quesada et al., 2008).

1.2.1 Implant bearing surfaces

Various hip prosthesis materials have been developed in the past. Repeated trials and experimentation with various materials and prosthetic designs culminated in the creation of the Charnley low-friction arthroplasty in the 1960s (Harris, 2009, Learmonth et al., 2007, Kolundzic et al., 2012). From this point, most hip prostheses would consist of an ultra-high-molecular-weight polyethylene (UHMWPE) acetabular cup and a metal-alloy femoral component. In cemented techniques, polymethylmethacrylate (PMMA) cement is used to fix the femoral component in bone, whereas in uncemented arthroplasties, the prosthesis interfaces with bone directly (Siopack and Jergesen, 1995). However, the discovery that UHMWPE wear and debris formation resulted in synovitis, joint instability, osteolysis, and prosthesis loosening (Catelas et al., 2011, Brown et al., 2006, Kolundzic et al., 2012) raised concerns about the long-term outcome of total joint replacement surgery. Specifically, UHMWPE wear debris was found to stimulate peri-prosthetic cells to express pro-inflammatory and pro-osteoclastic cytokines, which resulted in aseptic loosening (Gallo et al., 2013). This led to assessment of alternative bearing surfaces in an attempt to reduce wear and improve longevity of hip replacement procedures (Learmonth et al., 2007, Porat et al., 2012). The wear properties of polyethylene can be improved by cross-linking (Joyce et al., 2011). Depending on the processes used, cross-linking of UHMWPE alters the bonds between molecular chains, reduces crystallinity, alters the free radical content of the material and significantly influences the material's surface properties (Sethi et al., 2003). Laboratory hip simulators using cross-linked polyethylene have demonstrated significant decreases in wear rates in comparison to those of conventional UHMWPE (Hermida et al., 2003, Ries et al., 2001). Moreover, improved wear characteristics of this material

have been reported in short-term clinical trials (Learmonth et al., 2007, Joyce et al., 2011, Huo et al., 2011).

Additionally, hard-on-hard bearing combinations such as metal-on-metal (MoM) and ceramic-on-ceramic (CoC), have also been introduced because of their higher wear resistance based on volumetric material loss and the presumption that a reduction in wear rate would translate into fewer complications and improved implant lifetime (Catelas et al., 2011, Porat et al., 2012, Affatato et al., 2010). Alumina ceramics were introduced in the 1970s. They have a low coefficient of friction, superior wear rates, and are scratch-resistant (Learmonth et al., 2007). However, the major unique complications of ceramics are fracture because of their brittle nature (Learmonth et al., 2007, Porat et al., 2012) and noise generation (squeaking) (Huo et al., 2011, Porat et al., 2012). Modern day metal-on-metal total hip resurfacings were introduced approximately 14 years ago (Quesada et al., 2008). They represent approximately 10% of all hip arthroplasties in developed countries between 1990 and 2010 (Jiang et al., 2011, Corten and MacDonald, 2010). The Australian annual report from 2010 indicates that in 2009-2010, 35996 hip procedures were carried out in Australia and MoM accounted for 12% of all implanted arthroplasties (Australian Orthopaedic Association National Joint Replacement Registry, 2011). In 2010-2011, 11948 total hip replacements were performed in Canada from which 10.1% used MoM bearing surfaces (Canadian Joint Replacement Registry, 2013). Additionally, 491505 THA procedures were recorded between April 2003 and September 2011 in England and Wales and 8% involved MoM articulations (National Joint Registry, 2012). Metal bearing surfaces have low wear rates, are not brittle, and are self-polishing, allowing for self-healing of surface scratches (Learmonth et al., 2007). The most common metallic materials used in total hip joint replacements include titanium alloys, stainless steels and cobalt-chromium alloys (Antunes and Lopes de Oliveira, 2012). Furthermore, metal-on-metal hip resurfacing bearings are made from high-carbon CoCr alloy (Mahendra et al., 2009, Amstutz and Le Duff, 2006) due to their superior hardness and resistance to wear compared to Ti alloys. The relative softness of Ti alloys compared to CoCr alloys results in poor wear and frictional properties; Ti alloys are approximately 15% softer than CoCr alloys. For this reason, Ti alloys are

commonly used for non-weight bearing surface components such as femoral necks, stems, and porous coatings (Long, 2008, Navarro et al., 2008)

Even though MoM bearing technology was initially aimed to extend the durability of hip replacements and to reduce the requirement for revision, they have been reported to release at least three times more cobalt and chromium ions than metal-on-polyethylene hip replacements (Hart et al., 2006, Savarino et al., 2002, Keegan et al., 2007, Antoniou et al., 2008). As a result, the toxicity of metal particles and ions produced by bearing surfaces both locally in the peri-prosthetic space and systemically became a concern (Moroni et al., 2011). The following section gives a brief description of metal toxicity.

1.2.1.1 Metal toxicity

Metals are essential components of a variety of biological systems. For example, sodium, potassium, magnesium and calcium provide the basis for nerve conduction, muscle contraction, stabilization of nucleic acids and other biological systems and thus are the dominant metal ions in a cell (Bleackley and MacGillivray, 2011). Metals commonly occur in proteins modulating protein function (Okamoto and Eltis, 2011). Proteins that bind transition metals such as iron, copper, manganese, zinc, cobalt and nickel are often catalytic enzymes with the transition metal ion being essential for activity. Under physiological conditions, most transition metals can exist in multiple valence states, which allows them to participate in the control of various metabolic and signalling pathways such as electron transfer reactions, oxygen transport, gene regulation and structure stabilization. Metal ions are also found as components of prosthetic groups, cofactors and complexes prior to insertion into proteins (Okamoto and Eltis, 2011, Bleackley and MacGillivray, 2011)

Although some metals have specific biological functions, high metal concentrations can lead to toxicity often through the formation of oxygen radicals (Valko et al., 2005). The resulting reactive oxygen species can go on to damage cellular components including proteins, lipids and nucleic acids eventually leading to cell

death. Complex systems have evolved to maintain the delicate balance between transition metals as essential nutrients and their potentially damaging role as cytotoxins. Perturbations in this balance are observed in the genetic diseases of transition metal metabolism stemming from both overload and deficiency that manifest in a variety of symptoms (Bleackley and MacGillivray, 2011).

Metal compounds are found throughout the environment (Koedrith and Seo, 2011). Individuals who are subject to environmental overexposure to transition metals also exhibit a number of diseases related to the toxicity of the metals (Bleackley and MacGillivray, 2011). Industrial applications contribute significantly to human metal exposure (Koedrith and Seo, 2011) but with increasing numbers of joint replacement surgeries around the world; orthopaedic implants have become another important route of exposure. Some metals, including arsenic, cadmium, chromium, cobalt, lead, mercury, and nickel have been classified as human carcinogens or considered to be human carcinogens by the International Agency for Research on Cancer (Koedrith and Seo, 2011, Catalani et al., 2012).

The demand for metallic materials in medical devices is largely due to properties such as toughness, elasticity, rigidity, and electrical conductivity. They are widely used for orthopaedic implants, bone fixators, artificial joints, external fixators, among others (Vidal and Munoz, 2009). Metallic biomaterials are composed of a variety of metals including aluminium (Al), chromium (Cr), cobalt (Co), nickel (Ni), molybdenum (Mo), vanadium (V), titanium (Ti), and iron (Fe) (Cadosch et al., 2009). The compositions of metal alloys used in hip replacement implants are shown in Table 1.2.

Alloy	Ni	N	Co	Cr	Ti	Mo	Al	Fe	Mn	Cu	W	C	Si	V
Stainless steel														
(ASTM F138)	10.0 to 15.5	< 0.5	†	17.0 to 19.0	†	2.0 to 4.0	†	61.0 to 68.0	†	< 0.5	< 2.0	< 0.06	< 1.0	†
CoCrMo alloys														
(ASTM F75)	< 2.0	†	61.0 to 66.0	27.0 to 30.0	†	4.5 to 7.0	†	< 1.5	< 1.0	†	†	< 0.35	< 1.0	†
(ASTM F90)	9.0 to 11.0	†	46.0 to 51.0	19.0 to 20.0	†	†	†	< 3.0	< 2.5	†	14.0 to 16.0	< 0.15	< 1.0	†
Ti Alloys														
CPTi (ASTM F67)	†	†	†	†	99.0	†	†	0.2 to 0.5	†	†	†	< 0.1	†	†
Ti-6Al-4V (ASTM F136)	†	†	†	†	89.0 to 91.0	†	5.5 to 6.5	†	†	†	†	< 0.08	†	3.5 to 4.5

Table 1.2. Elemental compositions (% weight) of metal alloys used in orthopaedic implants. Alloy compositions are standardised by the American Society for Testing and Materials (ASTM). (CPTi: commercially pure titanium, Ti: titanium, Al: aluminium, V: vanadium, Co: cobalt, Cr: chromium, Mo: molybdenum, Ni: nickel, Fe: iron, Si: silicon, W: tungsten, Cu: copper, C: carbon, N: nitrogen). † indicates < 0.05% (Keegan et al., 2007, Hallab et al., 2001a, Singh and Dahotre, 2007).

CoCr alloy is used in joint replacement devices for knee, ankle, shoulder, elbow, wrist, and finger arthroplasty procedures (Long, 2008). Wear debris from these articulations is generated by mechanical wear, surface corrosion or a combination of both, and consists of both particles and ions (Keegan et al., 2007). Corrosion is the visible destruction of a metal caused by interactions with its environment, which may cause rupture of a structure or loss of function (Cadosch et al., 2009). The physiological environment is considered corrosive. This makes the corrosion of metallic materials a slow and continuous process, which leads to the release of metal ions (Singh and Dahotre, 2007, Cadosch et al., 2009).

It has been shown that wear debris generated from CoCr MoM articulations can lead to local soft-tissue inflammatory response that results in premature failure of the implant and systemic effects from prolonged exposure to Cr and Co ions (Davda et al., 2011, Griffin et al., 2012).

1.2.1.2 CoCr wear particles

The degradation products of any orthopaedic implant include only two basic types of debris: particles and soluble (or ionic) debris (Hallab and Jacobs, 2009). Particulate wear debris generated by MoM articulations is in the nanometre size range (Germain et al., 2003), the average particle size range being 30 to 100 nm in size (Catelas and Wimmer, 2011). The reduced size of nanoparticles allows their entrance into tissues and organs and diffusion throughout the body, and their interaction with different types of cells (Lucarelli et al., 2004).

It has been reported that the ingestion by cells of nanometersized wear particles occurs by endocytosis or pinocytosis (Shukla et al., 2005). Once ingested by macrophages, a host of biologic reactions can occur (Hallab and Jacobs, 2009). For example, macrophages may be able to process the particles in such a way that it could lead to activation of T cells through antigen presentation. Moreover, once inside the cell, the particles could interact directly with proteins or other intracellular molecules and interfere with normal biological processes. Additionally, particulate

wear debris corrodes and releases metal ions. Increased amounts of metal particle debris leads to increased metal ion concentrations, which could lead to release of proinflammatory mediators, cytotoxicity, DNA damage, and oxidative stress (Hallab et al., 2005b).

1.2.1.3 Chromium

Chromium is the 24th element of the periodic table and has a molecular weight of 51.9. It exists in a series of oxidation states (0, +3, +6). Trivalent (Cr^{3+}) and hexavalent (Cr^{6+}) compounds are thought to be the most biologically significant. Cr^{3+} is an essential dietary mineral in low doses. It is required to potentiate insulin action and for the normal glucose metabolism. Cr^{3+} is found in most fresh foods and drinking water. Dietary sources rich in chromium include bread, cereals, spices, fresh vegetables, meats, and fish (Valko et al., 2005). The recommended dietary intake of Cr ranges from 50 to 200 μg of Cr/day. Chromium plays a beneficial role in glucose tolerance and diabetes (Dillon et al., 2000). Its deficiency in humans will lead to impaired glucose tolerance, glycosuria, fasting hyperglycemia, and elevated circulating insulin and glucagon (Afolaranmi et al., 2008).

After entering the body from an exogenous source, Cr^{3+} binds to plasma proteins such as transferrin, an iron-transporting protein. Regardless of the source, Cr^{3+} is widely distributed in the body and accounts for most of the chromium in plasma or tissues. The greatest uptake of Cr^{3+} as a protein complex is *via* bone marrow, lungs, lymph nodes, spleen, kidney, and liver, the highest being in the lungs (Bagchi et al., 2002). Moreover, it has been shown that cell membranes are relatively impermeable to Cr^{3+} . When varying amounts of radioactive Cr^{3+} were added to whole blood *in vitro*, almost all of the radioactivity (94-99%) remained in the plasma with an insignificant count retained in the RBC after saline washing. Similar results were obtained *in vivo* (Gray and Sterling, 1950). Similarly, (Dillon et al., 2000) found low permeability of Cr^{3+} as shown by the lack of a detectable Cr accumulation in Chinese hamster lung V79 cells exposed to Cr^{3+} complexes. Additionally, it has been shown that the cellular uptake of Cr^{6+} is several fold greater than that of Cr^{3+} ion, because

trivalent chromium is predominantly octahedral and diffuses slowly (Biedermann and Landolph, 1990). In contrast to Cr^{3+} , Cr^{6+} is rapidly taken up by erythrocytes after absorption and reduced to Cr^{3+} inside the cell (Figure 1.4). Cr^{6+} enters the cell through non-specific anionic channels, such as the phosphate and sulphate anion exchange pathway (Tkaczyk et al., 2009, Raja et al., 2011). Once within the cell, Cr^{6+} is reduced metabolically by the redox system to short-lived intermediates Cr^{5+} , Cr^{4+} , and ultimately to the most stable species Cr^{3+} (Fornsaglio et al., 2005, Shrivastava et al., 2005, Afolaranmi et al., 2008). Cr^{3+} interacts and forms complexes with DNA, protein and lipids resulting in increased chromium intracellular levels (Fornsaglio et al., 2005, Shrivastava et al., 2005, Raja et al., 2011).

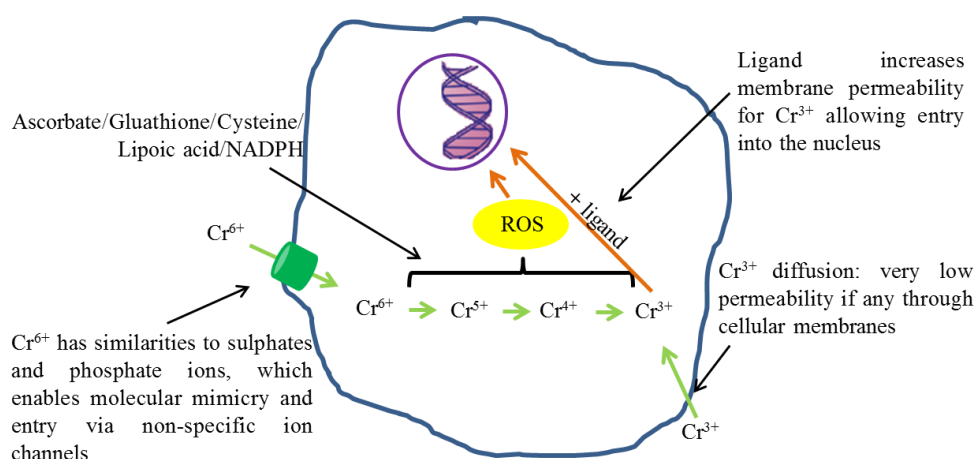


Figure 1.4. Schematic illustrating chromium uptake. This schematic depicts how Cr^{6+} enters cells readily, while Cr^{3+} on the other hand moves across the cell membrane via much slower diffusion and through other processes related to the chemical structure of the attached ligands. ROS: reactive oxygen species (adapted from (Gill et al., 2012a)).

Excretion of chromium occurs primarily via urine, with no major retention in organs. Approximately 10% of an absorbed dose is eliminated by biliary excretion, with smaller amounts excreted in hair, nails, milk, and sweat. Clearance from plasma is generally rapid (within hours), whereas elimination from tissues is slower (with a half-life of several days) (Valko et al., 2005).

The toxicity, mutagenicity, and carcinogenicity of chromium compounds are a well-established phenomenon (De Flora, 2000, Bagchi et al., 2002, Merritt and Brown, 1995, Tkaczyk et al., 2009). Long-term occupational inhalational exposure to chromium levels 100–1000 times higher than those found in the natural environment

have been associated with squamous cell carcinoma and adenocarcinoma in exposed workers (MacDonald, 2004). Epidemiological studies carried out in the U.K, Europe, Japan and the United States have consistently shown that workers in occupations where particulate chromates are generated or used have an elevated risk of respiratory disease, fibrosis, perforation of the nasal septum, development of nasal polyps, and lung cancer (Nickens et al., 2010). Additionally, during the intracellular reduction of Cr^{6+} to the stable Cr^{3+} , reactive intermediates (ROS, pentavalent and tetravalent chromium species) are generated, which cause a wide variety of DNA lesions including Cr–DNA adducts, DNA–protein crosslinks, DNA–DNA crosslinks, and oxidative damage (Valko et al., 2005, Codd et al., 2001).

1.2.1.4 Cobalt

Cobalt has a molecular weight of 58.9 and an atomic number of 27. It can occur in four oxidation states (0, +2, +3 and +4) (De Boeck et al., 2003). The most common oxidation numbers of cobalt are +3 [Co^{3+}], and +2 [Co^{2+}] which form a number of organic and inorganic salts (Valko et al., 2005). Cobalt and its salts are used in a variety of processes but the main consumption of Co nowadays is in the production of steel and alloys (Catalani et al., 2012).

For the general population the diet is the main source of exposure to Co and it is readily absorbed in the small intestine (Catalani et al., 2012, Valko et al., 2005). Most of the consumed cobalt is excreted in the urine and very little is retained, and it is mainly in the liver and kidneys (Valko et al., 2005). Under physiological conditions, this element is mostly accumulated in the liver, kidneys, heart, and spleen, while minimum concentrations are found in the blood serum and tissues of the brain and pancreas (Kravenskaya and Fedirko, 2011). Molecular details of cobalt uptake are not well known and whether Co enters mammalian cells via a specific transporter is not known either (Bleackley and MacGillivray, 2011, Catalani et al., 2012). However, it is likely that it is transported into the cells by broad-specificity divalent metal transporters (Bleackley and MacGillivray, 2011). It has been shown that P2X7, a transmembrane ionotropic receptor, is involved in the uptake of divalent

cations and Co (Virginio et al., 1997). In the same way, a protein named divalent metal transporter 1 (DMT1) has been shown to have a broad substrate specificity favouring divalent metals including Co^{2+} (Park et al., 2002, Griffin et al., 2005, Forbes and Gros, 2003). Additionally, (Kasten et al., 1992) suggested that the cellular uptake of Co was mediated by active transport ion pumps (i.e. $\text{Ca}^{2+}/\text{Mg}^{2+}$ ATPase and the Na^+/K^+ ATPase) and endocytosis.

The only biological known function of cobalt is its integral part of vitamin B12, which is incorporated into enzymes that participate in reactions essential to DNA synthesis, fatty acid synthesis and energy production (Bleackley and MacGillivray, 2011, Catalani et al., 2012). Examples of such enzymes are methyltransferases, such as methionine synthase (MetH), which catalyzes methionine biosynthesis both in mammals and bacteria (Randaccio et al., 2010).

Even though cobalt has a role in biological systems, overexposure results in toxicity due to excess (Bleackley and MacGillivray, 2011), which promotes the development of hypoxia and increases in the level of reactive oxygen species (ROS), suppresses synthesis of ATP, initiates apoptotic and necrotic cell death (Kravenskaya and Fedirko, 2011). Cobalt ions can directly induce DNA damage, interfere with DNA repair, DNA–protein crosslinking and sister chromatid exchange (Valko et al., 2005). The exact mechanism for cobalt carcinogenicity remains to be elucidated but it has been established that cobalt-mediated free radical generation contributes to the toxicity and carcinogenicity of cobalt (De Boeck et al., 2003).

1.2.1.5 Metal ion levels in patients with CoCr hip implants

Circulating physiological levels of cobalt and chromium are normally $<0.25\mu\text{g/l}$ ($0.005\mu\text{M}$). Elevated levels of cobalt and chromium ions occur in both the hip synovial fluid and in peripheral blood after MoM hip replacement (Andrews et al., 2011). Currently, whole blood is the most commonly used sample to monitor Co and Cr levels in the body (Liu et al., 2011). In blood, metal ions are transported both in the plasma and within the blood cells. In the case of chromium, it has been shown

that the ions are readily taken up by red blood cells causing variability in the ratio of metal in the intra- and extracellular compartments (Merritt and Brown, 1995). The concentration of metal ions in the serum corresponds only to the extracellular component. Therefore, determination of whole blood concentrations is a better measure of systemic exposure to metal ions (Daniel et al., 2007b).

There is concern about the toxicity and biological effects of such ions both locally and systemically since increased Co and Cr ion levels in blood have been reported in patients with CoCr implants (Clarke et al., 2003, Dunstan et al., 2005, Daniel et al., 2007a, Antoniou et al., 2008, Tkaczyk et al., 2010b, Bisseling et al., 2011, Lavigne et al., 2011, Friesenbichler et al., 2012, Penny et al., 2013). Moreover, there have been cases of particularly high blood ion concentrations. Wretenberg (2008) reported high concentrations of Co (22.92 $\mu\text{g/l}$) and Cr (19.43 $\mu\text{g/l}$) in blood from a patient with a McKee–Farrar MoM hip prosthesis after 37 years of implantation. Similarly, Fritzsche et al., (2012) reported high whole blood ion levels of Co (138 $\mu\text{g/l}$) and Cr (39 $\mu\text{g/l}$) in a 41-year-old patient with bilateral MoM Birmingham Hip Resurfacing (BHR) implants 3 months after surgery.

Several studies have been carried out to investigate the levels of metal ions release from well-functioning as well as failed MoM hip implants. As a result, a wide range of metal ion level values have been reported in whole blood and serum from a wide range of patients (Table 1.3). Higher levels of Co and Cr ions have been measured in blood of patients with MoM hip implants when compared to patients with metal-on-polyethylene (MoP) or ceramic-on polyethylene (CoP) devices (Dunstan et al., 2005, Hart et al., 2006, Rasquinha et al., 2006, Antoniou et al., 2008, Malviya et al., 2011, Moroni et al., 2012). Furthermore, elevated Co and Cr ion levels in blood and high wear volumes have been associated with pain (Davda et al., 2011, Hart et al., 2009, Langton et al., 2010) pseudotumors (Matthies et al., 2012, Hasegawa et al., 2012, Kwon et al., 2011), and implant failure (Hart et al., 2011, Davda et al., 2011, Hart et al., 2010).

Table 1.3 also shows that higher levels of Co ions, when compared to Cr, are generally measured. Cobalt corrodes faster than chromium under physiological conditions (Xia et al., 2011b) and, opposite to Cr, Co ions tend to remain mobile, which is reflected in the higher levels measured in blood, allowing them to reach remote organs (Afolaranmi et al., 2012). Elevated Co concentrations in patients with MoM implants are a concern, since increased cobalt levels in blood have also been reported to be associated with neurological (hand tremor, incoordination, cognitive decline, depression, vertigo, hearing loss, and visual changes) (Oldenburg et al., 2009, Tower, 2010), cardiac (myocardiopathy) (Gilbert et al., 2013, Dadda et al., 1994, Seghizzi et al., 1994) and endocrine (Keegan et al., 2007, Oldenburg et al., 2009) symptoms. Oldenburg et al. (2009) reported a case of severe cobalt intoxication due to prosthesis wear of a total hip arthroplasty. In this case a 55-year-old man developed hypothyroidism, peripheral neuropathy, and cardiomyopathy related to the deterioration of the metal femoral head and a Co concentration in blood of 625µg/l. Table 1.4 summarises the range of metal ions and metal particles typically measured in human body fluids and tissue with and without MoM replacements.

In addition to the above, data from the seventh annual report of the National Joint Registry for England and Wales showed high failure rates for MoM hip prostheses, which led to the market recall of the DePuy ASRTM, both the Resurfacing and XL Systems in August 2010 (DePuy International Ltd, Leeds, UK) (MDA/2010/069). Following this, the Medicines and Healthcare products Regulatory Agency (MHRA) safety alert in September 2010 drew attention to the long term biological safety of all types of MoM hips. In this document the MHRA explained the details behind the safety alert and included four situations in which measurement of blood metal ions in patients were recommended: 1) in patients who have symptoms associated with loose MoM bearings; 2) in patients showing radiological features associated with adverse outcomes including component position or small component size; 3) if the patient or surgeon are concerned regarding the MoM bearing; and 4) if there is concern about patients with higher than expected rates of failure. The MHRA have suggested that combined whole blood cobalt and chromium levels of greater than 7ppb (7µg/l) are

associated with significant soft-tissue reactions and failed MoM hips (MDA/2010/069).

Table 1.3. Metal ion levels measured in body fluids from patients with MoM hip replacements							
Author, date	Implant	Body fluid	Follow up	Mean concentration (µg/l)			
						Co	Cr
Clarke et al. (2003)	Birmingham hip resurfacing (BHR), Cormet 2000 (THA), both MoM	Serum	Median time 16 months	Resurfacing		2.24*	2.76*
				THA		1.30*	0.99*
Lhotka et al. (2003)	Metasul, SIKOMET-SM2, both MoM THA	Whole blood	42-48 months	Control	nanograms of element per gram of dry sample weight	0.70ng/g	0.21ng/g
				Metasul	immediate postoperative period	3.23ng/g	7.78ng/g
					42-48 months	16.95ng/g	25.62ng/g
				SIKOMET-SM21	immediate postoperative period	8.13ng/g	14.27ng/g
42-48 months	27.66 ng/g	36.35ng/g					
Dunstan et al. (2005)	THA MoM, MoP	Whole blood	Mean of 30 years	Control (no implants)		0.69ng/g	2.18ng/g
				MoP		0.48ng/g	2.00ng/g
				MoM revised to MoP		0.65ng/g	2.16ng/g
				MoM radiologically stable		1.97ng/g	2.17ng/g
				MoM radiologically loose		35.50ng/g	2.70ng/g
Hart et al. (2006)	THA MoP, MoM	Whole blood	Up to 60 months	MoP		2.48	0.28
				MoM		4.18	1.78
Iavicoli et al. (2006)	THA MoM	Serum	Mean of 15.3 months	Patients		14.00	2.88
				Controls		3.46	1.47

Table 1.3. Metal ion levels measured in body fluids from patients with MoM hip replacements						
Author, date	Implant	Body fluid	Follow up	Mean concentration (µg/l)		
					Co	Cr
Rasquinha et al. (2006)	THA MoM, CoP (ceramic-on polyethylene)	Serum	Minimum of 5 years	CoP	0.20	0.08
				MoM	2.35	3.48
Witzleb et al. (2006)	BHR (Resurfacing), Metasul (THA), both MoM	Serum	2 years	THA	1.70	1.22
				Resurfacing	4.28	5.12
				Control (implant free)	0.25*	< 0.25*
Daniel et al. (2007a)	MoM resurfacing	Whole blood	Up to 4 years	Pre-op	0.20	0.30
				1 year	1.30	2.40
				4 years	1.20	1.10
Grubl et al. (2007)	MoM THA	Serum	Minimum of 10 years	Median	0.75	0.95
Ziaee et al. (2007)	MoM resurfacing	Whole blood	Mean of 53 months	Control	0.34	0.20
				Patients	1.39	1.28
Antoniou et al. (2008)	MoM (THA and resurfacing), MoP (THA)	Whole blood	1 year	Control	1.75	0.05
				MoM THA	2.60	0.60
				MoM resurfacing	2.40	0.50
				MoP THA	1.65	0.05
De Haan et al. (2008)	MoM resurfacing	Serum	Mean of 3.4 years	steep (component abduction $\geq 55^\circ$)	9.80	9.70
				non-steep (component abduction $< 55^\circ$)	2.40	3.60
Wretenberg (2008)	MoM THA (Case report)	Whole blood	37 years		22.92	19.43
Hart et al. (2009)	Painful MoM resurfacings	Whole blood	median of 27 months	Unilateral	4.50*	3.00*
				Bilateral	10.60*	7.90*

Table 1.3. Metal ion levels measured in body fluids from patients with MoM hip replacements						
Author, date	Implant	Body fluid	Follow up	Mean concentration (µg/l)		
					Co	Cr
Lazennec et al. (2009)	MoM THA	Serum	9 years	Unilateral	1.55	1.49
				Bilateral	2.03	2.99
Hart et al. (2010)	Failed MoM resurfacing	Whole blood	Mean 51 months		112.64	61.71
Langton et al. (2010)	MoM resurfacing (ASR, BHR)	Whole blood	minimum of 12 months	ASR	2.74*	4.16*
				BHR	1.80*	4.19*
				Adverse reactions	69.00	29.30
Davda et al. (2011)	Symptomatic MoM, both THA and resurfacing	Synovial fluid	Mean of 36 months	Unexplained pain	1127.00*	1337.00*
				Defined cause of failure	1014.00*	1512.00*
Hart et al. (2011)	MoM, both THA and resurfacing	Whole blood	39-42 months	Failed	6.90*	5.00*
				Well-functioning	1.70*	2.30*
Kim et al. (2011)	MoM resurfacing	Serum	2 years	Pre-op	0.11	0.23
				2 years	1.79	2.70
Kwon et al. (2011)	Asymptomatic pseudotumors MoM resurfacing	Serum	Mean of 61 months	Control (MoP THA)	0.60	0.50
				Non-pseudotumor	1.90*	2.10*
				Pseudotumor	9.20*	12.00*
Malviya et al. (2011)	MoM, MoP, THA	Whole blood	2 years	MoM	5.21	2.78
				MoP	1.61	0.79
Fritzsche et al. (2012)	bilateral MoM resurfacing followed by unilateral MoM THA (Case report)	Whole blood, aspirate of pseudotumor	3 months after revision surgery	Blood	138.00	39.00
				Aspirate of pseudotumor	258.00	1011.00
Hasegawa et al. (2012)	MoM THA	Serum	2 years	Pre-op	0.30	0.20
				Well-functioning	2.30	1.60

Author, date	Implant	Body fluid	Follow up	Mean concentration ($\mu\text{g/l}$)			
					Co	Cr	
Matthies et al. (2012)	MoM, both THA and resurfacing	Whole blood	Median of 39 months	No pseudotumor	2.9	3.2	
				Pseudotumor	11.0	6.7	
Moroni et al. (2012)	MoP, MoM THA	Serum	Minimum of 18 months	MoP	Males	0.84	0.59
					Females	0.7	0.44
				MoM	Males	4.26	1.28
					Females	5.76	4.12

Table 1.3. Metal ion levels measured in body fluids from patients with MoM hip replacements. *Ion concentrations expressed as median values. THA= total hip arthroplasty, MoM= metal-on-metal, MoP= metal-on-polyethylene.

Human body fluids		Co ($\mu\text{g/l}$)	Cr ($\mu\text{g/l}$)
Serum	Control	0.20-3.46	0.15-1.47
	Well-functioning TJA	1.55-5.76	0.99-4.12
	Failed TJA	9.20	12.00
Synovial fluid	Control	5.00	3.00
	Well-functioning TJA	588.00	385.00
	Failed TJA	1127.00	1512.00
Whole blood	Control	0.20-2.48	0.28-4.00
	Well-functioning TJA	1.80-5.21	0.60-4.19
	Failed TJA	4.50-138	3.00-61.71
		Particle wear concentrations	
Peri-implant tissue		67.00mg-48.10g	

Table 1.4. Typical Concentrations of Metal in Human Body Fluids and in Human Tissue with and Without MoM Total Joint Replacements. Control: subjects without any MoM prosthesis (Matziolis et al., 2003, (Kempf and Semlitsch, 1990, Sargeant and Goswami, 2007, Hallab and Jacobs, 2009).

1.3 Immune response

Table 1.3 summarised part of the evidence demonstrating that blood cobalt and chromium ion levels are elevated in patients with MoM devices, which may lead to adverse immunological and cellular responses. In order to understand the biomaterial-tissue reactions following metal debris and ion release after hip arthroplasty, a broad overview of the immune system is given in this section.

The principal functions of the immune system are the recognition with subsequent elimination of foreign antigens, formation of immunologic memory, and development of tolerance to self-antigens (Luckheeram et al., 2012). The body is primarily protected from foreign invasion by the innate immune system, which is geared towards discriminating between self and alien/abnormal molecular patterns and mounting the first set of inflammatory and defence responses (Stow et al., 2009, Lucarelli et al., 2004).

An important feature for long-term survival and function of biomaterials is that they do not elicit a detrimental immune response. The foreign body reaction is the primary reaction of the nonspecific immune system that is evoked by the implantation of foreign materials (Luttikhuisen et al., 2006). *In vivo*, the initial responses are acute and chronic inflammation characterized by monocytes and lymphocytes, respectively (Brodbeck et al., 2005). Host response to a prosthesis or prosthetic debris results in the formation of a fibrous synovial-like membrane surrounding the prosthesis (Wang et al., 1996). This membrane consists predominantly of fibroblasts, macrophages, and endothelial cells and actively degrades the adjacent bone by the concerted action of the different cell types. A variety of factors, such as mechanical loading, may contribute to the formation of this membrane. However, little is known about the early phases of formation and it is considered to be a foreign body reaction initiated by wear debris particles from the prosthesis (Pap et al., 2001). A greater number of macrophages has been found in the interface membrane of patients with osteolysis compared to patients without osteolysis (Wang et al., 1996). It is believed that mononuclear phagocytic cells in the

pseudomembrane surrounding the implant phagocytose wear particles and become activated. This activation results in the release of pro-inflammatory cytokines, such as interleukin (IL) 6 (IL-6), tumour necrosis factor α (TNF- α), and inflammatory mediators, such as prostaglandin E₂ (PGE₂), which stimulate osteoclastic bone resorption (Ingham et al., 2000).

1.3.1 Monocytes and macrophages

Monocytes derive from the myeloid progenitor cells in the bone marrow (Hume, 2006). They circulate through the blood and lymphatic system and are recruited to sites of tissue damage and infection (Geissmann et al., 2010). Circulating monocytes give rise to a variety of tissue resident macrophages throughout the body, as well as to specialized cells such as dendritic cells (DCs) and osteoclasts (Gordon and Taylor, 2005). Pro-inflammatory, metabolic and immune stimuli elicit increased recruitment of monocytes to peripheral sites, where differentiation into macrophages and DCs occurs, contributing to host defence and tissue remodelling and repair (Geissmann et al., 2010).

Tissue macrophages have a broad role in the maintenance of tissue homeostasis, through the clearance of senescent cells and the remodelling and repair of tissues after inflammation (Gordon and Taylor, 2005). Macrophages are among the first innate immune cells recruited to a site of invasion, and to come into contact with foreign agents (Stow et al., 2009, Lucarelli et al., 2004). They are equipped with a broad range of pathogen-recognition receptors that make them efficient at phagocytosis (Geissmann et al., 2010) and induce production of inflammatory cytokines to recruit and activate other cells to initiate adaptive immune responses (Aderem and Ulevitch, 2000).

Macrophages become classically activated by exposure to two signals: response to interferon γ (IFN γ), which primes macrophages for activation, and Toll like receptor (TLR) ligation, which results from exposure to a microbe or microbial product such as lipopolysaccharides (LPS) (Mosser, 2003, Mantovani et al., 2002). Classical

macrophage activation gives rise to effector cells, usually referred to as M1, which kill microorganisms and tumour cells and produce inflammatory cytokines including IL-1 and TNF α (Lucarelli et al., 2004, Mantovani et al., 2004). On the other hand, IL-4 and IL-13 induce a distinct activation program, referred to as ‘alternative activation’, or M2 macrophages (Mantovani et al., 2004, Mantovani et al., 2002, Gordon and Martinez, 2010, Martinez et al., 2009), which tune inflammatory responses and adaptive T lymphocyte responses, allergy, immunoregulation, killing and encapsulation of parasites, matrix deposition and remodelling (Mantovani et al., 2004).

Macrophages that attach and recognize a foreign material show typically a classically activated phenotype secreting inflammatory cytokines, ROS, and degradative enzymes and displaying high phagocytic capacity (Xia and Triffitt, 2006). Macrophage phagocytosis of wear debris from joint replacement components is thought to be a crucial step in the pathogenesis of osteolysis and aseptic loosening. In addition to this, it has been suggested that biomaterial-adherent macrophages secrete cytokines that could attract and activate circulating T-lymphocytes, including IL-1 β , TNF α , IL-6, and IL-8 (Figure 1.5) (Brodbeck et al., 2005).

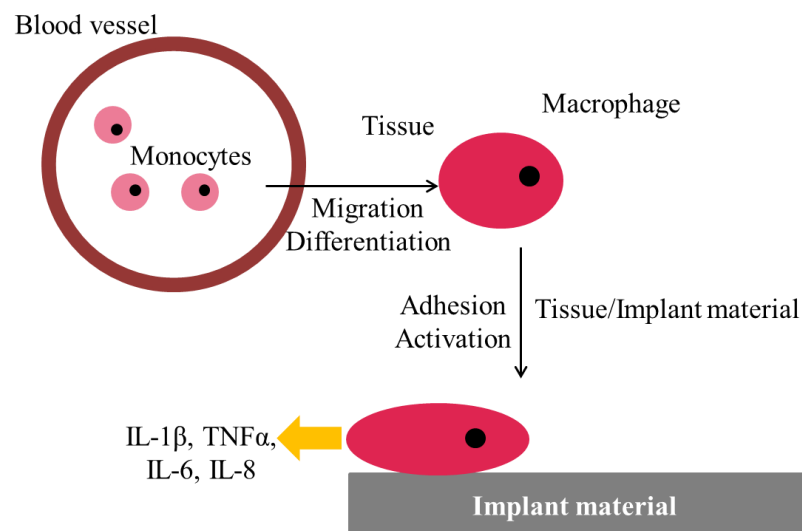


Figure 1.5. Schematic of the transition from blood-borne monocyte to biomaterial adherent monocyte/macrophage at the tissue/implant material interface.

1.3.1.1 U937 cells

The U937 cell line originated from a human histolytic lymphoma, possessing immature pro-monocytic characteristics, and is believed to retain the capacity to differentiate into monocytes/macrophages by various inducers such as PMA (phorbol 12-myristate 13-acetate) (Chabot et al., 2001), TPA (12-O-tetradecanoylphorbol-13-acetate), VD3 (1, 25-dihydroxyvitamin D3), retinoic acids, DMSO and IFN γ (Wang et al., 2011). It has been shown that U937 cells have comparable responses to polyethylene particles (Matthews et al., 2001) and metal ions (Wang et al., 1996, Petit et al., 2004b) to primary macrophages in terms of cytokine release.

Wang et al. (1996) evaluated the effects of titanium, cobalt and chromium ions, at concentrations ranging from 0.01 to 100ng/ml, on the release of bone-associated cytokines (IL-1 β , IL-6, TNF- α , and TGF- β 1) by primary human blood monocytes/macrophages and monocyte-like U937 cells upon lipopolysaccharide (LPS) stimulation. They also investigated the effects on cell viability and cell proliferation *in vitro*. They obtained comparable responses between human blood monocytes/macrophages and monocyte-like U937 cells and demonstrated that the three metal ions modulate cytokine release and cell proliferation *in vitro*. Specifically, their results show that the metal ions significantly enhanced the production of the bone-resorbing cytokines IL-1 β , IL-6, and TNF- α and the proliferation of monocytes/macrophages. On the other hand, these metal ions inhibited the production of the bone-forming cytokine TGF- β 1 after 24h of exposure.

In addition, a number of macrophage cell lines have been used to study the effects of prosthesis wear debris, e.g. murine cell lines J774, P388D1, and IC-21 (Glant and Jacobs, 1994, Shanbhag et al., 1994, Jones et al., 2006, Voronov et al., 1998, Schwab et al., 2006). However, the response of these cells has not been fully validated in comparison to primary macrophages or monocytes. Factors such as cell maturity or the stage of differentiation, or the species or donor tissue from which the cells were derived, could potentially affect their response (Matthews et al., 2001). All these led Matthews et al. (2001) to compare the response of three human cell lines of

monocytic lineage (Monomac-1, THP-1, and U937) challenged with polyethylene particles of known size and dose in order to identify a suitable model cell line for *in vitro* studies of cell-particle interactions. In this study, Monomac-1 cell line failed to synthesize osteolytic mediators in response to polyethylene particles. Furthermore the response of the THP-1 cells was shown to be very irregular. Whilst THP-1 cells were unresponsive to challenge with the 7.2 μm particle fraction they responded both to the very large particles (88 μm) at a ratio of 10mm³ per cell and to the other particle sizes at concentrations as low as 0.1 μm^3 particles per cell. Only the response of the U937 cell line was comparable to that of primary macrophages.

The human U937 macrophage-like cells have been chosen as the cell culture model in previous studies into the effects of different kinds of metals, particles, and ions. This cell line has also been chosen to study immune and molecular responses caused by prosthesis wear particles and ions by several authors. For example, Iwama et al. (2001) examined the effects of As₂O₃ on the activities of mitogen-activated protein (MAP) kinases, intracellular pH, and the production of reactive oxygen species in U937 cells to clarify the mechanism of induction of apoptosis in tumour cells by arsenic trioxide (As₂O₃). Ingham et al. (2000) compared the osteolytic potential of wear debris generated from different formulations of bone cement, used in total hip arthroplasty, in mononuclear phagocytes (U937 cells) *in vitro*. Similarly, Howling et al. (2003) investigated cytotoxic effects on U937 cells of the wear debris from carbon-based composite acetabular cup materials articulating against alumina ceramic femoral counterfaces. Germain et al. (2003) compared the effects cobalt–chromium and alumina ceramic wear particles at various doses on the viability of U937 cells. All these investigations illustrate how U937 cells have been selected to study an array of effects of wear debris particles of different nature.

Additionally, human macrophages (PMA-differentiated myelomonocytic U937 cells) were exposed *in vitro* to increasing concentrations of TiO₂, SiO₂, ZrO₂, or Co nanoparticles (up to 400 $\mu\text{g}/10^6$ cells), and their inflammatory response examined as the expression of TLR receptors and co-receptors, and cytokine production (Lucarelli et al., 2004). Tkaczyk et al. (2010a) studied the effect of chromium and cobalt ions

on the expression of antioxidant enzymes in U937 cells. Raghunathan et al. (2010) exposed FFC cell line and U937 cell line to 0, 0.05, 0.1, and 0.5 μ M Cr⁶⁺ continuously for 3 weeks and studied the changes in protein expression. These studies contribute to the body of evidence showing that the human U937 macrophage-like cells have been widely used as a cell culture model to investigate the effects and mechanisms of toxicity of a range of particles and ions. U937 cells are an alternative to isolating a pure population of monocytes/macrophages from human peripheral blood mononuclear cells, which could result in a mixed cell population. Moreover, they resemble macrophage behaviour *in vivo*, which are the main cells present in peri-prosthetic tissues that engulf foreign bodies by phagocytosis. Table 1.5 shows a compilation of investigations showing the U937 cell line as a model for studying the biological response to wear debris and ions.

Table 3.1. Studies of the effects of wear debris and ions derived from various materials on U937 cells		
Author	Aim/Treatment	Summary of Results
Wang et al. (1996)	Monocytes/macrophages were exposed to titanium, chromium or cobalt in vitro, and the production of IL-1 β , IL-6, TNF α and TGF- β 1 by the cells upon stimulation with lipopolysaccharide (LPS). This was done in order to test the hypothesis that soluble metals could modulate cytokine release by activated monocytes/macrophages.	The release of IL-1 β was enhanced by titanium, chromium and cobalt, the release of TNF- α by titanium and chromium, and of IL-6 by titanium. All three metal ions inhibited the release of TGF- β 1. Titanium and chromium, but not cobalt, enhanced blood monocyte/macrophage proliferation in response to LPS while only titanium enhanced U937 cell proliferation in response to LPS. The metals in concentrations ranging from 0.01 to 100ng/ml did not stimulate the cells to secrete detectable cytokines in the absence of LPS. The metals did not reduce cell viability and induce cell injury after 72 h incubation with the cells. The data suggest that the three metals at clinically relevant concentrations modulated cytokine expression, whereas they did not induce any cytotoxic effects.
Ingham et al. (2000)	Cement debris particles were co-cultured with U937 cells at two particle volume (μm^3) to cell number ratios of 10:1 and 100:1.	None of the cement particles tested at a ratio of 10 μm^3 particles/macrophage had any effect on IL-1, TNF- α or IL-6 production by the cells. When tested at the higher ratio of 100 μm^3 particles/macrophage, the cells were activated and released osteolytic cytokines. All seven cement debris types stimulated high levels of TNF- α and there were no statistically differences between the levels generated for each cement debris type. The levels of IL-6 and IL-1 β generated by macrophages in response to cement debris were considerably lower than the levels of TNF- α .
Matthews et al. (2000)	Particles with mean sizes of 0.24, 0.45, 1.71, 7.62 and 88 μm were co-cultured with cells for 24 hours prior to assessment of cell viability and production of the osteolytic mediators IL-1beta, IL-6, TNF α and, in supernatants from murine phagocytes, PGE2 and GM-CSF. All particle fractions were evaluated at particle volume (μm^3) to cell number ratios of 10:1 and 100:1 (and, additionally, 0.1:1 and 1:1 for U937 cells).	Although the results for the cell line were highly variable, stimulation with phagocytosable particles (range 0.1 to 15 μm) resulted in enhanced levels of cytokine secretion by both murine macrophages and U937 cells. The most biologically active particles were sub-micrometre in size. However, U937 cells responded to wear debris at much lower particle volume to cell number ratios (>0.1 μm^3 per cell) than the murine cells (> 10 μm^3 per cell). No GM-CSF was produced by particle or LPS stimulated murine macrophages. Similarly, U937 cells failed to secrete any IL-1 β . Neither macrophage population responded to stimulation with the largest (88 μm) particles.
Matthews et al. (2001)	The response of three human monocytic cell lines (Monomac-1, U937 and THP-1) to challenge with polyethylene particles of known size and dose was evaluated. Particles with a mean size of 0.21, 0.49, 4.3, 7.2, and 88 μm were co-cultured with the cells for 24 hours prior to the assessment of cell viability and production of the pro-inflammatory cytokines, IL-1 β , IL-6 and TNF α .	Only the response of the U937 cell line was demonstrated to be comparable to that of primary macrophages. Particle volume to cell number ratios of 10:1 or greater significantly enhanced levels of cytokine secretion with particles within the phagocytosable size range (0.1 to 10 μm) being the most biologically active.

Table 3.1. Studies of the effects of wear debris and ions derived from various materials on U937 cells		
Author	Aim/Treatment	Summary of Results
Germain et al. (2003)	The cytotoxicity of cobalt-chromium and alumina ceramic wear particles was compared to commercially available cobalt–chromium ($9.87 \pm 5.67\mu\text{m}$) and alumina ceramic ($0.503 \pm 0.19\mu\text{m}$) particles. The effects of the particles on the cells over a 5 day period at different particle volume (μm^3) to cell number ratios were tested and viability determined using ATP-Lite™.	Clinically relevant CoCr particles 50 and 5mm^3 per cell reduced the viability of U937 cells by 97% and 42% and reduced the viability of L929 cells by 95% and 73%, respectively. At 50mm^3 per cell, the clinically relevant ceramic particles reduced U937 cell viability by 18%. None of the other concentrations of the clinically relevant particles were toxic. The commercial CoCr and alumina particles did not affect the viability of either the U937 or the L929 cells.
Howling et al. (2003)	The effects on cell viability of the carbon–carbon composite material P25-CVD on U937 cells.	Culture of P25-CVD with U937 cells at all the particle-volume to cell-number ratios tested had no significant effect when compared to the cell-only controls and gave results very similar to the latex-bead controls.
Shardlow et al. (2003)	The aim was to generate particulate wear debris from a simulated stem-cement interface under sterile conditions. This debris was then co-cultured with U937 cells and the response measured by immunoassay of four of the cytokines implicated in the pathogenesis of periprosthetic osteolysis.	Polymethylmethacrylate (PMMA) pins containing different radiopaque additives, 9.2% barium sulphate (CMW 1; DePuy) and 15.6% zirconium dioxide (Palacos R; Schering-Plough, Welwyn, UK), were tested in sliding wear tests against a stainless-steel counterface with the Vaquasheen surface finish. Both cements stimulated the release of pro-osteolytic TNF α from the U937 monocytic cell line, in a dose-dependent fashion. There was a trend towards greater TNF α release with Palacos cement than CMW cement at the same dose. Palacos particles also caused significant release of IL-6, another pro-osteolytic cytokine, while CMW did not. The particulate cement debris produced did not stimulate the release of GM-CSF or IL1 β from the U937 cells. These results may explain the cytokine pathway responsible for bone resorption caused by particulate PMMA debris.
Williams et al. (2003)	The aim of this study was to examine the wear particles produced from thick ($>10\ \mu\text{m}$) surface engineered coatings: TiN, CrN or CrCN articulating with a CoCr alloy substrate. Surface engineered coatings were articulated against themselves in a simple geometry model. The wear particles generated were characterized by TEM and the cytotoxic effect on U937 macrophage and L929 fibroblast cells assessed.	The CrN and CrCN coatings showed a decrease in wear compared to the CoCr bearings and produced small (less than 40 nm in length) wear particles. The wear particles released from the surface engineered bearings also showed a decreased cytotoxic effect on cells compared to the CoCr alloy debris.

Table 3.1. Studies of the effects of wear debris and ions derived from various materials on U937 cells		
Author	Aim/Treatment	Summary of Results
Lucarelli et al. (2004)	PMA-differentiated U937 cells were exposed to non-toxic concentrations of TiO ₂ , SiO ₂ , ZrO ₂ , or Co nanoparticles, and the expression of TLR receptors and co-receptors, and cytokine production was examined.	Exposure to nanoparticles of ZrO ₂ upregulated expression of viral TLR receptors TLR3 and TLR7. TiO ₂ and ZrO ₂ nanoparticles also increased expression of TLR10. On the other hand, TLR9 expression was decreased by SiO ₂ nano-particles, and expression of the co-receptor CD14 was inhibited by Co nanoparticles. SiO ₂ nanoparticles induced production of inflammatory cytokines IL-1 β and TNF- α . Other ceramic nanoparticles had little influence on cytokine production, either in resting macrophages, or in LPS-activated cells. Generally, Co nanoparticles had an overall pro-inflammatory by reducing anti-inflammatory IL-1Ra and inducing inflammatory TNF- α .
Petit et al. (2004a)	The purpose of this study was to analyze the effect of Co ²⁺ and Cr ³⁺ ions on the expression of bcl-2, bax, caspase-3 and caspase-8 to better understand the mechanisms leading to ion-induced apoptosis in macrophages.	Co ²⁺ ions inhibited bcl-2 expression with significant effect (p<0.05) after 16 h and a maximal 52% inhibitory effect after 24 h. Co ²⁺ stimulated bax expression with a significant stimulation (p<0.05) after 8 h and a maximal 1.75-fold increase after 16 h. Co ²⁺ also stimulated the expression of the active fragment of caspase-3 as well as caspase-3 activity, with maximal increase after 24 h. Co ²⁺ ions had no effect on caspase-8 expression or activity. Cr ³⁺ ions inhibited bcl-2 expression with significant effect (p<0.05) after 16 h and a maximal 43% inhibitory effect after 24 h. Cr ³⁺ stimulated bax expression showed significant stimulation (p<0.01) after 8h and a maximal 2.25-fold increase after 24 h. Cr ³⁺ ions also stimulated the expression of the active fragments of caspase-3 and -8, as well as the activities of both proteases. The effect of Cr ³⁺ ions on the expression of both caspase active fragments was maximal after 16 h incubation.
Yagil-Kelmer et al. (2004)	The goal of this study was to compare the effect of two sizes of alumina ceramic particles, 0.5 and 1.5 μ m, on the cellular response of both U937 cells and primary human blood monocytes obtained from healthy volunteers. The cellular response was measured by quantifying gene expression of 12 cytokines using TaqMan RT-PCR.	Particle to cell ratio of 100:1, 0.5 μ m ceramic particles provoked higher amounts of IL-1 α , IL-1 β , IL-8, IL-10 and TNF- α steady state mRNA by U937 cells. Higher variability of cytokine expression in primary blood monocytes compared to the cell line, however, a similar trend was observed. A differential response to ceramic particle size was shown, which may imply that 0.5 μ m particles are less biocompatible.
Luo et al. (2005)	The effects of Co ²⁺ and Cr ³⁺ ions were examined on the expression of genes encoding MMP-1, one of the principal proteinases capable of degrading native fibrillar collagens in the extracellular matrix (ECM), its inhibitor TIMP-1, and TNF- α . Human U937 macrophages were incubated in suspension or on phosphorylcholine (PC)-polymer coated surfaces for 24h with Co ²⁺ and Cr ³⁺ ions.	Both Co ²⁺ and Cr ³⁺ ions induce the expression of MMP-1, TIMP-1, and TNF- α mRNA in a dose-dependent manner in cell suspensions. Tyrosine kinase inhibitors have different effects on these stimulatory effects. Indeed, genistein has only partial inhibitory effect on MMP-1 and TIMP-1, with even less effect on TNF- α expression. In contrast, herbimycin A completely blocks MMP-1 and TNF- α while partially inhibiting TIMP-1. However, Co ²⁺ and Cr ³⁺ ions had no effect on the expression of MMP-1 and TIMP-1 in macrophages cultured on the PC-polymer, suggesting that the attachment of U937 macrophages to the PC-polymer surfaces may modify their gene expression. These findings indicate that activation of MMP-1, TIMP-1, and TNF- α by Co ²⁺ and Cr ³⁺ ions is regulated by tyrosine kinases.

Table 3.1. Studies of the effects of wear debris and ions derived from various materials on U937 cells		
Author	Aim/Treatment	Summary of Results
Petit et al. (2005)	To investigate the putative modification of the cellular redox state by metal ions from MM prostheses, the study examines the effect of Co ²⁺ and Cr ³⁺ ions on protein oxidation in U937 cells.	Co ²⁺ and Cr ³⁺ ions induced a time- and dose-dependent protein oxidation reaching 6.5 and 2.9 times the control after 72 h, respectively, which were inhibited by the antioxidant glutathione monoethyl-ester. The oxidized proteins are mainly found in the cytoplasmic fraction of the cells and are absent from the nucleus.
Petit et al. (2006b)	To better understand the cellular effect of wear particles and metal ions, the aim was to investigate the effect of Co ²⁺ and chromium Cr ³⁺ ions, as well as UHMWPE and Al ₂ O ₃ particles, on the nitration of proteins in U937 cells.	Results showed that Co ²⁺ and Cr ³⁺ ions induced the nitration of a 79 ± 4kDa proteins in a time- and dose-dependent manner. The stimulation was significant (p < 0.05) after 24 h with 10 ppm Co ²⁺ and reached a plateau level between 48 and 72 h. With Cr ³⁺ , the stimulation was significant (p < 0.05) only after 48 and 72 h. The effect of both Co ²⁺ and Cr ³⁺ ions was inhibited by glutathione monoethyl-ester that provides protection against oxidative stress. However, ultrahigh-molecular-weight-polyethylene and alumina ceramic particles had no significant effect on the nitration of proteins. The nitrated proteins are mainly found in the cytoplasmic fraction of cells and are absent from the nucleus.
Sylvie et al. (2010)	The biological effects of bone substitutes presented to U937 cells in vitro as micron- or nanometer-sized particles were evaluated. The hydroxyapatite (HA) (550 nm) and beta-tricalcium phosphate (beta-TCP) (550 nm) nanoparticles were incubated with U937 cells, and cell cycle modification, specific antigen expression, and the extent of cell death determined.	Results provide evidence of the absence of cytotoxicity, and show that nanoparticles do not induce more apoptosis than microparticles in U937 cells. Although morphologic evidence of stimulation of U937-cells was found by confocal microscopy, neither bone substitute altered the distribution of the cells into different phases of the cell cycle. The flow cytometry results showed no differences in the expression of adherence and activation markers.

Table 1.5. Studies of the effects of wear debris and ions derived from various materials on U937 cells.

1.3.2 Lymphocytes

The lymphocyte population is mainly made up of the thymus-derived lymphocytes (T-lymphocytes), bone-marrow-derived (B-lymphocytes), and the natural killer cells (NK cells). T-lymphocytes mediating the cellular immunity, along with B lymphocytes mediating humoral immunity, provide adaptive immunity, which work in close collaboration with the innate immune system (Luckheeram et al., 2012).

The T-lymphocytes interact with other cell types by either direct cell-cell interactions or by soluble paracrine mechanisms (Brodbeck et al., 2005). The T-lymphocyte population may be further split into two subclasses, cytotoxic (CD8+) T-cells and T-helper (CD4+) cells. Cytotoxic T-cells interact directly with the target cell usually in response to intracellular invaders, such as viruses. The interactions between CD8+ T-lymphocytes and target cells lead to the induction of target cell apoptosis. On the other hand, CD4+ cells interact with a variety of cell types either directly or through cytokine messengers, inducing a variety of responses depending upon the nature of the original signal and the cytokines released (Luckheeram et al., 2012, Brodbeck et al., 2005).

Activated T lymphocytes at the implant site are assumed to be the source of both IL-4 and IL-13 and have been shown to enhance macrophage fusion to form foreign body giant cells on the surface of implanted biomaterials (Franz et al., 2011, Chang et al., 2009). The presence of lymphocytes surrounding the implant indicates that these cells may be the source driving the fusion and may play a critical role in the foreign body reaction (Anderson, 2009). Additionally, there is evidence of the involvement of lymphocytes in aseptic loosening from studies that correlated metal-specific lymphocyte response to poor implant performance (Hallab et al., 2005) and lymphocytic infiltration around metal-on-metal arthroplasties has also been reported (Davies et al., 2005).

1.3.3 Cytokines

Cytokines are protein, peptide or glycoprotein cell signalling immunomodulatory molecules that are primarily concerned with inter-cellular communication (Goodman and Ma, 2010). They elicit biological responses, including cell activation, proliferation, growth, differentiation, migration, and cytotoxicity (Tarrant, 2010). Cytokines generally have autocrine and paracrine functions, and act via specific cell-surface receptors as part of both the innate and adaptive immune response. When the receptors are activated, the result is a cascade of events leading to downstream signals that alter transcription factors, and up/down-regulation of specific genes. There is great redundancy in cytokine functions; several cytokines often have very similar actions (Goodman and Ma, 2010, Stow et al., 2009).

As mentioned in previous sections of this chapter, after implant stabilization in joint replacement occurs, wear of the bearing surfaces is the major issue limiting longevity of the prosthesis. The presence of wear debris stimulates both local and systemic cellular reactions. Cytokines are released by acute and chronic inflammatory cells and amplify the inflammatory response. The secretory pathways, routes, organelles and molecular machinery that control cytokine secretion must be regulated (Stow et al., 2009); otherwise, these cytokines could intensify the reaction to wear debris in an unfavourable way favouring osteolytic lesions.

1.4 Osteolysis and Aseptic loosening

Aseptic loosening was first recognized in the early 1960s by John Charnley (Archibeck et al., 2001). Osteolysis and subsequent aseptic loosening are the most common causes of failure of total joint replacement (TJR) (Geng et al., 2010). Initially termed “cement disease” and then “particle disease” (Harris, 1994) osteolysis is thought to occur as a host response to a variety of particles that may originate at several locations around a joint replacement (Germain et al., 2003). These locations include the articulating surfaces, modular component interfaces, fixation surfaces, and devices used for adjuvant fixation (Archibeck et al., 2001).

Although the wear volumes produced by MoM articulations have been estimated to be 40–100 times lower than metal-on-polyethylene bearings (Borruto, 2010), the main drawback of a metal articulation is the production of metal debris due to the combined effect of mechanical and corrosive wear (Langton et al., 2011). Current evidence indicates that the size of wear particles generated by MoM articulations is in the nanometre size range (Germain et al., 2003), the average particle size range being 30 to 100 nm in size (Catelas and Wimmer, 2011). The reduced size of nanoparticles allows their entrance into tissues and organs and diffusion throughout the body, and their interaction with different types of cells (Lucarelli et al., 2004).

The progressive loss of bone adjacent to an implant has been attributed to a granulomatous inflammatory reaction induced by particulate implant wear debris at the bone–implant interface (Vasudevan et al., 2012). Metal wear particles stimulate local macrophage and fibroblast recruitment (Gordon et al., 2010). Macrophages are unable to clear such particles because they are non-biodegradable. This results in the accumulation of wear debris in the bone-prosthesis micro-environment potentially leading to a chronic state of inflammation (Vasudevan et al., 2012). In addition, when particles are phagocytosed in sufficient amounts, the macrophages enter an active state of metabolism and release pro-inflammatory cytokines (Table 1.6), including IL-1, IL-6, and TNF α ; chemokines and growth factors that alter the balance of osteoclast and osteoblast activities. This accelerates osteoclast formation and bone resorption resulting in periprosthetic osteolysis (Matsusaki et al., 2007, Gordon et al., 2010). Figure 1.6 illustrates how complex the particle-induced osteolysis process can be.

Cytokine	Main Function
IL-1 α and IL-1 β	Produced by many cell types including macrophages. IL-1 activates macrophages, neutrophils and endothelial cells, stimulates fibroblasts and osteoclasts, and induces prostaglandin E ₂ and collagenase synthesis.
IL-6	Produced by macrophages, T cells, fibroblasts and other cell types. It activates T and B cells and induces B cells to differentiate and secrete immunoglobulins. It also stimulates bone resorption by recruiting mature osteoclasts and by activating them through an autocrine mechanism.
TNF α	Produced by activated lymphocytes, monocytes, macrophages and other cells. It stimulates fibroblasts and granulocytes. It stimulates bone resorption by enhancing the recruitment and the activation of osteoclasts
IFN γ	Produced by T cells, macrophages, and dendritic cells. It stimulates macrophages inducing direct antimicrobial and antitumor mechanisms as well as up-regulating antigen processing and presentation pathways. It enhances activated killer cells, orchestrates leukocyte attraction and directs growth, maturation, and differentiation of many cell types.

Table 1.6. Pro-inflammatory cytokines. Main pro-inflammatory cytokines reported to be produced at the peri-implant tissues related to osteolysis and aseptic loosening (Goodman and Ma, 2010, Valles et al., 2006, Schroder et al., 2004, Fiorito et al., 2003).

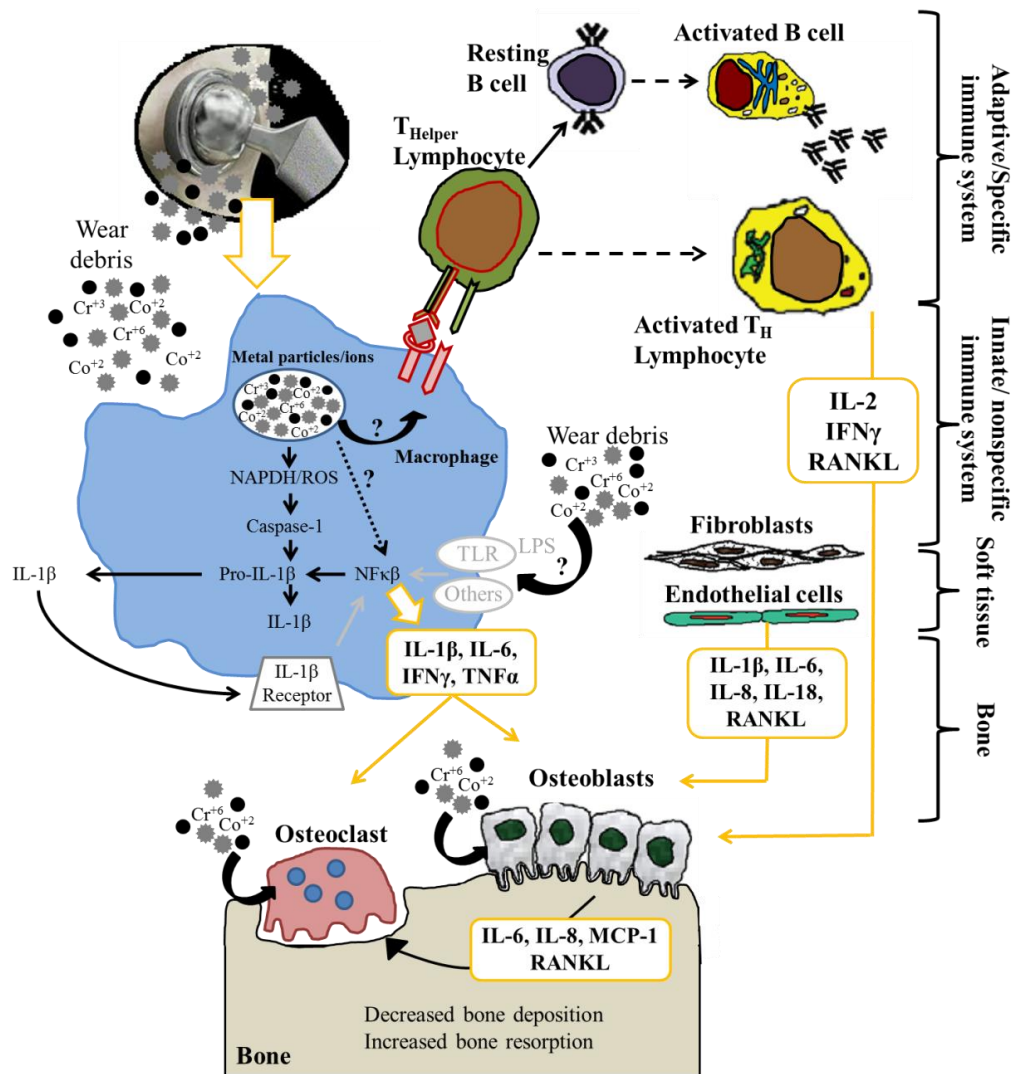


Figure 1.6. Schematic diagram of the debris-induced inflammation process. Process is mainly mediated by macrophages, where macrophages ingest debris which results in the release of cytokines causing inflammation and acceleration of osteoclast formation. NADPH: nicotinamide adenine dinucleotide phosphate. ROS: reactive oxygen species. IL-1 β : interleukin 1 β . NF κ B: nuclear factor kappa-B. IL-6: interleukin 6. IL-8: interleukin 8. IL-2: interleukin 2. IFN γ : interferon γ . TNF α : tumor necrosis factor α . MCP-1: monocyte chemotactic peptide-1. RANKL: Receptor activator of nuclear factor kappa-B ligand. TLR: Toll like receptor; LPS: lipopolysaccharides (adapted from Hallab and Jacobs, 2009).

In a TJR undergoing aseptic loosening, areas of lysis appear around the prosthesis at the bone-prosthesis interface. In the early stages, the condition is often asymptomatic, but as it progresses, the areas of lysis enlarge until the prosthesis becomes mechanically unstable and the patient experiences pain. In the later stages, the localized lysis may compromise bone stock (Atkins et al., 1997). When osteolysis is detected, revision surgery is required in order to avoid bone loss to an extent that would be too difficult to treat later on (Aspenberg et al., 2011).

1.5 Aims of the present study

Despite the success of hip replacements as a treatment for hip diseases, the sections above have summarised the present concern regarding the toxicity of metal particles and ions produced at the articulation site of a MoM implant. In addition to this, metal debris is thought to play an important part in osteolysis and subsequent aseptic loosening, which is the main cause of implant failure. It is essential to determine the potential effects of long-term exposure to metal ions and debris, as well as the implications of revision surgery in terms of metal pre-exposure. As a result, this thesis has been focussed on investigating the interactions of Co ions and metal wear debris with macrophages and lymphocytes, as well as their potential to affect gene expression. It was decided to focus on Co ions due to the potential of high levels of Co reaching remote organs, which poses a risk for multi-organ overexposure and toxicity in MoM hip replacements patients. The objectives of the individual studies comprising the thesis are:

- Assess the toxicity of Co-Cr nanoparticles released from a resurfacing implant and Co ions on U937 cells, an immortalised human monocyte-like cell line, *in vitro*.
- Explore the relationship between changes in gene expression and apoptosis *in vitro* with the release of metal ions derived from incubation with the metal wear debris.
- Assess the toxicity of Co-Cr nanoparticles released from a resurfacing implant and Co ions on primary human lymphocytes.
- Establish a storage protocol for fresh clinical blood samples collected with EDTA tubes from patients with hip implants, that allows extraction of RNA suitable for molecular applications.
- Explore whether *in vivo* gene expression in peripheral blood cells of key genes involved in bone remodelling process is related to circulating whole blood metal ion levels of patients with MoM hip implants.

2. GENERAL METHODS

This chapter contains general methods which were applied in several parts of the thesis. Some more specific methods are detailed in the relevant chapters.

2.1 Cells

The following cell types were used throughout the research:

- U937 cells, a human leukemic pre-monocyte lymphoma cell line (European Collection of Cell Cultures; Wiltshire, UK).
- Primary dendritic cells (DCs), derived directly from mouse bone marrow.
- Primary human lymphocytes, isolated from Buffy Coat (Scottish Blood Transfusion Service; Glasgow, UK) within 5h of preparation from blood samples.

2.1.1 Culturing of U937 cells

U937 cells were chosen for this investigation as they have been shown to have comparable responses to wear debris (Wang et al., 1996, Matthews et al., 2001, Petit et al., 2004b) to primary macrophages in terms of cytokine release. Moreover, these cells were available in the laboratory. Additionally, due to the cost of buffy coat, it was decided not to carry out experiments with primary cells.

U937 cells were cultured in 30ml of complete RPMI-1640 medium in 75cm² culture flasks (TPP; Switzerland) at 37°C, 5% (v/v) CO₂. Complete RPMI-1640 medium consisted of RPMI-1640 (Lonza, Slough, UK) medium supplemented with 10% (v/v) foetal calf serum (FCS), L-glutamine (2mM), penicillin (5000 units), streptomycin (5mg/ml) (all from Life Technologies; Paisley, UK). These cells were routinely split every three days at a ratio of 1:10. This was achieved by taking 3ml of cell suspension into a fresh 75cm² culture flask containing 27ml of fresh complete RPMI-1640 medium.

2.1.2 Activation of U937 cells

Phorbol 12-myristate 13-acetate (PMA) is commonly used to induce U937 cell differentiation into actively phagocytosing macrophages (Hewison et al., 1992, Chabot et al., 2001, Vongsakul et al., 2011, Huang et al., 2001, Boukes and van de Venter, 2012). After PMA exposure, monocytes become adherent and form cell aggregates indicative of differentiation into macrophages (Yagil-Kelmer et al., 2004, Blottiere et al., 1995, Matsusaki et al., 2007). However, different molar concentrations of PMA, ranging from 1nM to 100nM, have been used and the activation process has been reported to take place from 24h up to 5days after PMA exposure (Hewison et al., 1992, Vongsakul et al., 2011, Yagil-Kelmer et al., 2004, Matsusaki et al., 2007, Bainbridge et al., 2001, Lucarelli et al., 2004).

In this study, PMA (Sigma-Aldrich; Dorset, UK) was used to induce U937 cell activation. Three different concentrations of PMA were evaluated in order to determine the most appropriate concentration and exposure time. For this purpose, PMA was diluted to 5 μ M, 10 μ M, and 100 μ M in DMSO (Sigma-Aldrich; Dorset, UK). These concentrations were diluted 1:1000 in culture medium to treat the cells with 5nM, 10nM, and 100nM final concentrations of PMA. Cells were exposed for 5 days checking on adhesion and aggregation every 24 hours. Photos were taking on a Zeiss Imager.Z1 microscope and a Nikon DIAPHOT microscope with a Nikon CoolPix 4500 digital camera.

Each concentration of PMA was incubated in duplicate for each time point. Controls with no PMA were also incubated in duplicate. U937 cells were cultured in 24-well plates at a density of 2×10^5 cells/well. In order to avoid contamination, independent plates were used for each end point and each microscope. The size of the wells of 24-well plates combined with the diameter of the Zeiss microscope lenses restricts the visualisation area to the centre of the well. To be able to visualise the whole area cells were growing on, a sterile cover slip was placed into each of the wells before culturing the cells to be analysed with the Zeiss microscope. Plates were incubated at 37°C under 5% (v/v) CO₂. After 48 hours, 500 μ l of medium (from the initial 1ml)

was carefully removed from the wells and replaced with 1ml of fresh medium with the corresponding PMA concentration.

At each time point, images were taken from wells with a Nikon CoolPix 4500 digital camera using the Nikon microscope; and cover slips using both dry and wet lenses (20X) of the Zeiss microscope. For imaging with the wet lenses, cover slips were carefully washed with PBS before taking them into petri dishes. Then, 2ml of PBS were added to the petri dishes containing the cover slips for microscopy. Additionally, U937 cells were cultured in 96-well plates at a density of 2×10^4 cells/well and were incubated with each concentration of PMA being analysed by MTT assay at each time point. Controls with no PMA were also incubated in triplicate. At each end point, cells were washed with PBS. The MTT reduction assay was carried out as described in Section 2.1.8.

2.1.3 Assessment of activated U937 phagocytosis activity

Polymorphonuclear neutrophils (PMNs) and peripheral blood mononuclear cells (PMNCs), provide the first line of defence of the innate immune system and are commonly referred to as “professional phagocytes” due to their high phagocytic activity (Mesaik et al., 2008, Lunov et al., 2010, Colucci-Guyon et al., 2011). In order to provide evidence that activated U937 cells were capable of phagocytosis, they were incubated with latex beads and images were taken after 1, 2, 3, 4, 5, 24, 48, and 120h.

2.1.3.1 Preparation of Beads

200 μ l of latex bead suspension (carboxylate-modified polystyrene, fluorescent yellow-green- aqua suspension, 2.5% solids, 1 μ m particle size. Sigma-Aldrich; Dorset, UK) were added to 20ml of sterile PBS. 2ml of the bead suspension were then placed in sterile microtubes and centrifuged at 13,000rpm for 10 min. Most of the PBS was then removed, leaving approximately 100 μ l/tube. All beads were then

combined and transferred to a 25cm² tissue culture flask containing 5ml of serum-free RPMI. In order to sterilise the beads, the flask was left under UV light overnight.

2.1.3.2 Addition of beads to cells

It has been suggested that osteoblasts possess the ability to phagocytose particles <1µm in size (Lohmann et al., 2000, Saad et al., 1998, Reilly et al., 1997). Since the latex beads in this experiment are 1µm in size, immortalised rat osteoblast cells were used as controls. The cell line (Ost-5) was produced by transfecting neonatal rat osteoblasts at passage 4 with pUK42, a plasmid (10.9kb) containing the complete sequence of SV40, except for a 6bp deletion at the origin of replication. This plasmid also contains the RSVneo gene which provides Geneticin resistance, and selection of positively transfected cells was by resistance to the antibiotic Geneticin (G418, Gibco) (McKay et al., 1996). Ost-5 cells were seeded at 5x10⁴cells/well for the shorter end points and at 5x10³cells/well for the 48 and 120h end points. Activated U937 cells were seeded at 1x10⁵cells/well in a 24-well plate containing sterile 13mm glass coverslips. Cells were allowed to attach overnight. At this point 100µl of bead suspension was added to each well. Beads were incubated with cells for 1, 2, 3, 4, 5, 24, 48, and 120h in triplicates. At each time point coverslips were removed from the wells, transferred to petri dishes and cells washed gently with PBS. In order to visualise the cells, PI staining was carried out. Since PI is impermeable to intact plasma membranes but penetrates the plasma membrane of dead cells (Bank, 1988), cells were fixed with 4% (v/v) formalin for 20min and washed 3X with PBS. Following fixation, cells were stained with PI for 1min and washed 3X with PBS. 2ml of PBS were added and cells were viewed using a Carl Zeiss Axio Imager microscope under a 40X (numeric aperture of 0.80) water immersion lens. Fluorescence was excited using a mercury lamp and emission recorded using a fluorescein isothiocyanate (FITC)/Rhodamine filter block (485/515-530nm; 546/580-563nm). Digital images and z-stacks were captured and analysed using AxioVision 4.6 software.

2.1.4 Isolation of primary human lymphocytes

Human buffy coat samples were collected on the day of the experiment. All samples had been given by anonymous healthy donors no more than 5h before collection. Peripheral blood mononuclear cells (PBMCs) were isolated by density gradient centrifugation using Histopaque-1077 (Sigma-Aldrich; Dorset, UK) from 60ml of Buffy Coat under sterile conditions. In order to achieve this, 60ml of buffy coat were added to 60ml of serum free RPMI-1640. 30ml of diluted buffy coat were then gently layered onto 15ml of Histopaque-1077 in a 50ml centrifuge tube. The four tubes were then centrifuged at 600xg for 25 minutes, with the brake set to 'off', which allowed four distinct layers to be formed in each tube (Figure 2.1). Once the top layer was removed and discarded, the cellular layer from each tube was aspirated and resuspended in 45ml of serum free RPMI-1640. Cell suspensions were then centrifuged at 250xg for 10 minutes and the supernatant aspirated. This step was repeated twice more. Following this, lymphocyte enrichment was achieved as previously described (Martin-Romero et al., 2000). Briefly, PBMCs (2.5×10^6 cells/ml) were incubated in a 75cm² culture flask with complete RPMI-1640 for 1 hour at 37°C, 5% CO₂. The medium with the non-adherent cell suspension was then transferred to a fresh culture flask and incubated for a further hour to further deplete the monocyte population and yield an enriched lymphocyte population in suspension.

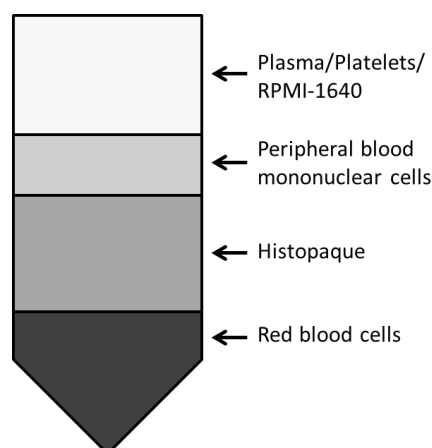


Figure 2.1 Isolation of peripheral mononuclear cells from buffy coat.

2.1.5 Isolation of primary murine dendritic cells (DCs)

Female BALB/c mice were killed by dislocation of the cervical vertebrae, and sprayed with alcohol. A pocket was cut in the skin of the rear leg and the skin was peeled away. Using a piece of tissue to help hold the lower part of the leg, the upper leg was pulled to dislocate the knee joint. Once dislocated, the femur was excised and the excess of muscle attached to it removed. It was then placed in serum free RPMI-1640 medium. The ankle joint was broken by pushing it against its natural direction. The tibia was then excised, cleaned and placed in serum free RPMI-1640 medium. When all the bones needed were excised, they were transferred to the cell culture laboratory.

Under sterile conditions the bones were transferred to the lid of a petri dish. To the bottom of the petri dish, 10ml of fresh serum free RPMI-1640 medium were added. The ends of the bone were carefully cut to expose the marrow. Using forceps, the bone was held over the fresh medium in the petri dish. Using a syringe (5-10ml) and a 26G needle (BD Bioscience; Oxford, UK), the marrow plug was flushed from the inside of the bone from both ends of the bone. With the needle, the bone marrow was aspirated to create a single cell suspension. Once all the bones had been flushed, the cells were transferred to a 50ml centrifuge tube and spun at 250xg for 5min. The supernatant was then removed and cells were resuspended in complete RPMI-1640 medium containing 10% (v/v) GM-CSF (culture supernatant from X63 myeloma cells transfected with mouse GM-CSF cDNA, kindly supplied by Dr Owain Millington; Strathclyde Institute of Pharmacy and Biomedical Sciences, University of Strathclyde, Glasgow, UK). Following this, the bone marrow cell concentration was adjusted to 5×10^5 cells/ml and cultured in 6-well plates (Nunc A/S; Roskilde, Denmark). Fresh complete medium was added to the cell cultures every 3 days.

2.1.6 Preparation of metal ion solutions

Freshly weighed cobalt chloride (CoCl_2) (Alfa Aesar; Lancashire, UK) was dissolved in sterile distilled water and filter-sterilized, using a 0.2 μm filter, to give a 100mM

stock solution of Co^{2+} . This was then used to prepare the required Co^{2+} concentration in complete RPMI-1640. These solutions were all made freshly on the day of the experiment.

2.1.7 Preparation of metal wear debris

CoCr wear debris was kindly donated by DePuy International (Leeds, UK). The wear debris was produced over 250,000 cycles from a size 39mm DePuy Articular Surface Replacement (ASR,) joint on a multistation hip joint simulator. This particular size was chosen as it represents a medium size hip. Additionally, hip joint simulators have been shown to produce clinically relevant cobalt–chromium wear particles (Germain et al., 2003, Papageorgiou et al., 2007a).

The wear debris, which was suspended in distilled water, was centrifuged at 3500xg for 10 minutes. The majority of the water was aspirated. The remaining suspension was heat treated (180°C for 5hr, 60kPa) in a Stable Temp vacuum oven (Cole-Parmer; London, UK) to eliminate the remaining water and destroy any endotoxins. The dry debris was then suspended in sterile phosphate buffered saline (PBS; Life Technologies; Paisley, UK), and stored at 4°C until required.

2.1.8 Assessing sterility of treated wear debris

In order to assess the presence of microbial contamination in the treated metal debris, DCs that had been growing for 6 days were washed with 2ml of complete RPMI-1640 medium and harvested. Cells were then seeded at 1×10^6 cells/well in two 6-well-plates in complete RPMI-1640 medium supplemented with GM-CSF. After an overnight incubation at 37°C and 5% (v/v) CO_2 , the supplemented medium was removed and replaced with complete RPMI-1640 and the appropriate treatments: debris (0.2mg/ 1×10^6 cells), lipopolysaccharide (1µl/ml; Sigma-Aldrich; Dorset, UK) or sterile PBS (100µl PBS/3ml RPMI). After 24h incubation, activation status of CD11c^+ DCs was characterized on a FACS Canto flow cytometer using the

monoclonal antibodies and relevant isotype controls (eBioscience; Hatfield, UK) listed in Table 2.1 and following the protocol described in Section 2.1.9.

Antibody	Isotype control	Purpose
CD11c-PE	Armenium hamster IgG-PE	Expressed on DCs
CD40-APC	Rat IgG2a-APC	Expressed on activated cells
MHC Class II FITC	Rat IgG2b-FITC	Expressed on activated cells

Table 2.1. Monoclonal antibodies and isotype controls used to assess CD11c⁺DC activation

2.1.9 Surface antigen staining of cells for flow cytometry

Cells in suspension were transferred to FACS tubes (BD Biosciences; Oxford, UK), centrifuged for 5min at 350xg and the supernatant aspirated off. The cells were then washed twice with FACS Buffer (10% (v/v) FCS and 0.02% (w/v) sodium azide (Sigma-Aldrich; Dorset, UK) dissolved in PBS), and then centrifuged for 5min (350xg) and the supernatant removed. In half the tubes, cells were then resuspended in FACS Buffer containing Fc block (2.4G2 hybridoma supernatant) and the appropriate combinations of fluorochrome-conjugated monoclonal antibody. In the other half, cells were resuspended in FACS Buffer containing Fc block and the relevant isotype control to identify any non-specific binding. All the tubes were then vortexed gently and incubated for 15min in the dark at room temperature. The tubes were then centrifuged for 5min at 350xg and the supernatant removed. 2ml of FACS buffer were added to each tube and they were then centrifuged for 5min at 350xg. The supernatant was removed and this step was repeated. Finally, the cells were suspended in 400µl FACS Flow and mixed thoroughly. The samples were then analysed on a FACS Canto flow cytometer using FACSDiva (BD Biosciences; Oxford, UK) software.

2.1.10 Characterisation of wear debris derived from a metal-on-metal hip resurfacing

CoCr wear debris was kindly donated by DePuy International (Leeds, UK) (details in section 2.1.7). Images were produced and the elemental composition of the CoCr wear debris analysed. A sample of the artificially produced wear debris suspended in distilled water as well as wear debris generated *in situ* from a hip implant patient (obtained during the revision surgery of a total hip replacement) were kindly processed and gold coated by Dr Thomas Yip using an Edwards S150 sputter coater at the Chemical and Process Engineering department, Strathclyde University. Briefly, debris was centrifuged and mounted on SEM stubs. Stubs were then placed in the vacuum chamber of the sputter coater, which was then sealed. The vacuum pump was switched on until the pressure in the chamber dropped to 8×10^{-2} torr. At this point, argon gas was released into the chamber until the pressure reached 2×10^{-1} torr. High voltage was then adjusted to 50mA to initiate plasma coating. To generate a thin layer of gold, coating was stopped after 1min. Argon gas was then released into the chamber to bring the pressure up to atmosphere. Following this, SEM stubs were taken to a Field Emission Scanning Electron Microscope (FE-SEM) (Hitachi SU-6600, Hitachi; Germany) to be imaged at magnifications of 100-1000x. The sample was then transferred to a Scanning Electron Microscope (SEM) (Hitachi TM-1000, Hitachi; Germany). Energy Dispersive X-ray Spectroscopy (EDS) was used for quantitative analysis of elemental composition. Hitachi TM-1000 and EDSwift-TM software was used to obtain the images and chemical spectra of the wear debris.

2.1.11 Exposure of U937 cells to wear debris and metal ions

Resting and activated U937 cells, with and without Co pre-treatment, (cultured as described in Section 2.1.1) were seeded at 1×10^5 cells per well in 96-well culture plates and incubated with 0.05mg/ 1×10^6 cells, 0.1mg/ 1×10^6 cells, and 0.2mg/ 1×10^6 cells wear debris in the absence or presence of Co ions in complete RPMI-1640 at 37°C, 5% (v/v) CO₂ for 24, 48, and 120 hours. Additionally, resting, Co pre-treated resting, activated and Co pre-treated activated U937 cells seeded at

1×10^4 cells per well in 96-well culture plates were exposed to 5mg/ 1×10^6 cells of wear debris and 0.1 μ M Co ions, individually and combined, in complete RPMI-1640 at 37°C, 5% (v/v) CO₂ for 24 and 120 hours.

2.1.12 Exposure of lymphocytes to wear debris and metal ions

Isolated peripheral human lymphocytes (prepared as described in section 2.1.4) were exposed to metal wear debris and Co²⁺ in a resting state. Lymphocytes were cultured (1×10^5 cells/well) in 96-well round-bottom plates (100 μ l/well) with 5mg wear debris/ 1×10^6 cells, 0.1 μ M of Co²⁺ and 5mg wear debris/ 1×10^6 cells combined with 0.1 μ M of Co²⁺ in complete RPMI-1640. Cultures were carried out for 24, 48, and 120h at 37°C under 5% (v/v) CO₂ air. For apoptosis analyses, debris concentration was 2.5mg wear debris/ 1×10^6 cells.

2.1.13 MTT assay for cell viability

The MTT assay is a colorimetric assay system, which measures the reduction of the yellow tetrazolium salt MTT (3-(4,5-Dimethylthiazol-2-yl)-2,5-diphenyltetrazolium bromide) into a blue formazan product by dehydrogenases and reducing agents present in metabolically active cells. The water-insoluble formazan that accumulates within viable cells may be extracted with organic solvents and estimated by spectrophotometry. The amount of formazan production is proportional to the number of viable cells, the dehydrogenase activity and the incubation time (Mosmann, 1983).

In order to make a 10mM solution of MTT, 414.3mg of MTT (Sigma-Aldrich; Dorset, UK) were dissolved in 100ml of PBS, which had been adjusted to pH 6.75 by the addition of HCl. This solution was sterile filtered with a 0.2 μ m filter and stored in the dark at 4°C until required.

At each culture end-point, 96-well plates (TPP; Switzerland) were centrifuged for 5min at 350xg. Supernatant was carefully removed and cells resuspended in 50 μ l of

MTT solution. Following an incubation period of 4h at 37°C, cells were centrifuged (350xg, 5min) and supernatant removed. Cells were then resuspended in 200µl of dimethyl sulfoxide (DMSO; Sigma-Aldrich; Dorset, UK) to dissolve the formazan product. The absorbance of light was measured at 540nm immediately using a Thermo Scientific Multiskan Ascent spectrophotometer plate reader.

2.1.14 Neutral red assay for cell viability

The Neutral Red (NR) assay is based on the ability of viable cells to incorporate and bind the NR dye in the lysosomes. Damage to cell surface or lysosomal membranes results in decreased dye uptake. The NR destain solution is used to extract the dye from the viable cells and the absorbance of solubilised dye is then determined spectrophotometrically. Quantification of the extracted NR by spectrophotometry has been correlated with cell numbers by equating the intensity of the red colour with the number of cells (Repetto et al., 2008).

5mg of NR powder (Sigma-Aldrich; Dorset, UK) were dissolved in 100ml of PBS pH 7.4. The solution was incubated overnight at 37°C and undissolved crystals were filtered out with a 0.2µm filter. The filtered solution was stored at 4°C. The NR destain was prepared by mixing together 50ml ethanol (Sigma-Aldrich; Dorset, UK), 1ml glacial acetic acid (Sigma-Aldrich; Dorset, UK) and 49ml distilled water and was then stored in a flammable solvent cupboard.

At each culture end point, 96-well plates were centrifuged for 5min at 350xg. Supernatant was carefully removed and cells resuspended in 100µl of NR solution. Following an incubation period of 3h at 37°C, cells exposed to NR were centrifuged (350xg, 5min) and supernatant removed. Cells were then resuspended in 200µl of PBS and centrifuged again. After discarding the supernatant, 100µl of NR destain solution was added. A homogeneous colour was obtained by placing the culture plate on an orbital shaker for at least 30min. The absorbance of light was measured at 540nm immediately using a Thermo Scientific Multiskan Ascent spectrophotometer plate reader.

2.1.15 Analysis of cell morphology and viability via microscopy

In order to assess the effects on cell morphology and viability, cells were stained with Acridine Orange (AO; Sigma-Aldrich; Dorset, UK) and Propidium Iodide (PI; Life Technologies; Paisley, UK). PI is impermeable to intact plasma membranes, but it easily penetrates the plasma membrane of dead or dying cells and intercalates with DNA or RNA forming a bright red fluorescent complex. AO is a membrane-permeable, monovalent, cationic dye which binds to nucleic acids in the cells to produce a fluorescent green product (Bank, 1987, Bank, 1988).

35mm² petri dishes (BD Falcon; Oxford, UK) were coated with 1ml 0.01% (v/v) poly-L-lysine (Sigma-Aldrich; Dorset, UK). After 10 minutes, the poly-L-lysine was aspirated off and petri dishes allowed to dry at room temperature overnight. Cells were then seeded onto the coated dishes. At each culture end point, medium was aspirated off and cells gently washed twice with PBS. 1ml of a 1:1 AO+PI solution was added and the cells incubated in the dark for 1 minute. The AO+PI solution was aspirated off and cells gently washed three times with PBS. 2ml of PBS were added and cells were viewed using a Carl Zeiss Axio Imager microscope under a 40X water immersion lens with a numeric aperture of 0.80. Fluorescence was excited using a mercury lamp and emission recorded using a fluorescein isothiocyanate (FITC)/Rhodamine filter block (485/515-530nm; 546/580-563nm) for AO and PI. Fluorescence was stable allowing digital images to be captured using AxioVision v.4.6 (Zeiss, Germany). Analysis of images was carried out with both AxioVision 4.6 and the freeware ImageJ v.1.47q (<http://rsbweb.nih.gov/ij/download.html>).

2.1.16 Cell proliferation assay

Cell proliferation was determined by a non-isotopic BrdU Cell Proliferation Immunoassay kit (Merck Chemicals; Nottingham, UK). This immunoassay quantifies cell proliferation by incorporating BrdU into the newly synthesized DNA

strands of actively proliferating cells. The kit provided all the agents and solutions required.

Briefly, the BrdU label was diluted 1:2000 into fresh complete RPMI-1640 medium. To label the DNA, 20µl of this working solution were added to cells in 96 well plates during the final 4 hours of the experiment. Plates were then centrifuged (300xg for 10min) and the supernatant aspirated. Cells were then fixed, permeabilized and DNA denatured by adding 200µl of the supplied fixative/denaturing solution to each well. Plates were incubated for 30min at room temperature and the fixative/denaturing solution was then aspirated. 100µl of anti-BrdU antibody diluted in antibody dilution buffer were added to each well and incubated with the cells for 1h at room temperature. Cells were washed 3 times with 1X wash buffer, making sure each well was filled completely. 100µl of peroxidase goat anti-mouse IgG HRP conjugate diluted in conjugate diluent were added to each well and incubated with the cells for 30min at room temperature. At the end of this time, cells were washed as described above. Plates were then flooded with dH₂O and contents removed by inverting them over the sink and tapping them on paper towels. 100µl of substrate solution were added to each well and the plates incubated in the dark at room temperature for 15min. 100µl of stop solution were added to each well in the same order as the previously added substrate solution. The absorbance was then measured in each well using a Thermo Scientific Multiskan Ascent spectrophotometer plate reader at dual wavelengths of 450-540nm.

2.1.17 ELISA

Cytokine levels were determined by collecting supernatants from appropriate cell cultures. These were then assayed using Ready-SET-Go! enzyme-linked immunosorbent assay (ELISA) kits (eBioscience; Hatfield, UK). The kit provided all components required except wash buffer, which consisted of 0.05% (v/v) Tween-20 (Sigma-Aldrich; Dorset, UK) diluted in PBS, and the stop solution (2M H₂SO₄, Fisher Scientific; Loughborough, UK).

Briefly, ELISA plates were coated with 100µl/well capture antibody diluted in coating buffer. Plates were sealed and incubated overnight at 4°C. Following this incubation, wells were aspirated and washed 5 times with 250µl/well wash buffer allowing the plate to soak for 1min between each wash. After the last wash, plates were dried by tapping them on paper towels. Plates were then blocked by adding 200µl/well of 1X assay diluent and incubating for 1h at room temperature. Liquid was aspirated and plates washed as described before. Standards, at concentrations between 0-500pg/ml for TNFα and IFNγ, 0-250pg/ml for IL-2, and 0-200pg/ml for IL-6 were prepared using 1X assay diluent to obtain a standard curve. 100µl/well of each standard or collected supernatant were added to the appropriate wells. Plates were sealed and incubated for 2h at room temperature. Following this period, wells were washed as described before, and 100µl/well of detection antibody diluted in 1X assay diluent were added to each well. Plates were sealed again, incubated for 1h at room temperature, then washed as previously described and 100µl/well of Avidin-HRP diluted in 1X assay diluent added. They were sealed and incubated for 30min at room temperature. Wells were then aspirated and washed 7 times allowing the plates to soak for 2min between each wash. 100µl/well of substrate solution were added, and the plates were sealed again, and incubated for 15min at room temperature. Following this final incubation period, 50µl/well of stop solution were added. The absorbance was finally measured using a Thermo Scientific Multiskan Ascent spectrophotometer plate reader at dual wavelengths of 450-570nm.

2.1.18 ICP-MS Analysis of metal ion concentrations

2.1.18.1 Metal ion concentrations in culture medium

Experiments were carried out to determine the extent of metal ion release when wear debris was incubated with cultured cells *in vitro*.

In order to assess the effects of foetal calf serum (FCS) and pH on the metal ion release, 2.5mg metal wear debris / 1×10^6 cells were incubated for 24h in RPMI-1640 medium in the presence and absence of FCS and complete RPMI-1640 medium, pH

4. Every condition was carried out in triplicate and controls of each condition with no metal debris were also present. To analyse the correlation between debris concentration and metal ions released 0.2, 0.5, 1, 2.5, and 5mg metal wear debris / 1×10^6 cells were incubated in complete RPMI-1640 for 24h at 37°C and 5% (v/v) CO₂. Every concentration was carried out in triplicate and controls with no metal debris were also present. At 24h, culture medium from each well was collected into microcentrifuge tubes and stored at -80°C until ICP-MS analysis. In addition to this, culture medium from cells exposed for 120h to 5mg debris/ 1×10^6 cells, 0.1µM Co, and a combination of 5mg debris / 1×10^6 cells and 0.1µM Co were also analysed.

All samples were diluted 10-fold in serum free RPMI-1640 medium, and centrifuged at 13,200 rpm for 15 minutes. Generally, 500µl of each sample were added to 4.5ml of RPMI-1640. Each sample was then sonicated. Standards were prepared by diluting Multielement Standard Solution 1 for ICP (Sigma-Aldrich (Fluka); Dorset, UK) in RPMI-1640 at the concentrations shown in Table 2.2. Samples were analysed using an Agilent 7700x octopole collision system ICP-MS (Agilent Technologies; Wokingham, UK) in helium gas mode using Scandium (Sc) as internal standard. The quantification is based on the maximum signal for a particular isotope, also referred to as peak height. Five readings are taken, and the result obtained is the mean value.

Standards	Metal Ions (µg/L)		
	Cobalt	Chromium	Molybdenum
Blank (0)	0	0	0
1	1	5	5
2	10	50	50
3	50	250	250
4	200	1000	1000
5	500	2500	2500

Table 2.2. ICP-MS standards.

2.1.18.2 Metal ion concentrations in U937 cells

In order to determine cellular up-take of the ions released into the culture medium during incubation with CoCr wear debris, resting U937 cells (cultured as described

in Section 2.1.1) were seeded at 1×10^5 cells/ml in 24-well plates and exposed to 0, 0.2, 0.5, 1, 2.5, and 5mg debris / 1×10^6 cells for 24h at 37°C and 5% (v/v) CO₂.

Cells in suspension were centrifuged at 350xg for 5min. Culture medium was aspirated off and cells were washed twice with PBS. After the second wash, PBS was discarded and pellets were sonicated for 30min at 45°C. Cell lysates were then resuspended in 1ml of ultrapure water (18mΩ) and stored at -20°C overnight. They were then allowed to thaw at room temperature and centrifuged at 13,200rpm for 15min. All samples were diluted 5-fold in 2% (v/v) HNO₃, and each sample was then sonicated. Standards were prepared by diluting Multielement Standard Solution 1 for ICP (Sigma-Aldrich (Fluka); Dorset, UK) in 2% (v/v) HNO₃ at the concentrations shown in Table 2.2. Samples were analysed as described in Section 2.1.13.1.

2.1.19 Flow cytometry analysis of apoptosis

Cell viability assays carried out in Chapter 3 will show that the 5mg debris/ 1×10^6 cells concentration was highly cytotoxic. As a result, the arbitrary 2.5mg debris/ 1×10^6 cells concentration was chosen for the analysis of apoptosis and gene expression. Although arbitrary 2.5mg debris/ 1×10^6 cells is still a high dose, it would allow to detect early apoptosis and isolate enough amounts of RNA. The concentration of Co ions was the same throughout this investigation as it represents the whole blood threshold suggested by the MHRA for patients with MoM articulations (MDA/2010/069).

Resting U937 cells and Co pre-treated resting U937 cells were seeded at 2.5×10^5 cells/ml in 12-well plates to be treated with 2.5mg/ 1×10^6 cells of metal debris, 0.1μM Co and a combination of 2.5mg/ 1×10^6 cells of metal debris and 0.1μM Co. Non-treated resting U937 cells were used as controls. Experiments with freshly isolated lymphocytes were carried out in a similar manner: cells were seeded at 2.5×10^5 cells/ml in 12-well plates to be treated with 2.5mg/ 1×10^6 cells of metal debris, 0.1μM Co and a combination of 2.5mg/ 1×10^6 cells of metal debris and 0.1μM Co. Non-treated lymphocytes were used as controls. In both cases, all treatments were

carried out in triplicate. Cells were exposed to the treatments for 24 and 48h before being analysed by FACS.

Cell suspensions were transferred into FACS tubes and centrifuged for 5min (350xg). The supernatant was aspirated and the cells resuspended in 200µl of FACS buffer. Following this, the cells were centrifuged for 5min (350xg) and supernatant discarded. The cells were then resuspended in 100µl Annexin binding buffer (0.01M HEPES, 0.14M NaCl and 2.5mM CaCl (all Sigma-Aldrich; Dorset, UK) in distilled water (pH 7.4)). 5µl of Annexin V- phycoerythrin (PE) and 5µl of 7-Aminoactinomycin D (7-AAD) (both BD Bioscience; Oxford, UK) were then added to each tube. Tubes were vortexed and incubated at room temperature for 15min in the dark. Following this incubation period, 200µl of Annexin binding buffer and 200µl of FACS Flow (BD Bioscience; Oxford, UK) were added to each tube. Calibrite™ beads (BD Bioscience; Oxford, UK) were used to adjust instrument settings, set fluorescence compensation, and check instrument sensitivity. The data were recorded using a FACSCanto flow cytometer (BD Bioscience; Oxford, UK) using FACSDiva software.

2.1.20 Western blot analysis of apoptosis

Resting U937 cells and Co pre-treated resting U937 cells were seeded at 2.5×10^5 cells/ml in 25cm^2 culture flasks (TPP; Switzerland) to be treated with 2.5mg/1x10⁶ cells metal debris, 0.1µM Co and a combination of 2.5mg/1x10⁶ cells metal debris and 0.1µM Co. Non-treated resting U937 cells were used as controls. Cells were exposed to the treatments for 24 and 48h before being analysed by western blot.

Anti-PARP recognizes Poly-ADP-Ribose-Polymerase (PARP; Roche; West Sussex, UK), a 113kD protein that binds specifically at DNA strand breaks (Demurcia and Demurcia, 1994). PARP is also a substrate for certain caspases (for example, caspase 3 and 7) activated during early stages of apoptosis (Nicholson et al., 1995). These proteases cleave PARP to fragments of approximately 89kD and 24kD. Detection of

the 89kD PARP fragment with anti-PARP thus serves as an early marker of apoptosis.

2.1.20.1 Preparation of cell homogenates

Cell suspensions were transferred from culture flasks to centrifuge tubes and centrifuged at 350xg for 5min. Culture medium was discarded and cells washed twice with PBS and centrifuged at 350xg for 5min between each wash. The pellet was resuspended in 500µl of 0.1M Sodium Phosphate buffer (NaPi) pH 7.6 (see composition in Appendix 1). Cells were then homogenised using seven strokes of a motor driven Teflon-glass homogeniser. Homogenates were split into three 150µl aliquots to be stored at -80°C for Western blotting and one 50µl aliquot to measure the total protein content.

2.1.20.2 Measurement of total protein content

Total protein content was determined for each sample with Lowry assay (Lowry et al., 1951). For this purpose, solution A (2% w/v Na₂CO₃, 1% w/v CuSO₄ and 1% w/v NaK tartrate; all Sigma-Aldrich; Dorset, UK) and solution B (1:4 dilution of Folin's in distilled H₂O; Sigma-Aldrich; Dorset, UK) were prepared. Bovine serum albumin standards (BSA; Sigma-Aldrich; Dorset, UK) were made up in test tubes as shown in Table 2.3. 50µl of each sample was diluted with 950µl 0.5M NaOH (Sigma-Aldrich; Dorset, UK). 5ml of solution A were added to standards and samples, which were mixed and incubated at room temperature for 10min. After this, 0.5ml of solution B were added and mixed immediately. Samples and standards were incubated at room temperature for 30min before being read at 725nm against water blank.

Protein Concentration µg/ml						
	0	25	50	100	150	200
BSA (ml)	0.000	0.125	0.250	0.500	0.750	1.000
0.5M NaOH (ml)	1.000	0.875	0.750	0.500	0.250	0.000

Table 2.3. Protein standards.

2.1.20.3 Sodium dodecyl sulfate polyacrylamide gel electrophoresis (SDS-PAGE)

Glass plates were cleaned with 70% (v/v) alcohol and assembled in the casting chamber. Gels were cast as shown in Table 2.4 (all reagents Sigma-Aldrich; Dorset, UK). Resolution gel was cast first and allowed to set. Stacking gel was cast over the resolution gel. Combs were inserted into the stacking gel before allowing it to set. Meanwhile, samples were prepared at 1mg/ml in Laemmli buffer (Sigma-Aldrich; Dorset, UK) and boiled for 2min in sure-lock microcentrifuge tubes. The gel sandwiches were then clicked into the electrode and the upper chamber filled with 1X electrophoresis buffer (Tris/Glycine/SDS; Sigma-Aldrich; Dorset, UK). Combs were removed making sure the buffer filled the wells, and the chamber was then placed in the tank and filled with buffer. Samples (10µg/well) were loaded in the wells, and the electrophoresis run at 50mA until it had run almost to the bottom of the gel.

Solutions	Stacking gel	10% Resolution Gel
Acrylamide/bis-acrylamide (40% stock)	1ml	5.625ml
Stacking gel buffer	2.5ml	-
Resolving gel buffer	-	5.625ml
1.5% ammonium persulfate	0.5ml	1.125ml
Distilled water	6ml	10.125ml
N,N,N',N'-Tetramethylethylenediamine (TEMED)	10µl	17.5µl

Table 2.4. Reagents for casting gels.

2.1.20.4 Western Blot

While the gels were running the transfer buffer (Towbin's buffer) was prepared as follows: 2100ml distilled water, 600ml methanol (Fisher Scientific; Loughborough, UK) and 300ml 10X Tris/Glycine transfer buffer (Sigma-Aldrich; Dorset, UK). The scotch brite pads and filter paper (Sigma-Aldrich; Dorset, UK) were soaked in the transfer buffer for 15min. The Immobilon-P membrane (Merck Millipore; Watford, UK) was soaked in methanol before placing it in transfer buffer for 15min. Once gels had run, the gel sandwich was removed from the tank and placed in transfer buffer

for a few minutes. Transfer cassettes were prepared as shown in Figure 2.2. Cassettes were placed in the tank which was partially filled with transfer buffer, with the black side of the cassette at the negative side of the tank. It was run overnight at 200mA.

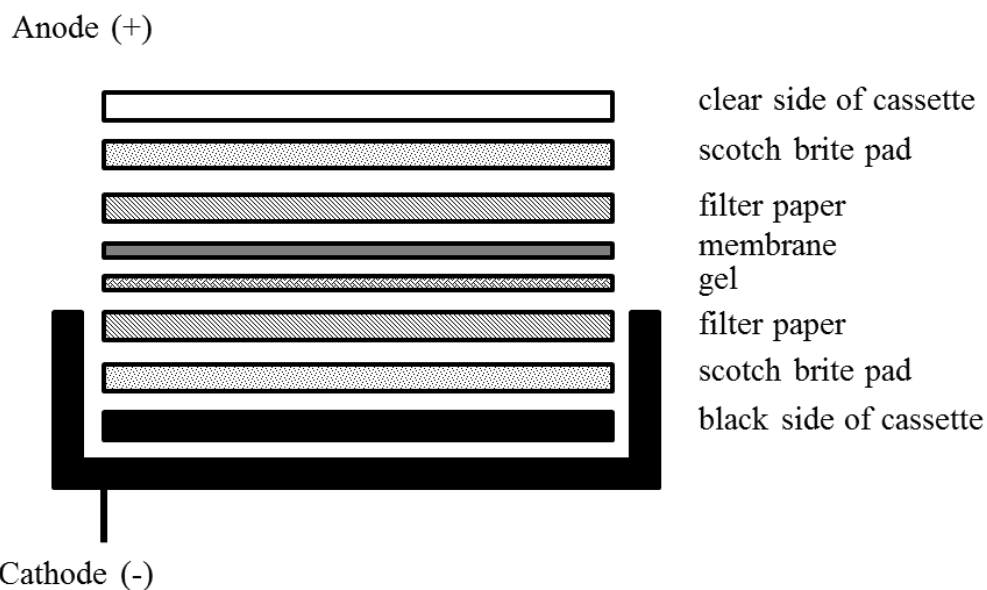


Figure 2.2. Transfer cassettes.

In order to develop the membranes, Tris Buffered Saline (TBS; Sigma-Aldrich; Dorset, UK) was prepared from 10X stock and then Tween Tris Buffered Saline (TTBS) was made up by adding 0.5ml of Tween 20 to 1L of 1X TBS. As blocking agent, 3% (w/v) gelatin (Sigma-Aldrich; Dorset, UK) was prepared in TTBS. The membranes were placed in this gelatine solution for 1hr at 37°C while shaking. The gelatin was then poured off, and membranes washed for 5min in TTBS while shaking. Anti-PARP (1:2000) in 1% (w/v) gelatin in TTBS was added, and the membranes shaken for 1hr at 37°C. Antibody was poured off and membranes washed 3 times with shaking in TTBS for 5min. Secondary antibody was prepared in 1% (w/v) gelatin in TTBS (anti rabbit IgG-ALP 1:1000; Bio-Rad; Hertfordshire, UK) and shaken with the membranes for 1hr at 37°C. Antibody was poured off and membranes washed twice shaking in TTBS and once in TBS for 5min. To visualise the bands on the membranes, the alkaline phosphatase detection system (Bio-Rad; Hertfordshire, UK) was used according to the manufacturer's recommendations. Membranes were then dried between 2 sheets of filter paper, scanned within a

CanoScan N670U scanner and the software CanoScan toolbox 4.1 (Canon; Middlesex, UK) to be analysed by ImageJ version 1.47q.

2.1.21 Minimum Information for Publication of Quantitative Real-Time PCR Experiments (MIQE)

The Minimum Information for Publication of Quantitative Real-Time PCR Experiments (MIQE) is a set of guidelines that describe the minimum information necessary for evaluating and publishing quantitative real-time PCR (qPCR) experiments results (Bustin et al., 2009, Bustin et al., 2010). The aim of the MIQE guidelines is to provide the reader with all the information required to either repeat the experiment or be able to judge whether the data are sound. The guidelines cover all the steps of a qPCR assay, which include sample acquisition, handling, and preparation, quantification of nucleic acids, reverse transcription, qPCR and data analysis. Figure 2.3 gives an overview of some of the suggested information to be included in a report or publication.

The MIQE guidelines were followed in the current study in both cells and whole blood experiments. Detailed information regarding each step of the RT-qPCR experiments is given in the appropriate sections. Additionally, a MIQE checklist is given in Appendix 3.

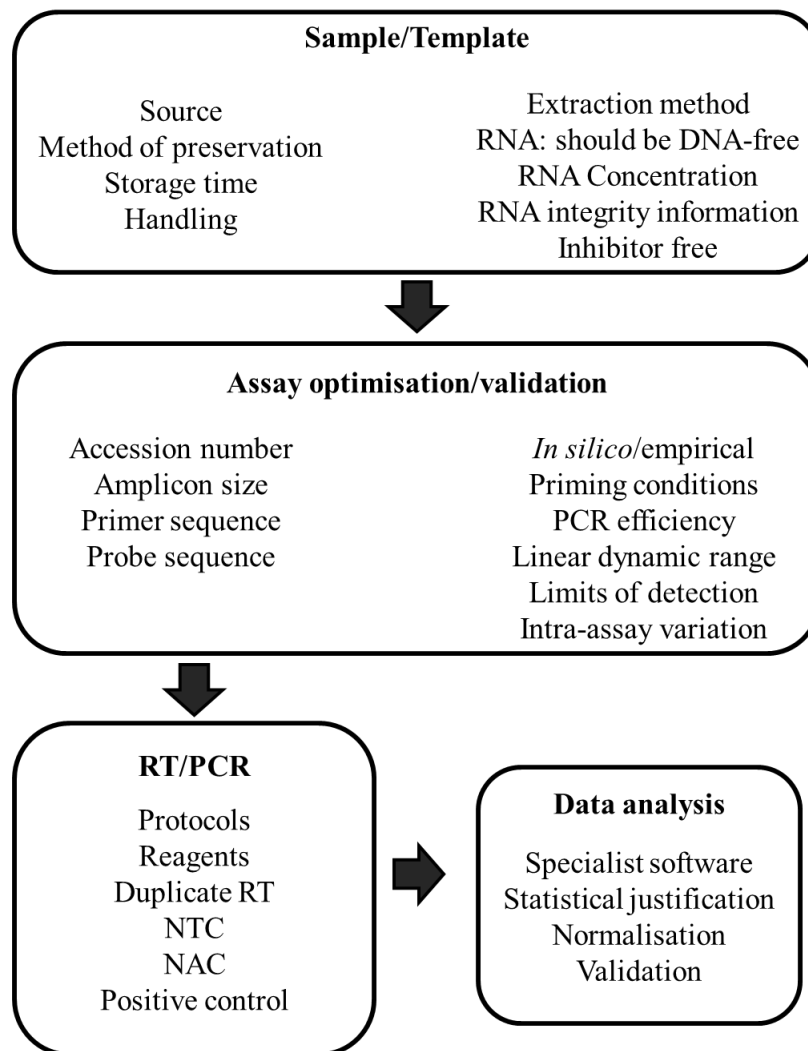


Figure 2.3. Key criteria delineating essential technical information required for the assessment of a RT-qPCR experiment. Accession number: unique identifier of a nucleotide sequence. *In silico*: BLAST specificity analysis. NTC: no template controls (H₂O). NAC: no amplification controls (RT- controls) (adapted from Bustin et al., 2010).

2.1.22 Isolation of total RNA

In order to extract total RNA from U937 cell cultures the GenElute Mammalian Total RNA Miniprep Kit (Sigma-Aldrich; Dorset, UK) was used. The protocol followed was the one suggested by the manufacturer in the kit manual. All steps were carried out at room temperature and an overview is given in Figure 2.4.

Briefly, resting and activated U937 cells were harvested and pelleted. Culture medium was removed and 500µl of lysis solution/2-mercaptoethanol mixture added

to lyse cells and inactivate RNases. To remove cellular debris and shear DNA, the lysed cells were pipetted into a GenElute filtration column. They were then centrifuged at maximum speed for 2min to complete the cell disruption and the filtration column discarded. 500µl of 70% ethanol solution were added, the mixture vortexed and 700µl of the lysate/ethanol mixture were taken into a GenElute binding column. Centrifugation at maximum speed for 15sec binds the total RNA in solution to the silica-based binding column. The flow-through liquid discarded. The binding column was placed back into the collection tube to apply any remaining lysate/ethanol mixture to the column. The centrifugation was repeated as described above. To remove any contaminating genomic DNA carryover which may interfere with the downstream reverse transcribed-PCR-based gene expression analysis, the optional on-column DNase I digestion procedure was included, which used an On-Column DNase I Digestion Set (Sigma-Aldrich, Dorset, UK). The binding column was then transferred to a fresh 2ml collection tube. 50µl of the elution solution were added to the binding column to release the total RNA and centrifuged at maximum speed for 1min. To maximise recovery, a second 50µl volume of the elution solution was added to the binding column and centrifuged at maximum speed for 1min. Both eluates were collected in the same tube. 5µl aliquots were taken to determine the purified RNA concentration, purity and integrity and the remaining RNA was stored at -80°C.

RNA concentration was determined in a 5µl aliquot by measuring the absorbance at 260 nm (A260) in a NanoDrop 2000c spectrophotometer (Labtech International, UK). RNA purity was also determined by the NanoDrop 2000c spectrophotometer as the ratio of the readings at 260 nm and 280 nm (A260/A280). Finally, RNA integrity was assessed in a 5µl aliquot by determining the RNA Quality Indicator (RQI) number, which is automatically generated by the Experion Automated Electrophoresis System (Bio-Rad; Hertfordshire, UK) using an algorithm that compares three regions of an electrophoretic profile to a series of degradation standards.

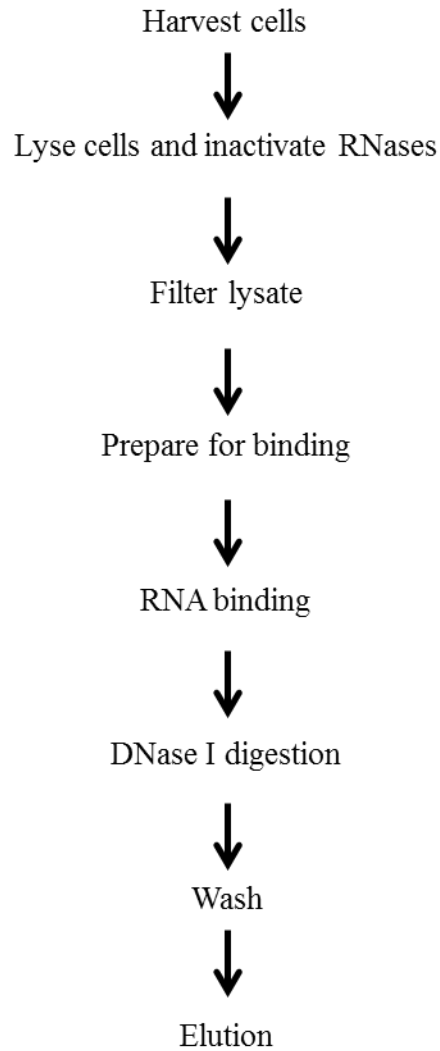


Figure 2.4. Overview of total RNA isolation from U937 cells.

2.1.23 cDNA synthesis

SuperScript III Reverse Transcriptase (Life technologies; Paisley, UK) was used to generate cDNA templates from the RNA extracted from U937 cells for use in reverse-transcribed polymerase gene reactions (RT-PCR). Briefly, 1 μ l of oligo(dT)₂₄ (500ng/ μ l, Eurofins MWG Operon; London, UK), 4 μ g of total RNA, 1 μ l of 10mM dNTP mix (Eurofins MWG Operon; London, UK) and nuclease-free water (Sigma-Aldrich; Dorset, UK) to 13 μ l were added to a nuclease-free microcentrifuge tube. The mixture was then heated to 65°C for 5min and incubated on ice for at least 1min. After this, the contents of the tube were collected by brief centrifugation and 4 μ l of 5X first-strand buffer, 1 μ l of 0.1M DTT, 1 μ l of RNaseOUT recombinant RNase

inhibitor (Life technologies; Paisley, UK) and 1µl of SuperScript III RT (200 units/µl) were added. Controls with nuclease-free water instead of SuperScript III were also carried out for each RNA sample. Such reactions were designated as the sample “RT-” control as it would provide a check for any persisting contaminating genomic DNA. A PCR carried out using an aliquot of this as the template should not generate any products. The cDNA reactions were mixed by pipetting gently before incubating at 50°C for 60min. In order to inactivate the reverse transcriptase, the reactions were heated at 70°C for 15min. cDNA was then stored at -20°C.

2.1.24 StellARray™ gene expression array

The StellARray™ Gene Expression System (Lonza; Switzerland) is a quantitative polymerase chain reaction (qPCR)-based method and provides profiling of biologically focused gene sets. Gene expression array analysis with the standard Human General Toxicology 96 StellARray™ was performed in order to identify genes related to the toxic effects of metal wear debris and ions on U937 cells. Cells were exposed to the combination of 2.5mg/1x10⁶cells wear debris and 0.1µM Co for 120h. Untreated resting U937 cells were used as control. The procedure was carried out as recommended by the manufacturer. Briefly, a supermix was prepared by adding 998µl nuclease free water to 1056µl SYBR® Select Master Mix (Applied Biosystems, UK). To obtain a sample-specific working solution, 106µl template (33.3ng/µl) cDNA was added to 2006µl supermix. Following this, the foil seal was removed from the StellARray plate and 20µl of sample-specific working solution were added to each well. Once it had been ensured that all reagents were at the bottom of the wells, the plate was sealed with an optical adhesive plate cover. The optical adhesive plate cover is an optically clear plate seal designed for optical assays, such as real-time PCR. The plate was incubated at room temperature for 15min. prior to loading into a StepOnePlus Real-Time PCR system (Applied Biosystems, UK). Thermal cycling conditions were set for a standard run as shown on Table 2.6 (Section 2.1.19), which was followed by a melting curve analysis to check for nonspecific amplification. Quantification cycles (Cq) from the amplification curves were obtained from the Applied Biosystems StepOne Plus

software v2.1. Further data analysis was performed with the Global Pattern Recognition™ software (Bar Harbor Biotechnology Inc, USA) which is partnered with the StellarRay™ system.

2.1.25 Primer design and efficiency determination

Individual SYBR green primer sets for dye-base quantitative real-time PCR were designed using the software GeneRunner (Hasting Software, USA). The parameters for designing the primers were: have a length between 20 and 25 nucleotides, have a melting temperature (T_m) higher than 59°C but lower than 62°C, have a percentage of guanine-cytosine (GC) of between 40-60%, and produce an amplicon between 100 and 150bp long. Although a DNase treatment was included in the RNA isolation process to avoid genomic DNA contamination, primer sets were designed to span exon-exon junctions. In this way, only cDNA from mRNA gene transcripts will be amplified, not genomic copies of the gene (Sandhu and Acharya, 2005, Del Aguila et al., 2005). In the cases where the introns were smaller than 100bp, primers were designed to sit on the exon-exon junctions in a 50/50 ratio. Thus, if an intron were to be present (i.e. genomic DNA) only 50% of the primer sequence would anneal and the amplification reaction would not take place. Since some of the target genes have several variants, the multiple sequence alignment software, MUSCLE (Edgar, 2004); <http://www.ebi.ac.uk/Tools/msa/muscle/>) was used to align the variants and help with the process of targeting a unique region for a particular transcript. Specificity of each set of primers was verified with the Primer-BLAST tool (Ye et al., 2012); <http://www.ncbi.nlm.nih.gov/tools/primer-blast>) to make sure that the primers would not amplify unwanted products. Primer sequences, T_m, and amplicon size are summarised in Table 2.5.

In order to avoid under- or overestimation of the expression levels of 8 target genes, the efficiencies of each primer set were calculated. For this purpose, cDNA from untreated U937 cells was diluted to 100, 50, 10, 4, and 1ng. Triplicate real-time PCR reactions were run for each sample, containing 10µl SYBR® Select Master mix (Applied Biosystems, UK), 3µl of forward primer (1pmol/µl), 3µl of reverse primer

(1pmol/μl) and cDNA template to a total volume of 20μl with molecular biology-grade H₂O.

Gene	Primer sequences (5'→3'), (nucleotides)	T _m	Amplicon size (bp)
NOS2	Sense GTGCAAACCTTCAAGGCAGCCT (22)	59.3	127
	Anti-sense TGAGTCCTGCACGAGCCTGTAGTG (24)	60.3	
LTA	Sense TGCTGCTCACCTCATTGGAGACC (23)	60.1	123
	Anti-sense CTGGTGGGGACCAGGAGAGAATT (23)	59.2	
BAG1	Sense TGCCCAAGGATTTGCAAGCTG (21)	59.7	113
	Anti-sense TTCTGGCAGGATCAGTGTGTCAATC (25)	59.9	
GADD45A	Sense AACATCCTGCGCGTCAGCAAC (21)	59.7	137
	Anti-sense AGATGAATGTGGATTCGTCACCAGC (25)	60.1	
FOS	Sense ACGCAGACTACGAGGCGTCATCC (23)	61.3	142
	Anti-sense GCCAGGTCCGTGCAGAAGTCC (21)	60.4	
B2M	Sense AGATGAGTATGCCTGCCGTGTGAAC (25)	60.3	110
	Anti-sense CAAATGCGGCATCTTCAAACCTC (23)	59.5	
HPRT1	Sense CCCTGGCGTCGTGATTAGTGATG (23)	60.2	138
	Anti-sense CGAGCAAGACGTTTCAGTCCTGTCC (24)	60.9	
GAPDH	Sense AGCCTCCCGCTTCGCTCTC (20)	58.2	125
	Anti-sense ACCAAATCCGTTGACTCCGACC (23)	58.7	

Table 2.5 Primer sequences, melting temperatures (T_m) as calculated by GeneRunner and amplicon size.

2.1.26 SYBR Green quantitative real-time PCR

U937 cell gene expression assays were carried out using SYBR Green-based quantitative real-time RT-PCR. Oligonucleotide primers for these assays were designed as described in Section 2.1.25.

Briefly, for each reaction, 10μl of SYBR Select Master Mix (2X, Life Technologies; Paisley, UK), 3μl of forward primers (1pmol/μl), 3μl of reverse primers (1pmol/μl),

1µl cDNA (33.3ng/µl) and 3µl of nuclease-free water were added to a nuclease-free microcentrifuge tube. Negative controls with nuclease-free water and “RT-”cDNA reaction mixture were also set up. Master mixes for each assay were prepared with the primers, nuclease-free water and SYBR select. The components were mixed thoroughly and centrifuged briefly to eliminate any air bubbles. 19µl of each master mixture were transferred to the corresponding wells of optical 8-tube strips (Applied Biosystems; Paisley, UK). Finally, 1µl of cDNA was added to the reactions, and 1µl of nuclease-free water or “RT-”cDNA reaction product was added to the corresponding controls. Tubes were sealed with optical 8-cap strips (Applied Biosystems; Paisley, UK) and loaded into a StepOnePlus Real-Time PCR system (Applied Biosystems; Paisley, UK). Thermal cycling conditions were set for a standard run as shown on Table 2.6, which was followed by a melting curve analysis to check for nonspecific amplification. Quantification cycle (Cq) values were calculated by the StepOnePlus software (v2.1). Once finished, the reactions were stored at 4°C to be further analysed via horizontal electrophoresis.

Standard Cycling Mode (Primer T_m ≥60°C)			
Step	Temperature	Duration	Cycles
UDG Activation	50°C	2min	Hold
AmpliTaq DNA Polymerase, UP Activation	95°C	2min	Hold
Denature	95°C	15sec	40
Anneal/Extend	60°C	1min	

Table 2.6. PCR thermal cycling conditions

2.1.27 Horizontal gel electrophoresis

In order to verify that the primer sets were working appropriately, gel electrophoresis was carried out using a horizontal submarine mini-gel apparatus (Bioscience Services, London, UK). For this purpose, a 2% (w/v) agarose gel solution was prepared by adding 1g of AgarGel H/M (Continental Laboratory Products; Northampton, UK) to 50ml of 1X Tris-Borate-EDTA (TBE; Sigma-Aldrich; Dorset, UK) buffer. This solution was microwaved at high power for 1 minute and 30 seconds. 2µl of a 10mg/ml solution of ethidium bromide (Sigma-Aldrich; Dorset, UK) were added to the agarose solution, which was then poured into the

electrophoresis chamber. The comb was positioned and the gel was allowed to set for 10 minutes. 6µl of ethidium bromide were added to 80ml of TBE for the running buffer. Once the gel set, the running buffer was poured into the chamber and the comb removed. 6µl of HyperLadder II (Bioline; London, UK) were loaded into the first well to serve as molecular weight marker lane. 15µl of each PCR reaction were mixed with 2µl of DNA loading buffer (Bioline; London, UK) and loaded into the corresponding well. The gel was run for 1h at 50 volts using a BioMax MBP300 electrophoresis powersupply (Kodak, London, UK). The ethidium bromide stains DNA during the electrophoresis and this enables the PCR products to be visualised under UV light. Once finished, the gel was imaged and analysed with the InGenius Bio Imaging system (Syngene; Cambridge, UK) and GeneSnap image acquisition software (Syngene; Cambridge, UK).

2.2 Analysis of blood samples

2.2.1 Storing clinical blood samples

Whole blood samples were collected in EDTA tubes and delivered to the laboratory on the same day of collection. Upon arrival at the laboratory, blood samples were divided into 500µL aliquots. To minimise RNA degradation, 1.2ml of *RNAlater*[®] (Life Technologies; Paisley, UK) was added to each sample. Samples were incubated overnight at 4°C and then stored at -80°C.

2.2.2 ICP-MS Analysis of metal ions

Metal ion concentrations were measured in whole blood. All samples were diluted 10-fold using the solubilisation matrix solution (Table 2.7; all reagents Sigma-Aldrich; Dorset, UK). 500µl of whole blood was mixed with 2.5ml of the dilution matrix in a plastic vial and 2ml of ultrapure water (18mΩ) were added. The final solution was then sonicated. Standards were prepared by diluting Multielement Standard Solution 1 for ICP (Sigma-Aldrich (Fluka); Dorset, UK) in 2% (v/v) HNO₃. The samples were then analysed using ICP-MS as described before.

Reagent	% in solution (w/v)	Quantity for 1L solution
1-Butanol	1.5%	15ml
EDTA (acid)	0.01mM	2.9224mg
Triton X-100	0.07%	0.7ml
Ammonium hydroxide	0.7mM	26.92ml
Ultrapure Water	Make up to volume	Make up to 1l

Table 2.7. Preparation of solubilisation matrix solution

2.2.3 Isolation of total RNA that includes the small RNA fraction

In order to extract RNA from blood samples the RiboPure™-Blood Kit (Life Technologies; Paisley, UK) was used. Using the modified protocol provided with the kit, total RNA that includes the small RNA fraction (RNA < 200nts) was isolated.

2.2.3.1 Sample Collection, Cell Lysis, and RNA Purification

Initial experiments were conducted to show the efficacy of *RNAlater* in terms of preservation of blood RNA. The maximum period of RNA stability under different conditions was assessed and details of these experiments are given in Chapter 6.

Samples in *RNAlater* solution were centrifuged for 1min at maximum speed in a microcentrifuge. Supernatant was then aspirated and discarded. Archive samples (not stored in *RNAlater* solution) were mixed by gently inverting the collection tube several times. After this, 800µl Ribopure lysis solution were added to 300–500µl anticoagulated whole blood in a 2ml microfuge tube, or to the cell pellet from *RNAlater*-stabilized samples. Samples were then vortexed vigorously inverting the tube to be sure the solution was homogenous. 10µl of the Ribopure sodium acetate solution were added, and the samples were vortexed and stored on ice for 5min. 500µl of the Ribopure supplied Acid-Phenol:Chloroform were added to the cell lysate, after which it was vortexed for 30sec. To separate the aqueous and organic phases, samples were centrifuged at room temp for 1min at maximum speed in a

microcentrifuge. The aqueous (upper) phase containing the RNA was then transferred to a 15ml screw-cap tube and the lower phase was discarded. 1ml of Ribopure denaturation solution and 2.7ml of 100% ethanol were sequentially added and each mixed thoroughly by vortexing.

Before starting the process of final RNA purification, 110 μ l per sample of elution solution were heated to 75°C in an RNase-free tube. The RNA sample was bound to a Ribopure filter cartridge by successively applying 700 μ l of sample, centrifuging for a few seconds to let the liquid pass through, emptying the collection tube and repeating. The filter flow-through liquid was discarded every time. The Ribopure filter cartridge was then transferred into a 2ml collection tube, 700 μ l of 70% ethanol/30% denaturation solution applied to the filter cartridge and the sample centrifuged for 5–10sec to allow the solution to pass through the filter. The flow-through liquid from the collection tube was discarded and the filter cartridge was replaced into the same collection tube. This process was repeated twice with 700 μ l aliquots of 80% ethanol/50mM NaCl. After discarding the flow-through from the last wash, the filter cartridge was replaced in the same collection tube and centrifuged for 1min to remove residual fluid from the filter. The Ribopure filter cartridge was transferred into a labelled collection tube and 150 μ l elution solution applied to the centre of the filter. The cap was closed and the assembly was left at room temp for 1min to allow dissociation of the RNA from the column. It was then centrifuged for 20–30sec at maximum speed to recover the RNA in the collection tube.

2.2.3.2 DNase I Treatment

To remove any contaminating genomic DNA from the eluted RNA, 1/20th volume 20X DNase Buffer and 1 μ l DNase I (8U/ μ l) were added to the RNA and mixed gently. The samples were then incubated for 30min at 37°C. Following this, a volume of Ribopure DNase inactivation reagent equal to 20% of the volume of RNA treated was added. Tubes were vortexed briefly to thoroughly mix the DNase inactivation reagent with the RNA, and incubated at room temperature for 2min. The tubes were vortexed twice during this period to resuspend the DNase inactivation

reagent. Samples were then centrifuged at maximum speed for 1min in a microcentrifuge to pellet the DNase inactivation reagent. 5µl aliquots were taken to determine the purified RNA concentration and integrity and the remaining RNA was stored at -80°C.

RNA concentration, purity and integrity were determined as described in Section 2.1.22 of the current Chapter.

2.2.4 cDNA synthesis

First-strand synthesis of cDNA from RNA obtained from whole blood was carried out using Superscript III reverse transcriptase as in Section 2.1.23, however, for the whole blood studies, 400ng of RNA was used in each reverse transcriptase reaction.

2.2.5 Stability of RNA after up to 10 Freeze/Thaw Cycles of storage

Whole blood samples in the presence and absence of *RNAlater* were frozen at -80°C for 15 minutes and thawed at room temperature for 15 minutes. This was repeated several times in an attempt to replicate the real life situation where clinical samples may undergo several freeze/thaw cycles. RNA was extracted with the RiboPure Blood Kit after 0, 3, 6, and 10 freeze/thaw cycles, and RNA concentration and integrity were assessed as previously described.

2.2.6 Taqman quantitative real-time PCR

In order to analyse gene expression of clinical whole blood samples, TaqMan Gene Expression Assays (Table 2.8.) and TaqMan Gene Expression Master Mix (all Applied Biosystems; Paisley, UK) were used.

Briefly, for each reaction 1µl of 20X TaqMan® Gene Expression Assay, 10µl 2X TaqMan® Gene Expression Master Mix, 1µl cDNA (8ng/µl) and 8µl of nuclease-free water were added to a nuclease-free microcentrifuge tube. Negative controls

with nuclease-free water and “RT-”cDNA reaction product were included. Master mixes for each assay were prepared with the primers, nuclease-free water and TaqMan® Gene Expression Master Mix. The components were mixed thoroughly and centrifuged briefly to eliminate any air bubbles. 19µl of each master mixture were transferred to the corresponding wells of optical 8-tube strips. Finally, 1µl of cDNA was added to the reactions, and 1µl of nuclease-free water or “RT-”cDNA reaction product was added to the corresponding controls. Tubes were sealed with optical 8-cap strips and loaded in a StepOnePlus Real-Time PCR system. Thermal cycling conditions were set for a standard run as shown on Table 2.6. Cq values were calculated by the StepOnePlus software (v2.1)

Gene	Assay	Assay ID	Amplicon length
TNF receptor-associated protein 1 (TRAP1)	TaqMan® Probes TRAP1	Hs00212474_m1	64
Folypolyglutamate synthase (FPGS)	TaqMan® Probes FPGS	Hs00909430_m1	69
2,4-dienoyl CoA reductase 1, mitochondrial (DECRI)	TaqMan® Probes DECRI	Hs01051812_m1	67
Peptidylprolyl isomerase B (cyclophilin B) (PPIB)	TaqMan® Probes PPIB	Hs00168719_m1	67
Tumor necrosis factor (ligand) superfamily, member 11 (RANKL)	TaqMan® Probes TNFSF11	Hs00243522_m1	67
Tumor necrosis factor receptor superfamily, member 11b (OPG)	TaqMan® Probes TNFRSF11B	Hs00900358_m1	74
Tumor necrosis factor receptor superfamily, member 11a, NFκB activator (RANK)	TaqMan® Probes TNFRSF11A	Hs00187192_m1	67

Table 2.8. TaqMan gene expression assays.

2.2.7 Effects of RNA integrity on qRT-PCR results

qRT-PCR reactions were carried out with RNA of varying qualities extracted from fresh whole blood samples obtained from patients with metal on metal hip implants. For this purpose, RNA was extracted as previously described from whole blood samples in the presence of *RNAlater* that had undergone freeze/thaw cycles. cDNA was synthesised from both intact and degraded RNA (Section 2.2.4) and real time

PCR reactions carried out (Section 2.2.6) for four genes that have been previously validated as whole blood reference genes in humans (Stamova et al., 2009).

3. EFFECTS OF COBALT IONS AND WEAR METAL DEBRIS DERIVED FROM A HIP RESURFACING ON U937 CELLS *IN VITRO*

3.1 Introduction

The most common cause of failure of total hip arthroplasty is aseptic loosening of the implant. The adverse tissue response to prosthesis wear particles is an important contributor to bone loss around the implant (Luo et al., 2005). As discussed in Chapter 1, host response to a prosthesis or prosthetic debris results in the formation of a fibrous synovial-like membrane surrounding the prosthesis (Wang et al., 1996). It is believed that mononuclear phagocytic cells in the pseudomembrane surrounding the implant phagocytose wear particles and become activated. This activation results in the release of pro-inflammatory cytokines, such as IL-6 and TNF- α , and inflammatory mediators, such as PGE₂, which stimulate osteoclastic bone resorption (Ingham et al., 2000).

As mentioned in Chapter 1, U937 cells have been used as cell culture model for a variety of research related to implant wear debris. However, the mechanisms of toxicity of metal particles and ions are poorly understood. This raises concerns about the long term effects of exposure to metal debris particularly as younger, more active patients are being offered MoM joint replacement for end-stage bone disorders (Rao et al., 2012). In spite the number of investigations that have been carried out, none of them have treated the cells with metal ions (i.e. Co) before exposing the cells to wear particles.

In the current study, U937 cells in both resting and activated states were exposed to metal wear debris derived from a MoM resurfacing implant and Co ions in order to evaluate their toxicity in terms of changes in cell morphology, viability, cytokine production, and proliferation. Moreover, in an attempt to understand host response to a device after revision surgery, U937 cells were treated with Co ions before being exposed to the metal wear debris. Since the MHRA have suggested combined whole blood cobalt and chromium levels of 7ppb (7 μ g/l) as a threshold for patients with

MoM devices (MDA/2010/069), 0.1 μ M Co was chosen as the cobalt concentration for the treatments.

3.2 Aims

To assess the toxicity of Co-Cr nanoparticles released from a resurfacing implant and Co ions, as well as the effect of treating cells with Co ions prior to exposure to wear debris, on an immortalised human cell line *in vitro* by:

- MTT and NR assays for viability
- Fluorescent microscopy to evaluate changes in morphology
- ELISA to measure cytokine production
- BrdU proliferation test

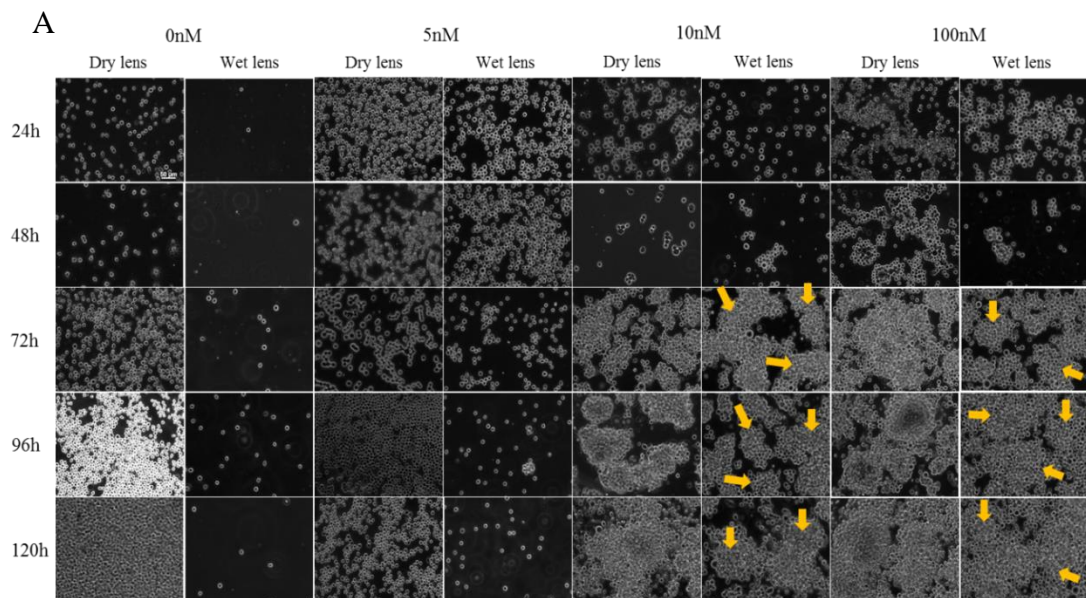
3.3 Results

3.3.1 Activation of U937 cells with PMA

As discussed previously, the human U937 cell line is a common model for the investigation of monocyte/macrophage characteristics and phagocytosis. Upon stimulation with PMA, U937 cells become adherent, form cell aggregates, the number of lysosomes and phagosomes in the cytoplasm increases (Lessig et al., 2011), and they develop phagocytosis activity (Spittler et al., 1997, Boukes and van de Venter, 2012). In this study, U937 cells were exposed to different concentrations of PMA for 5 days in order to determine the appropriate concentration and exposure time that would result in cell activation. Changes in cell aggregation and adhesion were documented every 24h by imaging the cultures (Figure 3.1 and Figure 3.2).

Even though resting U937 cells are non-adherent cells, they tend to sit at the bottom of the wells creating a homogenous layer giving the impression that they have adhered to the surface (Figure 3.1 (20X dry lens images) and Figure 3.2). In order to avoid mistaking this phenomenon with actual cell activation, it was decided to image

cells by using both wet and dry coverslips. When comparing the dry and wet lens images (20X) in Figure 3.1, it becomes clear that non-adherent cells are easily washed off the coverslips. It can also be seen in both figures that adhesion and aggregation occur when cells are exposed to 10 and 100nM PMA for at least three days when compared to the control (0nM). However, such changes were not observed when cells were exposed to 5nM PMA. In Figure 3.1 and Figure 3.2, the 10nM and 100nM images from 72h of exposure show cell aggregates characteristic of the differentiation process of U937 cells.



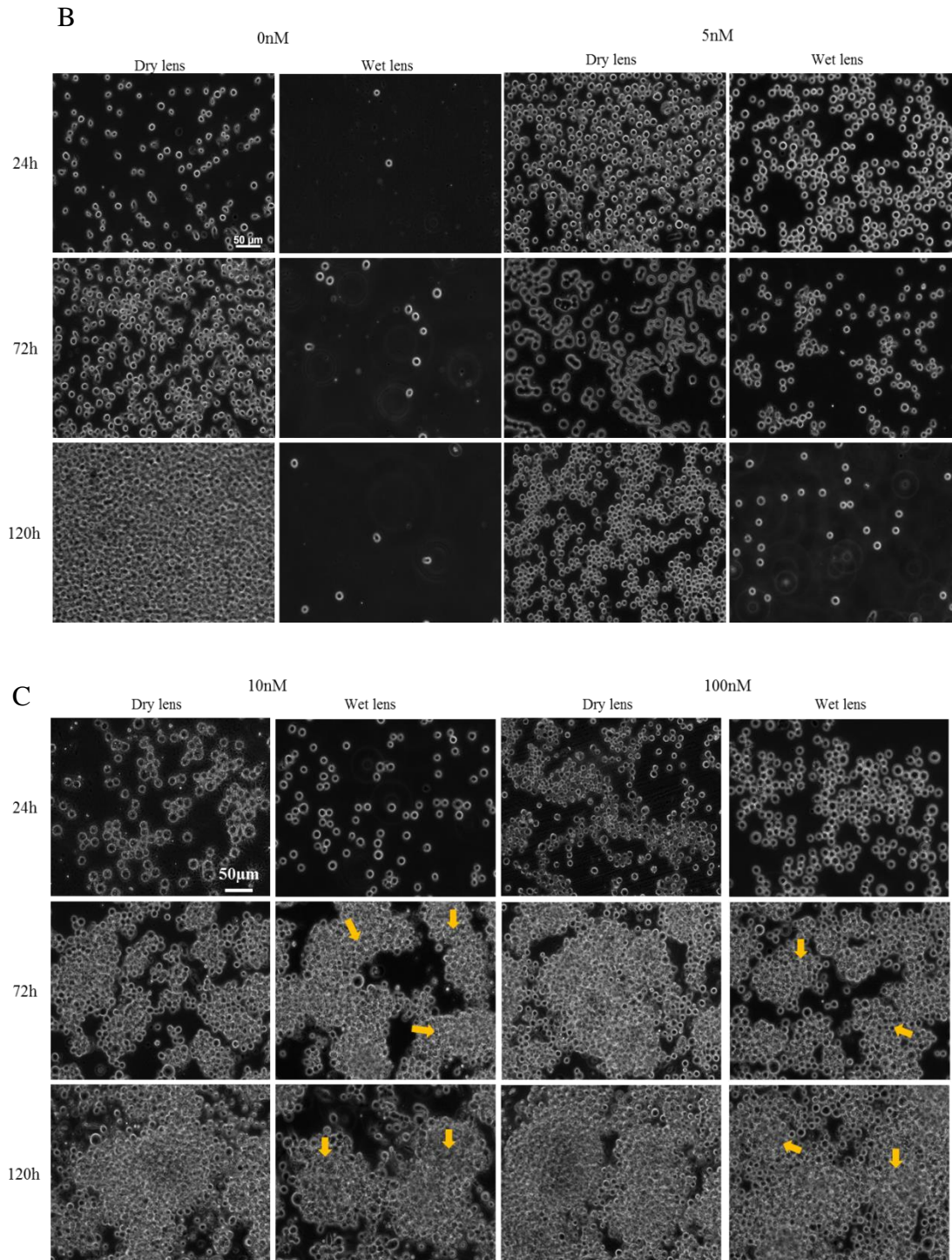
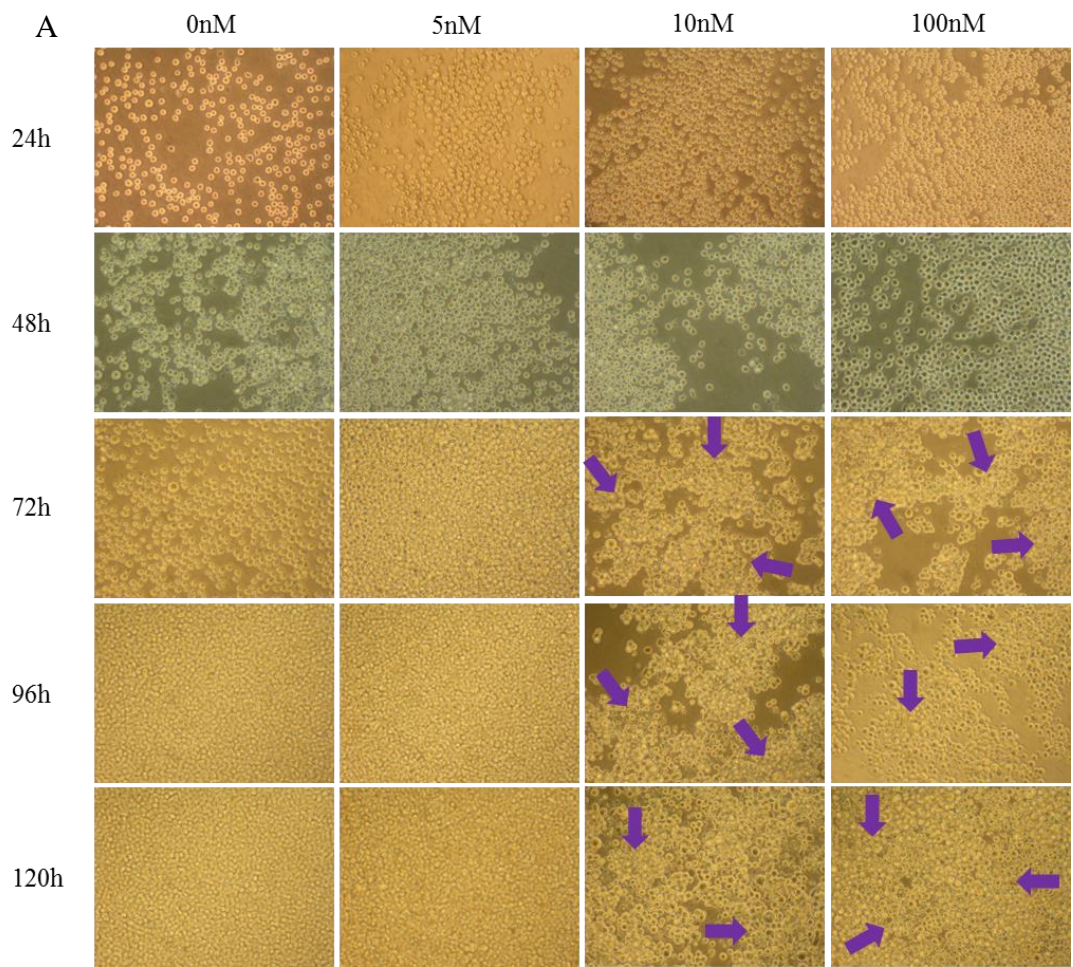


Figure 3.1 Carl Zeiss Axio Imager Microscope images of U937 cells. U937 cells exposed to different concentrations of PMA (0, 5, 10 and 100nM) for five days and imaged every 24h with both dry and wet lenses (20X). A: all PMA concentrations and time points. B: Larger images of 0 and 5nM PMA concentrations at 24, 72 and 120h. C: Larger images 10 and 100nM PMA concentrations at 24, 72 and 120h. Yellow arrows point to cell aggregates indicative of activation.



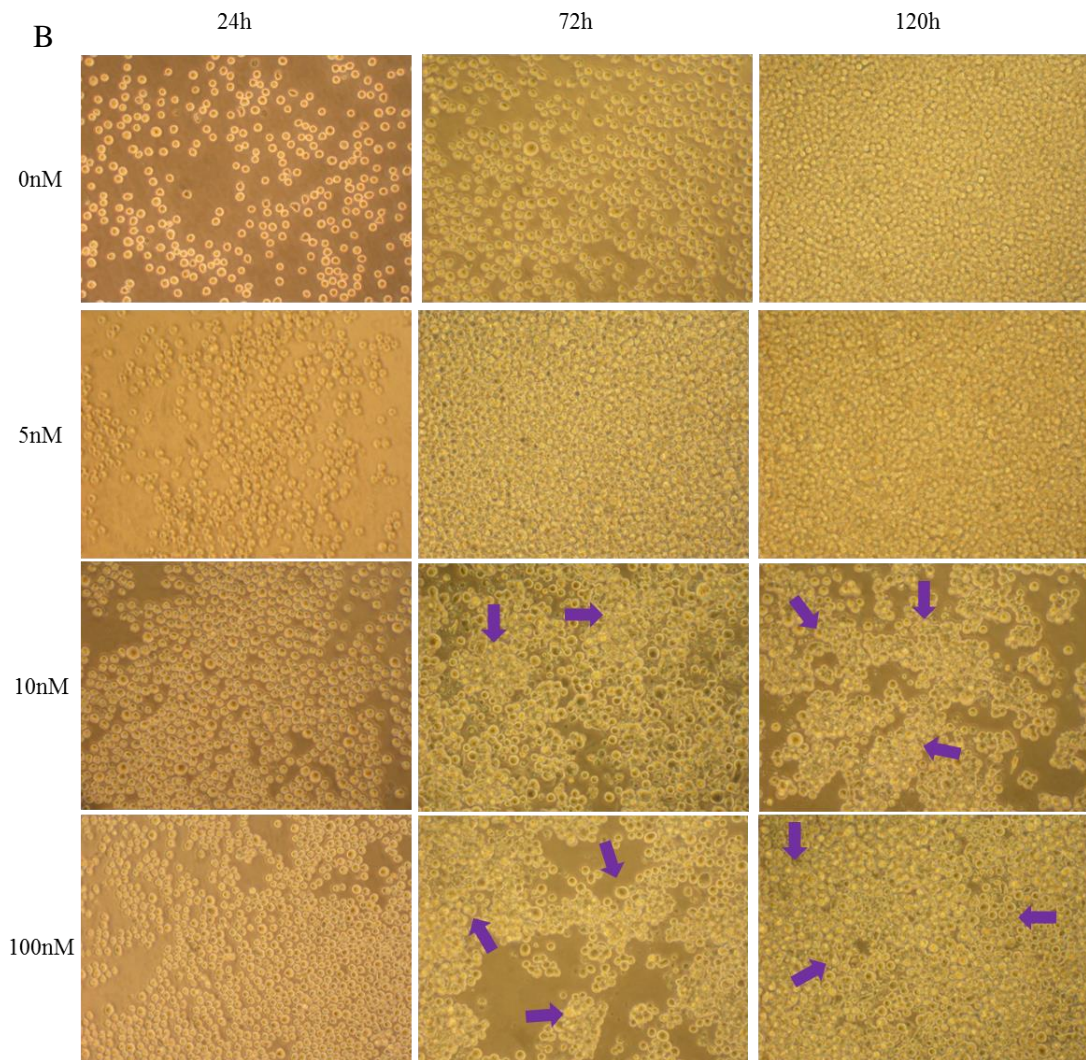


Figure 3.2. Nikon Microscope images of U937 cells (20X). U937 cells exposed to different concentrations of PMA (0, 5, 10 and 100 nM) for five days and imaged every 24h. Purple arrows point to cell aggregates indicative of activation. A: All PMA concentrations and timepoints. B: Larger images at 24, 72 and 120h.

The differentiation of U937 cells was also verified with a MTT metabolic assay after a 24, 48, 72, 96, and 120h exposure to PMA. MTT shows that there was a significant increase ($p < 0.05$) in adherent cell numbers after being exposed to 10 and 100nM of PMA for at least 72h (Figure 3.3). These results are in agreement with the observations discussed above. Resting cells tend to sit at bottom of the wells but are easily whashed off during the performance of the MTT assay. Contrary to this, activated cells adhere to the surface and remain in the wells throughout the assay and therefor significantly higher amounts of formazan can be measured. There was no significant difference between the effect caused by 10 and 100nM concentrations.

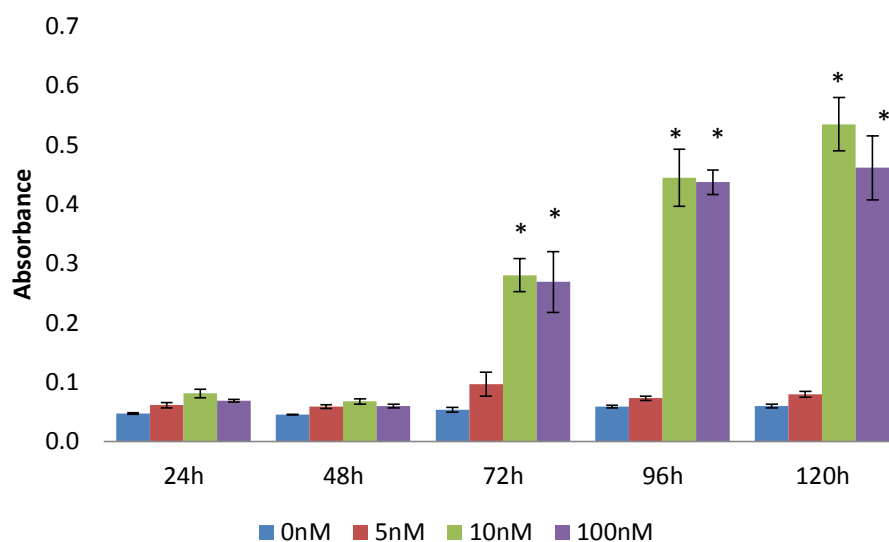


Figure 3.3. Presence of U937 cells after 24, 48, 72, 96 and 120h exposure to PMA, measured by MTT. Results are absorbance values (Mean \pm SEM, n=3). 0nM corresponds to control values. *Significantly different from control values ($p < 0.05$) by one-way ANOVA followed by Dunnett's multiple comparison test.

3.3.2 Activated U937 phagocytosis activity

Fluorescent latex beads were used in order to provide evidence of activated U937 cells phagocytosis activity (Figure 3.5). This activity was documented after 1, 2, 3, 4, 5, 24, 48, and 120h. Ost-5, an immortalised rat osteoblast cell line was used as a control (Figure 3.4). Images suggest that the beads remain mainly in suspension for the first 2h since only a few beads could be observed after 2h of incubation. Nevertheless, the amount of precipitated beads increased over time. When comparing the images between the two cell lines over time, there seems to be fewer beads directly on the plastic surface of the U937 cultures. This could be an indication of the phagocytosis activity of the activated U937 cells. Additionally, the fact that beads seem to be restricted to the cell shape, particularly evident in Figure 3.5.F, also suggests that the beads are being phagocytised by the activated U937 cells.

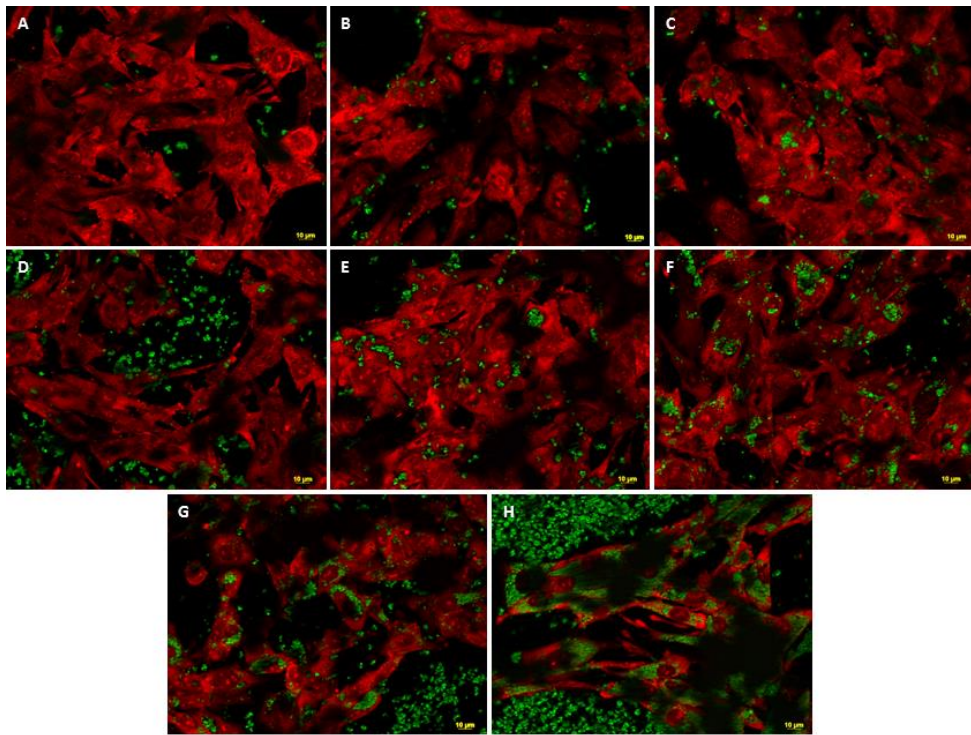


Figure 3.4. Fixed Ost-5 cells and latex beads (40X). PI stained activated cells (red) and FITC-modified latex beads (green). A) 1h, B) 2h, C) 3h, D) 4h, E) 5h, F) 24h, G) 48h and H) 120h.

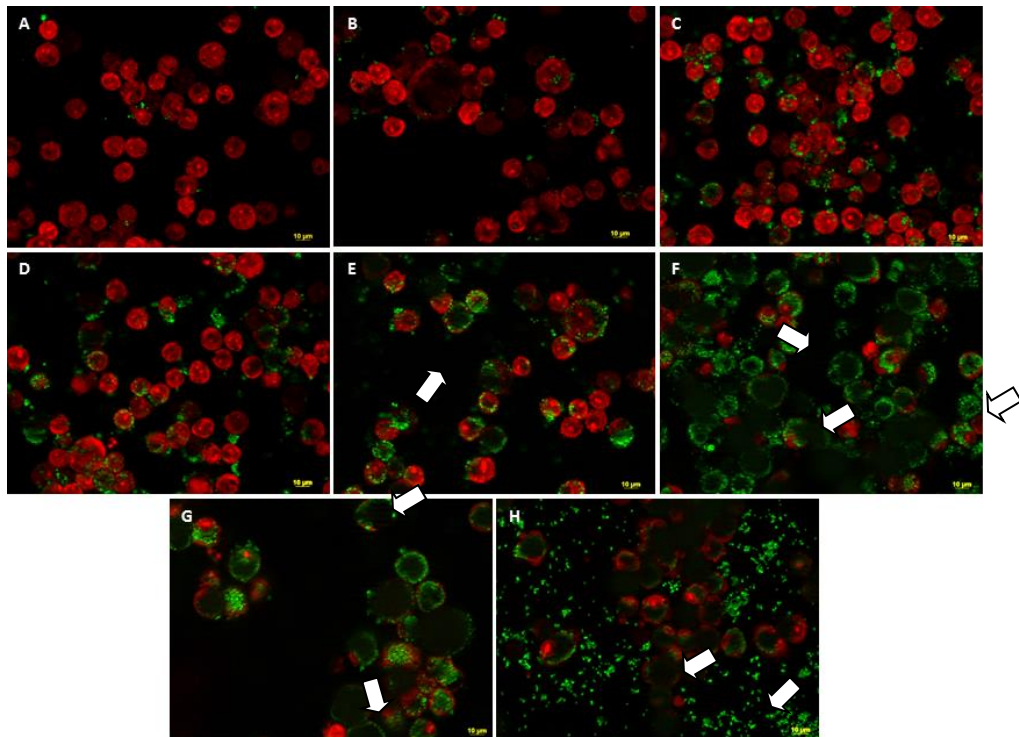


Figure 3.5. Fixed activated U937 cells and latex beads (40X). PI stained activated cells (red) and FITC-modified latex beads (green). A) 1h, B) 2h, C) 3h, D) 4h, E) 5h, F) 24h, G) 48h and H) 120h.

In order to further show that latex beads were not just sitting on top of the activated U937 cells, images of planes at various depths within a sample (z-stacks) were taken at various time points. In Figure 3.6 two individual cells are followed from the top surface through to the bottom after 5h incubation with the latex beads. The average size of U937 cells is approximately 15 μm (Opydo-Chanek et al., 2010, Lessig et al., 2011). Fluorescence slides were captured using the z-stack imaging technique, over a total distance of 13.905 μm . Moving through the sequence (following the cell circled in red) we can see the latex beads within the cells come into focus at a depth of approximately 5.208 μm (slide 3, Figure 3.6) and then moving out of focus again at a depth of approximately 12.161 μm (slide 7, Figure 3.6); the localisation of the beads in this central region indicates they have been internalised and are fully encapsulated by the cells.

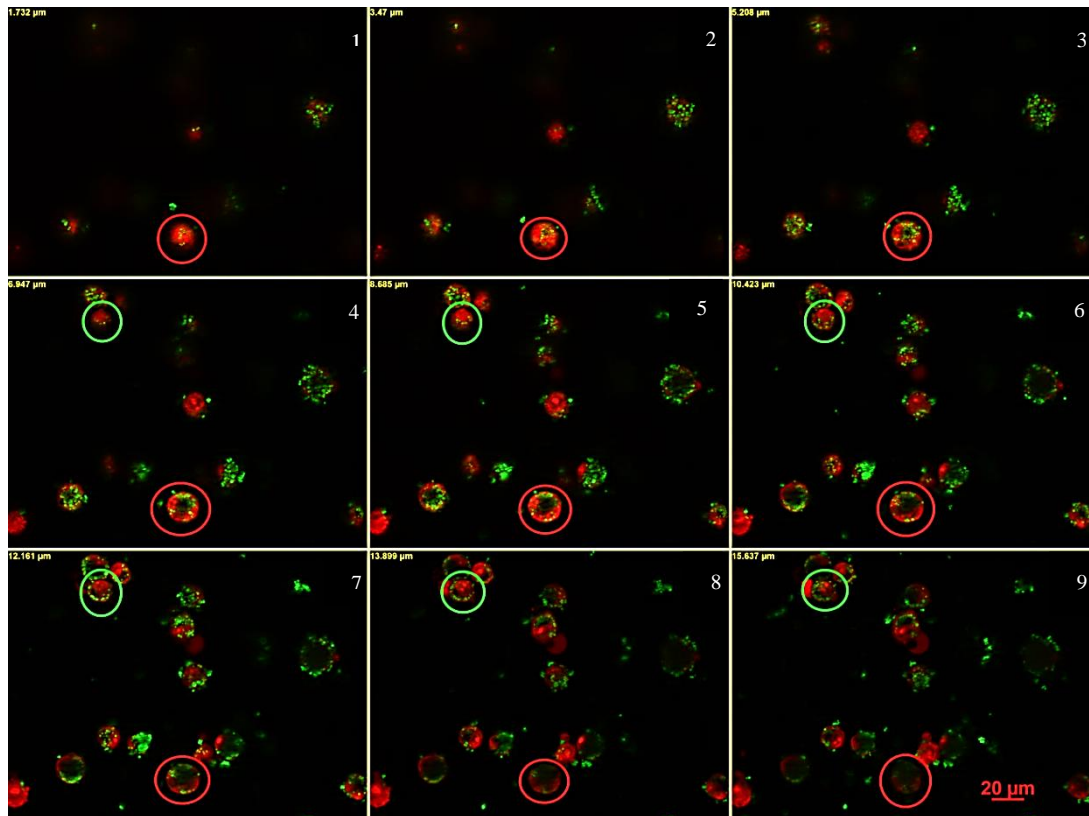


Figure 3.6. Images of planes at various depths within a 5h activated U937 cell sample (40X). PI stained activated cells (red) and FITC-modified latex beads (green). Coloured circles follow single cells through the changing depth. Sequence starts at the left upper corner. Image depths are at the left upper corner of each individual image and are as follows: 1) 1.732 μm , 2) 3.470 μm , 3) 5.208 μm , 4) 6.947 μm , 5) 8.685 μm , 6) 10.423 μm , 7) 12.161 μm , 8) 13.899 μm and 9) 15.637 μm .

3.3.3 Characterisation of CoCr wear debris

Wear debris produced on a hip simulator from a DePuy ASR resurfacing implant is shown in Figure 3.7. The hip simulator replicates the motion of the human hip. The acetabular cup can be positioned in a number of ways relative to the machine axes. Either the ball or cup can be the fixed or mobile partner. A Plexiglas chamber or flex sleeve surrounds the hip joint to hold the lubricating fluid. A physiological load profile mimics the *in vivo* walking load with a frequency of typically one cycle per second (Brown and Clarke, 2007). For this investigation, the acetabular inserts were mounted at 35° to the horizontal plane and positioned anatomically. The femoral components were positioned vertically below the cups resulting in the contact region developing on the pole. The simulator had flexion–extension -15° to 30° (on the head) and internal–external rotation of ±10° (on the cup) to replicate the motions and kinematic paths applied during normal gait. The lubricant (distilled water) was collected at the end the 250,000 cycles.

The SEM images show different shapes and sizes varying from the nano to the micro scale. These images suggest that the particulate debris aggregates. Infiltrate from a hip implant patient obtained during the revision surgery was also imaged (Figure 3.8). Similarly, there seems to be different shapes and varying sizes. Additionally, this particulate debris appears to be aggregated and attached to protein.

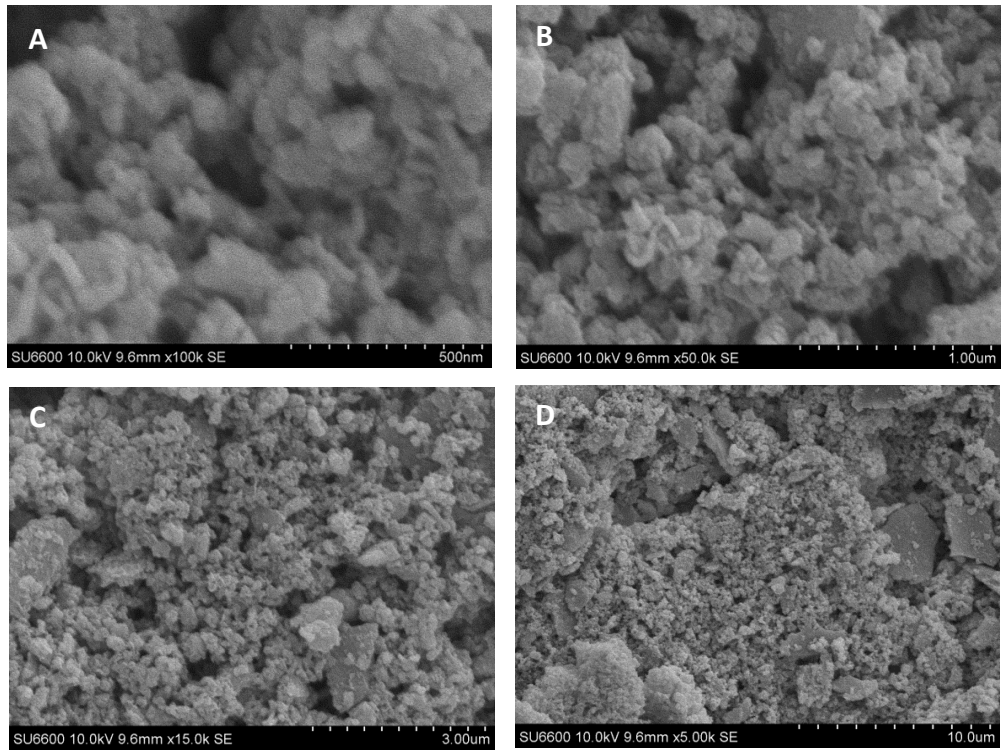


Figure 3.7. Scanning Electron Microscopy images of simulator generated wear debris from an ASR hip implant. Images taken at A) 100kX, B) 50kX, C) 15kX and D) 5kX with a FE-SEM Hitachi SU-6600.

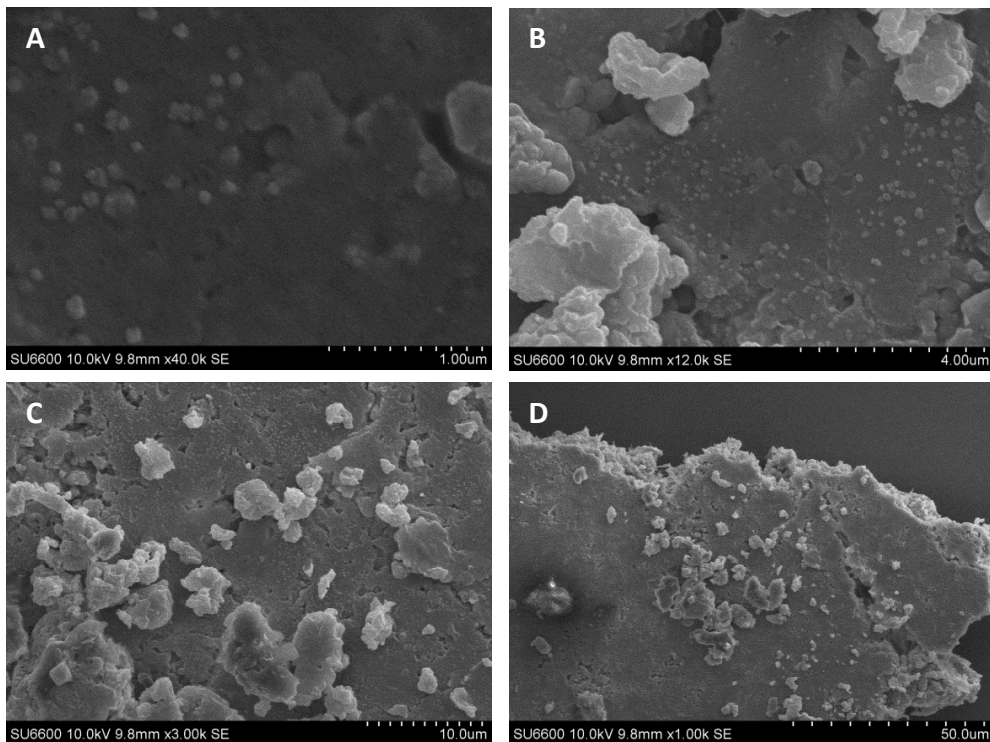


Figure 3.8. Scanning Electron Microscopy images of wear debris from the implant retrieved from a patient undergoing revision surgery. Images taken at A) 40kX, B) 12kX, C) 3kX and D) 1kX with a FE-SEM Hitachi SU-6600.

The composition of simulator generated wear debris (Figure 3.9) and an implant retrieved from a patient undergoing revision surgery (Figure 3.10) was analysed with Energy Dispersive X-ray Spectroscopy (EDS), which indicated that both types of debris are primarily composed of cobalt and chromium.

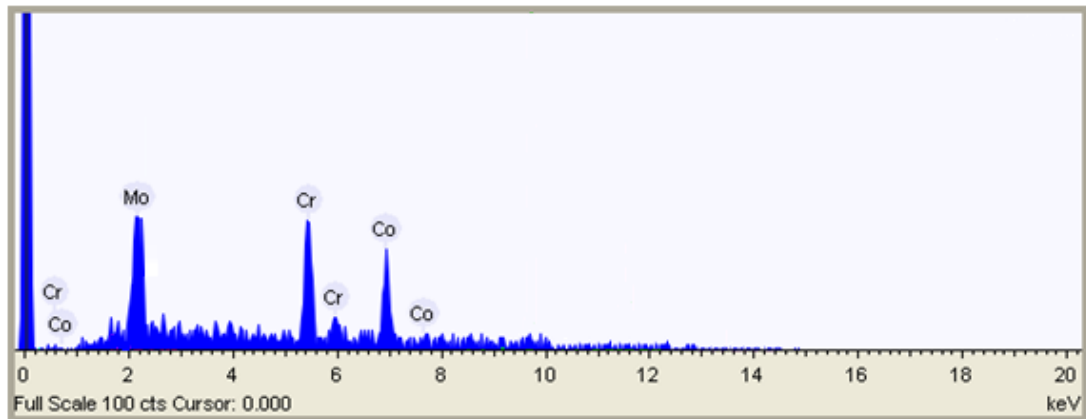


Figure 3.9. Energy Dispersive X-ray Spectroscopy of simulator generated wear debris from an ASR hip implant.

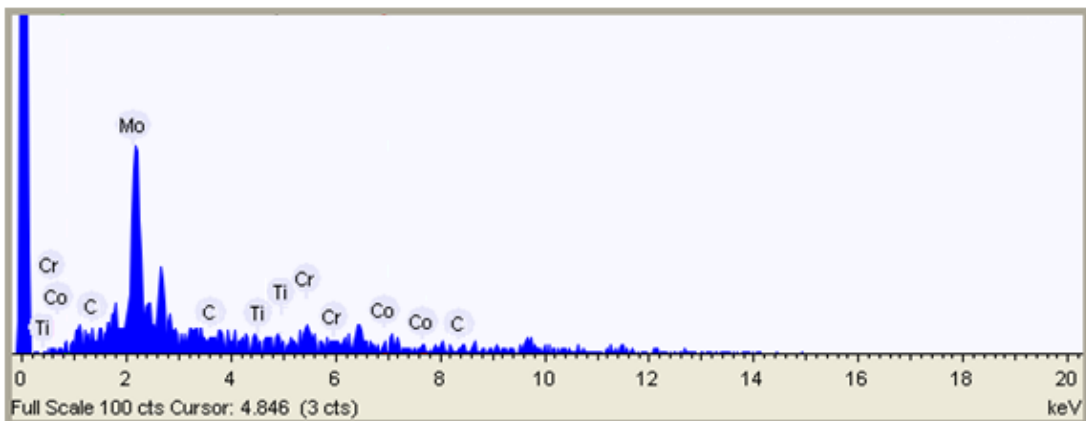


Figure 3.10. Energy Dispersive X-ray Spectroscopy of sample from a patient undergoing revision surgery.

Analysis of 25 simulator generated particles showed a mean composition of 59.57% cobalt and 40.43% chromium (Figure 3.11). On the other hand, 25 particles from the infiltrate of a patient undergoing revision surgery showed a mean composition of 10.43% cobalt, 83.05% chromium and 6.52% titanium (Figure 3.11). Interestingly, traces of organic material (i.e. carbon) were also detected. In both cases, molybdenum could not be detected. It is important to note that the retrieved implant

debris sample was composed of a much greater percentage of chromium than the debris from the artificial simulator.

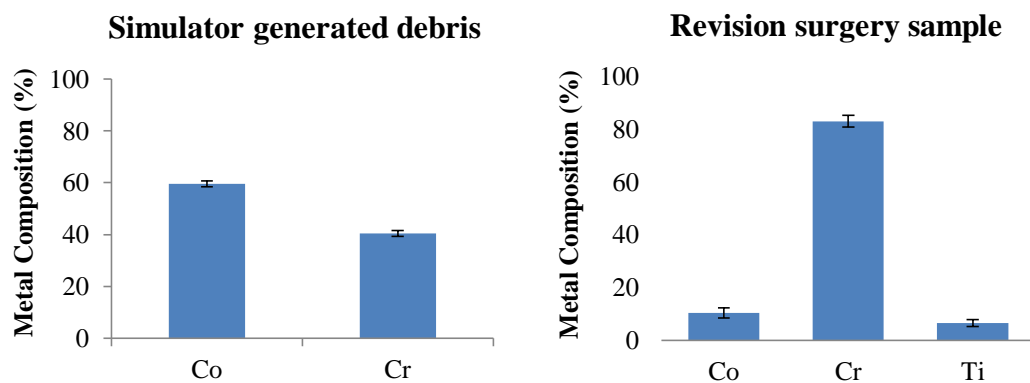


Figure 3.11. Composition of simulator generated CoCr wear debris from an ASR hip implant and infiltrate from a patient undergoing revision surgery, analysed by EDS. Results are means \pm SEM, n=1 (25 independent measurements of 1 biological replicate).

3.3.4 Sterility of CoCr wear debris to be used in cell culture experiments

The sterility of the simulator generated CoCr alloy metal wear debris was evaluated in order to avoid the possibility that the effects observed and measured would be the result of exposure to contaminants present in the particles and not the particles themselves.

For this purpose, dendritic cells (DCs) were cultured in complete RPMI-1640 alone or supplemented with sterile PBS, 1 μ g LPS, or 0.2mg metal debris /1x10⁶cells. DCs express receptors, such as TLR, which upon binding their ligands activate the cells by triggering differentiation pathways that culminate in the acquisition of a mature phenotype characterized by high surface expression of MHC class II (MHC II) and T cell co-stimulatory molecules (e.g. CD80, CD86, and CD40) (Vega-Ramos and Villadangos, 2013). Exposure of DCs to LPS (positive control) resulted in cell activation documented as a significant increase in surface expression of both stimulatory proteins CD40 and MHC II (Figure 3.12). On the other hand, endotoxin free PBS did not elicit a cell response. Moreover, heat-treated metal debris

resuspended in endotoxin free PBS did not cause an increase of either of the stimulatory proteins validating the sterility of the particles.

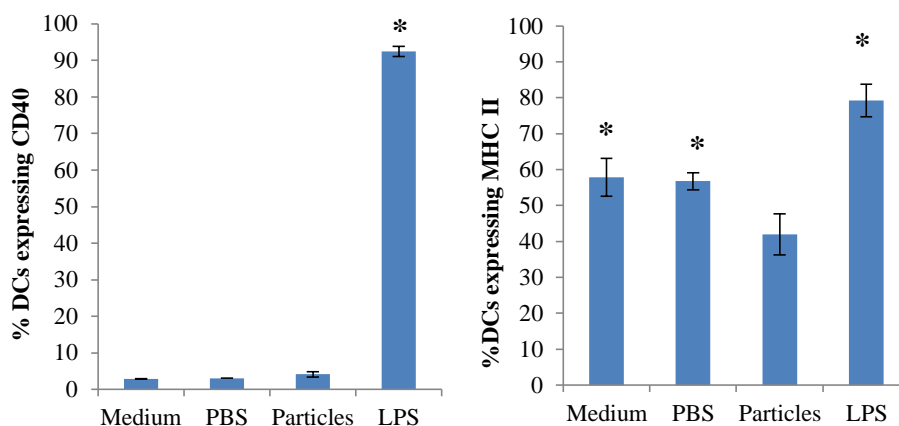


Figure 3.12. Activation of CD11c+ dendritic cells (DCs). Results are mean percentages of DCs expressing stimulatory surface proteins (\pm SEM, n=3) following 24h culture in complete RPMI-1640 alone or supplemented with sterile PBS, 1 μ g LPS or 0.2mg metal debris / 1×10^6 cells. *Significantly different from metal debris values ($p < 0.05$) by one-way ANOVA followed by Dunnett's multiple comparison test.

3.3.5 Effects of metal debris and ions on cell viability measured by MTT and NR

3.3.5.1 Resting U937 cells exposed to CoCr wear debris and Co ions

The effects of three different concentrations of CoCr wear debris on the viability of resting U937 cells were measured in terms of metabolic activity (MTT) and cell number (NR). For this purpose, cells were exposed to 0.05mg/ 1×10^6 cells, 0.1mg/ 1×10^6 cells and 0.2mg/ 1×10^6 cells wear debris for 24, 48, and 120h. Figure 3.13 summarises the results of both MTT (Figure 3.13.A) and NR (Figure 3.13.B). There was a significant increase in metabolic activity of cells exposed for 24h to all three concentrations of debris, as measured by the increase of MTT. This initial increase gradually decreases reaching control levels at 120h as seen in Figure 3.13.A. On the other hand, no significant difference in NR results suggested no change in cell number in cells treated with metal debris when compared to controls (Figure 3.13.B). These results seem to suggest that at low concentration, CoCr wear debris may not affect cell viability.

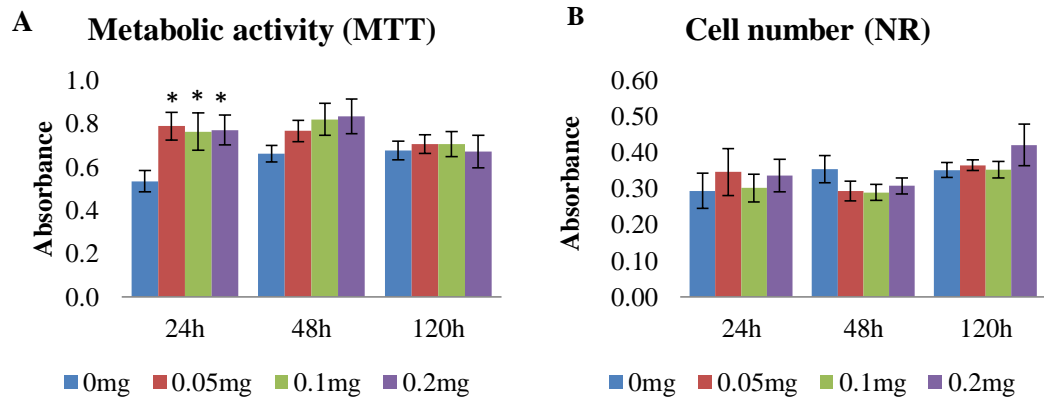


Figure 3.13. Resting U937 cell viability after 24, 48 and 120h of exposure to 0.05mg/1x10⁶ cells, 0.1mg/1x10⁶ cells and 0.2mg/1x10⁶ cells wear debris. Results are absorbance values (\pm SEM, n=15) where 0mg represents control untreated cells.*Significantly different from control values ($p < 0.05$) by one-way ANOVA followed by Dunnett's multiple comparison test.

Aseptic loosening usually leads to revision surgery (Maezawa et al., 2009, Naal et al., 2011, Sehatzadeh et al., 2012). In an attempt to elucidate what the effects of the metal ions that are already present in these patients may have in terms of the biological response to the new device, cells were pre-treated with 0.1 μ M Co for 4 days before being treated with metal wear debris and a combination of debris and 0.1 μ M Co. Following treatments, cell viability was measured in terms of metabolic activity (MTT) and cell number (NR) after 24, 48 and 120h. Figure 3.14 summarises the results from both MTT (Figure 3.14.A-C) and NR (Figure 3.14.D-F) assays. Similarly to the results discussed above, there was a significant increase of metabolic activity in resting cells treated for 24h with debris and the combination of debris and Co, as measured by an increase in MTT. Such increase was also observed in Co pre-treated cells. At 48 and 120h, metabolic activity continued to be elevated particularly in cells exposed to the combination of wear debris and 0.1 μ M Co. In general, cell number did not seem to be affected by the treatments as no significant differences were measured by the NR assay, the exception being cells exposed to 0.2mg/1x10⁶ cells metal debris for 120h. These results seem to suggest that these treatments may not be toxic for resting U937 cells. Additionally, at each end point, MTT and NR results from non Co pre-treated cells were compared to results from Co pre-treated cells to determine if the Co pre-treatment had an impact on cell viability.

Although some differences were observed, it is difficult to establish a general conclusion since a general trend could not be observed.

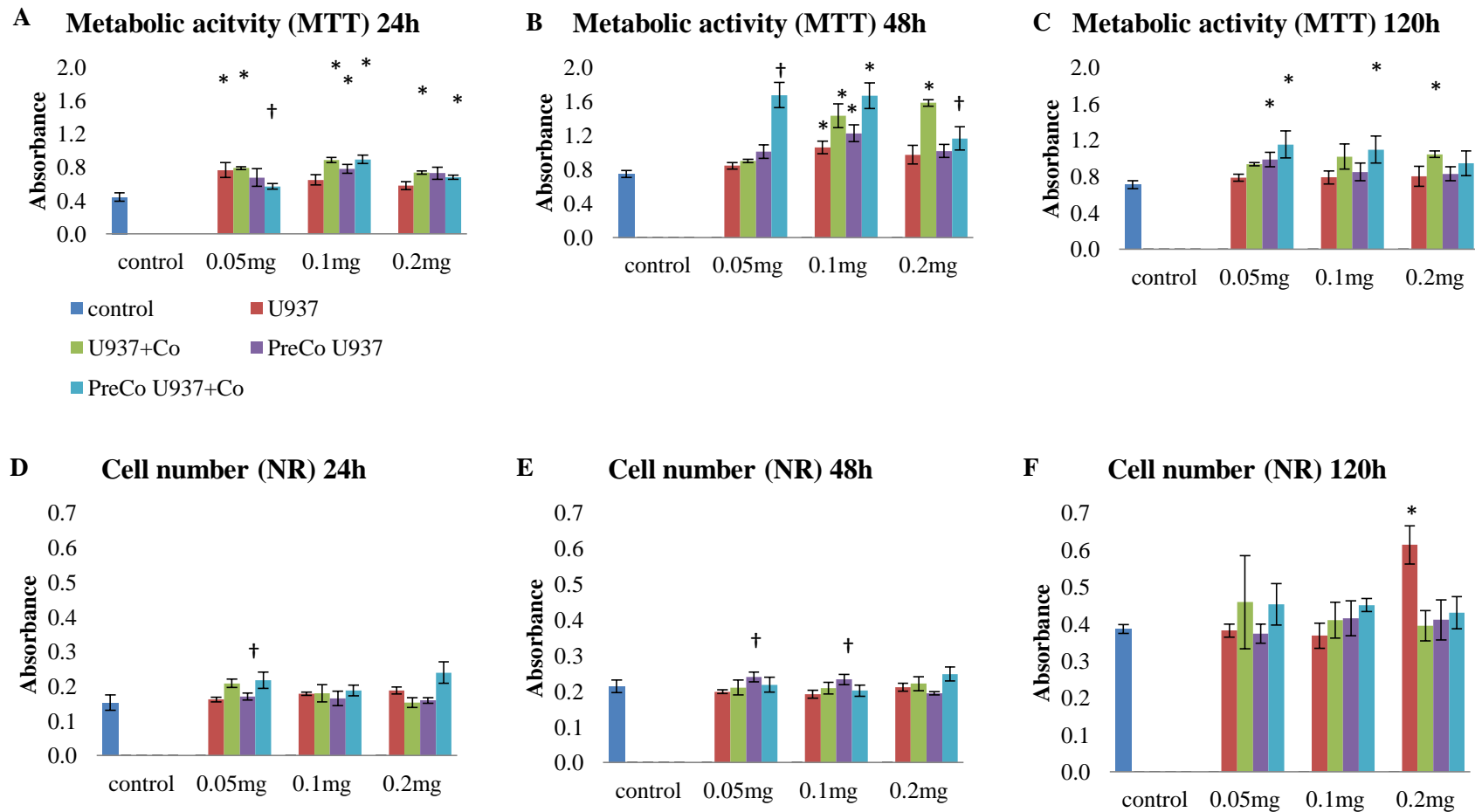


Figure 3.14 Resting and resting Co pre-treated U937 cell viability after 24, 48 and 120h of exposure to 0.05mg/1x10⁶cells, 0.1mg/1x10⁶cells and 0.2mg/1x10⁶cells wear debris. Results absorbance values (\pm SEM, n=6) where controls are untreated cells (0mg). *Significantly different from control values. †Significant difference between non Co pre-treated cell and Co pre-treated cell values (p<0.05) by 2 sample t-Test.

Since the debris concentrations used in the previous experiments did not seem to have a major effect on cell viability and high metal particles and ions concentrations in tissue surrounding the implant at revision surgery have been previously reported (Matziolis et al., 2003, Maezawa et al., 2009, Sehatzadeh et al., 2012), it was decided to increase the wear debris concentration. As a consequence, resting and Co pre-treated resting U937 cells were exposed to 5mg debris/ 1×10^6 cells, $0.1 \mu\text{M}$ Co and the combination of 5mg debris/ 1×10^6 cells with $0.1 \mu\text{M}$ Co. Viability was assessed after 24 and 120h of treatment in terms of metabolic activity (MTT) and cell number (NR). Figure 3.15 summarises the results from both assays.

After 24h of exposure, MTT shows significant increase in cell metabolic activity in cells treated with Co ions and the combination of Co ions and debris. Moreover, MTT shows significant increase in metabolic activity of Co pre-treated cells exposed to debris and Co ions separately. (Figure 3.15.A). However, NR shows a significant decrease on cell number for Co pre-treated resting cells treated with wear debris and the combination of wear debris and Co ions when compared to control untreated resting U937 cells (Figure 3.15.C). After 120h, NR shows a significant decrease in cell number for both resting U937 and Co pre-treated resting U937 cells compared to control when treated with 5mg debris/ 1×10^6 cells and the combination of metal debris with $0.1 \mu\text{M}$ Co (Figure 3.15.D). Similarly, MTT shows a significant decrease in cell metabolic activity for both resting U937 and Co pre-treated resting U937 cells compared to control when treated with 5mg debris/ 1×10^6 cells and the combination of metal debris with $0.1 \mu\text{M}$ Co (Figure 3.15.B). Interestingly, there was a significant increase in both cell number and metabolic activity of cells treated with Co ions alone, as measured by NR and MTT. In addition to the above, the effects on resting U937 and Co pre-treated resting U937 cells were compared in order to establish if the pre-treatment with Co ions made a difference to the effects caused by the exposure to metal debris and Co. At 24h, there is a significant difference in the effect caused by 5mg debris/ 1×10^6 cells in cell number and on the effect of the combination of 5mg debris/ 1×10^6 cells and $0.1 \mu\text{M}$ Co on metabolic activity. At 120h, there is a significant difference on the effects of combined 5mg debris/ 1×10^6 cells and $0.1 \mu\text{M}$

Co on cell number. These results seem to suggest that chronic exposure to high concentrations of wear metal debris could have a detrimental effect on cell viability.

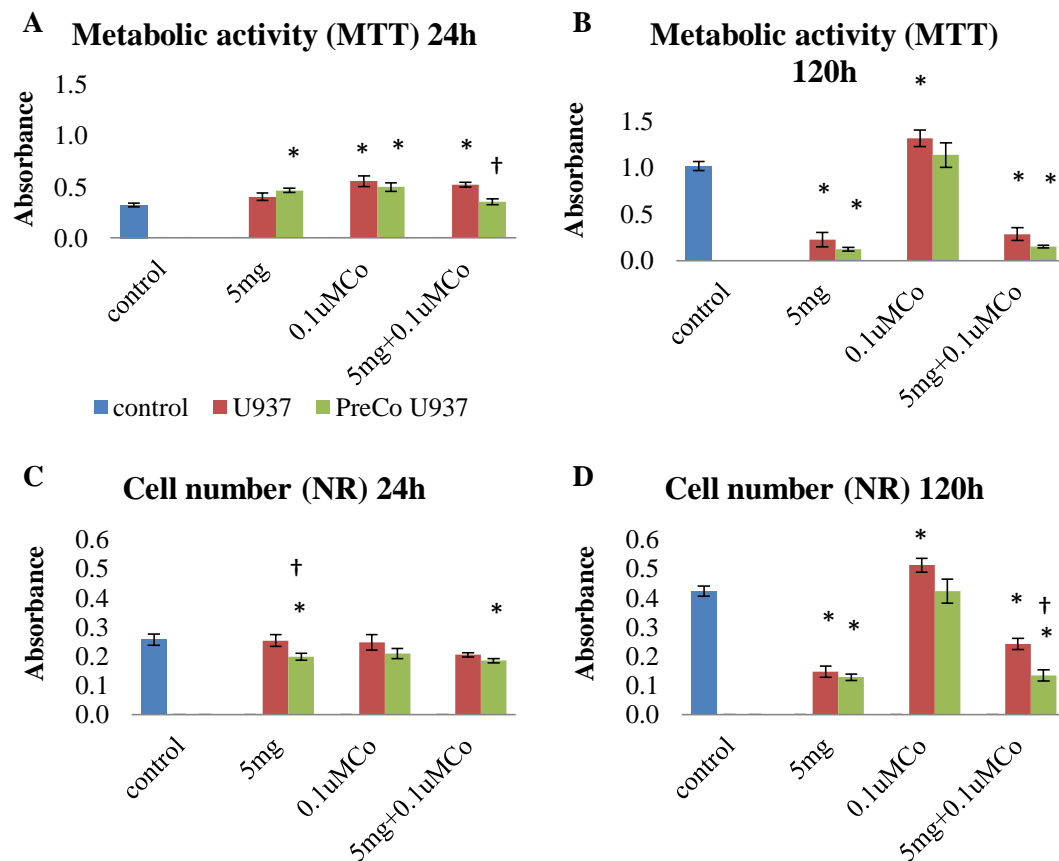


Figure 3.15 Cell viability at 24 and 120h measured by Neutral Red and MTT. Results are absorbance values (Mean \pm SEM, n=9) where control values correspond to resting untreated cells. *Significantly different from control values ($p < 0.05$) by one-way ANOVA followed by Dunnett's multiple comparison test. †Significant difference between non Co pre-treated cell and Co pre-treated cell values ($p < 0.05$) by 2 sample t-Test.

3.3.5.2 Activated U937 cells exposed to CoCr wear debris and Co ions

The experiments with resting U937 cells described above were also carried out with activated U937 cells. Therefore, the viability of activated U937 cells was measured in terms of metabolic activity (MTT) and cell number (NR) after a 24, 48, and 120h exposure to 0.05mg/1x10⁶cells, 0.1mg/1x10⁶cells, and 0.2mg/1x10⁶cells wear debris. Figure 3.16 summarises the results from both MTT (Figure 3.16.A) and NR (Figure 3.16.B). There was a significant increase in metabolic activity of cells exposed to 0.2mg debris /1x10⁶cells for 24h, which decreased by 48h. There was no significant

difference in number of treated cells and controls. These results seem to suggest that low concentrations of CoCr debris do not have a detrimental impact on activated U937 cell viability, which is in agreement with the effects observed on resting U937. However, these findings seem to indicate that the metabolic activity of activated cells was less affected than the activity of resting cells, as measured by MTT after 24h of treatment.

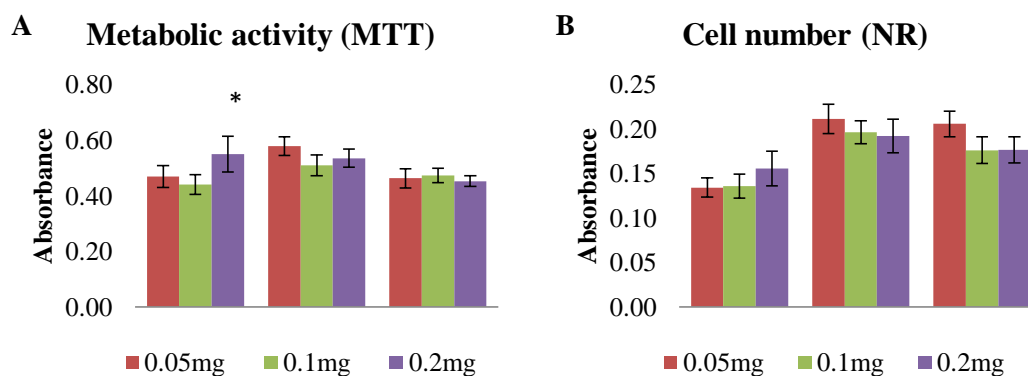


Figure 3.16 Activated U937 cell viability after 24, 48 and 120h of exposure to 0.05mg/1x10⁶cells, 0.1mg/1x10⁶cells, and 0.2mg/1x10⁶cells wear debris. Results are absorbance values (\pm SEM, n=15) where control are untreated cells (0mg). *Significantly different from control values ($p < 0.05$) by one-way ANOVA followed by Dunnett's multiple comparison test.

Additionally, activated cells were also pre-treated with 0.1 μ M Co before being treated with metal debris and a combination of debris and Co. Cell viability was then measured in terms of metabolic activity (MTT) and cell number (NR) after 24, 48, and 120h. Figure 3.17 summarises the results from both MTT (Figure 3.17.A-C) and NR (Figure 3.17.D-F). The main effects were observed after 120h of treatment. These results suggest that activated U937 cell were more susceptible to chronic exposure to the combination of debris and Co ions, as there was significant increase in both MTT and NR (Figure 3.17.C and F). These findings differ from the effects observed on resting cells, which may suggest different mechanisms of wear debris toxicity depending on cellular activation state. Furthermore, at each end point, MTT and NR results from non-Co pre-treated cells were compared to results from Co pre-treated cells to determine if the Co pre-treatment had an impact on the biological response to wear debris in terms of cell viability. Significant differences were

observed mainly in cell number, as measured by NR, after 120h of treatment with the combination of debris and Co ions (Figure 3.17). These differences suggest that the pre-exposure to Co ions could affect the biological response to wear debris. Moreover, these results in conjunction with the results from resting cells seem to indicate that cells respond differently to metal wear debris depending on their activation state.

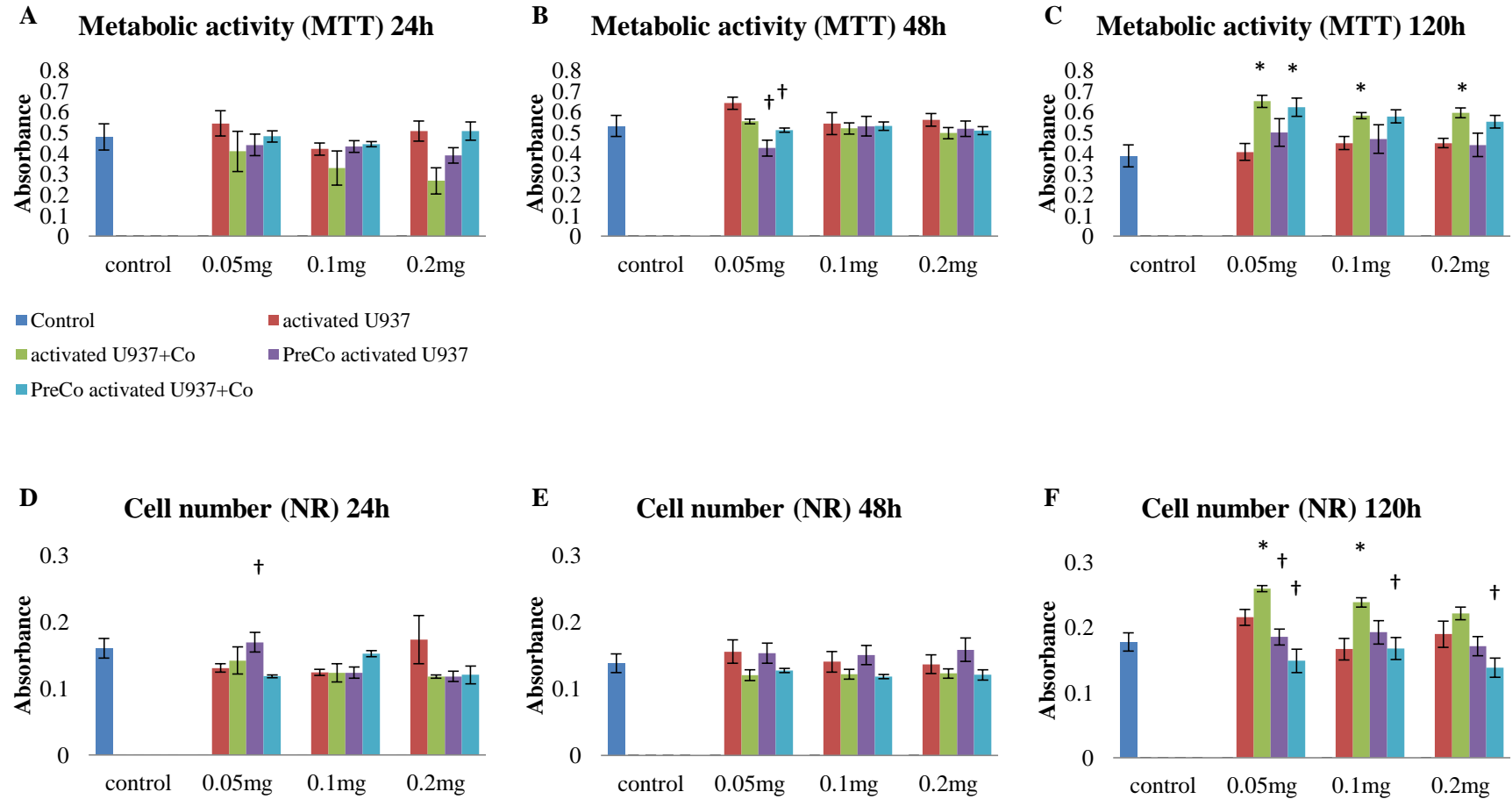


Figure 3.17 Activated and activated Co pre-treated U937 cell viability after 24, 48, and 120h of exposure to 0.05mg/1x10⁶cells, 0.1mg/1x10⁶cells and 0.2mg/1x10⁶cells wear debris. Results are absorbance values (\pm SEM, n=6) where controls are untreated cells (0mg). *Significantly different from control values (p<0.05) by one-way ANOVA followed by Dunnett's multiple comparison test. †Significant difference between non Co pre-treated cell and Co pre-treated cell values (p<0.05) by 2 sample t-Test.

In addition to the above, activated cells were also exposed to higher concentrations of wear debris. For this reason, activated and Co pre-treated activated U937 cells were exposed to 5mg debris/ 1×10^6 cells, 0.1 μ M Co, and the combination of 5mg debris/ 1×10^6 cells with 0.1 μ M Co. Viability was assessed after 24 and 120h of treatment in terms of metabolic activity (MTT) and cell number (NR). Figure 3.18 summarises the results from both assays.

Opposite to the effects seen with the resting cells, after 24h of treatment there were no significant differences in cell viability of activated cells as measured with both MTT and NR (Figure 3.18.A and C). On the other hand and similarly to resting cells, activated cells showed significant decrease in both cell number and metabolic activity after being exposed to 5mg debris/ 1×10^6 cells and the combination of debris and 0.1 μ M Co for 120h (Figure 3.18.B and D). These findings suggest that chronic to metal wear debris has detrimental effects on cell viability. Furthermore, the effects on activated U937 and Co pre-treated activated U937 cells were compared in order to establish if the pre-treatment with Co of the cells affected their response to the exposure to metal debris and Co. Significant differences were mainly observed on metabolic activity as measured by MTT after 24h of treatments (Figure 3.18.A). These differences may indicate that the pre-exposure to Co ions could modulate the cellular response to metal wear exposure. This could be of great importance to patients with MOM implants undergoing revision surgery as it could potentially mean that the metal ions that are already present in their system may affect the biological response to the new device.

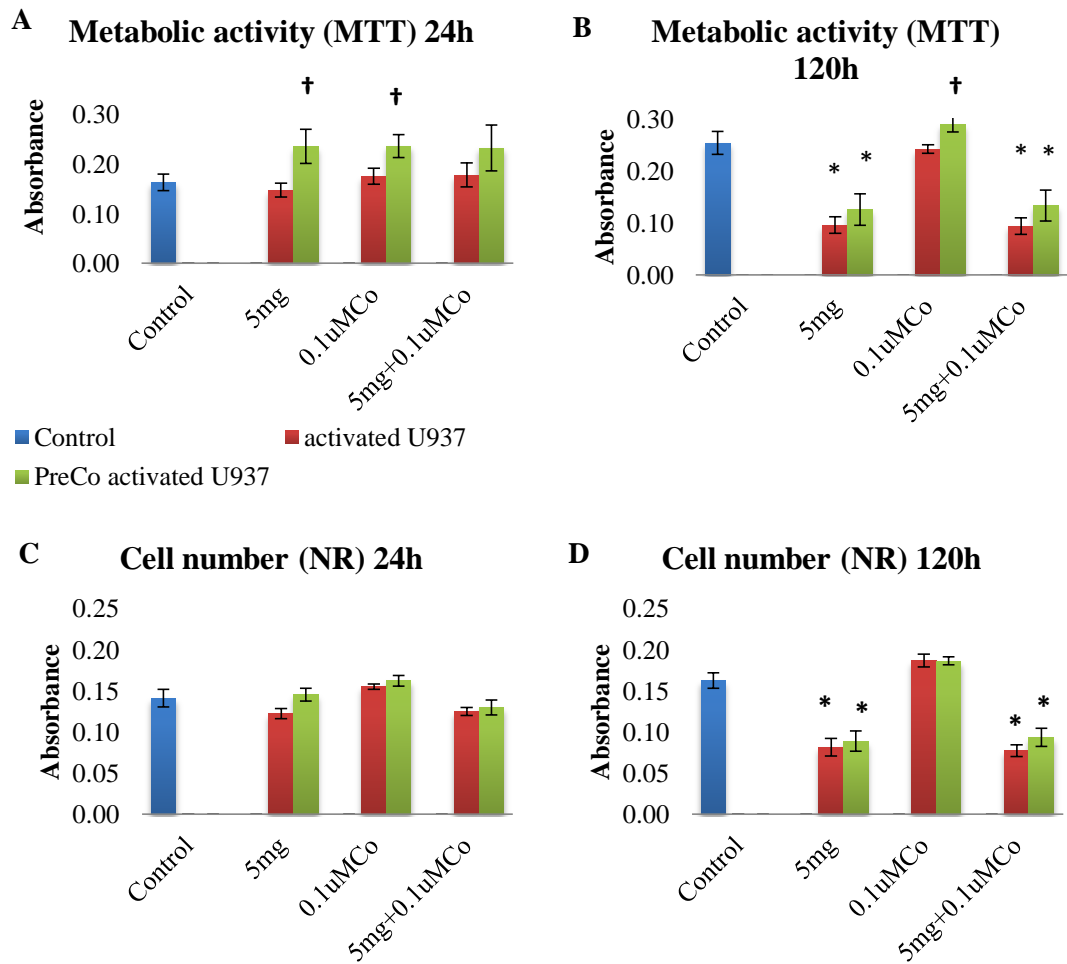


Figure 3.18 Cell viability at 24 and 120h measured by Neutral Red and MTT. Results are absorbance values (Mean \pm SEM, n=9) control values are untreated activated cells. *Significantly different from control values ($p < 0.05$) by one-way ANOVA followed by Dunnett's multiple comparison test. †Significantly different from non Co pre-treated cell values ($p < 0.05$) by 2 sample t-Test.

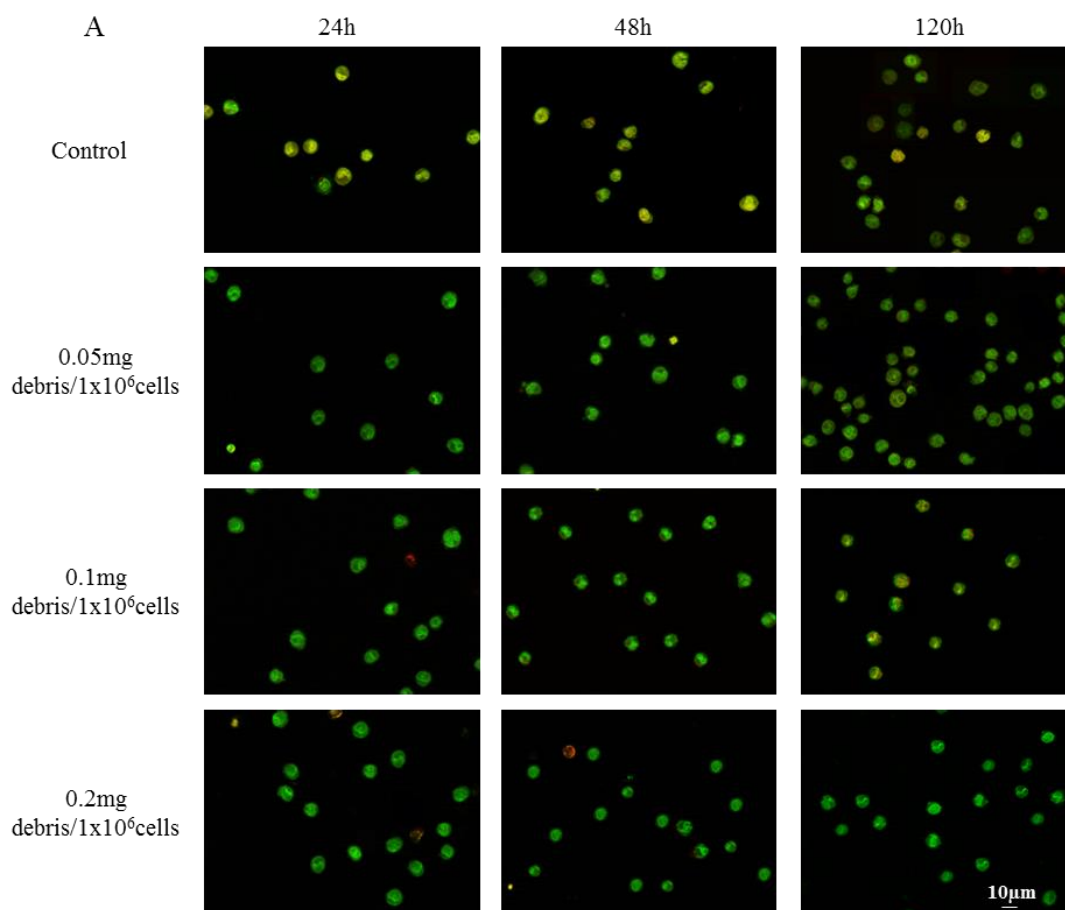
3.3.6 Effects of metal debris and ions on cell morphology assessed with fluorescence microscopy

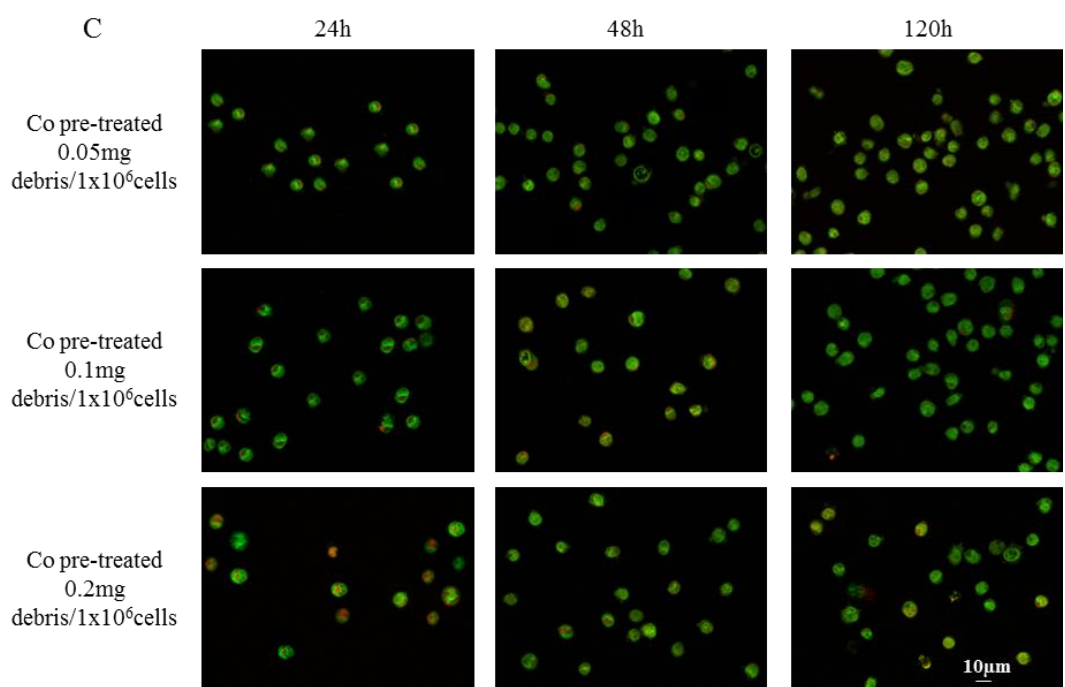
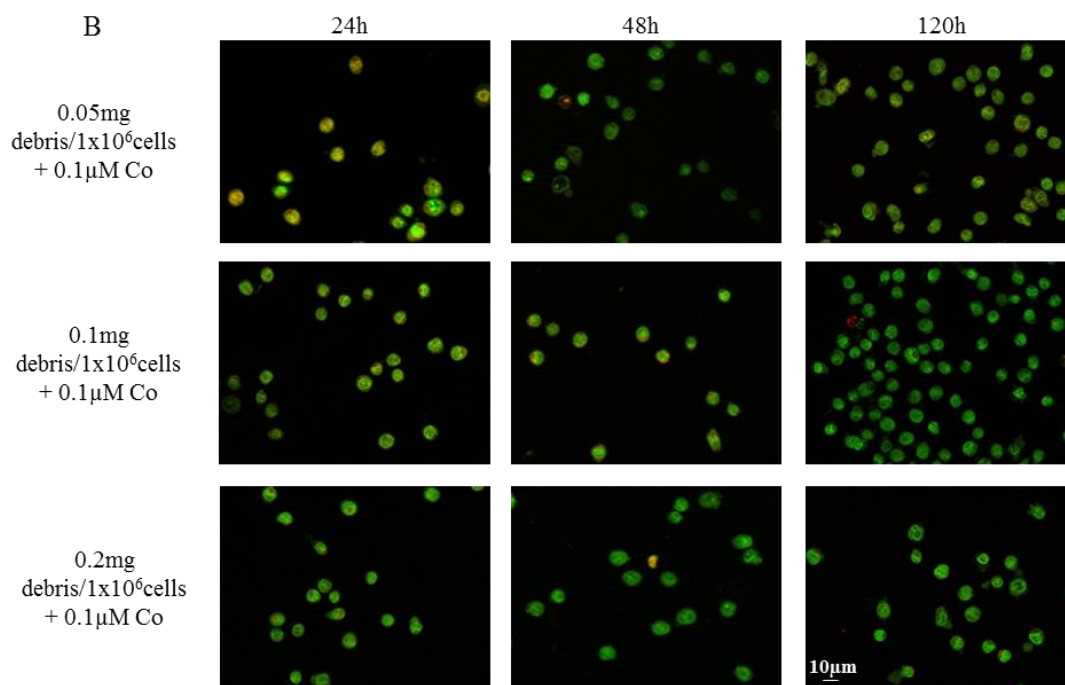
3.3.6.1 Resting U937 cells exposed to CoCr wear debris and Co ions

The effects of three different concentrations of CoCr wear debris on cell morphology of resting and Co pre-treated resting U937 cells were assessed with fluorescence microscopy at each end point. Cells were treated with 0.05mg/1x10⁶cells, 0.1mg/1x10⁶cells, and 0.2mg/1x10⁶cells wear debris and the combination of debris and 0.1µM Co. Following staining with acridine orange (AO) and propidium iodide

(PI) at 24, 48 and 120h, cells were viewed under a Carl Zeiss Axio Imager microscope (Figure 3.19.A-D, more detail can be seen in larger images in Appendix 2.1).

No obvious effect of any of the treatments on cell morphology on either resting or Co pre-treated resting U937 cells was observed when compared to controls after 24, 48 and 120h of exposure.





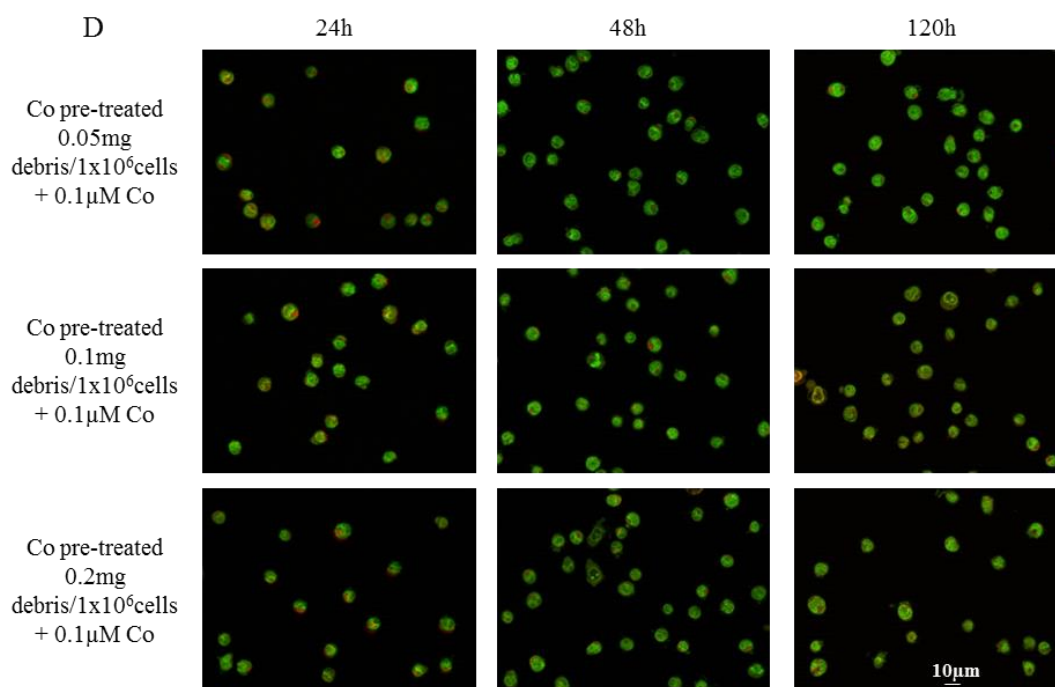


Figure 3.19 Fluorescence microscopy images (40X) following PI (Dead cells, red)/AO (Live cells, green) staining of resting U937 and Co pre-treated resting U937 cells exposed to 0.05mg/ 1×10^6 cells, 0.1mg/ 1×10^6 cells, and 0.2mg/ 1×10^6 cells wear debris for 24, 48 and 120h. A: Resting U937 cells exposed to 0.05mg/ 1×10^6 cells, 0.1mg/ 1×10^6 cells and 0.2mg/ 1×10^6 cells wear debris. B: Resting U937 cells exposed to 0.05mg/ 1×10^6 cells, 0.1mg/ 1×10^6 cells and 0.2mg/ 1×10^6 cells wear debris in combination with 0.1 μ M Co. C: Co pre-treated resting U937 cells exposed to 0.05mg/ 1×10^6 cells, 0.1mg/ 1×10^6 cells and 0.2mg/ 1×10^6 cells wear debris. D: Co pre-treated resting U937 cells exposed to 0.05mg/ 1×10^6 cells, 0.1mg/ 1×10^6 cells and 0.2mg/ 1×10^6 cells wear debris in combination with 0.1 μ M Co. Images are representative of 5 independent images from each sample at each end point.

The effects of high wear debris concentrations on cell morphology of resting and Co pre-treated resting U937 cells were also assessed. Figure 3.20 and Table 3.1 show the effects of 5mg debris/ 1×10^6 cells, 0.1 μ M Co and 5mg debris/ 1×10^6 cells+0.1 μ M Co after 24 and 120h exposure on cellular morphology following staining with AO and PI. Cells were mainly circular and fluoresced green indicating that they were generally healthy following 24h treatment (Figure 3.20.A) and an evident change in the morphology of either resting nor Co pre-treated resting U937 cells was not observed when compared to control. After 120h, cells treated with 0.1 μ M Co did not seem to change morphologically. However, in the presence of metal debris the majority of cells appeared apoptotic; there was cell blebbing and shrinkage (Figure 3.20). Moreover, a decrease in cell number when compared to control was observed (Figure 3.20.B and Table 3.1, more detail can be seen in larger images in Appendix 2.2).

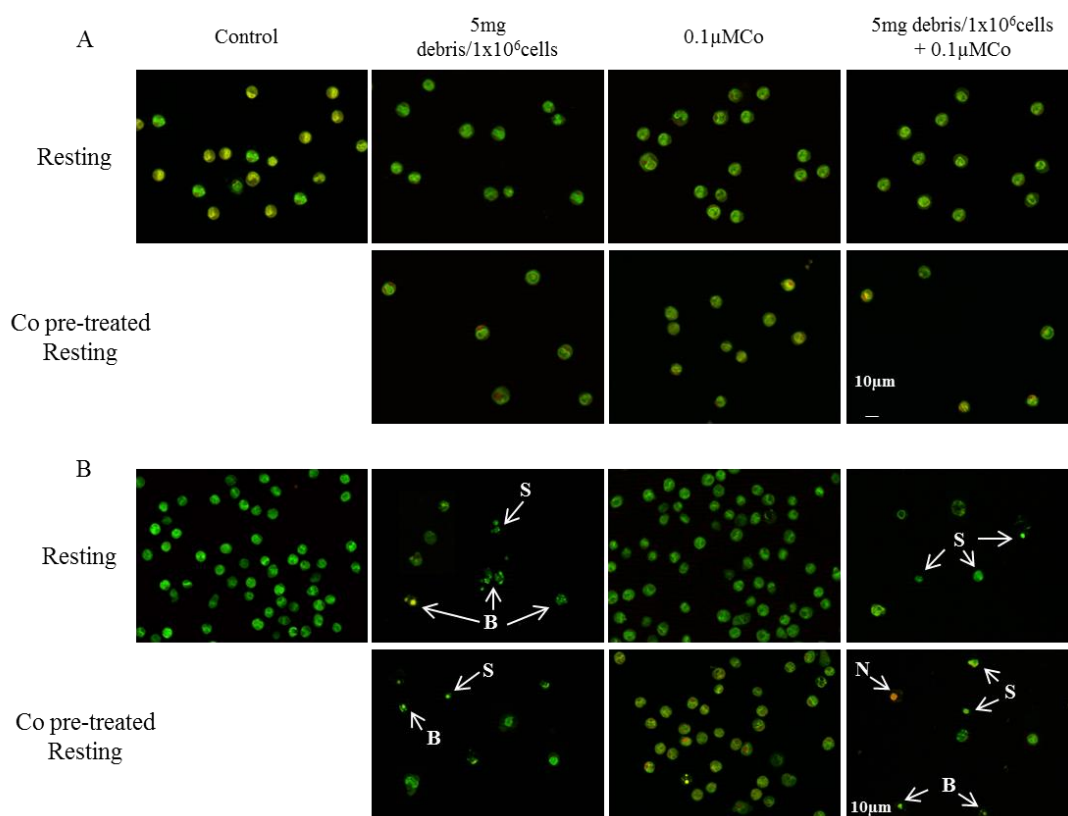


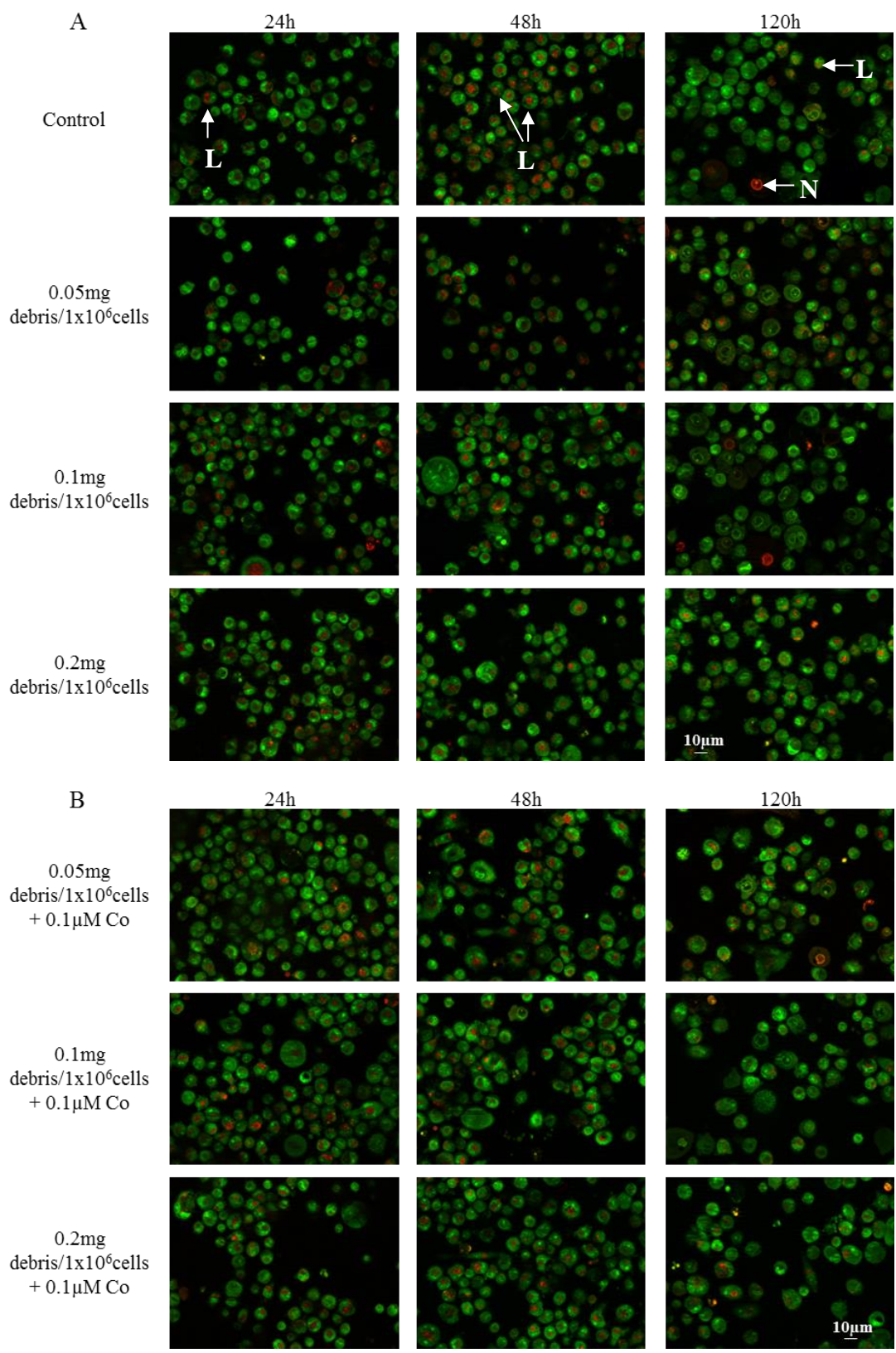
Figure 3.20. Fluorescence microscopy images (40X) following PI (Dead cells, red)/AO (Live cells, green) staining of resting U937 and Co pre-treated resting U937 cells exposed to 5mg debris/ 1×10^6 cells, $0.1 \mu\text{M}$ Co and 5mg debris/ 1×10^6 cells + $0.1 \mu\text{M}$ Co. A: 24h of exposure. B: 120h of exposure. Images are representative of 5 independent images from each sample at each end point. “B” indicates cell blebbing, “S” indicates cell shrinkage and “N” indicates necrotic.

End point	U937 cells	Mean number of viable cells (AO, live cells, green) \pm SEM			
		Control	5mg debris/ 1×10^6 cells	$0.1 \mu\text{M}$ Co	5mg debris/ 1×10^6 cells + $0.1 \mu\text{M}$ Co
24h	Resting	13.80 \pm 2.10	9.50 \pm 1.31	8.36* \pm 1.06	6.50* \pm 0.78
	Co pre-treated resting	-	7.45* \pm 1.58	5.77* \pm 0.54	5.42* \pm 0.83
120h	Resting	29.86 \pm 5.76	4.60* \pm 0.93	42.60 \pm 6.67	4.20* \pm 0.73
	Co pre-treated resting	-	2.50* \pm 0.34	29.13 \pm 3.44	2.33* \pm 0.42

Table 3.1. Mean number of viable resting U937 cells as recorded by Confocal Laser Scanning Microscopy following staining with Acridine Orange and Propidium Iodide. Results are data recorded from a total of 30 independent images from each sample (Mean \pm SEM). *Significantly different from control values ($p < 0.05$) by one-way ANOVA followed by Dunnett’s multiple comparison test.

3.3.6.2 Activated U937 cells exposed to CoCr wear debris and Co ions

The effects of the three low concentrations of CoCr wear debris on cell morphology were also assessed on activated and Co pre-treated activated U937 cells with fluorescence microscopy at each end point. For this reason, cells were treated with 0.05mg/1x10⁶cells, 0.1mg/1x10⁶cells, and 0.2mg/1x10⁶cells wear debris and the combination of debris and 0.1µM Co. Following staining with AO and PI at 24, 48, and 120h, cells were viewed under a Carl Zeiss Axio Imager microscope. AO is a weak base that accumulates mainly in the acidic compartments, preferentially lysosomes (Olsson et al., 1989, Canonico and Bird, 1969, Antunes et al., 2001, Hornung et al., 2008, Kirkegaard et al., 2010). AO fluoresces green in its monomeric state and binds to nuclear and cytosolic DNA and RNA. When AO concentrates in the lysosomes, the formation of dimers takes place and they fluoresce red (Liao et al., 2008, Lessig et al., 2011, Hornung et al., 2008, Denamur et al., 2011). In addition to this, increased numbers of cellular organelles in the cytoplasm, namely mitochondria and lysosomes, is considered a feature of macrophage differentiation (Lopes et al., 2006, Lessig et al., 2011, Daigneault et al., 2010). Figure 3.21 seem to show greater accumulation of AO in activated U937 cells when compared to resting U937 cells (Figure 3.19), which could be indicating an increased in the number of lysosomes, providing another evidence of cell activation. Following 24, 48, and 120h treatment, cells were mainly circular and fluoresced green indicating that they were generally healthy. Some of the images in Figure 3.21 show a few bigger cells, which could due to cells going through division cycle. However, it would seem that cells, particularly cells pre-treated with Co after 120h treatment, were displaying some apoptotic features (more detail can be seen in larger images in Appendix 2.3).



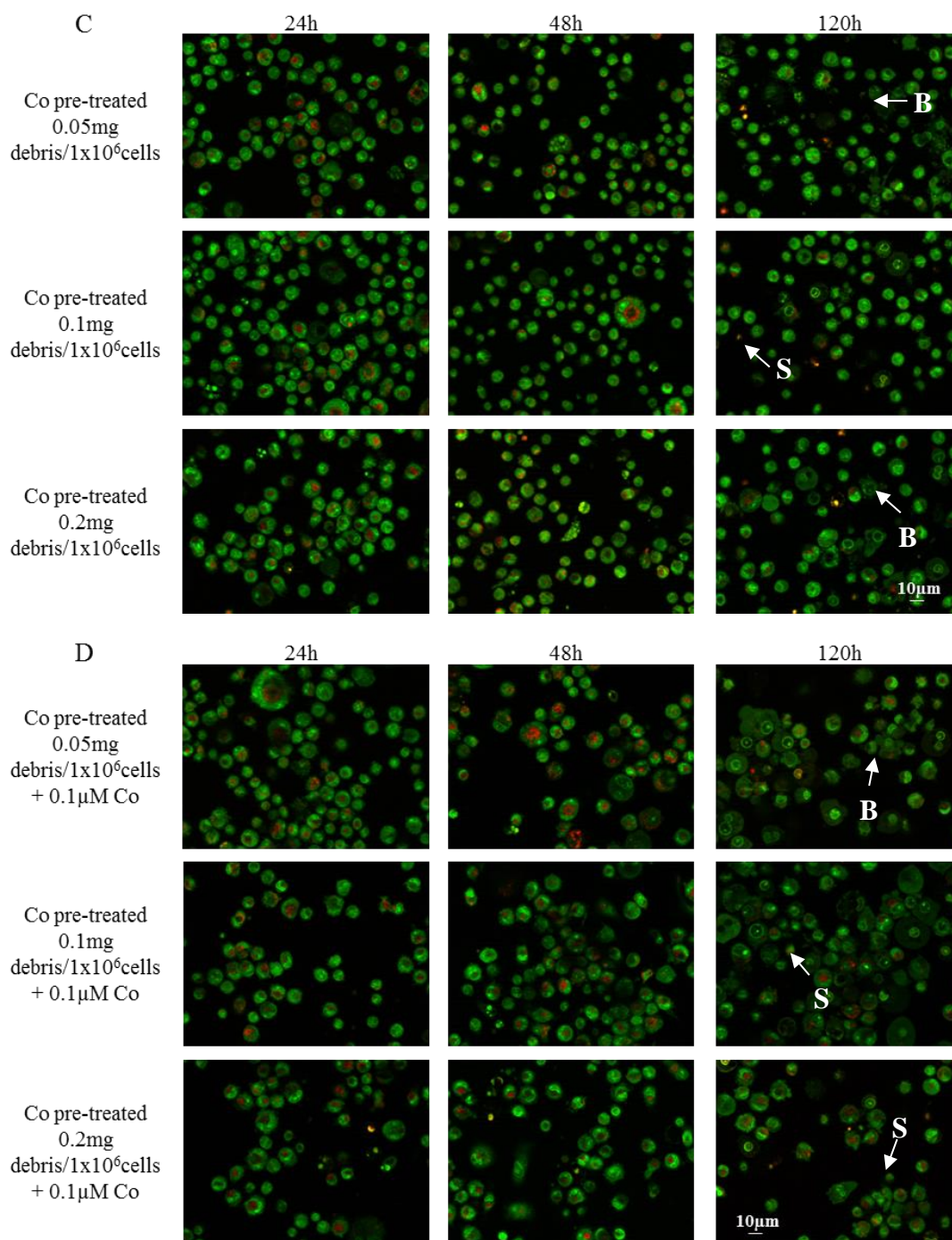


Figure 3.21. Fluorescence microscopy images (40X) following PI (Dead cells, red)/AO (Live cells, green) staining of activated U937 and Co pre-treated activated U937 cells exposed to 0.05mg/ 1×10^6 cells, 0.1mg/ 1×10^6 cells and 0.2mg/ 1×10^6 cells wear debris for 24, 48 and 120h. A: Activated U937 cells exposed to 0.05mg/ 1×10^6 cells, 0.1mg/ 1×10^6 cells and 0.2mg/ 1×10^6 cells wear debris. B: Activated U937 cells exposed to 0.05mg/ 1×10^6 cells, 0.1mg/ 1×10^6 cells and 0.2mg/ 1×10^6 cells wear debris in combination with 0.1µM Co. C: Co pre-treated activated U937 cells exposed to 0.05mg/ 1×10^6 cells, 0.1mg/ 1×10^6 cells and 0.2mg/ 1×10^6 cells wear debris. D: Co pre-treated activated U937 cells exposed to 0.05mg/ 1×10^6 cells, 0.1mg/ 1×10^6 cells and 0.2mg/ 1×10^6 cells wear debris in combination with 0.1µM Co. “L” indicates lysosomes, “B” indicates cell blebbing, “S” indicates cell shrinkage and “N” indicates necrotic.

The effects of high debris concentrations on activated cell morphology were also assessed. Figure 3.22 shows the effects of 5mg debris/ 1×10^6 cells, $0.1 \mu\text{M}$ Co and 5mg debris/ 1×10^6 cells + $0.1 \mu\text{M}$ Co after 24 and 120h exposure on cellular morphology following staining with AO and PI (more detail can be seen in images of Appendix 2.4). After 24h of exposure, there does not seem to be an evident change in the morphology of neither activated nor Co pre-treated activated U937 cells when compared to control. However, after 120h treatment, there was a decrease in cell number of cells in the presence of debris but not Co ions. Furthermore, the few cells observed appeared to be mainly apoptotic (Figure 3.22.B, more detail can be seen in larger images in Appendix 2.4).

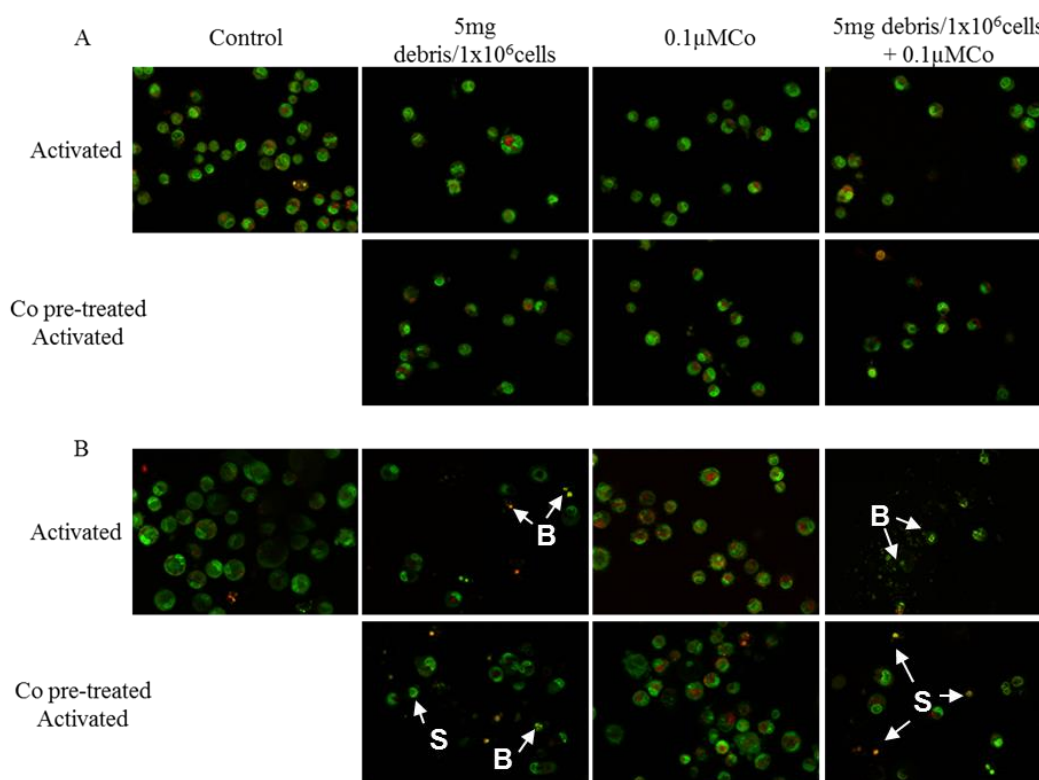


Figure 3.22. Fluorescence microscopy images (40X) of activated U937 and Co pre-treated activated U937 cells exposed to 5mg debris/ 1×10^6 cells, $0.1 \mu\text{M}$ Co and 5mg debris/ 1×10^6 cells + $0.1 \mu\text{M}$ Co. A: 24h of exposure. B: 120h of exposure. “B” indicates cell blebbing, “S” indicates cell shrinkage.

End point	U937 cells	Mean number of viable cells (AO, live cells, green) \pm SEM			
		Control	5mg debris/ 1×10^6 cells	0.1 μ M Co	5mg debris/ 1×10^6 cells + 0.1 μ M Co
24h	Activated	17.79 \pm 2.58	12.36 \pm 1.75	15.71 \pm 1.22	10.64* \pm 1.05
	Co pre-treated activated	-	15.62 \pm 3.00	13.77 \pm 1.92	9.69* \pm 1.12
120h	Activated	16.86 \pm 1.41	5.79* \pm 1.30	15.93 \pm 1.70	5.21* \pm 1.09
	Co pre-treated activated	-	5.57* \pm 0.84	17.90 \pm 1.99	5.00* \pm 0.90

Table 3.2. Mean number of viable activated U937 cells as recorded by Confocal Laser Scanning Microscopy following staining with Acridine Orange and Propidium Iodide. Results are data recorded from a total of 30 independent images from each sample (Mean \pm SEM). *Significantly different from control values ($p < 0.05$) by one-way ANOVA followed by Dunnett's multiple comparison test.

3.3.7 Effects of metal debris and ions on U937 proliferation as measured by BrdU

In the previous sections of this chapter, it was shown that the main effects on cell viability and morphology were observed in the presence of a high wear debris concentration. Consequently, it was decided to assess the effects of such high concentration on cell proliferation and cytokine production. In this section, changes in cell proliferation in response to metal debris and ions exposure are described.

3.3.7.1 Resting U937 cells exposed to CoCr wear debris and Co ions

In order to determine if high concentrations of metal wear debris could have an effect on cell proliferation, resting and Co pre-treated resting U937 cells were exposed to 5mg debris/ 1×10^6 cells, 0.1 μ M Co and the combination of 5mg debris/ 1×10^6 cells and 0.1 μ M Co. Proliferation was then measured via BrdU assay following 24h exposure. Cells in the presence of metal debris seem to have had lower proliferation (Figure 3.23). Additionally, the effects on resting U937 and Co pre-treated resting U937 cells were compared in order to establish if the pre-treatment with Co influenced the cell

response to the treatments. Co pre-treated resting cells proliferated significantly less than non Co pre-treated resting cells when exposed to 0.1 μ M Co alone, as measured by BrdU (Figure 3.23). These findings could suggest a potential role of Co ions in the inhibition of resting U937 cell proliferation.

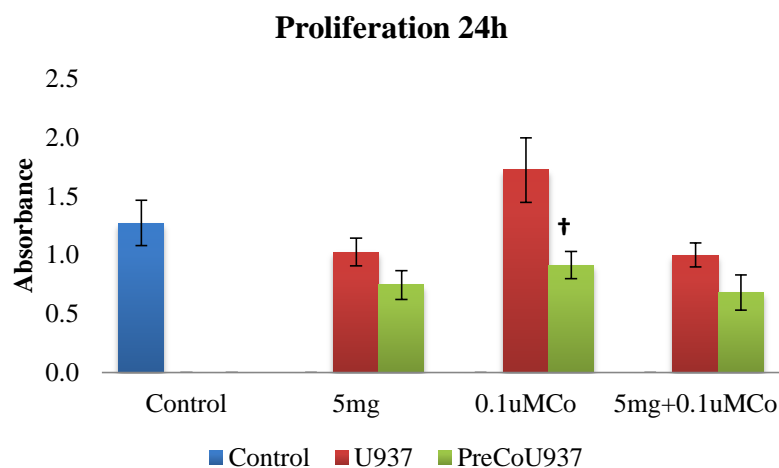


Figure 3.23 Resting U937 cell proliferation at 24h measured by BrdU. Results are absorbance values (Mean \pm SEM, n=8) where controls are resting untreated cells. †Significant difference between non Co pre-treated cell and Co pre-treated cell values ($p < 0.05$) by 2 sample t-Test.

3.3.7.2 Activated U937 cells exposed to CoCr wear debris and Co ions

Activated U937 and Co pre-treated U937 cells were also exposed to 5mg debris/ 1×10^6 cells, 0.1 μ M Co and the combination of 5mg debris/ 1×10^6 cells and 0.1 μ M Co. The effects on cell proliferation were determined with the BrdU assay following 24h exposure. Contrary to the observations from resting U937 cells, the exposure to 0.1 μ M Co caused a significant decrease in the proliferation of activated U937 cells (Figure 3.24). Moreover, the effects on activated U937 and Co pre-treated activated U937 cells were compared in order to establish if the pre-treatment with Co influenced the cell response to the treatments. Figure 3.24 shows that Co pre-treated activated cells proliferated more than non Co pre-treated activated cells in the presence of metal wear debris but no difference was observed in the presence of Co ions alone. These findings differ from the results of resting cells, which suggest that

cellular activation state may influence the biological response to metal particles and ions.

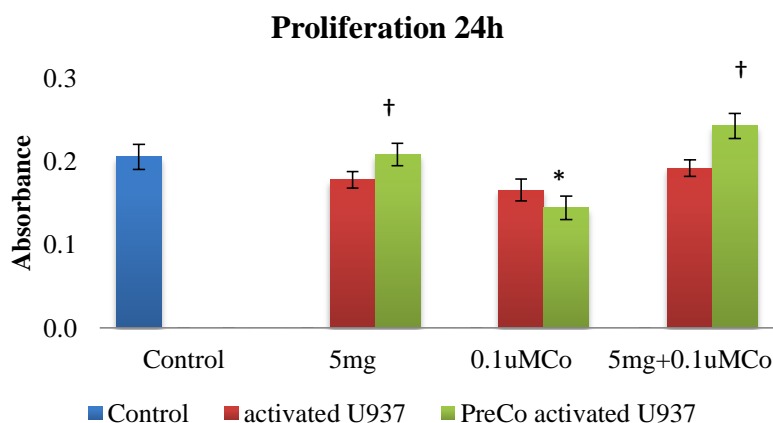


Figure 3.24 Activated U937 cell proliferation at 24h measured by BrdU. Results are absorbance values (Mean \pm SEM, n=8) where controls are activated untreated cells. *Significantly different from control values ($p < 0.05$) by one-way ANOVA followed by Dunnett's multiple comparison test. †Significant difference between non Co pre-treated cell and Co pre-treated cell values ($p < 0.05$) by 2 sample t-Test.

3.3.8 Effects of metal debris and ions on cytokine release measured by ELISA

As mentioned before, the main effects on cell viability and morphology were observed in the presence of a high wear debris concentration. In an attempt to better understand how such high debris concentration was affecting the cells, the levels of production of IL-6, TNF- α , and IFN- γ were measured by ELISA and results are described below.

3.3.8.1 Resting U937 cells exposed to CoCr wear debris and Co ions

Resting and Co pre-treated resting U937 cells were exposed to 5mg debris/ 1×10^6 cells, $0.1 \mu\text{M}$ Co and the combination of 5mg debris/ 1×10^6 cells and $0.1 \mu\text{M}$ Co for 24 and 120h. At each end point, the levels of IL-6, TNF- α , and IFN- γ secreted by the cells were measured in the culture medium of each sample.

Figure 3.25 shows that untreated resting cells (controls) were secreting the three cytokines at each culture end point. It also shows that there was no statistical

difference between the levels of cytokines secreted by treated and untreated cells. Results from resting and Co pre-treated resting U937 cells were compared in order to establish if the pre-treatment with Co affected the response to the exposure to metal debris and Co. The Co pre-treatment did not cause a significant difference to the levels of cytokine secretion at either 24 or 120h.

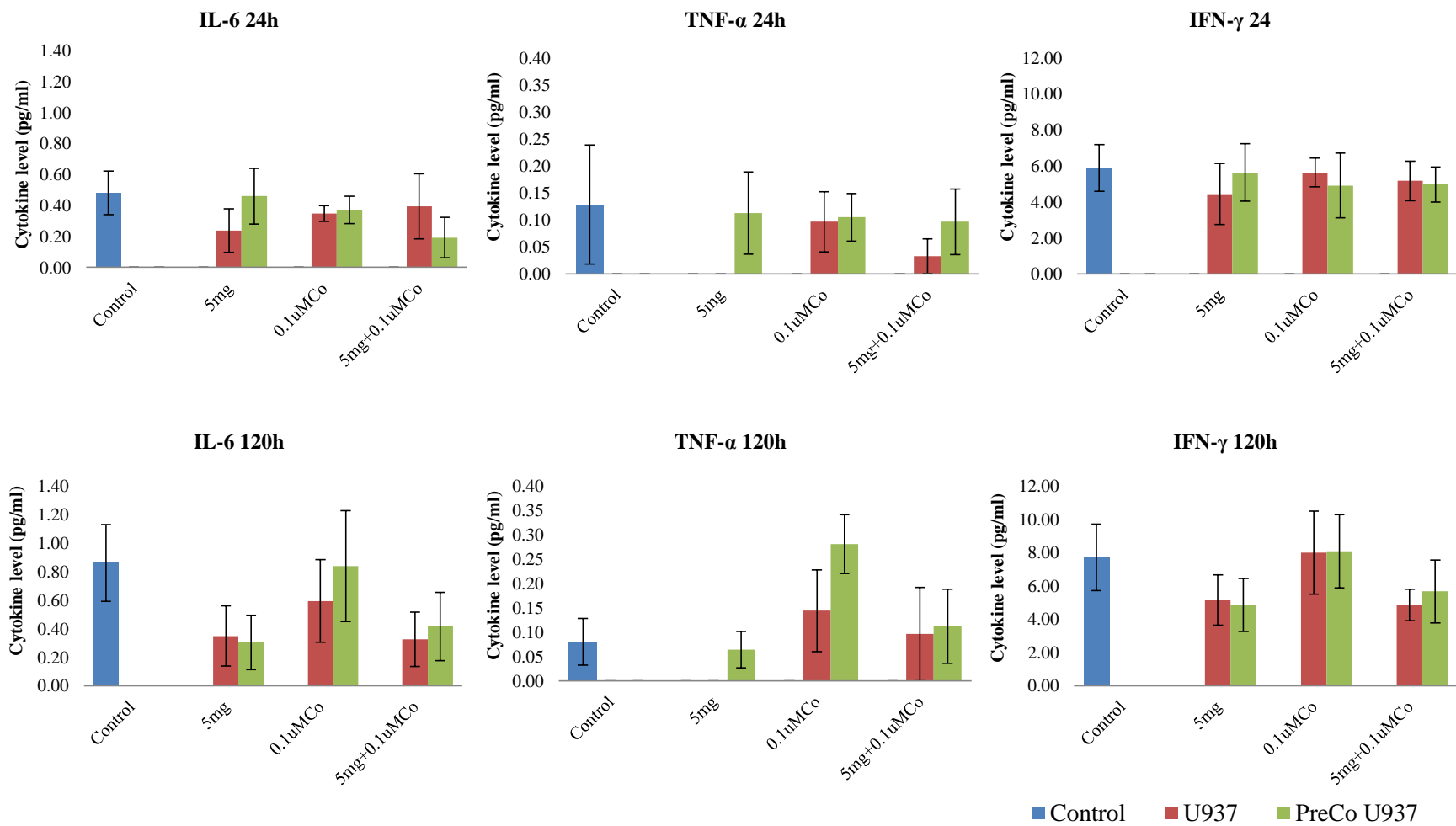


Figure 3.25. Cytokine secretion levels of resting and Co pre-treated resting U937 cells at 24 and 120h of exposure to 5mg debris/ 1×10^6 cells, 0.1 μ M Co and 5mg debris/ 1×10^6 cells + 0.1 μ M Co.

3.3.8.2 Activated U937 cells exposed to CoCr wear debris and Co ions

Secretion levels of IL-6, TNF- α , and IFN- γ were also measured in the culture medium of activated and Co pre-treated activated U937 cells exposed to 5mg debris/ 1×10^6 cells, 0.1 μ M Co and the combination of 5mg debris/ 1×10^6 cells and 0.1 μ M Co for 24 and 120h. Figure 3.26 shows that untreated activated cells (controls) were secreting the three cytokines at each culture end point. It also shows that secretion by treated cells of IL-6 and TNF- α significantly decreased after 24h exposure. However, IFN- γ secretion levels did not seem to be affected by the treatments. After 120h exposure, cells in the presence of metal debris, but not Co ions alone, secreted significantly less IL-6 than control cells. Moreover, all treatments caused significant decrease in the secretion of TNF- α but did not seem to affect the secretion of IFN- γ . Additionally, results from activated and Co pre-treated activated U937 cells were compared in order to establish if the pre-treatment with Co made a difference to the effects caused by the exposure to metal debris and Co. Co pre-treated activated cells exposed to 0.1 μ M Co for 120h secreted significantly less TNF- α than non Co pre-treated cells.

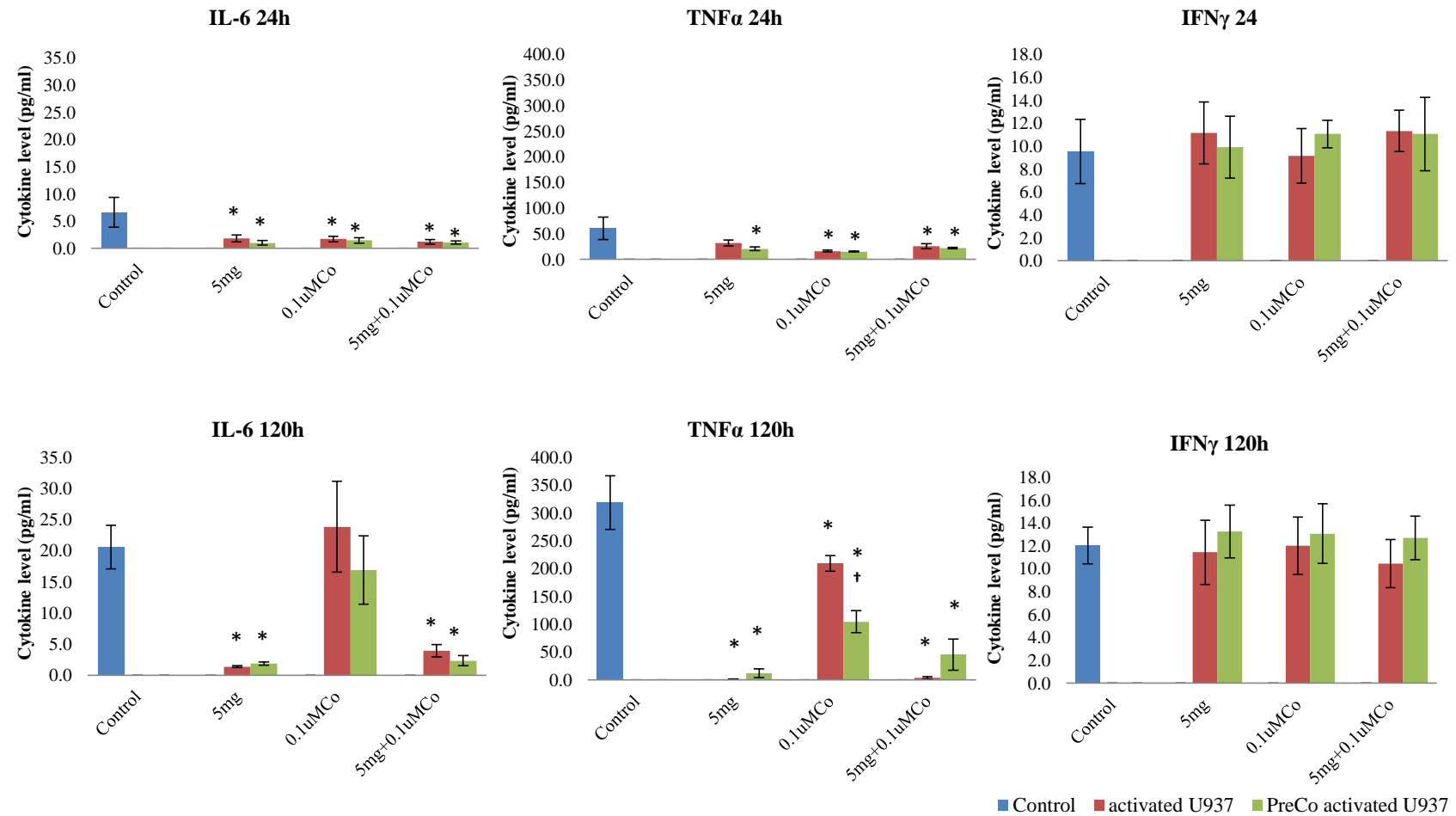


Figure 3.26. Cytokine secretion levels of activated and Co pre-treated activated U937 cells at 24 and 120h of exposure to 5mg debris/ 1×10^6 cells, 0.1 μ M Co and 5mg debris/ 1×10^6 cells + 0.1 μ M Co. *Significantly different from control values ($p < 0.05$) by one-way ANOVA followed by Dunnett's multiple comparison test. †Significant difference between non Co pre-treated cell and Co pre-treated cell values ($p < 0.05$) by 2 sample t-Test.

3.3.9 Summary of major findings

In this chapter, the effects of Co ions and CoCr wear debris derived from a hip resurfacing on cell morphology, viability, proliferation, and cytokine secretion by resting and activated U937 cells have been studied. The main findings of this investigation are:

- Low concentrations of metal debris (0.05mg/1x10⁶cells, 0.1mg/1x10⁶cells, and 0.2mg/1x10⁶cells wear debris) did not seem to be cytotoxic for either resting or activated cells
- High concentrations of metal debris (5mg debris/1x10⁶cells) had a detrimental effect on the viability of both resting and activated U937 cells
- The high debris concentration was more toxic for resting cells after pre-treating cells with Co ions (Figure 3.15)
- Exposure to 5mg debris/1x10⁶cells for 24h did not seem to affect cell proliferation
- Cytokine release by U937 cells was affected by both metal debris and metal ions

Results from this chapter are also summarised in Table 3.3.

U937 cells	Parameter	Metal wear debris concentration $\pm 0.1\mu\text{M Co}$	
		Low (0.05, 0.1 and 0.2mg debris/ 1×10^6 cells)	High (5mg debris/ 1×10^6 cells)
Resting	Viability	Did not cause a significant effect on cell viability.	A significant decrease in both cell number and metabolic activity was observed even at the 24h time point. The high debris concentration was more toxic for resting cells after pre-treating resting cells with Co ions.
	Morphology	No obvious effect on cell morphology on either resting or Co pre-treated resting U937 cells was observed when compared to controls after 24, 48 and 120h of exposure.	After 120h of exposure, very few cells could be visualised and a great number of them appeared to be apoptotic.
	Proliferation	Parameter not evaluated with low metal debris doses.	Although there was no significant difference when compared to controls, cells in the presence of metal debris seem to have had lower proliferation.
	Cytokine secretion	Parameter not evaluated with low metal debris doses.	There was no statistical difference between the levels of cytokines secreted by treated and untreated cells.
Activated	Viability	Did not cause a significant effect on cell viability.	Significant decrease in both cell number and metabolic activity after 120h of exposure.
	Morphology	No obvious effect on cell morphology. However, increased number of lysosomes and cell size, compared to resting cells, were observed.	After 120h of exposure, there was a decrease in cell number of cells that could be visualised. The few cells observed appeared to be mainly apoptotic
	Proliferation	Parameter not evaluated with low metal debris doses.	Opposite to the effects seen in resting cells, a significant decrease in the proliferation of activated cells was observed in cells treated only with $0.1\mu\text{M Co}$
	Cytokine secretion	Parameter not evaluated with low metal debris doses.	Contrary to results from resting cells, there was a significant decrease in IL-6 and TNF- α secretion by activated cells.

Table 3.3. Summary of main results from Chapter 3.

3.4 Discussion

Cobalt and chromium ions have been the subject of many studies because metal on metal hip implants are mainly cobalt chromium (CoCr) alloys. Co–Cr alloys are usually composed of 62–67% Co, 27–30% Cr, 5–7 % Mo, and ~1% Ni (Singh and Dahotre, 2007) and relative percentage weight estimations (by SEM) of metals from Co-Cr implants showing 52.5% Co, 43.5% Cr, and 3.9% Mo have been reported (Case et al., 1994). The femoral and acetabular components of ASR implants (Articular Surface Replacement; DePuy; Leeds, UK) are made of high carbon ($\geq 0.2\%$) content CoCr alloy (ISO 5832-12: Co Balance, Cr 26.0–30.0%, Mo 5.0–7.0%, Ni 1.0% max., Si 1.0% max., Mn 1.0% max., Fe 0.75% max., C 0.35% max., N 0.25% max.) (Dearnley, 1999). EDS analysis of the simulator generated wear debris from an ASR implant showed a metal composition consistent with the composition of the CoCr alloy used in the fabrication of such implants. On the other hand, tissue retrieved from a patient undergoing revision surgery showed a higher percentage of Cr than Co. Similarly to these findings, Xia et al. (2011) performed EDS analysis on biopsies from MoM peri-implant tissue retrieved at a revision surgery and found Cr but not Co to be the predominant component of the wear nanoparticles in the tissue. Metal particles have been shown to accumulate in tissues adjacent to the implant (Case et al., 1994, Langton et al., 2010). As these particles corrode, Cr and Co ions are released. Since Co is more soluble than Cr, Co corrodes faster leaving mainly Cr in the local environment (Xia et al., 2011a). It was described in Chapter 1 how Cr and Co ions enter the cells and bind in tissues. Contrary to Cr, Co ions tend to remain mobile, as greater Co concentration (compared to Cr) in blood and remote organs have been reported (Afolaranmi et al., 2012). These interaction mechanisms of the metal ions may explain why a higher percentage of Cr than predicted from alloy composition of retrieved implant was observed.

In the current study, CoCr wear debris from an ASR hip implant was found to range in size and shape. These irregularly shaped particles ranged from the nanometre scale to micrometre particles; some of the latter were aggregates of the smaller particles. These observations are in agreement with a variety of studies that have reported the

tendency of nanoparticles to aggregate in solution and body fluids (Domingos et al., 2009, Ward et al., 2009, Sajjadi et al., 2013). Additionally, previous SEM images of simulator generated CoCr wear particles (Germain et al., 2003, Papageorgiou et al., 2007a) and CoCr particles retrieved from patients (Xia et al., 2011a, Topolovec et al., 2013) have revealed particle aggregates. The composition analysis of the particles retrieved from the revision patient showed organic material (i.e. C) providing evidence that the metal wear debris binds to macromolecules such as proteins. These findings also agree with previous reports of deposition of CoCr wear particles in MoM peri-implant surrounding tissues *in vivo* (Korovessis et al., 2006, Papageorgiou et al., 2007b, Mahendra et al., 2009). The aggregation of the nanoparticles in conjunction with the protein binding could potentially mitigate the adverse immunological response *in vivo*, since by being bound to autologous proteins the immune cells may not recognise the particles as foreign bodies.

In addition to the above, due to the irregular nature of the wear particles it was difficult to accurately quantify their number or measure their surface area. Therefore, the dose for *in vitro* studies was quantified as a dry mass which could easily be suspended in sterile PBS and added to the culture medium.

Clinically, the acetabular cup is commonly positioned at an angle of 45° to the vertical axis of the acetabulum (Figure 3.27). During gait, the direction of the force vector is approximated as 10° medial, resulting in a 55° angle between the face of the cup and the direction of the joint reaction force vector (Williams et al., 2008). However, even small variations in the positioning angle may have a detrimental effect in terms of wear volumes, as it has been reported that cup angles with a mean of 57° resulted in edge loading and increased wear (Morlock et al., 2006). Previous simulator testing of 39mm ASR™ bearings positioned at a 55° angle over 2 million cycles showed a wear rate production of around 8mm³ of debris per million cycles during both the initial bedding-in stage (between zero and 1 million cycles) and the steady-state (Leslie et al., 2008, Williams et al., 2008). The wear debris used in the current study was also produced from a size 39mm ASR™ joint. Since these conditions mentioned above emulate the common clinical practice, the wear rate

production of 8mm^3 of debris per million cycles was assumed to represent the physiological scenario for a 39mm ASR™ joint.

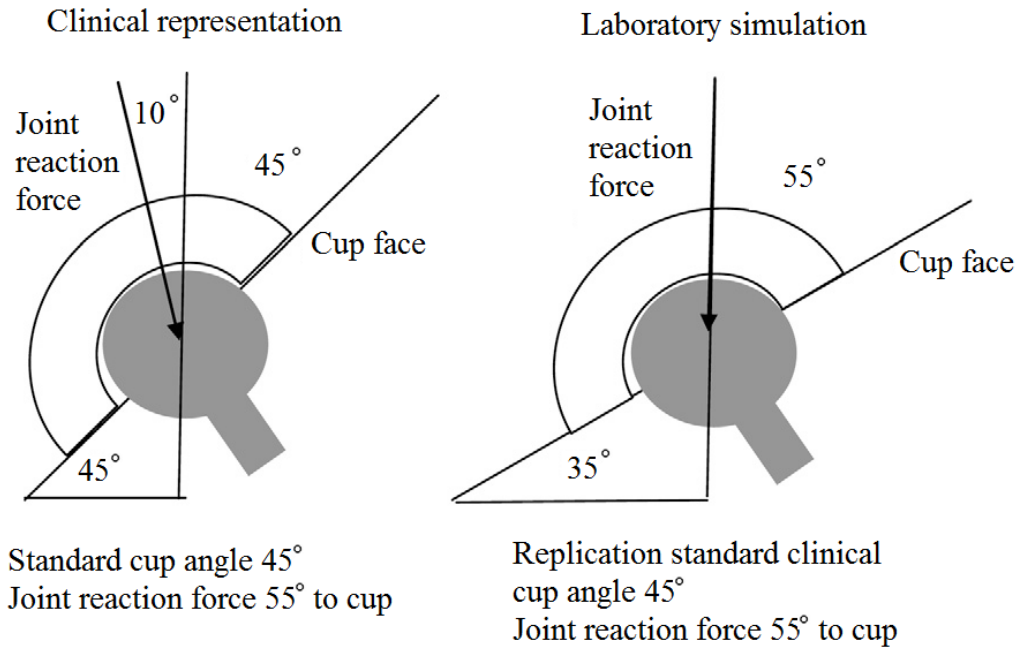


Figure 3.27. Cup angular position *in vivo* and in the simulator (Williams et al., 2008).

The density of the CoCr alloy used to produce the wear debris was $\sim 8.32\text{mg}/\text{mm}^3$ (Medley et al., 1996), as a result, 8mm^3 of wear would equate to 66.56mg of debris per million cycle. It has been reported that a very active person can walk up to 3.5 million cycles per year (Schmalzried et al., 1998, Gill et al., 2012b), assuming that the prosthesis is *in situ* for 25 years that would equate to 5824mg of debris produced in the total life-time of the prosthesis. There are 5-6 litres of blood in an adult male human and 4-5 litres in an adult female human. There are an average of 7000 white blood cells per microlitre of blood (range: 5000-10000cells/ μl) in an adult human (Martini et al., 2011). Taking 5 litres as the average volume of blood, there are $\sim 35000 \times 10^6$ white blood cells in an adult human. This equates to white blood cells being exposed to $\sim 0.2\text{mg}/1 \times 10^6$ cells. As a consequence, a concentration of 0.2mg debris/ 1×10^6 cells was implemented as the top debris concentration for the initial viability and morphology testing. Since this represents a life-time quantity of wear debris produced in the conditions described above, the author acknowledges that 0.2mg debris/ 1×10^6 cells is a high dose. However, a number of investigations

studying the biological effects of CoCr wear nanoparticles have been carried out, with higher doses ranging from 1.6mg/1x10⁶cells to 83.2mg/cell (Germain et al., 2003, Papageorgiou et al., 2007b, Papageorgiou et al., 2007a, Williams et al., 2003, Mostardi et al., 2010). Interestingly, they do not mention how they determined such concentrations.

A number of studies have shown that metal wear particles and high levels of metal ions, particularly cobalt and chromium, have a cytotoxic effect on a variety of cells *in vitro* (Allen et al., 1997, Fleury et al., 2006, Petit et al., 2006). Most of these investigations have been focused mainly on the short-term exposure, acute cell response, or limited to evaluation of one parameter like cell viability or cytokine levels. Moreover, studies carried out with U937 cells have been performed either with resting U937 cells or activated U937 cells. In this study, exposure for up to 5 days to debris concentrations up to 0.2mg/1x10⁶cells wear debris were not found to be cytotoxic for either resting or activated U937 cells.

Metallosis is a complication of total joint replacement (Romesburg et al., 2010, Day et al., 2013). The term metallosis is used to describe the infiltration of metallic wear debris into the periprosthetic structures, including soft and bony tissues (Chang et al., 2005, Khan et al., 2009, Romesburg et al., 2010). It can occur in the joint capsule, around the acetabular cup, and around the femoral stem. It can be the result of dissociation, fracture or wear and corrosion of the joint prostheses components (Khan et al., 2009, Chang et al., 2005, Sporer and Chalmers, 2012). Amounts of material wear ranging from 67mg (Matziolis et al., 2003) to 48.1g (Kempf and Semlitsch, 1990) have been reported. Metallosis has been associated with adverse tissue reactions and increased ion concentrations in peri-implant tissue and whole blood (O'Brien et al., 2013). It can cause pain, formation of a mass with occasional cystic change, osteolysis and systemic effects related to metal hypersensitivity (Romesburg et al., 2010). A hallmark of metallosis is that of metallic staining of the tissues. Macroscopically, the hip pseudocapsule contains a black-stained synovium. Microscopically, there is local necrosis with histiocytic and granulomatous reaction around the deposits of metallic particles. In cases of severe metallosis, there is

radiographic opacification of the peri-prosthetic soft tissue planes by the deposition of metallic debris (Khan et al., 2009), known as the “bubble sign” (Su et al., 2003), as well as osteolytic lesions (Chang et al., 2005).

Both resting and activated U937 cells were studied and a high wear debris concentration was chosen in an attempt to mimic a metallosis environment surrounding an implant. *In vitro*, the pathophysiological pathways of the inflammatory cascade triggered by Toll-like receptor-4 are widely studied using stimulation of macrophages with lipopolysaccharide (LPS) derived from Gram-negative bacteria (Okoko and Oruambo, 2008, Hougee et al., 2005, Chen et al., 2010, Dorresteijn, 2006). However, *in vitro* protocols using various stimuli (i.e. DMSO, Retinoic acid, Vitamin D3, phorbol 12-myristate 13-acetate (PMA), IFN- γ), either alone or in combination, have been developed to induce U937 terminal differentiation into mature macrophages and study the inflammatory response (Baek et al., 2009, Blottiere et al., 1995, Liao et al., 2008, Larrick et al., 1980, Caron et al., 1994). PMA exerts its biologic effects by altering gene expression through the activation of protein kinase C (PKC) and modulating the activity of transcriptional factors such as nuclear factor kappa-light-chain-enhancer of activated B cells (NFkB) and activator protein 1 (AP1) (Garcia et al., 1999, Daigneault et al., 2010). To the author’s knowledge, there is no evidence in the literature of U937 cells being stimulated with LPS to study the biological effects of hip implant wear debris. Contrary to this, PMA has been used previously to activate U937 cells in implant wear debris related studies (Matsusaki et al., 2007, Yagil-Kelmer et al., 2004, Bainbridge et al., 2001, Lucarelli et al., 2004). As a consequence, PMA was chosen as the U937 cell activating stimulus.

In the current study, it has been shown that the metal wear debris used is free of endotoxins, which means that the changes seen in the cells exposed to the debris are due to the metal debris and not to contaminants that could have been present within the debris. The high metal debris concentration, 5mg/1x10⁶cells, proved to be cytotoxic for both resting and activated U937 cells. Evidence of this can be found on the Carl Zeiss Axio Imager Microscope images as well as the Neutral Red and MTT

results, mainly after 120h of treatment when very few cells could be found. This could explain why no morphology changes were observed. Since the 5mg/1x10⁶ cells of metal debris are so toxic, cells died before we observed a change to their morphology. The evidence gathered in this study is probably not enough to conclude whether or not exposure to the Co ions or the metal debris resulted in the maturation and activation of resting U937 cells. However, *in vivo* studies have reported high numbers of macrophages in tissues surrounding metal-on-metal prosthesis (Catelas and Wimmer, 2011, Bhamra and Case, 2006, Tuan et al., 2008) and their activation upon interaction with metal wear nanoparticles has been suggested to be a nonspecific inflammatory response to the wear products (Catelas and Wimmer, 2011, Kranz et al., 2009, Catelas et al., 2011).

Bone necrosis is a feature of metallosis (Ollivere et al., 2009). The findings in the current study suggest that the extensive necrosis associated with metallosis (Ollivere et al., 2009, Romesburg et al., 2010) is not limited to bone and includes other cell types. Typical histological changes related to metallosis include perivascular lymphocyte infiltration, inflammation, and the accumulation of macrophages loaded with metal debris (Ollivere et al., 2009). These factors in conjunction with the high levels of osteolytic cytokines released by the macrophages eventually lead to bone loss and aseptic loosening (Romesburg et al., 2010).

Severe metallosis often requires the complete removal of all hip replacement components (Kempf and Semlitsch, 1990, Ollivere et al., 2009, Matziolis et al., 2003, Ebreo et al., 2011). However, with extensive metallosis, excision of the pseudomembrane using electrocautery can produce sparks, which are potentially hazardous (Su et al., 2003). The deposition of metallic debris could also be so extensive that excision of all the compromised tissue may not be possible. In the current investigation, a pre-treatment with cobalt ions was carried out to simulate the conditions of a revision surgery in order to find out if such pre-exposure would have an effect on cell response to newly derived metal wear debris and ions. Results seem to indicate that the exposure to wear debris had a pronounced detrimental effect on cell number and metabolic activity of cells pre-treated with Co, especially after an

incubation period of 120h. It has to be taken into account that cells pre-treated with Co at the 120h end point would have been exposed to Co for 9 days in total. This suggests that the toxic effects of the treatments could be the result of a chronic exposure rather than an acute one. This could mean that in patients the effects of cobalt ions and nanoparticles released from metal implants may be additive in terms of adverse effects. Since resting U937 cells are not mature active phagocytes, these findings suggest that it is the Co ions rather than the metal wear debris that are causing the cellular response. In addition to this, the metal particles could be releasing soluble products, such as Co and Cr ions, which could be internalised by the resting cells causing the effects seen.

It is accepted that the presence of implant devices and wear debris incites a foreign body inflammatory reaction (Anderson et al., 2008). The macrophages that engulf the particles release inflammatory cytokines that may cause the peri-prosthetic osteolysis leading to implant loosening (Romesburg et al., 2010). In the present study, secretion of IL-6, TNF- α , and IFN- γ by U937 cells exposed to wear debris and Co ions was examined. The lower secretion of IL-6 and IFN- γ by resting cells treated with 5mg/1x10⁶ cells of metal debris after 120h are in agreement with lower cell numbers, as measured by NR. However, TNF- α levels did not seem to have been affected by the metal debris treatments. Since there are fewer cells to produce this cytokine, these results could actually indicate a higher TNF- α level of expression. Moreover, when the resting U937 cells were pre-treated with Co, all treatments caused higher TNF- α release when compared to the non-pre-treated cells. These findings support the hypothesis that the cellular response is caused by chronic exposure to metal particles and ions. Moreover, they suggest that the Co ions released from the implant and from the wear particles play an important role in long-term survival of a MoM implant *in vivo*. For example, for a patient that has one MoM device, this could mean that, if in need of a second MoM hip implant on the other hip, the survival and function of this new joint may be impaired by the presence of the Co ions derived from the first device. In the case of activated cells, the lower level of secretion of IL-6 and TNF- α by cells treated with 5mg/1x10⁶ cells of metal debris after 120h could be due to the lower cell number. On the other hand,

IFN- γ levels do not seem to have been affected by the metal debris treatments. Given that there are fewer cells to produce and release this cytokine, these results could potentially be indicating a higher IFN- γ level of expression. In addition to this, when the activated U937 cells were pre-treated with Co, all treatments caused higher IFN- γ release when compared to the non-pre-treated cells. These results again suggest a larger impact of a chronic exposure and a key role of Co ions. They also suggest that the biological response may be influenced by the cellular activation state.

Previous studies have reported that nanoparticles can adsorb cytokines, such as IL-6 and TNF- α , distorting ELISA assay outcomes (Veranth et al., 2007, Kocbach et al., 2008, Brown et al., 2010, Kroll et al., 2012). Thus, it is possible that the reduction in cytokines release levels detected in the current study might be a result of the cytokine adsorption onto the CoCr particles. However, such a decrease was not seen evenly across samples and cytokine levels from resting cells were affected differently than levels from activated cells. As a consequence, the findings from this investigation cannot be entirely attributed to particle adsorption.

Bone remodelling involves tight regulation of three proteins, receptor activator of NF- κ B ligand (RANKL), receptor activator of NF- κ B (RANK), and osteoprotegerin (OPG). These proteins are key determinants of osteoclastogenesis and regulate bone resorption (Takayanagi, 2005). As mentioned in Chapter 1, pro-inflammatory cytokines such as IL-6, and TNF- α can accelerate osteoclast formation and bone resorption. By upregulating RANKL expression on osteoblasts, these pro-inflammatory cytokines accelerate RANKL signalling, and thus directly contribute to osteolysis (Oishi et al., 2012). In biomaterials research, TNF- α , IL-1, and other pro-inflammatory cytokines are also known as mediators of the foreign body reaction, an inflammatory response that can cause both severe tissue damage and premature failure of implanted materials (Mountziaris and Mikos, 2008). IFN- γ promotes innate immune responses by activating macrophages. In parallel, IFN- γ exerts regulatory functions to limit tissue damage associated with inflammation-like suppressing osteoclastogenesis (Hu and Ivashkiv, 2009).

According to the above, the results from this study seem to suggest that the high concentration of metal debris in combination with Co ions not only have a direct effect on cell viability but also influence cell function. Moreover, these findings could potentially mean that the survival and well-functioning of MoM devices could be compromised in patients undergoing revision surgery or receiving a second device. The potential increase in TNF- α level by the resting cells could be a factor contributing to the osteolysis process, while the potential increase in IFN- γ production by the activated cells could be a cellular effort to counteract tissue damage. This also suggests that the cellular activation state affects the biological response to wear debris and caution should be taken when choosing *in vitro* models to study immune and molecular responses.

4. CORRELATION BETWEEN GENE EXPRESSION, APOPTOSIS AND METAL ION LEVELS ON U937 CELLS *IN VITRO*

4.1 Introduction

The previous chapters have described how particulate debris can provoke biological tissue responses, including vascularized granulomatous tissue formation along the implant-to-bone interface, inflammatory cell (macrophages, lymphocytes) influx, bone resorption, osteolysis, and finally loss of prosthesis fixation (Zhang et al., 2009).

Over the past few years numerous investigations have been carried out to study the effects of different ions and particulate wear debris on the expression of an array of genes *in vitro*. TNF- α , IL-1, and IL-6 are cytokines that have been reported as playing a central role in the induction of implant osteolysis (Algan et al., 1996, Merkel et al., 1999, Stea et al., 2000b). Extensive work has been carried out on cytokine production by macrophages in response to wear debris. Sethi et al. (2003) studied the macrophage response to cross-linked UHMWPE and compared it to conventional UHMWPE as well as titanium-alloy (TiAlV) and cobalt–chrome alloy (CoCr). At 24 and 48h, macrophages cultured on TiAlV and CoCr alloy expressed higher levels of IL-1 α , IL-1 β , IL-6 and TNF- α and than when grown on UHMWPE materials according to qRT-PCR analysis. Jakobsen et al. (2007) compared surfaces of as-cast and wrought CoCrMo alloys and TiAlV alloy when incubated with mouse macrophage J774A.1 cells and reported a significant increase in the levels of expression of TNF- α , IL-6, IL-1 α and β from cells incubated with alloys compared to non-stimulated cells. Garrigues et al. (2005) used microarrays to investigate alterations in the phenotype of macrophages as they interact with UHMWPE and TiAlV alloy particulate wear debris. Their findings further validate the important roles of TNF- α , IL-1 β , IL-1 α , IL-6, MIP1 α and MIP1 β in osteolysis.

As well as macrophages, other cell types have been reported as being involved in the biological response to implant wear debris. As a result, there are similar studies on

monocytes, lymphocytes, osteocytes, and osteoblasts. For example, the effects of CoCr particles on osteocytes were tested by Kanaji et al. (2009) CoCr treatment of MLO-Y4 osteocytes significantly up-regulated TNF α gene expression after 3 and 6h and TNF- α protein production after 24h, but down-regulated IL-6 gene expression after 6h. MG-63 osteoblasts were treated by Vermes et al. (2001) with titanium, titanium alloy, chromium orthophosphate, polyethylene and polystyrene particles and they reported that each type of particle significantly suppressed procollagen alpha1[I] gene expression ($p < 0.05$), whereas other osteoblast-specific genes (osteonectin, osteocalcin, and alkaline phosphatase) did not show significant changes. Koulouvaris et al. (2008) studied the role of particulate debris in macrophage activation and inhibition of osteogenic signalling *in vitro* by exposing human monocytes and MG-63 cells to Ti and PMMA particles. Both Ti and PMMA particles induced up-regulation of chitinase (CHIT1) in human CD14+ monocytes. Titanium particles reduced expression of a regulator of osteogenesis (BMP4) and induced IL-8 expression in MG-63 cells. Murine MC3T3-E1 preosteoblasts were treated with TiO₂ nanoparticles of different sizes (32nm and 5nm) by Zhang et al. (2005) and they found that these nanoparticles increased granulocyte-macrophage colony stimulating factor (GM-CSF) and granulocyte colony-stimulating factor (G-CSF) gene expression. The effect of particulate derivatives of nickel and cobalt alloys on the mRNA levels of chemokine receptors CCR1 and CCR2 on monocytes/macrophages from whole blood were analysed by Fujiyoshi and Hunt (2006). Although there were no significant differences in the level of CCR1 mRNA in monocytes/macrophages incubated with NiCr particulates, there was a down-regulation in the level of CCR2 in cells incubated with NiCr and CoCr particles. All these investigations indicate that wear debris and metal ions derived from MoM implants can cause an adverse tissue response by modulating gene expression on several types of cells, which suggests that osteolysis and subsequent aseptic loosening is the result of the concerted action of the different cell types.

Previous studies have stated that ions released from the wear debris could also affect gene expression. It has been reported that Cr⁺³ and Co⁺² ions could induce damage to proteins in macrophage-like cells *in vitro*, probably through the formation of reactive

oxygen species (ROS) (Petit et al., 2005, Petit et al., 2006a). U937 cells were exposed to Cr^{+6} and Co^{+2} ions by Tkaczyk et al. (2010). Cr^{+6} induced the protein expression of Mn-superoxide dismutase, Cu/Zn superoxide dismutase, catalase, glutathione peroxidase, and heme oxygenase-1 (HO-1) but had no effect on the expression of their mRNA whereas Co^{+2} induced the expression of both protein and mRNA of HO-1. The overexpression of HO-1 has been suggested to play an important role in cellular protection against oxidant-mediated cell damage (Chen et al., 2000, Rothfuss and Speit, 2002). This suggests that the results from Tkaczyk et al., (2010) show that Cr and Co ions cause oxidant-mediated cell damage. Type-I collagen gene expression was evaluated by Hallab et al. (2002) treating MG-63 cells with increasing concentrations (from 0.001 to 10 mM) of a variety of metal ions including Co and Cr. At toxic concentrations (1mM), Co depressed osteoblast function by significantly decreasing the levels of type I collagen gene expression to 40% of control values. Queally et al. (2009) showed that 10ppm cobalt ions induce chemokine secretion in primary human osteoblasts by measuring the up-regulation of IL-8 and MCP-1 gene expression in osteoblasts stimulated with 0–10 ppm Co^{2+} . The level of expression of matrix metalloproteinases and tissue inhibitors of metalloproteinases in U937 cells exposed to Co^{2+} and Cr^{3+} ions for 24h was determined by Luo et al. (2002) who showed that these ions induce up-regulation in a dose-dependent manner. These findings suggest that Co and Cr ions may modulate bone tissue remodelling. These studies provide more evidence of potential gene expression modulation by wear debris and ions derived from MoM implants.

A great number of investigations have looked at various aspects of aseptic loosening. As mentioned above, the response of various cell types including macrophages, fibroblasts and osteoblasts to implant wear debris has been explored and the molecular mechanisms of this process have been proposed. In the current study, a general human toxicology microarray assay was carried out in order to select a short list of genes for further analysis. Based on the results from this assay, the genes lymphotoxin alpha (LTA), BCL2-associated athanogene (BAG1), growth arrest and DNA-damage-inducible alpha (GADD45A), inducible nitric oxide synthase (NOS2)

and FBJ murine osteosarcoma viral oncogene homolog (FOS) were selected to be analysed in the context of prosthetic wear debris.

LTA (lymphotoxin alpha, $LT\alpha$), a member of the TNF family, is an inflammatory mediator that influences multiple processes such as activation, proliferation, differentiation, and death induction in many different cell types. It is mainly produced by lymphocytes during a variety of autoimmune and infectious diseases (Kagi et al., 1999). $LT\alpha$ is secreted as the homotrimer $LT\alpha_3$ or complexed on the cell surface with $LT\beta$, predominantly as $LT-\alpha_1\beta_2$ heterotrimers (Chiang et al., 2009). Induction of $LT\alpha$ and $LT\beta$ gene transcription is tightly regulated by specific transcription factors in hematopoietic and non-hematopoietic cells. Uncontrolled activation of these genes leads to inflammatory-associated disorders (Remouchamps et al., 2011). It has been shown to induce apoptosis in murine and human T lymphocytes *in vitro* (Sarin et al., 1995), to be one of the main messengers involved in the response to acute toxic stress caused by LPS (Novoselova et al., 2006), and to mediate the monocyte–endothelial interaction via the classical NF κ B pathway following TNFR1/PI3K activation in human umbilical vein endothelial cells (Suna et al., 2009).

BAG1 (BCL2-associated athanogene) is a multifunctional protein able to delay cell death by a synergistic action with BCL2 (Aveic et al., 2011). It exists as multiple isoforms which are differentially localized in the cell and interacts with a diverse array of molecular targets, including the BCL2 apoptosis regulator (Townsend et al., 2005). It has been described as a part of the regulation of apoptotic, transcriptional, and proliferative pathways, as well as cell signalling and differentiation (Aveic et al., 2011). Since the initial demonstration of BAG1 as an antiapoptotic molecule, BAG1 overexpression has been shown to inhibit apoptosis induced by a wide range of inducers in various cell types, including activation of cell surface death receptors, radiation, chemotoxic drugs and heat shock (Townsend et al., 2003). This has led to several reports on the significance of BAG1 in human cancer (Townsend et al., 2003, Turner et al., 2001, Tang, 2002, Cutress et al., 2002).

The family of growth arrest and DNA damage (GADD) proteins is comprised of five members that are mostly localized in nuclei and co-ordinately regulated. These include GADD34, GADD45 α , GADD45 β , GADD45 γ , and GADD153 (Siafakas and Richardson, 2009). The GADD group of nuclear proteins are regulatory molecules that function primarily to protect cells and ensure survival by inducing cell cycle arrest, DNA repair and ultimately promoting apoptosis (Siafakas and Richardson, 2009). Expression of GADD45 α is stimulated by a range of DNA-damaging agents including UV radiation, hypoxia, peroxy nitrite free radicals, low pH, arsenic, Cr(VI) compounds, cisplatin, cadmium, and many other soil, air, and water pollutants (Moskalev et al., 2012, Hollander et al., 1993, Son et al., 2010, Nickens et al., 2010). GADD45 proteins also modulate immune responses by stimulating proliferation of T helper 1 cells (Moskalev et al., 2012).

The FOS (FBJ osteosarcoma oncogene) gene family consists of 4 members: FOS, FOSB, FOSL1, and FOSL2. These genes encode leucine zipper proteins that can dimerize with proteins of the JUN family, thereby forming the transcription factor complex AP-1 (Marks-Konczalik et al., 1998). FOS is a critical factor involved in osteoclast development and activation (Chen et al., 2011). The bones of FOS-deficient mice are osteopetrotic and highly deficient in osteoclasts (Regunathan et al., 2002). The effects of heavy metals on FOS expression have been studied. It has been shown that tungsten, nickel, and cobalt cause dose-related induction of FOS expression (Miller et al., 2004). There are also several studies on the effects of cadmium on the levels of expression of FOS (Chen et al., 2011, Kondo et al., 2012) and the role of FOS in cadmium-induced bone loss (Regunathan et al., 2002, Bhattacharyya, 2009). Moreover, it has been suggested to have a pivotal role in nitric oxide synthase 2 (NOS2) expression in airway epithelial cells (Chambellan et al., 2009, Marks-Konczalik et al., 1998). NOS2, which is inducible in diverse cell types by cytokines, converts L-arginine to L-citrulline, and nitric oxide (NO) (Xu et al., 2003). NOS2 is widely expressed in every type of tissue and cell after transcriptional induction following exposure to a vast array of immunologic and inflammatory stimuli (Marks-Konczalik et al., 1998, Zeidler and Castranova, 2004). Activity of NOS2 has been associated with inflammatory tissue damage in human diseases (Xu

et al., 2003). NO produced by macrophages is an important component of host defense against pathogens and tumor cells (Kim et al., 2002). It has been reported that mercury inhibits NO and NOS2 expression induced by interleukin-1 β (IL-1 β) in pancreatic islet β -cells (Eckhardt et al., 1999) and that in BALB/c murine macrophage cells (J774A.1) it inhibits NO production through decreases in NOS2 mRNA and protein (Kim et al., 2002). On the other hand, it has been shown that lead treatment *in vitro* at early developmental stage of bone marrow-derived macrophages enhances NOS2 gene expression and NO production through IL-1 β and IL-6 (Song et al., 2001).

As mentioned above, even though a vast spectrum of toxicology studies has been carried out on LTA, BAG1, GADD45A, FOS, and NOS2, their gene expression levels have not been analysed from the orthopaedic point of view. In addition to this, the general human toxicology microarray assay results seemed to suggest that the expression of these genes could be affected by metal ions released from MoM implants. These genes are involved in key cellular and immunological processes which could potentially be unbalanced by particulate and soluble wear debris derived from implant devices. Understanding the impact of CoCr wear debris on the expression of these genes may contribute to even better comprehension of the periprosthetic osteolysis process and the potential effects of circulating debris.

In addition to gene modulation contributing to wear particle-induced osteolysis, some recent *in vivo* and *in vitro* studies showed that direct or indirect induction of cell death was involved in the wear particle-induced bone resorption (Zhang et al., 2012b). Apoptosis is a complex, highly regulated cell death process that can result from a range of developmental, genetic, and environmental cues including injury, mild toxic stimuli, loss of cell attachment to matrices, and loss of trophic signals needed to maintain cell viability (Cardoso et al., 2009). It is a necessary biological process involved in embryonic development, tissue remodelling, and regulation of the immune system. Yet, several pathological conditions have been associated with unintended or uncontrolled induction of apoptosis (Au et al., 2006), as seen in

cancer, autoimmune disorders, neurodegenerative disease and toxin-induced disease (Li et al., 2000).

Apoptosis can be initiated either via an extrinsic or intrinsic pathway, with the extrinsic pathway being initiated by cell surface receptors and the intrinsic pathway being initiated by a mitochondria mediated death signalling cascade (Chen et al., 2001, Shin et al., 2009). The early apoptotic events include changes in membrane structure, membrane permeability and mitochondrial potential. These early changes are followed by alterations in the chromatin structure, DNA strand breaks with formation of DNA fragments, decreases in nuclear DNA content and shrinkage in cell size (Ciapetti et al., 2002).

A variety of signalling systems activate apoptosis, such as surface receptors for cytokines (mainly TNF), expression of genes (c-myc, bax), DNA injury through a mechanism driven by p53 protein, injury to the cell membrane or to mitochondria (Stea et al., 2000a). Macrophage apoptosis in the interface membrane has been suggested to play an important role in the pathogenesis of aseptic loosening. It has been shown that apoptosis occurs in the interface membrane of aseptic loosening of total hip/knee replacements by using 20 specimens of bone-implant interface membrane for *in situ* localization of apoptotic changes, namely bcl-2/bax expression and DNA fragmentation (Zhang and Revell, 1999). In a similar study, 54 biopsies taken from the tissue surrounding loosened hip joint prostheses were examined. *In situ* apoptotic cell identification was performed by the detection of single- and double-stranded DNA breaks that occurred in the early stages of apoptosis. Apoptotic cells were present in a higher percentage in tissue sections where metal particles were present (24% apoptotic cells) if compared to areas where no metallic wear (6%), or plastic wear (2.8%) or ceramic wear (1.5%) was observed (Stea et al., 2000a). Using TUNEL staining, DNA laddering and immunodetection of PARP, a high incidence of apoptosis in cells at the interface membranes harvested at the time of hip revision surgery from 25 failed THRs was also revealed (Huk et al., 2001).

It has also been suggested that different apoptosis pathways may be triggered by implant wear debris. Fas receptor, BAK and caspase-3 cleavage were evaluated immunohistochemically in capsules and interface membranes from patients with aseptic hip implant loosening. A strong expression of cleaved caspase-3, Fas and BAK in macrophages, giant cells and T-lymphocytes was observed. The fibroblasts showed cleaved caspase-3 and BAK, but no Fas staining. Increased proliferation of macrophages and fibroblasts was also found (Landgraeber et al., 2008). Analysing periprosthetic interface membranes from 23 patients undergoing revision operations for aseptic loosening of hip joint prostheses, it was reported that death receptor pathway, mitochondria/cytochrome c caspase-dependent pathway and endoplasmic reticulum stress pathway are involved in the process of macrophage apoptosis (Yang et al., 2011). Similarly, it has been reported that the mode of cell death is dependent on the ion type and concentration as well as the duration of incubation. With short incubation times, the non-inflammatory process of apoptosis was predominant. With longer incubation times and high concentrations of ions, however, necrosis predominated (Huk et al., 2004). In lymphocytes from interface membranes from patients with aseptic hip implant loosening, (Landgraeber et al.) (2009) observed that the intensity of the apoptotic process tended to follow the radiological changes and stages of osteolysis.

Using an *in vivo* murine air pouch model of inflammation, the apoptotic changes associated with various shapes of UHMWPE particles were evaluated for the correlation of wear debris-induced inflammation and macrophage apoptosis by (Yang et al.) (2002). At 7 days post-particle introduction, there was a significant increase in the number of apoptotic cells present in the air pouch membrane containing the elongated-UHMWPE particles, compared with pouches containing globular particles or non-particle controls. The apoptotic cells were predominantly focused within the contact zone of the UHMWPE particle deposit, and often accompanied by local inflammatory reactions.

The bone marrow stroma contains mesenchymal stem cells (MSCs), multipotential cells capable of differentiating into various mesenchymal lineages such as bone,

cartilage, tendon, ligament, and muscle (Bruder et al., 1994). In procedures such as THA, the MSCs are likely to be subjected to prolonged and direct exposure to implant devices (Wang et al., 2003). (Haleem-Smith et al.) (2012) observed that exposure to submicron-size titanium (Ti) particles results in reduced osteogenic differentiation and proliferation, and enhanced apoptosis in human (h) MSCs. (Wang et al.) (2003) reported direct and indirect induction of apoptosis in hMSCs in response to titanium particles. Exposure of hMSCs to commercially pure Ti (cpTi) particles diminished cell viability through the induction of apoptosis in a manner dependent on particle dosage and time. Following 72h culture in conditioned medium collected from cpTi-loaded cell cultures, hMSCs exhibited increased apoptosis compared to cells cultured in conditioned medium from non-particle-loaded controls suggesting that soluble factors released in response to particulate stress are capable of inducing apoptosis.

Cytotoxicity and genotoxicity of metal compounds have been studied in a variety of systems in human carcinogenesis (Akita et al., 2007). Apoptosis was originally viewed as a normal physiologic process by which correct functional cellular population dynamics are maintained through the apoptotic loss of cell populations carrying abnormal genetic information. It is known that metals under certain circumstances can induce apoptosis (Chen et al., 2001). Some researchers have suggested that the preferential induction of macrophage apoptosis in peri-prosthetic tissue would be a desirable therapeutic modality since no inflammatory response is generated and therefore it may create a more favourable peri-prosthetic environment (Huk et al., 2001, Catelas et al., 2001). On the other hand, the presence of apoptosis in the peri-prosthetic membrane may be alternatively considered as a contributing detrimental factor in arthroplasty failure rather than a preventive element of osteolysis (Sabbatini et al., 2010). If uncontrolled apoptosis is induced, recognition and clearance of cells undergoing apoptosis may be overwhelmed and cells would start leaching their contents perpetuating the inflammatory response. Moreover, chronic and lower dose exposure of cells or tissues to metals may perturb or even inhibit appropriate apoptosis, leading to the accumulation of cells with carcinogenic potential (Chen et al., 2001).

4.2 Aims

The aim of this chapter was to explore the relationship between changes in gene expression and apoptosis *in vitro* with the release of metal ions derived from incubation of culture medium with the metal wear debris. Of particular interest was to assess the potential effect of cell pre-treatment with Co ions on gene expression and apoptosis.

4.3 Results

4.3.1 Protocol development for ICP-MS analysis of culture medium

ICP-MS analysis was carried out in order to find out if metal ions were being released from the CoCr wear debris used to treat the cells, and, if so, to quantify the levels of such ions. In the current study, a protocol for the processing and ICP-MS analysis of cell culture medium was developed. This development was necessary due to the lack of an existing protocol in the research laboratory to carry out this analysis. Details of this development are given below. As a starting point culture medium samples were diluted with the solubilisation matrix solution used for whole blood samples. Briefly, all samples and standards were diluted using the solubilisation matrix solution used for whole blood samples (Table 2.6, Section 2.2.2). 500µl of culture medium sample or standard was added to 2.5ml of the dilution matrix in a plastic vial. 2ml of deionized water (18mΩ) was then added into each vial. A final solution of 5ml was attained giving a 10X dilution of the samples and each sample was then sonicated. Standards were prepared by diluting TraceCERT[®], 1000mg/l Co in nitric acid, TraceCERT[®], 1000mg/l Cr in nitric acid and TraceCERT[®], 1000mg/l Mo in nitric acid (all Sigma-Aldrich (Fluka); Dorset, UK). Final concentration of standards used were 0.001, 0.01, 0.1, 1, 10, and 100µg/l. Samples were then analysed using an Agilent 7700x octopole collision system ICP-MS (Agilent Technologies; Wokingham, UK) in helium gas mode using Rhodium as internal standard.

Results from this first analysis showed that the detection limits required could not be achieved due to poor internal standard recovery from the culture medium samples. Figure 4.1 shows that the internal standard recovery was outside the 90-110% range in the samples. The instability of the analysis was likely to be due to a space charge effect as a result of the EDTA salt, which would cause a reduction in sensitivity. A space charge effect is an effect created by matrix ions interfering with the ion focussing of the analyte ions, which leads to poor sensitivity and detection limits (Thomas, 2008). This realisation led to reviewing the matrix components and preparing a new matrix with EDTA acid. Additionally, even though the set of data obtained could not be considered due to the poor internal standard recovery, it seemed to suggest that the ion concentration in some samples were outside the 0-100 μ g/l range. Moreover, it came to our attention that the standard solutions were not the most appropriate for ICP-MS analysis. Consequently, a new set of standards were prepared by diluting Multielement Standard Solution 1 for ICP (Sigma-Aldrich (Fluka); Dorset, UK) in the modified solubilisation matrix to obtain 0, 0.1, 1, 10, 50, 100 and 500 μ g/l final concentrations of Cobalt. Since the multielement standard solution composition includes 22 elements in different concentrations, Cobalt (10mg/l) was chosen as the reference to prepare the standards. Figure 4.2 shows that although the internal standard (Rh) recovery remained within the 90-110% range, it fluctuated greatly during the run.

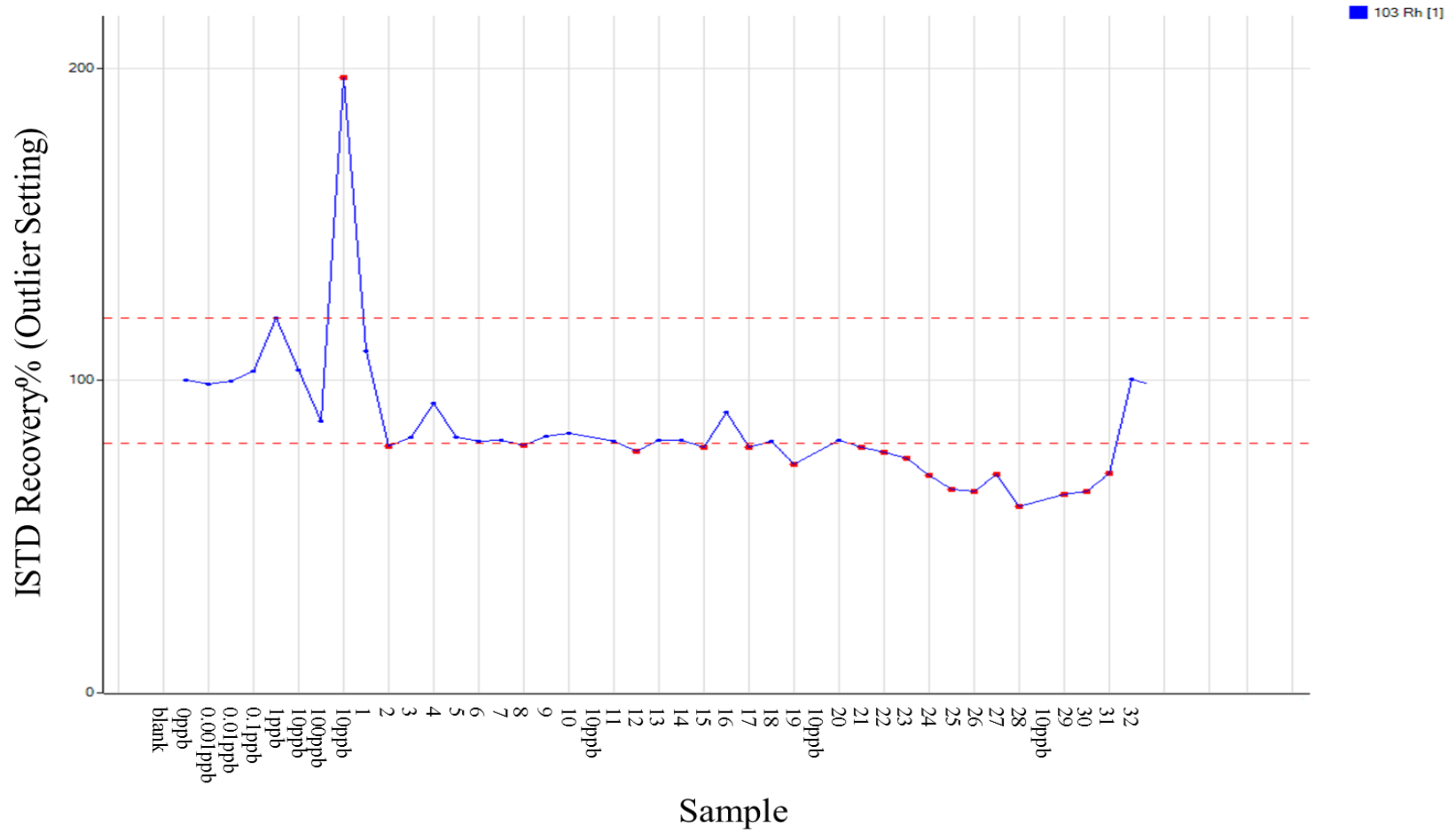


Figure 4.1. ICP-MS Internal standard (ISTD) recovery. Red dotted line marks acceptable range limits (90-110%) for internal standard recovery. Red dots represent the samples that are outside the range (outlier setting) Rh: Rhodium. Standards: 0, 0.001, 0.01, 0.1, 1, 10, and 100ppb (0, 0.001, 0.01, 0.1, 1, 10, and 100µg/l).

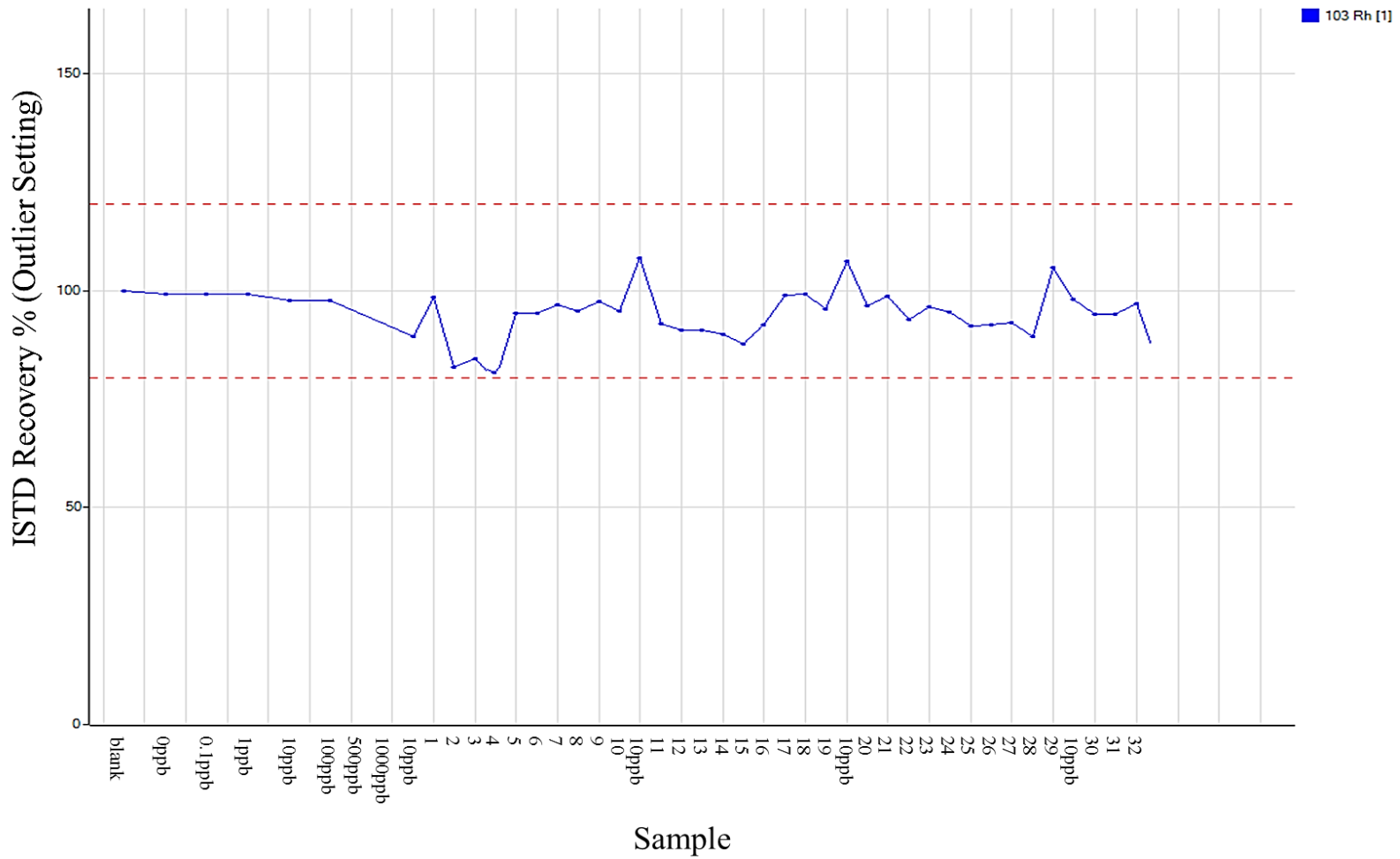


Figure 4.2. ICP-MS Internal standard (ISTD) recovery. Red dotted line marks acceptable range limits (90-110%) for internal standard recovery. Rh: Rhodium. Standards: 0, 0.1, 1, 10, 100, 500 and 1000ppb (0, 0.1, 1, 10, 100, 500 and 1000µg/l).

Based on this, the possibility of the culture medium samples not being stable in the dilution matrix was considered and an analysis of internal standard recovery (Rh, Sc, In) in a set of standards diluted in serum-free RPMI-1640 was performed. Figure 4.3 shows that there is minimal fluctuation in the internal standard recovery of the three candidates for internal standard. The generally flat slope of the internal standard recovery curve shows that there was no loss of sensitivity when implementing RPMI-1640 as the diluting matrix. Additionally, the mean (\pm SEM, n=3) detection limit for Co and Cr was $0.048\mu\text{g/l}$ (± 0.019) and $0.097\mu\text{g/l}$ (± 0.028), respectively. As a result, from this point on, analysis of metal ion levels in culture medium samples were carried out by diluting the samples in serum-free RPMI-1640 and following the protocol described in Section 2.1.18.1. In Chapter 7, it is shown that Sc is the least fluctuating internal standard in the analysis of whole blood samples. So, it was decided to use Sc as internal standard for all ICP-MS analysis. Figure 4.4 shows that the recovery of the internal standard from culture medium samples was stable with minimal fluctuation during the analysis.

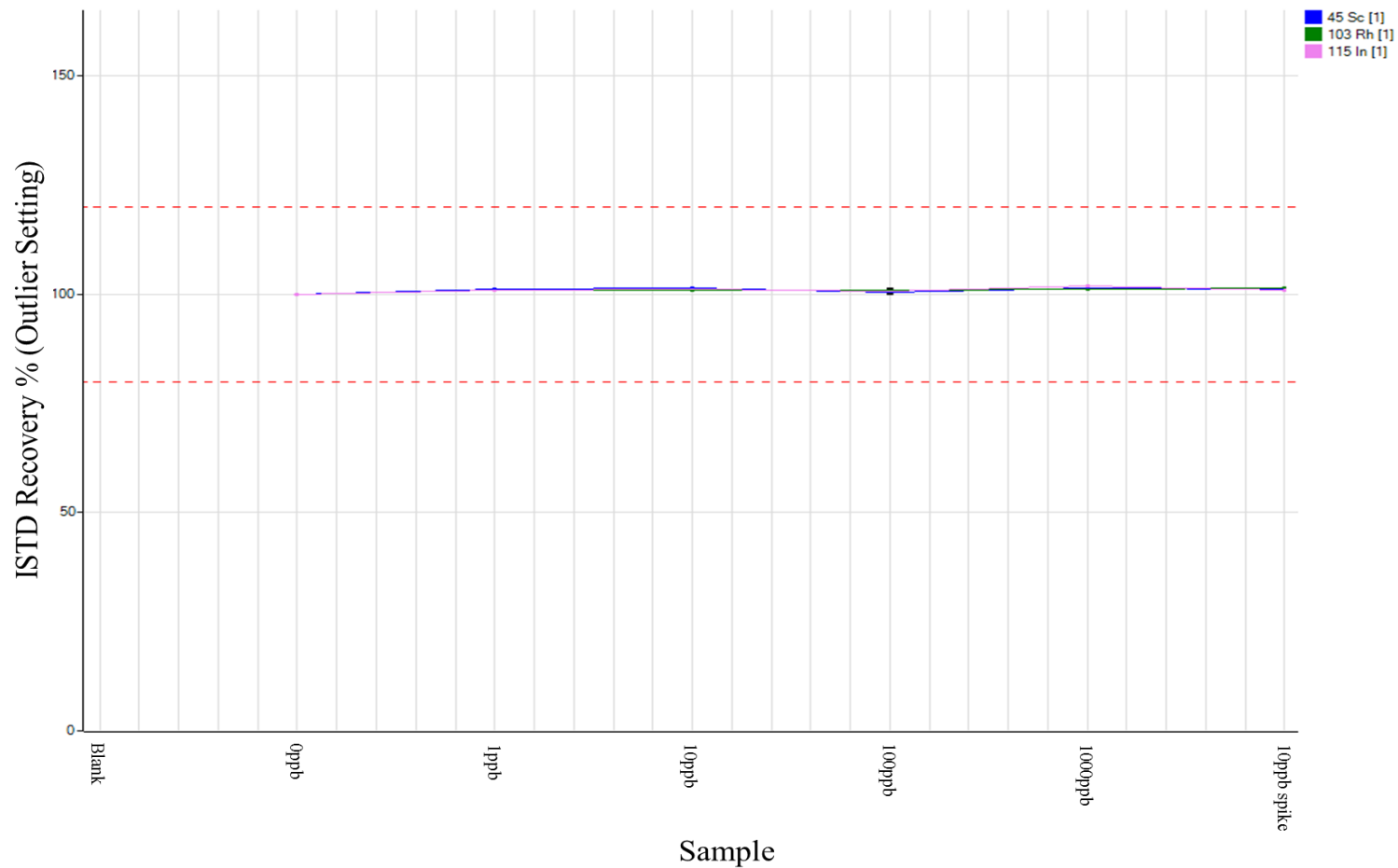


Figure 4.3. ICP-MS internal standard recovery of the candidates Sc, Rh, In. Red dotted line marks acceptable range limits for internal standard recovery. Graph representative of three independent repetitions. Sc: Scandium. Rh: Rhodium. In: Indium.

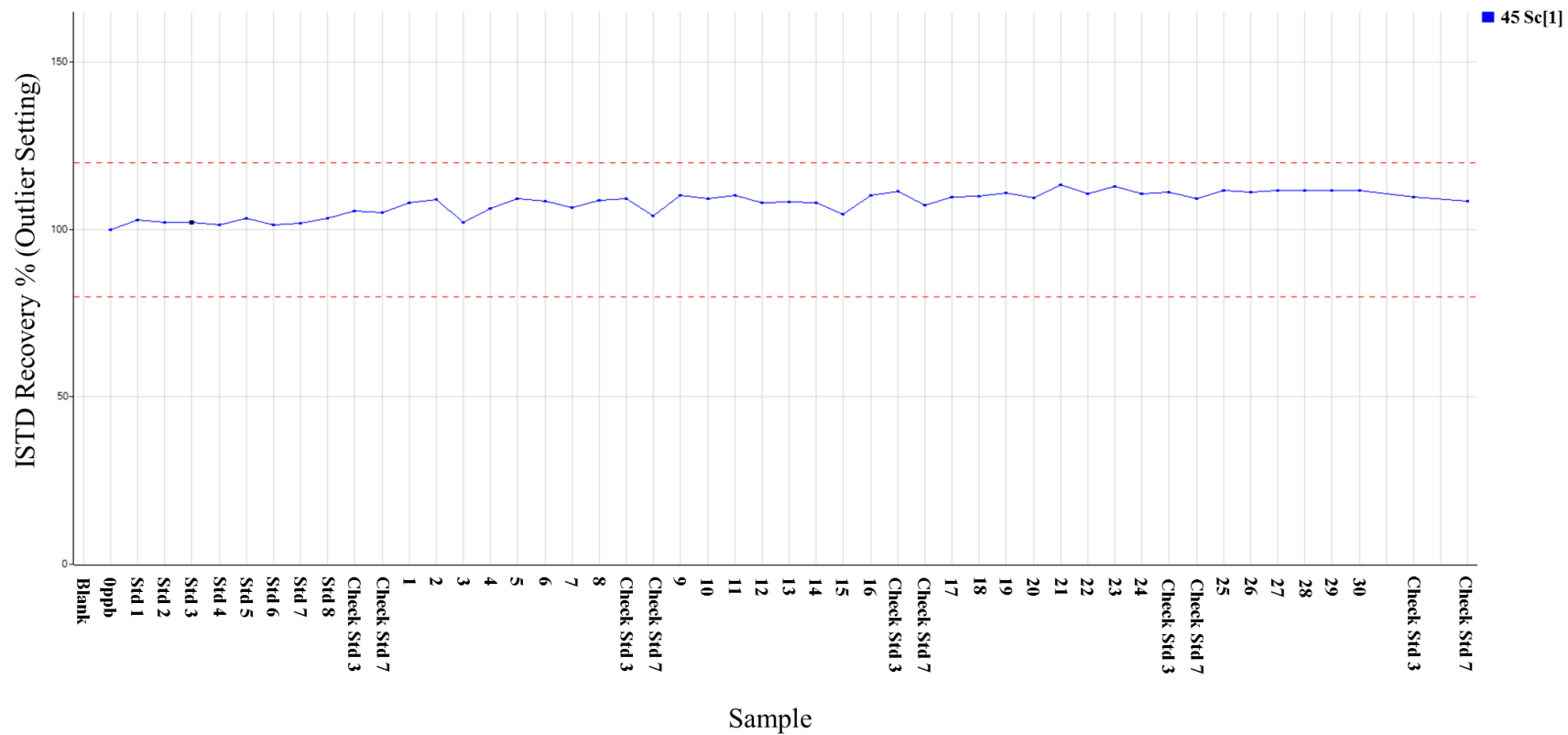


Figure 4.4. ISTD recovery from ICP-MS analysis of culture medium samples. Red dotted line marks acceptable range limits for internal standard recovery. Sc: Scandium. Std: standard Graph representative of three independent repetitions.

4.3.2 Metal ions release into cell culture medium

Experiments were carried out to determine the extent of metal ion release when wear debris was incubated with cultured cells *in vitro*.

Metal debris was incubated under different conditions (Section 2.1.17.1) in order to analyse the effects that some variables have on the amount of metal ions released into the culture medium. Analysis of ICP-MS results found that CoCr wear debris release metal ions into culture medium (Table 4.1 **Error! Reference source not found.**). There was no significant difference ($p > 0.05$) in ion release in the presence and absence of FBS. However, the acidic pH had a considerable effect as seen in the significant increase ($p < 0.05$) in the ion concentrations measured. Co was the ion predominantly released in all cases.

Condition	Mean Concentration [$\mu\text{g/l}$] \pm SEM		
	Cr	Co	Mo
RPMI - FBS	0.15 \pm 0.12	0.03 \pm 0.03	3.17 \pm 0.33
RPMI + 10% FBS	0.19 \pm 0.06	0.09 \pm 0.09	6.32 \pm 0.16
RPMI - FBS + CoCr wear debris	15.91 \pm 1.65*	1226.56 \pm 38.97*	127.82 \pm 4.28*
RPMI + 10% FBS + CoCr wear debris	18.18 \pm 2.64*	1259.41 \pm 39.58*	124.60 \pm 2.70*
pH4 RPMI + 10% FBS + CoCr wear debris	372.10 \pm 14.45*	3182.85 \pm 115.68*	222.26 \pm 7.69*

Table 4.1. Metal ions in RPMI-1640 in the presence and absence of metal wear debris. Results are expressed as mean values (\pm SEM, n=3). *Significantly different from RPMI + 10% FBS values ($p < 0.05$) by one-way ANOVA followed by Dunnett's multiple comparison test.

Different concentrations of metal debris (0, 0.2, 0.5, 1, 2.5, and 5mg debris/ 1×10^6 cells) were incubated in cell culture medium for 24h at 37°C and 5% (v/v) CO₂ in order to analyse the correlation between debris concentration and metal ions released (Table 4.2). Analysis of ICP-MS results found a significantly ($p < 0.05$) increasing amount of ions released with increasing wear debris concentrations. Once again, Co was the ion with the highest concentrations detected.

Debris concentrations (mg/10⁶ cells)	Cr (µg/l) Mean± SEM	Co (µg/l) Mean± SEM	Mo (µg/l) Mean± SEM
0.2	2.61±0.54	165.85±13.90	12.47±1.41
0.5	4.94±0.54	329.73±19.28	28.49±1.82
1.0	10.08±0.20	731.95±16.00	60.53±1.58
2.5	19.47±0.33	1560.06±30.60	147.97±2.32
5.0	26.83±0.80	2485.11±101.83	245.90±10.10

Table 4.2. Metal ions released from different concentrations of wear metal debris. Results are expressed as mean values (\pm SEM, n=6). All values are significantly different from control (0mg debris/1x10⁶cells) values ($p < 0.05$) by one-way ANOVA followed by Dunnett's multiple comparison test.

Considering these findings and to complement the viability and cytokine release results discussed in chapter 3, metal ion levels were measured in culture medium from resting (Figure 4.5) and activated (Figure 4.6) cells exposed for 24 and 120h to 5mg debris/1x10⁶cells, 0.1µM Co and a combination of 5mg debris/1x10⁶cells and 0.1µM Co.

ICP-MS results showed significantly ($p < 0.05$) higher concentrations of Cr and Co ions in the culture medium of both resting and activated cells exposed to metal wear debris when compared to control. In the presence of wear debris, significantly higher levels of Co and Cr ions were measured after 120h exposure compared to levels at 24h. Additionally, significantly higher levels of both metal ions were observed in cells pre-treated with 0.1µM Co compared to non-Co pre-treated cells. Moreover, significantly higher concentrations of Co than Cr were measured in the medium from both resting and activated cells in the presence of metal debris and 0.1 µM Co.

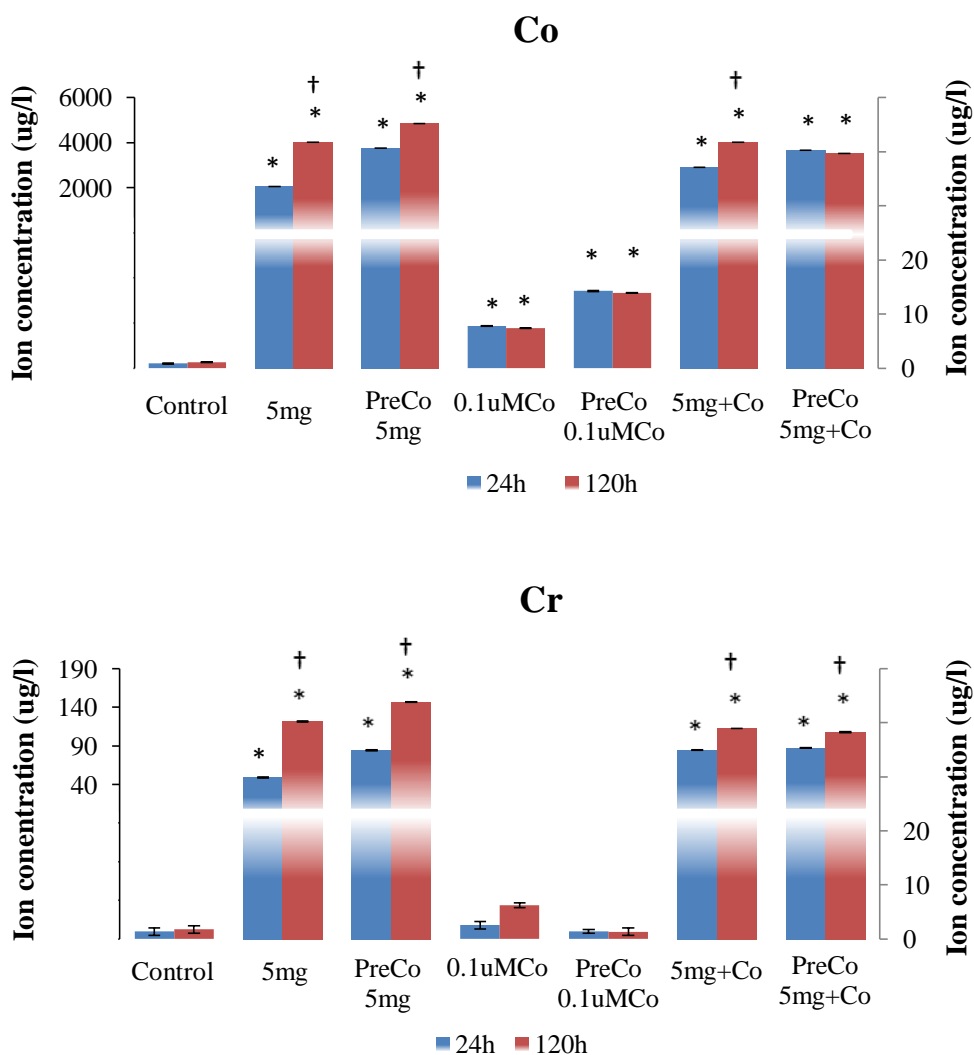


Figure 4.5. Metal ion concentrations in culture medium from resting U937 cells. Cells were exposed for 24 and 120h to 5mg debris/ 1×10^6 cells, $0.1 \mu\text{MCo}$ and a combination of 5mg debris/ 1×10^6 cells and $0.1 \mu\text{MCo}$. PreCo: cells pre-treated with $0.1 \mu\text{M Co}$. Results are expressed as mean values (\pm SEM, $n=3$). *Significantly different from control (untreated resting cells) values ($p < 0.05$) by one-way ANOVA followed by Dunnett's multiple comparison test. †120h values significantly different from 24h values by two-sample t-Test ($p < 0.05$).

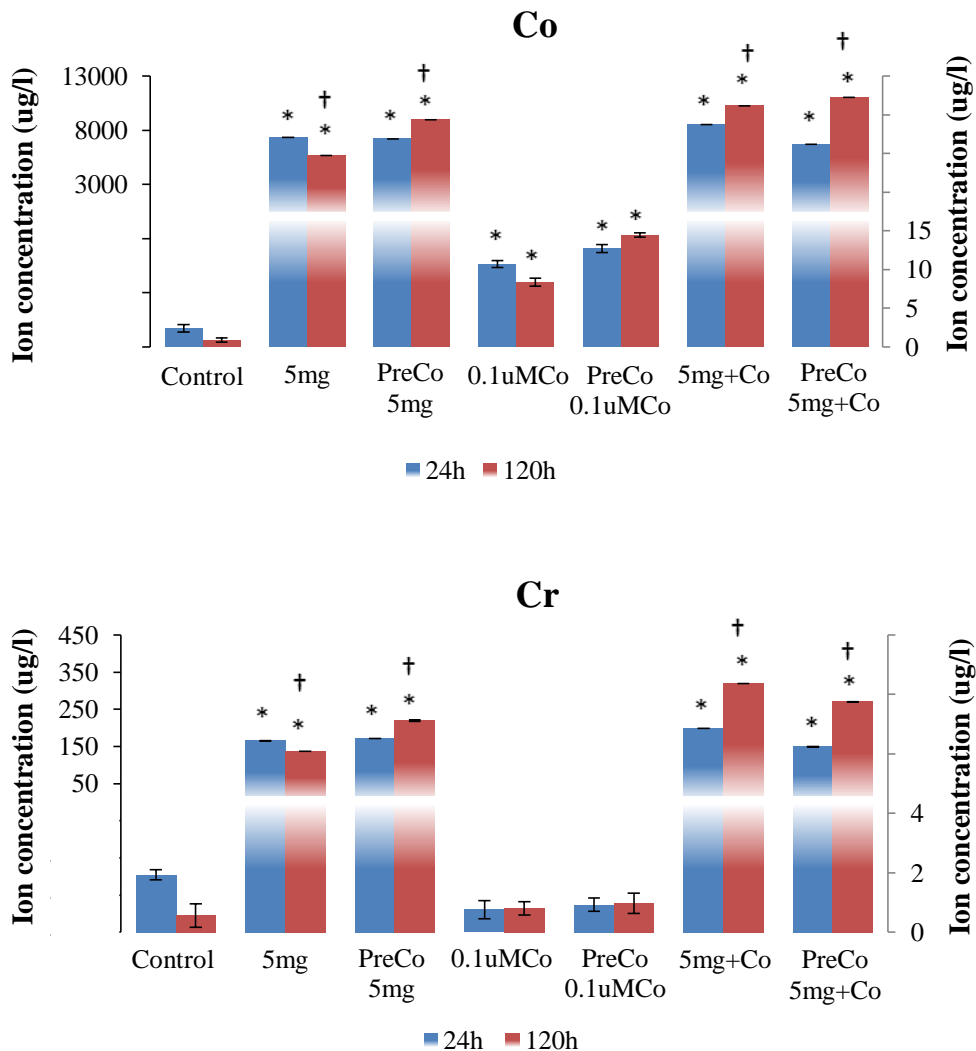


Figure 4.6. Metal ion concentrations in culture medium from activated U937 cells. Cells were exposed for 24 and 120h to 5mg debris/ 1×10^6 cells, $0.1 \mu\text{M}$ Co and a combination of 5mg debris/ 1×10^6 cells and $0.1 \mu\text{M}$ Co. PreCo: cells pre-treated with $0.1 \mu\text{M}$ Co. Results are expressed as mean values (\pm SEM, $n=3$). *Significantly different from control (untreated resting cells) values ($p < 0.05$) by one-way ANOVA followed by Dunnett's multiple comparison test. †120h values significantly different from 24h values.

Co and Cr ion levels measured in culture medium from activated cells were significantly higher than levels in medium from resting cells in the presence of metal debris. Activated macrophages contribute to the extracellular acidification during inflammatory reactions (Park et al., 2012), which in turn would enhance the release of ions from the metal debris. These findings complement the results documented in Chapter 3 and illustrate the contribution of metal ions in metal wear debris toxicity.

4.3.3 Cellular metal ion up-take

U937 cells were exposed to varying metal debris concentrations (0, 0.2, 0.5, 1, 2.5, and 5mg debris/ 1×10^6 cells) for 24h at 37°C and 5% (v/v) CO₂ in order to detect cellular up-take of ions released into the culture medium during incubation with CoCr wear debris. Analysis of ICP-MS results found significantly higher ($p < 0.05$) levels of Co than Cr in cells after all treatments (Table 4.3). Mo could not be detected (mean detection limit \pm SEM, 0.040 ± 0.020 , $n=6$). There is an increase in ion levels with increasing wear debris concentrations. However, there is a slight decrease in ion levels when cells were exposed to 5mg debris/ 1×10^6 cells probably due to the fact that this concentration has been shown to be cytotoxic (Chapter 3). Once again, these findings demonstrate that the toxicity seen in Chapter 3 is not solely due to the metal nanoparticles and that metal ions contribute greatly to such toxic effects.

Debris concentrations (mg/ 10^6 cells)	Cr (fg/cell) Mean \pm SEM	Co (fg/cell) Mean \pm SEM
0.2	3.18 \pm 1.27	10.18 \pm 0.64
0.5	5.09 \pm 0.64	24.17 \pm 1.27
1.0	3.75 \pm 0.06	32.44 \pm 1.10
2.5	16.54 \pm 0.64	122.14 \pm 2.92
5.0	14.63 \pm 0.64	110.05 \pm 3.18

Table 4.3. Cellular ion up-take. Results are expressed as mean values (\pm SEM, $n=6$). All values are significantly different from control (0mg debris / 1×10^6 cells) values ($p < 0.05$) by one-way ANOVA followed by Dunnett's multiple comparison test.

4.3.4 Apoptosis analysis of U937 cells following exposure to CoCr wear debris and Co ions

In order to assess apoptosis, 1×10^5 cells/ml resting U937 cells, with and without Co pre-treatment, were exposed for 24 and 48h to 2.5mg debris/ 1×10^6 cells, 0.1 μ M Co and 2.5mg debris/ 1×10^6 cells plus 0.1 μ M Co, in 12-well plates at 37°C and 5% (v/v) CO₂.

4.3.4.1 Flow cytometry of resting U937 cells following 24 and 48h exposure to CoCr wear debris and Co ions

Flow cytometry using Annexin V/FITC and 7-AAD double staining allowed distinction between cells that were viable, in early stages of apoptosis, in late stages of apoptosis and necrotic. This was possible as Annexin V binds to the negatively charged phospholipid phosphatidylserine (PS) which is redistributed from the inner to outer layer of the cell membrane during apoptosis. Cells in early stages of apoptosis are not permeable to 7-AAD but bind to Annexin V. Cells which bind to Annexin V, and are permeant to 7-AAD, are in the later stage of apoptosis as the cell membrane is compromised. Cells which have 7-AAD bound to DNA, but are not Annexin V positive are said to be necrotic, as they are non-viable but not through apoptotic mechanisms.

Flow cytometry analysis revealed that after exposure to 2.5mg debris/ 1×10^6 cells and 2.5mg debris/ 1×10^6 cells with 0.1 μ M Co, the number of cells with externalized PS started to increase by 24h of treatment. This increase became significant by 48h of exposure. Metal wear debris induced a greater PS externalization in cells that had been pre-treated with Co (Figure 4.7).

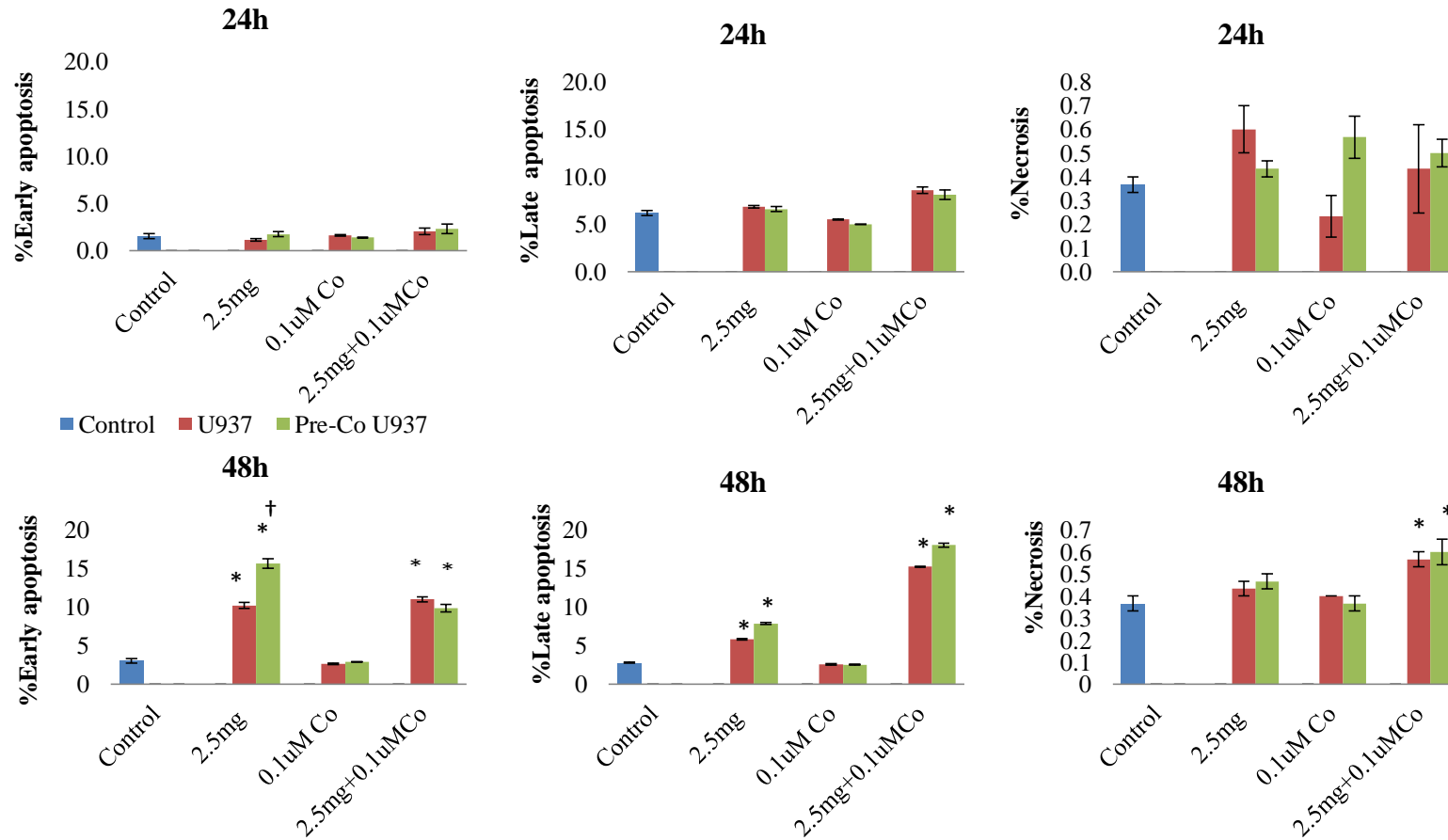


Figure 4.7. Early apoptosis, late apoptosis and necrosis of resting U937 and Co pre-treated resting U937 cells measured by FACS. Cells were exposed for 24 and 48h to 2.5mg debris/ 1×10^6 cells, 0.1µM Co and a combination of 2.5mg debris/ 1×10^6 cells and 0.1µM Co. Results are mean values (\pm SEM, n=6). PreCo: cell pre-treated with 0.1µM Co. *Significantly different from control values ($p < 0.05$) by one-way ANOVA followed by Dunnett's multiple comparison test. †Significantly different from non-Co pre-treated cells.

4.3.4.2 Western blot of resting U937 cells following 24 and 48h exposure to CoCr wear debris and Co ions

Western blot analysis validated the flow cytometry results by showing the fragmentation of PARP after 48h of exposure to 2.5mg debris/ 1×10^6 cells and 2.5mg debris/ 1×10^6 cells with $0.1 \mu\text{M}$ Co (Figure 4.8). PARP is cleaved by members of the caspase family (for example, caspase 3 and 7) during early apoptosis (Nicholson et al., 1995, Ding et al., 2009). These proteases cleave PARP to fragments of approximately 89kD and 24kD and detection of one or both fragments has been used as a hallmark of apoptosis (Mudter and Neurath, 2007, Gambi et al., 2008).

Figure 4.8 shows the fragmentation of PARP in the presence of wear debris but not in the presence of $0.1 \mu\text{M}$ Co after 48h of treatment. These results together with flow cytometry findings suggest that the mechanism of cell death could correlate to particle concentration. High concentrations of wear debris may be more likely to induce necrosis, results in Chapter 3 are evidence of this; and lower concentrations may be more likely to induce apoptosis.

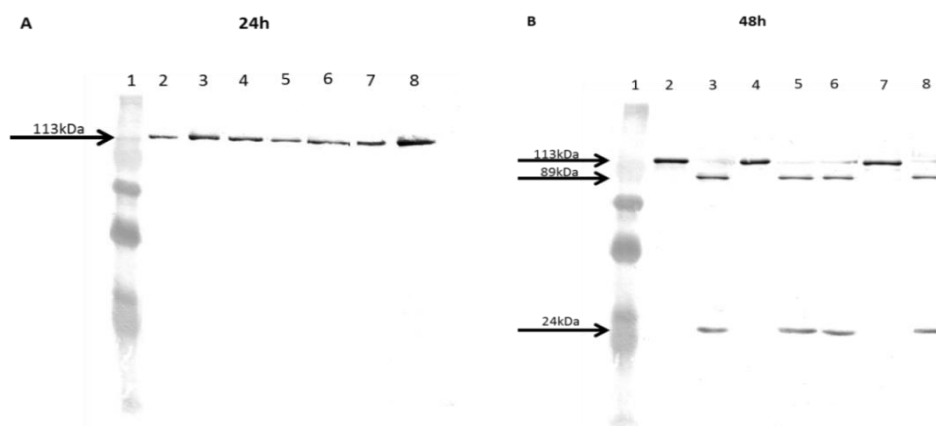


Figure 4.8. Detection of PARP and PARP fragments by western blot as indication of early apoptosis of resting U937 and Co pre-treated resting U937 cells. Cells were exposed for 24 and 48h to 2.5mg debris/ 1×10^6 cells, $0.1 \mu\text{M}$ Co and a combination of 2.5mg debris/ 1×10^6 cells and $0.1 \mu\text{M}$ Co. Lane 1: Molecular marker. Lane 2: untreated cells (control). Lane 3: U937 cells + 2.5mg debris/ 1×10^6 cells. Lane 4: U937 cells + $0.1 \mu\text{M}$ Co. Lane 5: U937 cells + 2.5mg debris/ 1×10^6 cells with $0.1 \mu\text{M}$ Co. Lane 6: Co pre-treated U937 cells + 2.5mg debris/ 1×10^6 cells. Lane 7: Co pre-treated U937 + $0.1 \mu\text{M}$ Co. Lane 8: Co pre-treated U937 cells + 2.5mg debris/ 1×10^6 cells with $0.1 \mu\text{M}$ Co. Figure A shows intact PARP (113kDa) after 24h for all treatments. Figure B shows fragmentation of PARP (89kDa and 24kDa) after 48h of treatment with debris and debris with Co.

4.3.5 Gene expression analysis of resting U937 cells following 120h exposure to CoCr wear debris and Co ions

4.3.5.1 StellARray[®] gene expression array

This toxicology array used here was specifically designed to profile the expression of the 94 top ranked genes important for monitoring the metabolic responses against drugs and other toxins. Primer pairs present on this array are specific for genes involved in DNA damage and repair processes, apoptosis, cell cycle, electron transport, growth and proliferation, metabolite transporters, and stress response genes.

Lonza recommend the use of the Global Pattern Recognition™ (GPR) software (Bar Harbor Biotechnology Inc, USA) with the StellARray system data to define the invariant normalizer genes from the experiment. Analysis is performed by logging into [Gene Expression Arrays System](https://www.bhbio.com/BHB/(S(pbw4hguf2capymwtwa13fam5))/GUI/Account/Login.aspx?ReturnUrl=%2fBHB%2fGUI%2fAP%2fGPR.aspx) ([https://www.bhbio.com/BHB/\(S\(pbw4hguf2capymwtwa13fam5\)\)/GUI/Account/Login.aspx?ReturnUrl=%2fBHB%2fGUI%2fAP%2fGPR.aspx](https://www.bhbio.com/BHB/(S(pbw4hguf2capymwtwa13fam5))/GUI/Account/Login.aspx?ReturnUrl=%2fBHB%2fGUI%2fAP%2fGPR.aspx)), selecting the appropriate StellARray product, uploading the data and submitting it for analysis. A HTML or Excel formatted file is generated which gives a ranked list of genes and links to MGI and NCBI gene pages.

In the current study, the standard Human General Toxicology 96 StellARray was used in order to identify genes related to the toxic effects of metal wear debris and ions on resting U937 cells. The procedure was carried out as recommended by the manufacturer and is detailed in Section 2.1.23. GPR compared the qPCR results from treated and untreated cells and gave a ranked list of genes by fold change value (Table 4.4).

Rank	Gene Name	Fold Change	Rank	Gene Name	Fold Change	Rank	Gene Name	Fold Change
1	AHR	-21.92	33	XPC	-2.09	65	FOS	3.40
2	PPARD	-10.88	34	E2F1	-2.06	66	UNG	3.67
3	CDK2	-9.09	35	ERCC3	-1.72	67	CYP2F1	3.75
4	ABCC1	-7.08	36	DNAJA1	-1.72	68	BAG1	3.96
5	BCL2L1	-6.89	37	EPHX1	-1.67	69	CYP2D6	4.55
6	RAD23A	-5.48	38	CASP8	-1.60	70	FGF2	4.61
7	CYB5R3	-5.18	39	NFKB1	-1.58	71	ABCC2	4.71
8	MYC	-4.70	40	RAD51	-1.37	72	MAOA	6.22
9	ERBB2	-4.70	41	TNF	-1.35	73	TRPV6	7.34
10	XDH	-4.51	42	MLH1	-1.32	74	CYP2A13	9.16
11	HSPA5	-4.42	43	BCL2	-1.29	75	FASLG	17.58
12	GSR	-4.33	44	CASP3	-1.28	76	LTA	22.25
13	PPARGC1A	-4.24	45	CYP27B1	-1.26	77	NOS2	25.74
14	SOD1	-3.96	46	HSPA1B	-1.08	78	ABCB1	37.69
15	GPX1	-3.93	47	XRCC2	-1.07	79	ESR2	50.07
16	IGF1R	-3.90	48	ACADSB	1.11	80	CYP3A4	50.77
17	ARNT	-3.57	49	CYP1A1	1.15	81	EGFR	74.85
18	MDM2	-3.42	50	HSPB1	1.17	82	CYP1A2	154.99
19	HSPA1A	-3.40	51	TNFRSF1A	1.23	83	CYP7A1	228.49
20	BAX	-3.28	52	CYP8B1	1.31	84	CYP1B1	234.92
21	XPA	-3.13	53	HSPA1L	1.33	85	CYP4B1	297.35
22	CHEK2	-3.10	54	CCND1	1.39	86	ABCB4	329.93
23	CDK4	-3.02	55	POR	1.43	87	MGMT	483.04
24	ERCC1	-2.86	56	CDKN1A	1.51	88	CYP7B1	514.13
25	DDIT3	-2.82	57	CDKN1B	1.52	89	IGFBP6	659.85
26	HSP90AA1	-2.63	58	NQO1	1.81	90	CYP11A1	659.85
27	CCNE1	-2.57	59	TRADD	1.81	91	CYP2B6	895.16
28	BRCA1	-2.42	60	CYP2E1	1.82	92	CYP2C9	952.78
29	MSH2	-2.37	61	GPX2	1.99	93	CYP24A1	1301.54
30	CAT	-2.34	62	HIF1A	2.24	94	FMO1	2313.72
31	CDKN2A	-2.32	63	FMO4	2.47			
32	PRDX1	-2.12	64	GADD45A	2.98			

Table 4.4. GPR results derived from resting U937 cells treated with 2.5mg/1x10⁶ cells wear debris and 0.1µM Co for 120h. Fold change values are displayed with respect to the control group. For example, AHR (rank position 1) is down-regulated ~22 fold in treated cells. The genes of interest are highlighted in gray.

Gene Set Enrichment Analysis (GSEA) is a microarray data analysis method that uses predefined gene sets and ranks of genes to identify significant biological changes in microarray datasets (Tang et al., 2013). The gene sets are groups of genes that share common biological function, chromosomal location, or regulation and are defined based on prior biological knowledge, e.g., published information about biochemical pathways or co-expression in previous experiments. The goal of GSEA is to determine whether members of a gene set S are randomly distributed throughout the list L or primarily found at the top or bottom, in which case the gene set is correlated with phenotypic difference (Subramanian et al., 2005). Toppgene is an on-line portal for GSEA and candidate gene prioritization based on functional annotations and protein interactions (Chen et al., 2009). Exposure to metal ions may cause early cellular changes that could induce a deviation from a normal biological pathway. As the cellular levels of exposure increase, the metal ions could potentially interact with a molecular target to induce perturbation of cellular function (Figure 4.9). At low levels of exposure, adaptive stress responses are activated to try to restore the pathway to produce its normal outputs. At high enough levels of exposure and internal dose, perturbation exceeds the homeostatic capacity of the adaptive responses, and cell injury occurs (Bushnell et al., 2010).

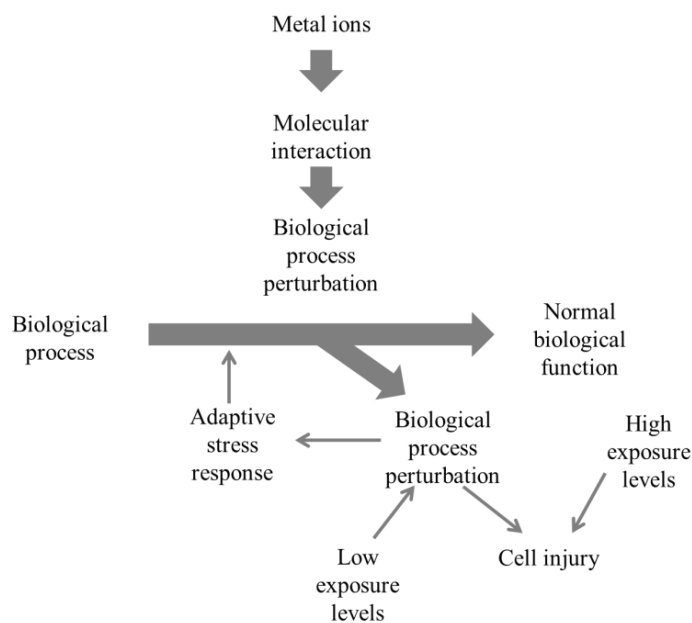


Figure 4.9. Schematic overview of a biological process perturbation. (adapted from Bushnell et al., 2010).

The StellarRay gene set was submitted to Toppgene for analysis. After screening the biological processes identified by this on-line portal and taking into account the results from the StellarRay profiling, five genes were chosen (Table 4.5) for further expression investigation in U937 cells treated with metal debris and ions.

Biological Process	Gene Name
Regulation of cell death	BAG1, LTA
Regulation of programmed cell death	BAG1, LTA
Response to toxin	FOS
Negative regulation of growth	LTA
Response to metal ions	BAG1, FOS
Regulation of cell proliferation	NOS2, LTA
Nitric oxide metabolic process	NOS2
Oxygen and reactive oxygen species metabolic process	GADD45A, NOS2

Table 4.5. Genes chosen for further expression analysis. LTA (lymphotoxin alpha): inflammatory mediator that influences multiple processes such as activation, proliferation, differentiation, and death induction in many different cell types (Kagi et al., 1999). BAG1 (BCL2-associated athanogene): multifunctional protein able to delay cell death by a synergistic action with BCL2 (Aveic et al., 2011). GADD45A (growth arrest and DNA damage): nuclear protein involved in cell cycle arrest, DNA repair and apoptosis (Siafakas and Richardson, 2009). FOS (FBJ osteosarcoma oncogene): involved in osteoclast development and activation (Chen et al., 2011). NOS2 (inducible nitric oxide synthase): inducible by cytokines, converts L-arginine to L-citrulline, and nitric oxide (Xu et al., 2003).

4.3.5.2 Primer specificity

Forward and reverse SYBR Green primers were then designed for each of the shortlisted genes to target all their variants and to generate a product bigger than 100bp but smaller than 150bp. SYBR Green is a dye that binds in the minor groove of double-stranded DNA (dsDNA) in a sequence independent way. When it binds, its fluorescence increases over 100-fold (Deprez et al., 2002). However, since SYBR Green binds indiscriminately to dsDNA, primer-dimer artifacts or other non-specific products contribute to the detected fluorescence (Zipper et al., 2004), which is why it requires melting curve analysis to determine the specificity of the amplification (VanGuilder et al., 2008).

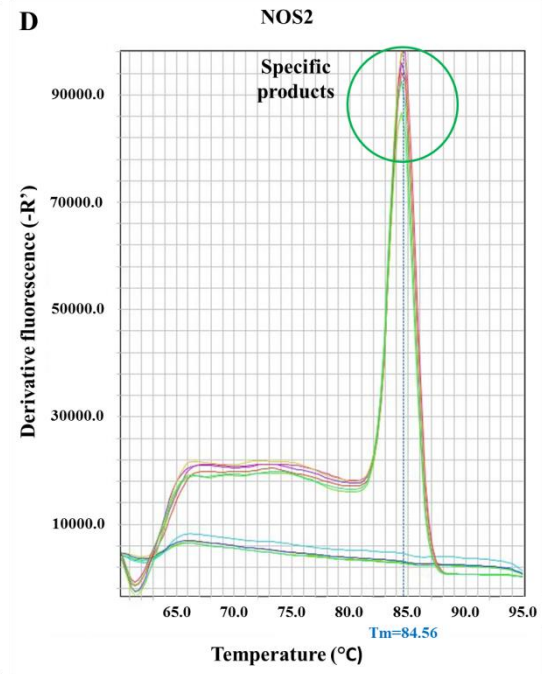
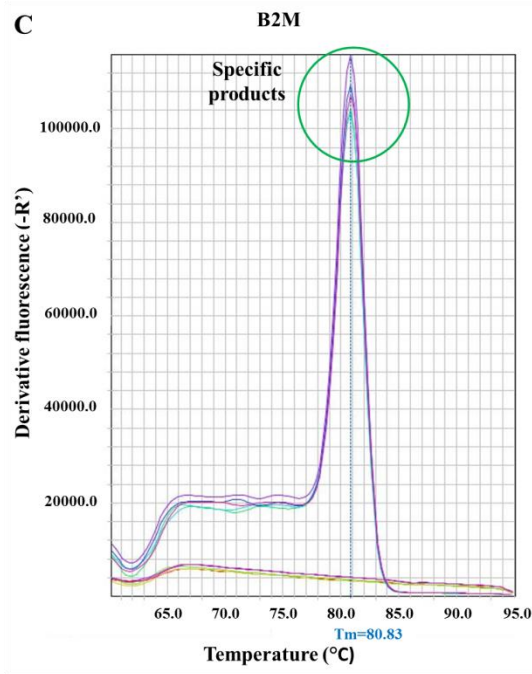
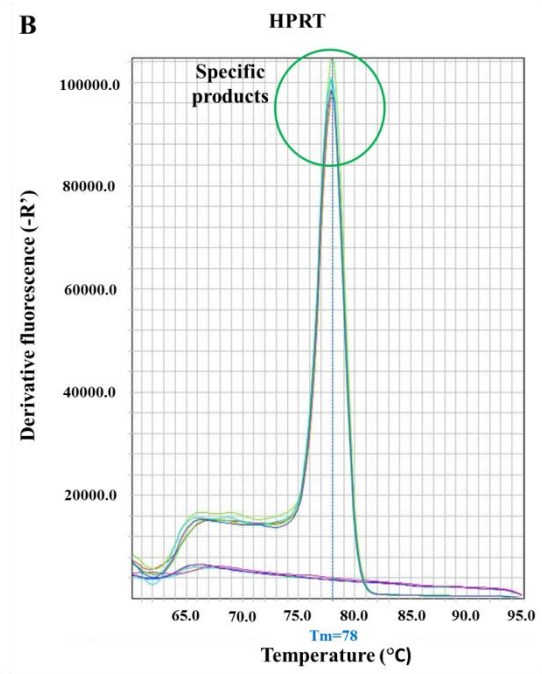
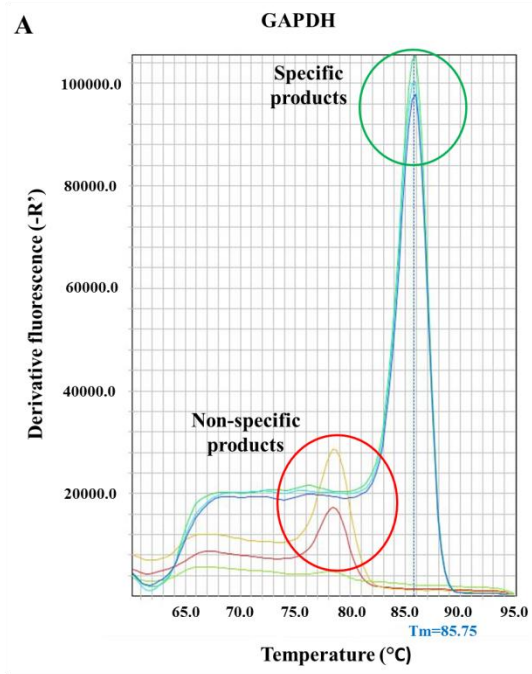
Post-PCR melting curve analysis is a technique used for determining the presence of primer-dimer artifacts or other non-specific products and to ensure reaction

specificity. PCR products can be distinguished by their melting curves because the melting curve of a product is dependent on GC content, length and sequence (VanGuilder et al., 2008).

If the fluorescence of SYBR Green is monitored continuously throughout a temperature cycle, product denaturation can be observed as a rapid loss of fluorescence near the melting (denaturing) temperature (Wittwer et al., 1997). A melt curve is produced by gradually increasing the temperature, thereby gradually denaturing an amplified DNA target. Since SYBR Green is only fluorescent when bound to dsDNA, fluorescence decreases as duplex DNA is denatured. The highest rate of fluorescence decrease is generally at the melting temperature of the DNA sample (T_m) (Ririe et al., 1997). The T_m is defined as the temperature at which 50% of the DNA sample is double-stranded and 50% is single-stranded. The T_m is typically higher for DNA fragments that are longer and/or have a high GC content (von Ahsen et al., 2001).

Since a SYBR Green dye-based chemistry was used in the current study, specificity of qRT-PCR was assessed with melting curve analysis after every run (Figure 4.10) and with horizontal gel electrophoresis (Section 2.1.20).

The StepOne™ software v2.1, plots the melt curve as derivative fluorescence ($-R'$) vs. temperature. A single peak at a high temperature ($>75^\circ\text{C}$) in all reactions and nothing, or very little, detected in the no-template controls, showed high specificity (Figure 4.10). Since some of melting curve analysis showed non-specific product formation, the PCR reactions were qualitatively assessed on ethidium bromide-stained agarose gels. Each gene expression assay displayed a single product of the desired length and no bands were present in the negative controls. Only PCRs with cDNA from cells treated with $2.5\text{mg}/1 \times 10^6$ cells wear debris showed non-specific products in the presence of GAPDH primers. These non-specific products are likely to be primer dimers (primers attached to each other) due to the lack of a full length amplicon resulting in an excess of primers (Figure 4.12.A).



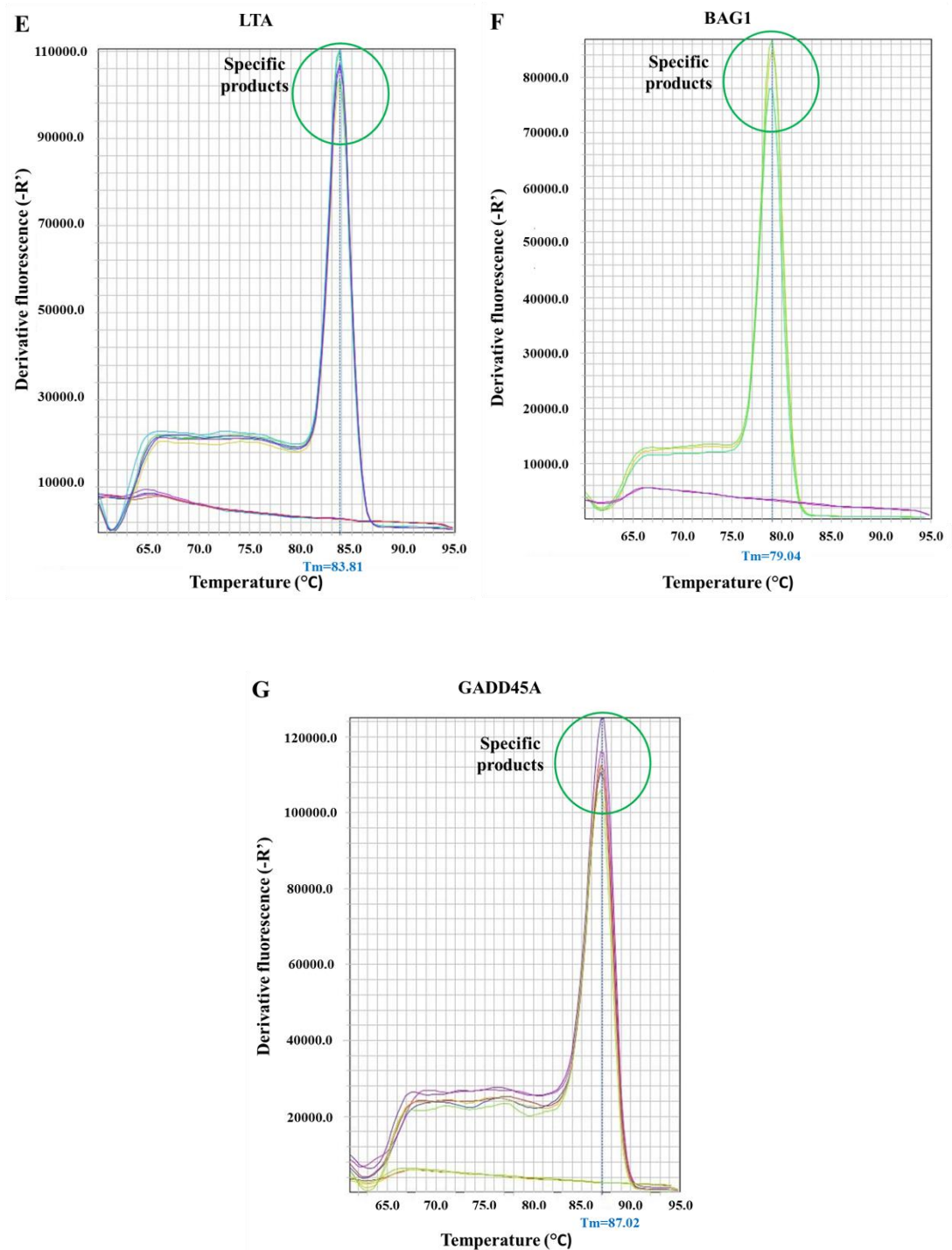


Figure 4.10. Melting curve analysis. Curves showing peaks of specific product at $>78^{\circ}\text{C}$ and some non-specific product at lower temperatures. A) GAPDH. B) HPRT. C) B2M. D) NOS2. E) LTA. F) BAG1. G) GADD45A.

Following PCR, horizontal gel electrophoresis of negative control and cDNA reaction mixtures was performed as a qualitative assessment of the real-time PCR. Two different negative control reactions were included for each gene, namely H_2O

and RT-. Negative controls were included to monitor contamination to ensure that the fluorescence measured during the PCR corresponds to product amplification (Bustin et al., 2010). H₂O reactions helped monitor PCR contamination and contained all the PCR reagents but instead of 1µl of cDNA template, 1µl of nuclease free water was added. In a similar way, RT- reactions helped monitor potential carry over contamination from the cDNA synthesis. These reactions contained all the PCR reagents but instead of 1µl of cDNA template, 1µl of reverse transcriptase free reaction (from the cDNA synthesis) was added. These reactions should not generate amplification products during the PCR process.

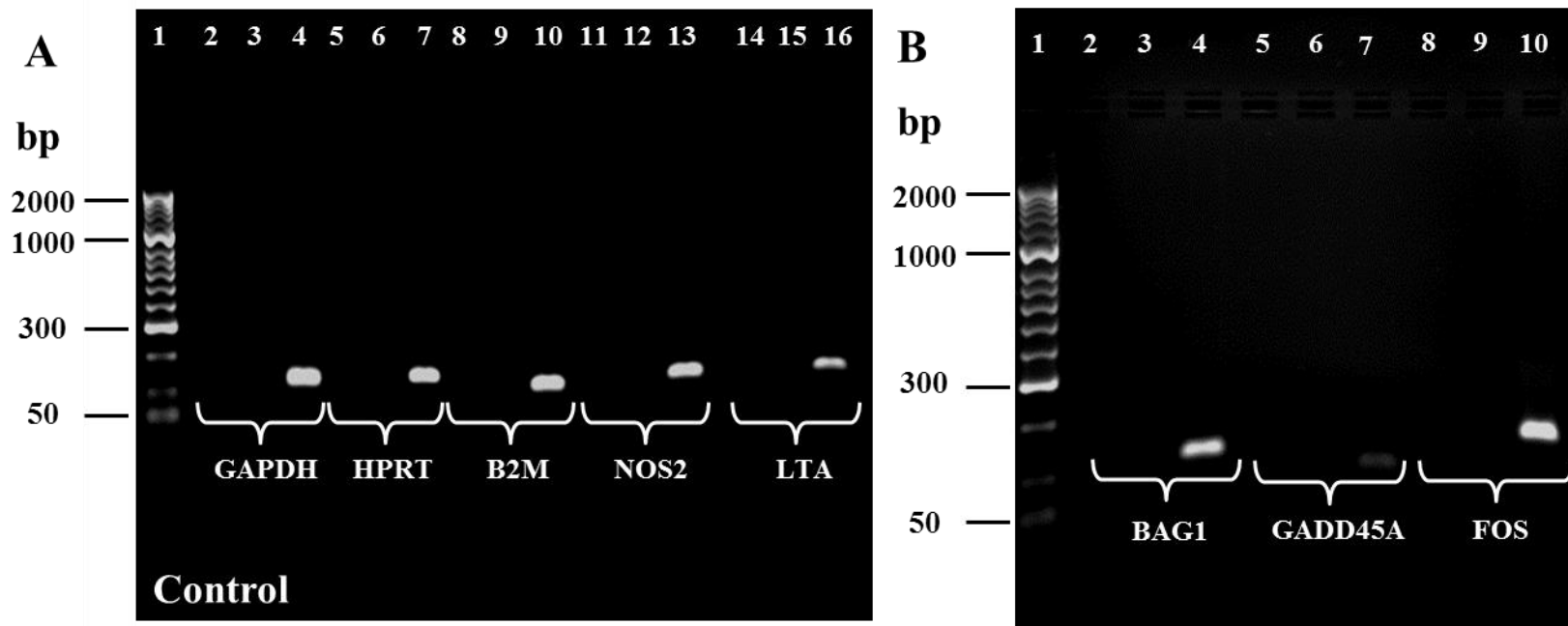


Figure 4.11. Horizontal gel electrophoresis of PCR amplification products from untreated resting U937 cells (control). HyperLadder II (Bioline, UK) molecular ladder was used. A) Amplification products of GAPDH (lanes 2-4), HPRT (lanes 5-7), B2M (lanes 8-10), NOS2 (lanes 11-13) and LTA (lanes 14-16). C) Amplification products of BAG1 (lanes 2-4), GADD45 (lanes 5-7) and FOS (lanes 8-10). Lane 1 in B) and B) shows the HyperLadder II molecular ladder. There are three lanes for each gene: the first two lanes are negative control reactions (H_2O and RT-) and the third lane is the cDNA reaction.

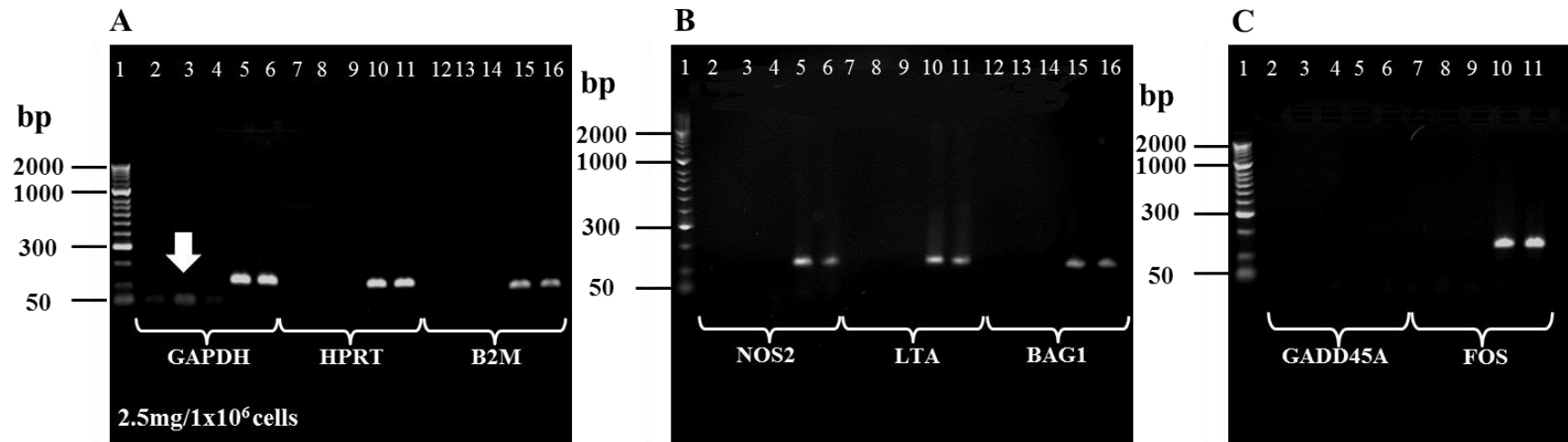


Figure 4.12. Horizontal gel electrophoresis of PCR amplification products from resting and Co pre-treated resting U937 cells exposed to 2.5mg debris/1x10⁶ cells for 120h. A) Amplification products of GAPDH (lanes 2-6), HPRT (lanes 7-11), B2M (lanes 8-10), B) NOS2 (lanes 11-13) and LTA (lanes 14-16). C) Amplification products of BAG1 (lanes 2-4), GADD45 (lanes 5-7) and FOS (lanes 8-10). Lane 1 in A), B) and C) shows the HyperLadder II molecular ladder. There are five lanes for each gene. The first three lanes are negative control reactions (H₂O, RT_{U937}⁻ and RT_{PreCoU937}⁻). The fourth lane is the cDNA_{U937} reaction and the fifth is the cDNA_{PreCoU937} reaction.

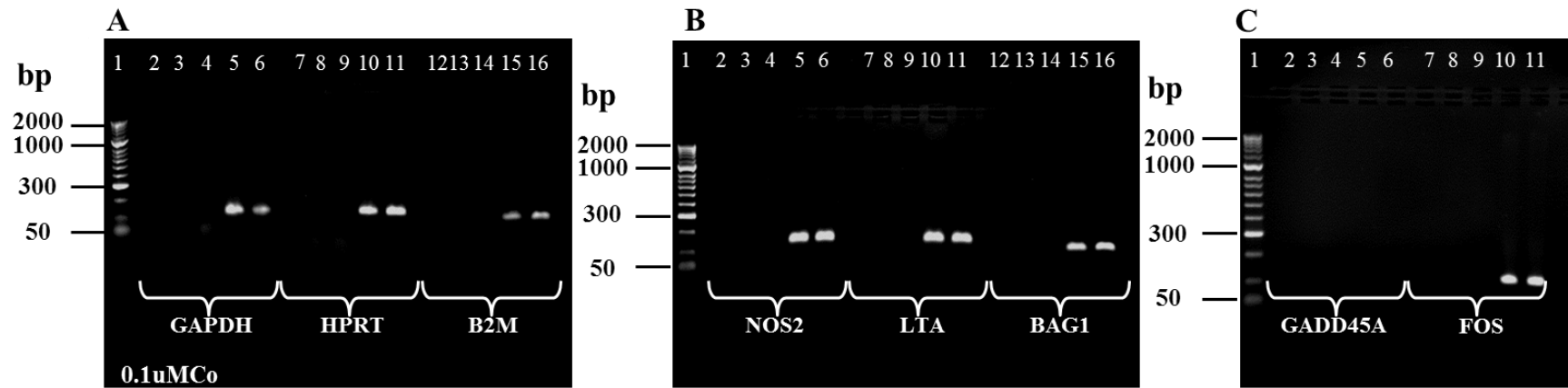


Figure 4.13. Horizontal gel electrophoresis of PCR amplification products from resting and Co pre-treated resting U937 cells exposed to 0.1μM Co for 120h. A) Amplification products of GAPDH (lanes 2-6), HPRT (lanes 7-11), B2M (lanes 8-10). B) NOS2 (lanes 11-13) and LTA (lanes 14-16). C) Amplification products of BAG1 (lanes 2-4), GADD45 (lanes 5-7) and FOS (lanes 8-10). Lane 1 in A), B) and C) shows the HyperLadder II molecular ladder. There are five lanes for each gene. The first three lanes are negative control reactions (H_2O , RT_{U937^-} and $RT_{PreCoU937^-}$). The fourth lane is the $cDNA_{U937}$ reaction and the fifth is the $cDNA_{PreCoU937}$ reaction.

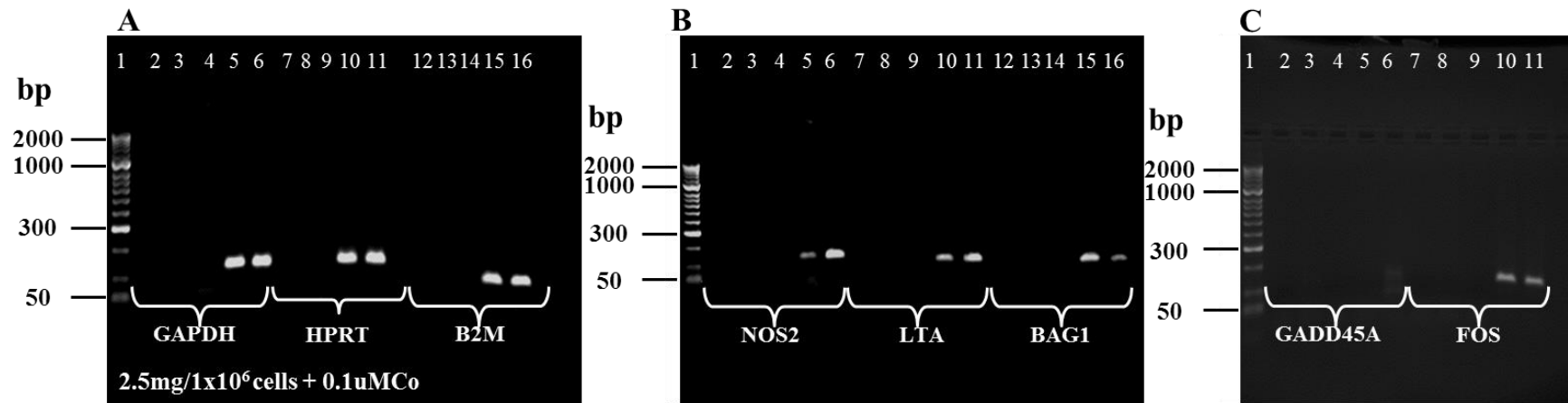


Figure 4.14. Horizontal gel electrophoresis of PCR amplification products from resting and Co pre-treated resting U937 cells exposed to 2.5mg debris/1x10⁶ cells+0.1μM Co for 120h. A) Amplification products of GAPDH (lanes 2-6), HPRT (lanes 7-11), B2M (lanes 8-10). B) NOS2 (lanes 11-13) and LTA (lanes 14-16). C) Amplification products of BAG1 (lanes 2-4), GADD45 (lanes 5-7) and FOS (lanes 8-10). Lane 1 in A), B) and C) shows the HyperLadder II molecular ladder. There are five lanes for each gene. The first three lanes are negative control reactions (H₂O, RT_{U937}⁻ and RT_{PreCoU937}⁻). The fourth lane is the cDNA_{U937} reaction and the fifth is the cDNA_{PreCoU937} reaction.

These results show that the set of primers designed were specific, giving single products of the predicted size. This means that the fluorescent signal measured in the PCR reactions is due to the single desired product and there is no contribution to the signal from misprime-derived products or primer dimer formation which might complicate analysis.

4.3.5.3 Reference gene determination

Resting and activated U937 cells and Co pre-treated U937 cells were exposed for 120h to three different treatments: 2.5mg metal wear debris, 0.1 μ M Co and 2.5mg metal wear debris plus 0.1 μ M Co. Total RNA was extracted at 120h, from which cDNA was then synthesised. Quantitative real-time PCR was carried out to analyse the effect of the treatments on the expression of NOS2, LTA, BAG1, GADD45A, and FOS. These five genes were selected due to their response to metal debris and ions as seen on the General Human Toxicology StellarArray® qPCR Array plates and the analysis of such results.

Normalization is an essential component of a reliable qPCR assay because this process controls for variations in extraction yield, reverse-transcription yield, and efficiency of amplification, thus enabling comparisons of mRNA concentrations across different samples (Bustin et al., 2009). Normalising to a reference gene is the most common method for internally controlling for error in real-time RT-PCR. However, the chosen genes must be experimentally validated for particular tissues or cell types and specific experimental designs (Bustin et al., 2010). The most commonly used reference genes, also referred to as classic reference genes, include β -actin, glyceraldehyde-3-phosphate dehydrogenase (GAPDH), 2-microglobulin (B2M), hypoxanthine-guanine phosphoribosyl transferase (HPRT) and 18S ribosomal RNA (Huggett et al., 2005, Thellin et al., 1999, Lee et al., 2002). It is surprising to see the variety of studies that have chosen these genes but show no evidence or mention of a validation process (Sethi et al., 2003, Jakobsen et al., 2007, Bastonini et al., 2011, Liew et al., 2002) even though there have been a number of reports that demonstrate that such genes can vary extensively depending on the

experimental conditions and are unsuitable for normalisation purposes (Dheda et al., 2004, Bas et al., 2004, Bemeur et al., 2004, Schmid et al., 2003, Tricarico et al., 2002). GAPDH, HPRT1, and B2M have been selected previously as reference genes in gene expression studies with U937 cells and primary human monocytes (Bastonini et al., 2011, Van Brussel et al., 2012, Liew et al., 2002, Koulouvaris et al., 2008). In the current study, these three genes were included in the analysis as potential reference genes.

As the expression level of these genes may vary among tissues or cells and may change under certain circumstances, the selection of housekeeping genes is critical for gene expression studies (Silver et al., 2006). Furthermore, the validation of more than one reference gene for particular tissues or cell types and specific experimental designs are part of the MIQE guidelines (Bustin et al., 2009). In order to determine the most appropriate reference gene for resting U937 cells, GAPDH, HPRT1, and B2M were evaluated for their stability under the treatment with metal debris and ions.

Several mathematical approaches have been published that deliver suitable reference genes with the lowest variation and with high stability across the biological samples (Jacob et al., 2013). The four most commonly used approaches are GeNorm (Vandesompele et al., 2002), NormFinder (Andersen et al., 2004), BestKeeper (Pfaffl et al., 2004), and the comparative ΔC_t (ΔC_q) method (Silver et al., 2006). In the current study, quantification cycle (C_q) values from control and treated cells were analysed by RefFinder, an online tool that integrates the four approaches mentioned to compare and rank the tested candidate reference genes (Xie et al., 2012). The C_q value, originally referred to as C_T , is a cycle number where the PCR kinetic curve reaches a user or program-defined threshold amount of fluorescence. This intersection point is set in the exponential phase above the background level and before reaching the retardation phase (Figure 4.15) (Luu-The et al., 2005, Schefe et al., 2006).

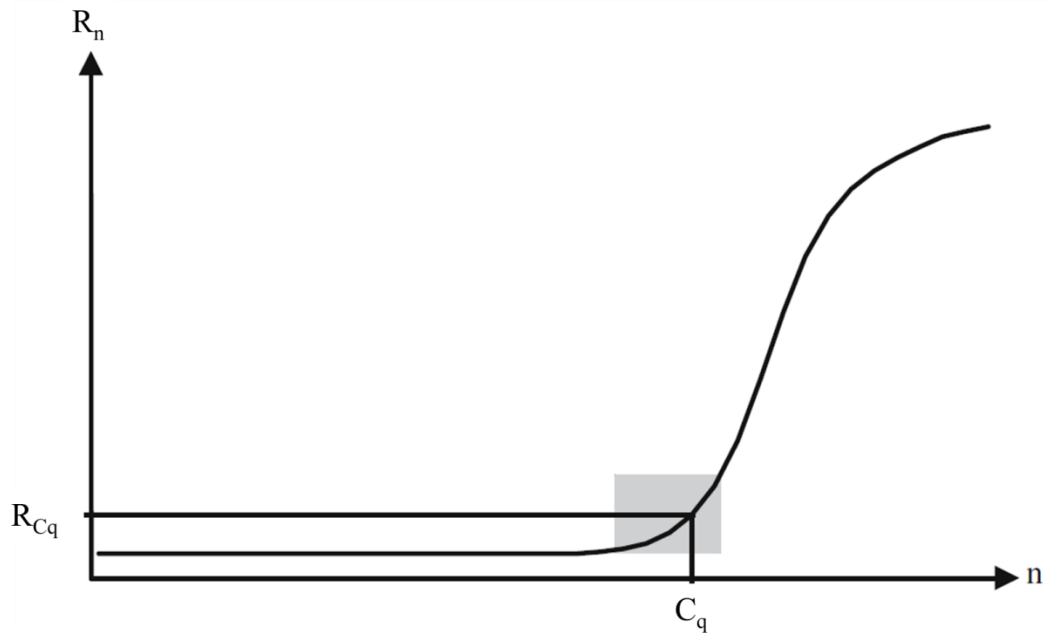


Figure 4.15. qPCR amplification plot. The grey square indicates the exponential region, where the threshold for C_q value determination is set. n number of cycles, R_n fluorescence amount after n cycles, R_{C_q} fluorescence amount after C_q cycles (adapted from (Schefe et al., 2006)).

Based on the rankings from each programme, RefFinder assigns a weight to each gene and calculates the geometric mean of their weights for the overall final ranking (Table 4.6 and Figure 4.16).

Ranking Order (Better--Good--Average)			
Method	1	2	3
Delta C_T	GAPDH	HPRT1	B2M
BestKeeper	HPRT1	B2M	GAPDH
Normfinder	GAPDH	HPRT1	B2M
Genorm	GAPDH-HPRT1		B2M
Recommended comprehensive ranking	GAPDH	HPRT1	B2M

Table 4.6. Ranking of the reference genes candidates. RefFinder analysis shows that GAPDH is the most stable and B2M is the least stable of the three candidate genes.

Comprehensive gene stability

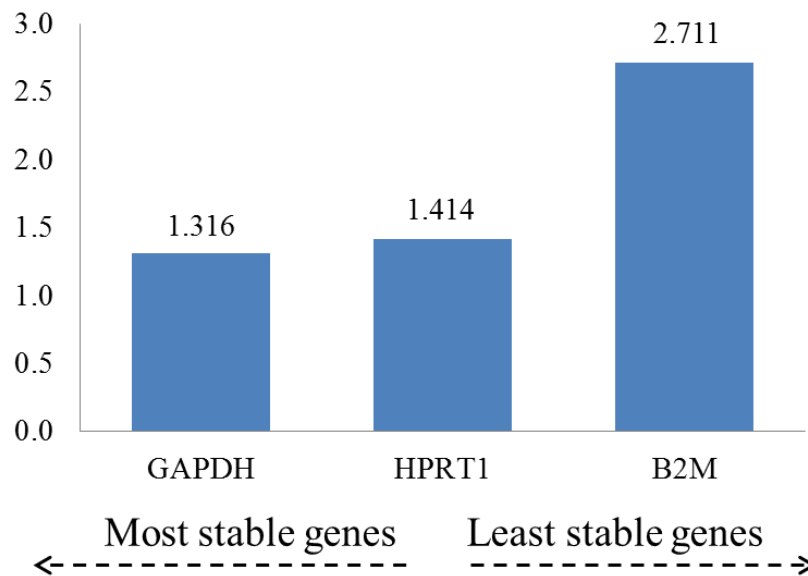


Figure 4.16. RefFinder results. Comprehensive gene stability integrates the four commonly used approaches to compare and rank the tested candidate reference genes calculating the geometric mean of their weights for the overall final ranking.

According to this, GAPDH would be the most appropriate reference gene followed by HPRT1 for the analysis of the effects of CoCr wear debris and ions on the gene expression of resting U937 cells. However, melting curve analysis and horizontal gel electrophoresis showed specificity issues of the GAPDH primers, which meant the data from their assays would be unreliable. Since this made GAPDH unsuitable for use as a reference gene for the current study, results were normalized to HPRT1.

4.3.5.4 Primer efficiency

The PCR efficiency can be defined as the increase in amplicon per cycle (Ruijter et al., 2009). Ideally, the efficiency (E) of a PCR reaction should be 100% ($E=2$), meaning the template doubles after each thermal cycle during exponential amplification. Experimental factors such as the length, secondary structure, and GC content of the amplicon can influence PCR efficiency (Liu and Saint, 2002). Robust and precise PCR assays are usually correlated with high PCR efficiency (Bustin et al., 2009). According to the MIQE guidelines, the PCR efficiency of newly designed

assays should be reported as part of the validation process (Bustin et al., 2010). Consequently, the efficiencies for each of the newly designed primer set were calculated. For this purpose, a dilution series of known cDNA (1 to 100ng) concentrations was performed. The log of each concentration in the dilution series (x-axis) was plotted against the C_q value for that concentration (y-axis) for each primer set. The slope from each standard curve is a measure of reaction efficiency. A slope of -3.32 corresponds to a PCR efficiency of 2 (100%) as determined by the following equation (Pfaffl, 2001):

$$E = 10^{(-1/\text{slope})}$$

Table 4.7 summarises the efficiencies of the designed primer sets.

Gene	Efficiency	%
HPRT	1.84	84.09
NOS2	2.13	112.80
LTA	2.88	188.46
BAG1	1.85	84.71
GADD45A	1.75	75.26
FOS	1.83	82.87

Table 4.7. Primer set efficiencies. Efficiency values were calculated according to the equation $E = 10^{(-1/\text{slope})}$. Percentages were determined by the equation $\% = (10^{(-1/\text{slope})} - 1) \times 100$.

The relative expression ratio of the target genes were then calculated (section 4.3.5.5) based on E and the ΔC_q of the sample versus the control, and expressed in comparison to the reference gene according to the equation (Pfaffl, 2001):

$$\text{ratio} = E_{\text{target}}^{\Delta C_{q\text{target}}(\text{control-sample})} / E_{\text{ref}}^{\Delta C_{q\text{ref}}(\text{control-sample})}$$

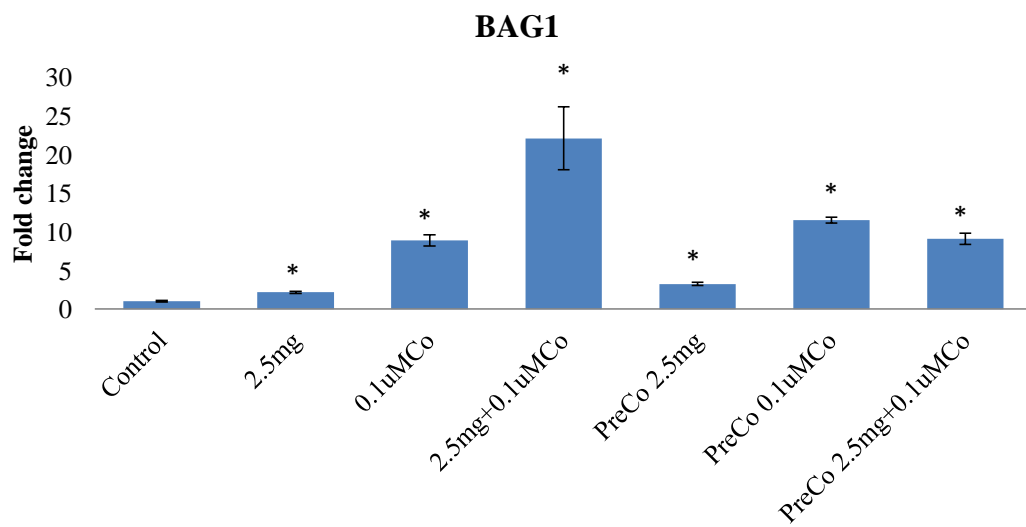
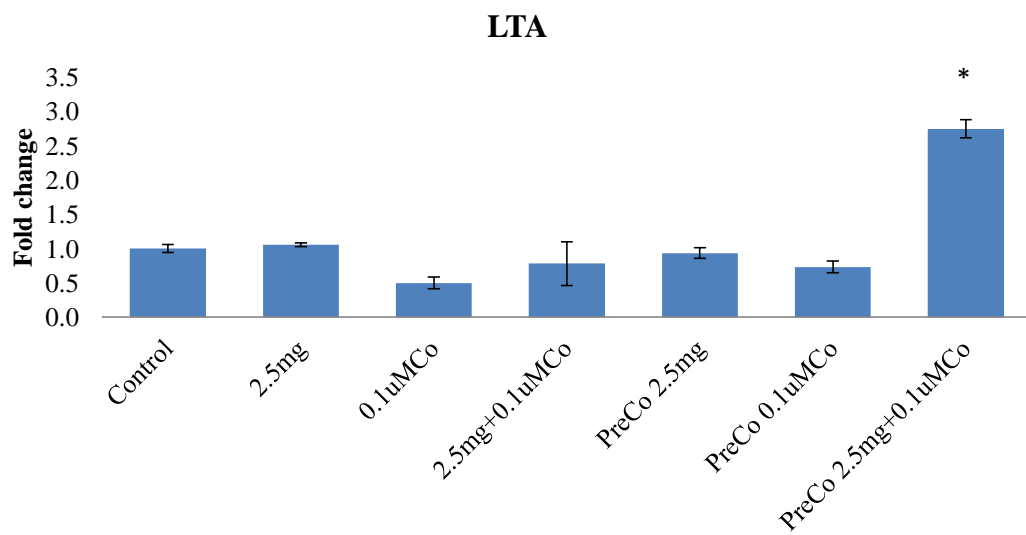
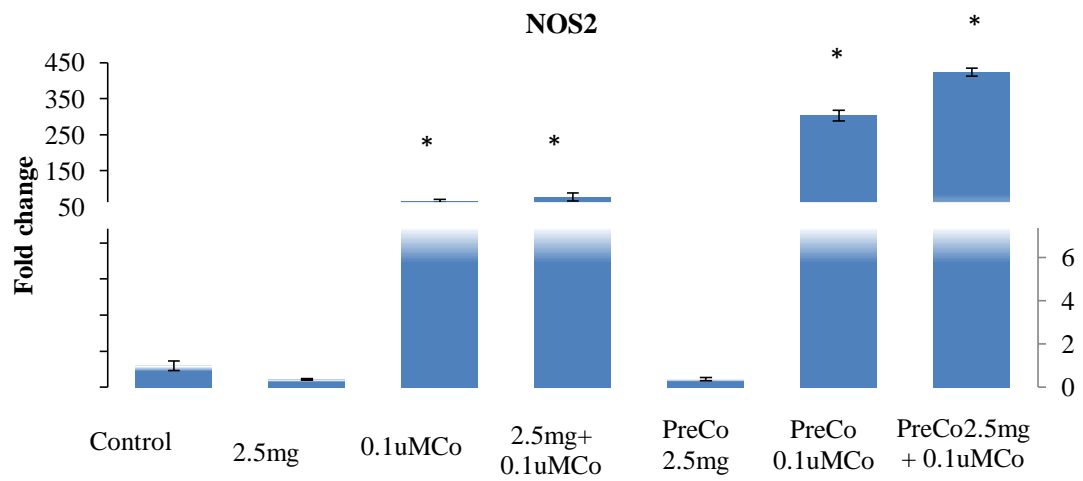
4.3.5.5 Effect of metal debris and Co ions on gene expression

To address the effect of wear particles on resting U937 cells, the mRNA expression of general human toxicology related genes NOS2, LTA, BAG1, GADD45A, and FOS was studied 120h after treatment with 2.5mg debris/1x10⁶ cells, 0.1 μ M Co and

2.5mg debris/1x10⁶cells plus 0.1μM Co. Since accuracy of the calculated gene expression is affected by the efficiency of the reaction, fold variation relative to controls was calculated by the $\Delta\Delta C_T$ ($\Delta\Delta C_q$) method assuming a primer efficiency of 100% (Figure 4.17) and also by taking into account the primer efficiencies calculated in the previous section (4.4.5.4) (Figure 4.18).

The efficiency of the reaction had an impact on the fold variation values. However, the changes in gene expression had similar trends in both analyses. The main difference is that unadjusted results show up-regulation of BAG1 and FOS in cells treated with debris alone whereas adjusted results show up-regulation of LTA and FOS. These findings exemplify the importance of validating the performance of qPCR and how the analysis of results can be affected by it. Moreover, they are in agreement with previous studies such as the one performed by Ruijter et al. (2009) where they observed that changes in the PCR efficiency values had an impact on the fold-changes results.

As seen in the StellarArray results, NOS2, LTA, BAG1, GADD45A, and FOS gene expression was up-regulated in response to 2.5mg debris/1x10⁶cells plus 0.1μM Co treatment validating the StellarArray gene expression assay. However, the magnitudes of the fold changes were different. This could probably be due to the fact that the reference gene in the StellarArray assay (Human 18S ribosomal subunit) differs from HPRT1, which in turn affects the normalization process and thus the fold change results.



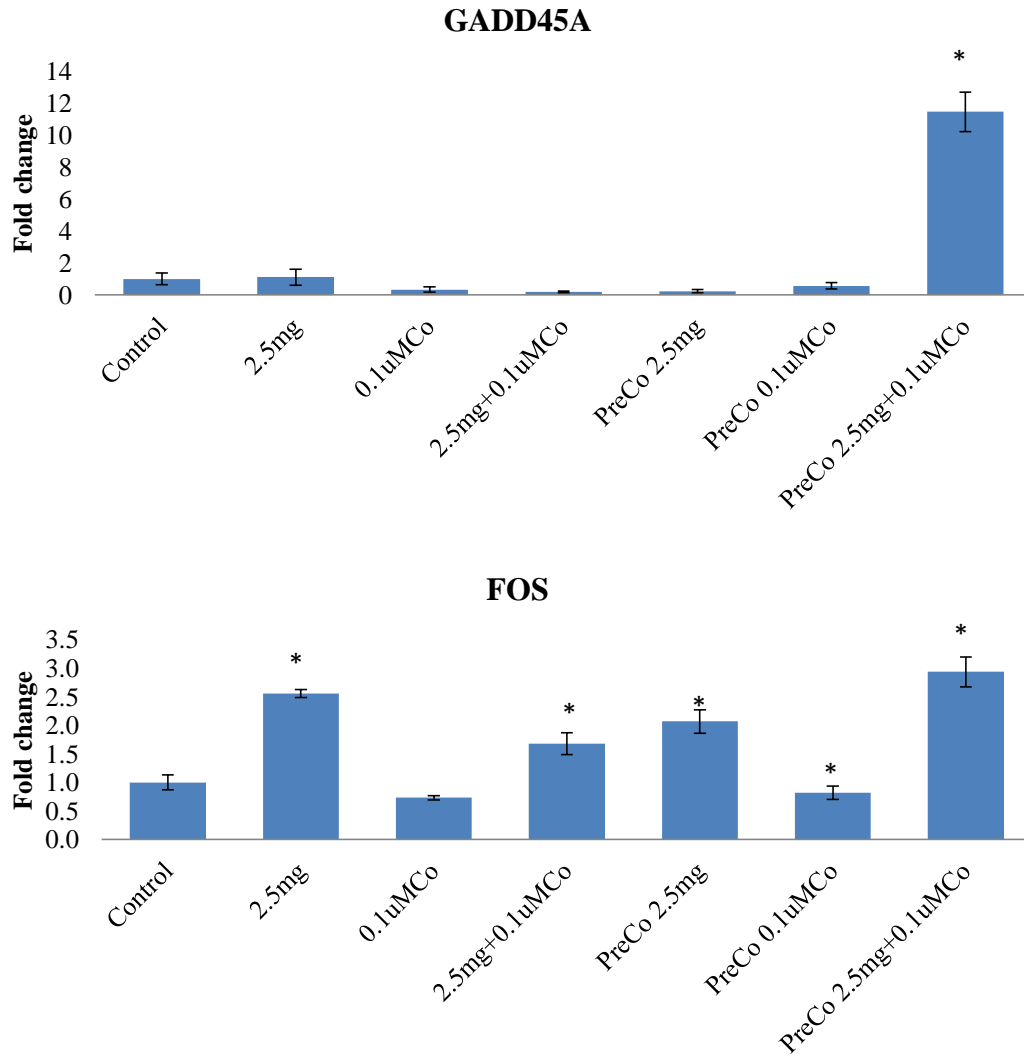
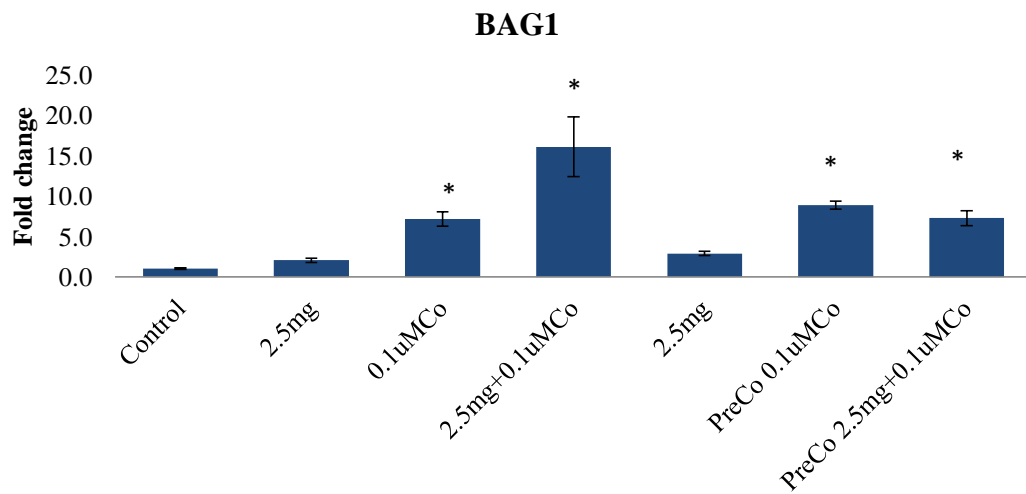
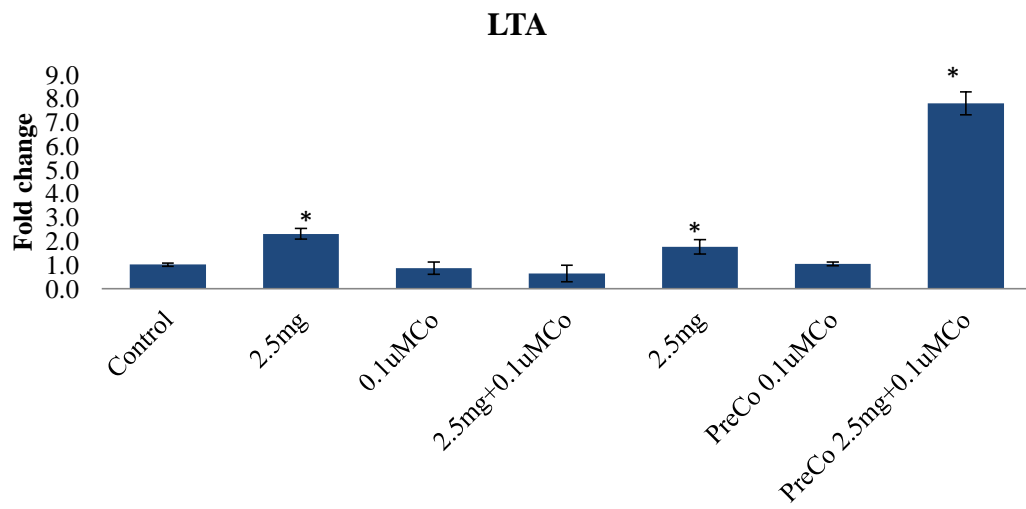
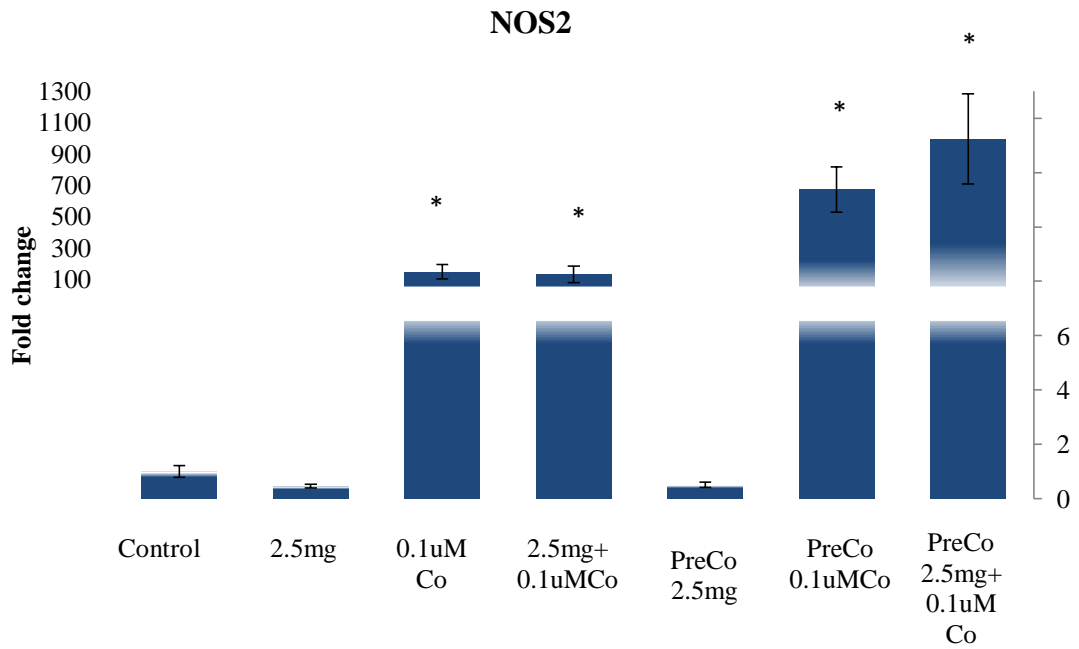


Figure 4.17. Gene fold change assuming 100% primer efficiency. Fold variation of NOS2, LTA, BAG1, GADD45A and FOS (\pm SEM, n=3). Controls are untreated resting U937 cells.*Significantly different from control (0mg debris / 1×10^6 cells) values ($p < 0.05$) by one-way ANOVA followed by Dunnett's multiple comparison test.



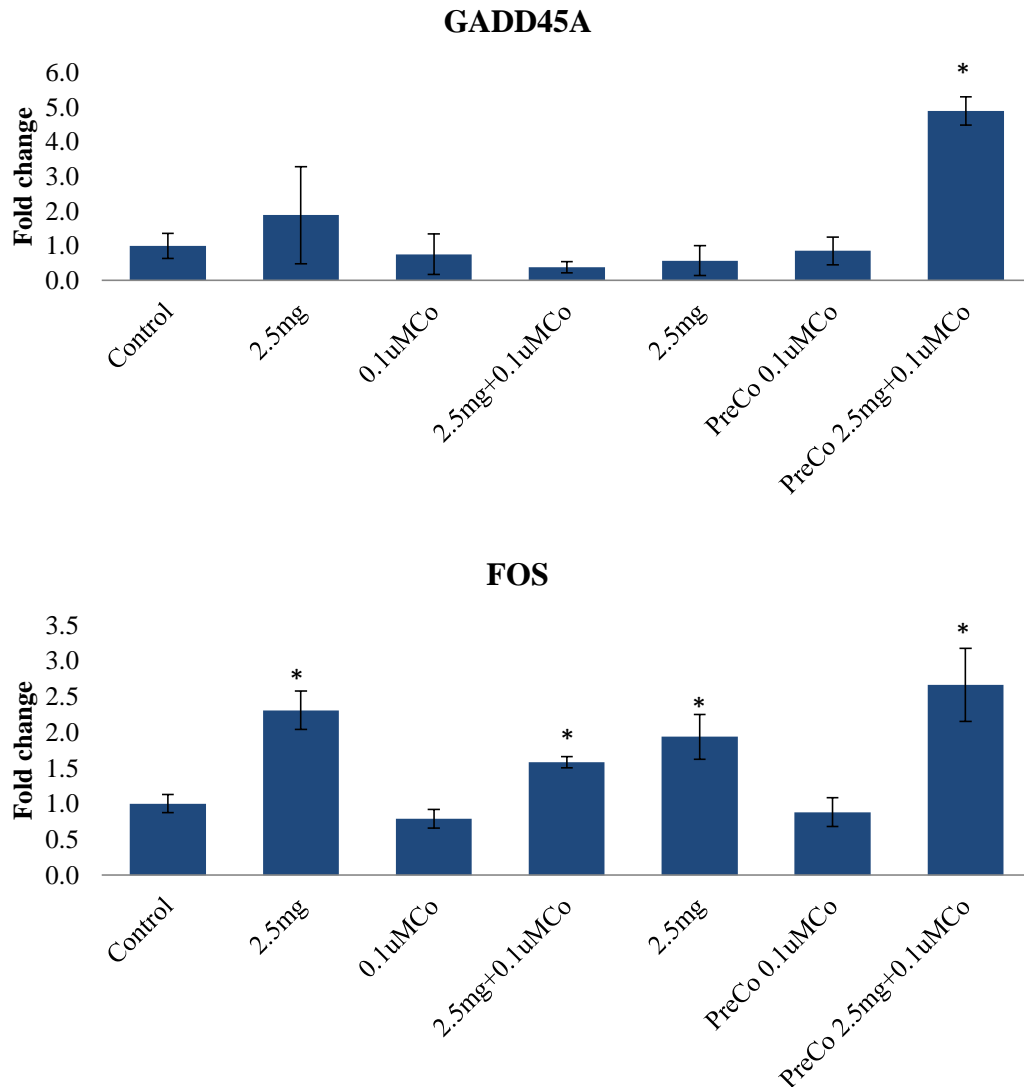


Figure 4.18. Gene fold change corrected to primer efficiency. Fold change of NOS2, LTA, BAG1, GADD45A and FOS (\pm SEM, n=3). Controls are untreated resting U937 cells.*Significantly different from control (0mg debris / 1×10^6 cells) values ($p < 0.05$) by one-way ANOVA followed by Dunnett's multiple comparison test.

Despite the magnitude differences in the analysis methods, BAG1 and NOS2 were the genes most affected by the treatments. Co ions seem to have had a significant effect on the up-regulation of both BAG1 and NOS2. FOS expression increased in the presence of metal debris suggesting that this gene may be affected by the presence of Cr ions. Expression of LTA increased significantly in the presence of both debris and Co when cells were pre-treated with Co. Of the 5 genes under study, GADD45A was the least affected but still showed significant up-regulation when Co pre-treated cells were exposed to both debris and Co. In general, pre-treatment with

Co resulted in the biggest fold changes suggesting that chronic exposure to Co ions induced changes in gene expression.

4.4 Discussion

The progressive loss of bone adjacent to an implant has been attributed to a granulomatous inflammatory reaction induced by particulate implant wear debris at the bone–implant interface (Vasudevan et al., 2012). Degradation products of metallic biomaterials include particulate wear debris, free metallic ions and inorganic metal salts or oxides (Hallab et al., 2001a). These are released into surrounding tissue by various mechanisms, including corrosion, wear, and mechanically accelerated electrochemical processes such as stress corrosion, corrosion fatigue and fretting corrosion (Okazaki and Gotoh, 2005).

Corrosion is a natural phenomenon where higher energy states of a metal attain equilibrium by transforming to such constituents as natural ore, which have lower energy states (Sargeant and Goswami, 2007). All metals in contact with biological systems corrode (Hallab et al., 2001a). Under physiological conditions, corrosion occurs as an electrochemical process in which electron exchange occurs at the metal surface (Steinemann, 1996). The rate of this phenomenon is determined, in part, by the surface area. Since wear debris released from metal components is in the nanometre size range, it has a high surface area that increases the rate of corrosion. Their small size allows the metal particles to migrate from the joint tissues surrounding the prosthesis, leading to systemic effects of the metal ions (Sargeant and Goswami, 2007). Since it has been well documented that patients receiving metal-on-metal hip replacements have increased metal ion concentrations in blood and urine analyses (Table 1.3, Chapter 1), metal ion release from prostheses is of much concern. For this reason, Co and Cr ions released from Co-Cr metal wear debris were measured in this study. ICP–MS is widely regarded as a powerful technique for the quantification elemental composition (Allouni et al., 2012). Once a protocol for preparation sample was established, culture medium from cells exposed to metal wear debris was analysed. At varying incubation conditions and debris

concentrations, results showed higher concentrations of Co than Cr, which could be explained by the alloy composition (62–67% Co, 27–30% Cr, 5–7 % Mo, and ~1% Ni (Singh and Dahotre, 2007)) but also but the fact that cobalt is preferentially released from Co–Cr–Mo alloy during the corrosion process (Hanawa, 2004). It has also been reported that in body fluids, cobalt is dissolved while chromium remains in the oxide layer on the metal surface (Hanawa et al., 2001). Higher cellular uptake of Co could also be due to the fact that there is more availability of this ion than there is of Cr.

The released ions can activate the immune system by forming complexes with native proteins (Hallab et al., 2001a). Chromium and cobalt have similar protein binding affinity, chromium and cobalt bind to protein in proportion to the added concentration ratio (Yang and Black, 1994). Once a metal is bound to a protein, it can be systemically transported and either stored or excreted (Sargeant and Goswami, 2007). Additionally, the presence of wear debris in the peri-implant area leads to macrophage phagocytosis of particulate debris and activation, to stimulate the release of a variety of mediators, such as free radicals and nitric oxide, and a myriad of proinflammatory cytokines and chemokines (Sethi et al., 2003). It has been reported that local acidification may develop during acute and chronic inflammation (Rajamaki et al., 2013) and high hydrogen ion concentrations down to pH 5.4 have been found in inflamed tissue (Steen et al., 1995). In turn, such an acidic environment created by actively metabolizing immune cells may enhance the corrosion process of the nanoparticles increasing the metal ions being released. In this study, ICP-MS analysis showed significantly higher concentrations of Co and Cr when incubating wear debris at low pH. Moreover, higher metal levels were measured in the activated U937 cells culture medium compared to resting cells medium. These findings could suggest that the osteolysis process generated by wear debris may be exacerbated by the lowering of pH at the inflammation site, which would be in line with reports of synovial-fluid acidosis correlating with radiological joint destruction in rheumatoid-arthritis knee joints (Geborek et al., 1989, Mansson et al., 1990)

Cobalt ions and cobalt nanoparticles are cytotoxic and induce apoptosis and, at higher concentrations, they induce necrosis with an inflammatory response (Simonsen et al., 2012). Catelas et al. (2005) demonstrated that macrophage mortality induced by metal ions depends on the type and concentration of metal ions as well as the duration of their exposure. Overall, apoptosis was predominant after 24 h with both Co^{2+} (0-10ppm) and Cr^{3+} (0-500ppm) ions, but high concentrations induced mainly necrosis at 48 h. This same group also showed that Co^{2+} and Cr^{3+} induced TNF α secretion, mortality, and more specifically apoptosis, in J774 macrophages (Catelas et al., 2001, Catelas et al., 2003). Granchi et al. (1998) demonstrated that both cobalt and chromium ions induced apoptosis at 24 h, but that high concentrations of cobalt (50 and 25%) produced necrosis at longer incubation times (48 and 72h, respectively). In a similar way, Akbar et al. (2011) reported that exposure to high concentrations of metal ions (10 and 100 μM Cr^{6+} , 100 μM Co^{2+}) initiate apoptosis that results in decreased lymphocyte proliferation. Another investigation showed that up to 24h, Co^{2+} (0-10ppm) and Cr^{3+} (0-500ppm) ions induced the presence of caspase-3, a protease of the caspase family implicated in the majority of the apoptosis pathways, and particularly in the cleavage of poly-(ADP-ribose) polymerase (PARP). The degree of cell response depended on ion concentration and exposure time. Additionally, they also reported the induction of macrophage apoptosis by Co^{2+} and Cr^{3+} ions requires the modulation of the expression of Bcl-2 and bax and activity of several caspase proteins (Petit et al., 2004a). Results from this study showed that apoptosis started to increase after 24h of exposure to wear debris, and wear debris combined with Co ions, which became significant after 48h as seen in both FACS and western blot analysis. Co ions on their own did not induce apoptosis probably due to low concentration (0.1 μM Co). The apoptotic effects of cobalt ions have mainly been reported at concentrations starting from 100 μM , where Co induced cell death and apoptosis in a dose and time dependent manner (Araya et al., 2002, Zou et al., 2001, Akbar et al., 2011). Results reported herein seem to support these observations. This could mean that the increase in ion release at the acidic peri-implant environment enhances cell death intensifying the immune reaction. Several cellular components functioning in apoptosis have been reported. Among them, Bcl-2 is known to suppress multiple forms of apoptosis

(Willis et al., 2003). It has been shown that co-expression of BAG1, Bcl-2 association athagogene 1, and Bcl-2 increases protection from cell death (Takayama et al., 1995, Terada et al., 1999). In the present study, up-regulation of BAG1 was observed in treated U937 cells compared to controls. This suggests that BAG1 could be part of a defence mechanism for delaying cell death in response to metal toxicity, particularly cobalt toxicity.

Activated macrophages possess the ability to kill and degrade intracellular microorganisms, and for several years, this was the functional criterion used to define an activated macrophage (Mosser, 2003). This killing is accomplished by an increase in the production of toxic oxygen species and an induction of the inducible NO synthase (iNOS or NOS2) gene to produce nitric oxide (NO) (Mosser, 2003, Song et al., 2001, Chauhan et al., 2004, Mantovani et al., 2004). NO has been proposed to exhibit a pro-inflammatory action by enhancing NF- κ B activation in response to inflammatory agents. Such activation of NF- κ B has been linked to NO-induced enhancement of the production of TNF- α and IFN- γ (Zeidler and Castranova, 2004). In addition, it has been shown that cobalt could function as a microglial activator to induce the production of NO and some cytokines such as TNF- α and IL-6 (Mou et al., 2012). Results reported in this chapter show up-regulation of NOS2 gene expression. Since the induction of NOS2 is characteristic of activated macrophages, these findings suggest that metal debris and ions have the potential to activate resting macrophages. Moreover, such over expression of NOS2, which leads to an over production of NO, could have a predominant role in the inflammation and acidification of the peri-implant microenvironment discussed above. Additionally, lymphotoxin alpha (LTA) is an effector in innate and adaptive immune responses (Banks et al., 2006) and is produced by activated lymphocytes, and monocytes (Detogni et al., 1994). Ligation of LTA and receptor (TNFR and LT β R) results in the activation of genes involved in pro-inflammatory reactions, including chemokines, such as macrophage inflammatory protein-1 β (MIP-1 β) and MIP-2, as well as integrins, such as vascular cell adhesion molecule 1 (VCAM-1), attracting and localizing leukocytes to areas of inflammation (Schneider et al., 2004). Up-regulation of LTA in response to chronic exposure to metal debris and ions could

also be a contributing factor to inflammation and recruitment of immune cells at the peri-implant site. On the other hand, GADD45A is a member of a group of genes that are induced by DNA damaging agents and growth arrest signals (Zhan, 2005). Activation of GADD45A indicates a potential damage at the genomic level (Miller et al., 2004). Up-regulation of this gene suggests a DNA damage-related toxicity mechanism by chronic exposure to metal debris and ions, leading to growth arrest or apoptosis depending on DNA damage extent.

Several reports indicate that particulate debris generated from mechanical wear of prosthetic components plays a critical role in the process of aseptic loosening and osteolysis (Zhang et al., 2009). FOS protein is required for formation and activation of osteoclasts from their monocyte precursors (Chen et al., 2011, Miller et al., 2004). When HepG2 cells were incubated with 0, 0.3, 0.75, 1.5, or 3 μ g Co for 48h, Co exposure induced a 2 to 8 fold induction of FOS (Miller et al., 2004). In the present study, FOS expression was up-regulated, which suggests that metal ions may induce osteoclast differentiation. This in turn may impair osteoblast/osteoclast balance leading to stimulation of osteolysis and subsequent aseptic loosening. Since the up-regulation was observed in the presence of metal debris, it could be suggested that either Cr ions play an important part of this process or that this is the result of synergistic action of Co and Cr ions.

To summarise, gene expression results suggest different mechanisms for transcriptional activation of the genes investigated in this study. This could indicate that gene expression is modulated in a dose-dependent manner and as the result of several signals coming together. When this is considered together with the metal ion level and apoptosis analyses, it is easy to see that the biological response to metal ions is a complex reaction involving regulation at different cellular and molecular levels, to try and maintain intra- and extra-cellular homeostasis. When cells fail, they tip the balance towards inflammation and acidification. This exacerbates the adverse reaction ultimately resulting in osteolysis and subsequent aseptic loosening. Moreover, since the main gene expression changes and apoptosis were observed in cells pre-treated with Co ions, patients with a MoM implant undergoing revision

surgery or receiving a second MoM device may potentially be at higher risk of implant failure.

5. EFFECTS OF COBALT IONS AND WEAR METAL DEBRIS DERIVED FROM A HIP RESURFACING ON FRESHLY ISOLATED HUMAN LYMPHOCYTES *IN VITRO*

5.1 Introduction

It has been established that macrophages are key mediators of osteolysis. Lymphocytes are known to be important regulators of macrophage function (Arora et al., 2003). Previous studies of peri-prosthetic tissue have shown the involvement of both a nonspecific foreign body reaction involving phagocytic macrophages, but few T lymphocytes (Goodman, 2007), as well as a specific T-cell-mediated immune response (Arora et al., 2003). T cells are recognized as modulators of immune response pathways as a result of stimulation of either the Th1 or Th2 pathway, which involves cell types and cytokines that may influence loosening of total hip replacements (Cachinho et al., 2013). The Th1-cell response is crucial to the activation of macrophages and cytotoxic T-lymphocytes and is involved in the cell-mediated immune response. On the other hand, Th2-cell response is the most effective activator of B-lymphocytes and is associated with humoral immunity (Cachinho et al., 2013).

Hypersensitivity can involve an immediate humoral response. This response is initiated by an antibody or by the formation of antibody-antigen complexes of type-I, II, and III reactions. Alternatively, hypersensitivity can be a delayed cell-mediated response (Akdis, 2006). Implant-related hypersensitivity reactions are generally the latter type of response, in particular type-IV delayed-type hypersensitivity (DTH). Type IV hypersensitivity involves a specific antigen, co-stimulatory molecules, an antigen-presenting cell and T lymphocytes (Posadas and Pichler, 2007). In hypersensitivity reactions, T lymphocytes play a prominent role in sustaining the chronic inflammatory response. Diseases such as rheumatoid arthritis and lupus erythematosus are thought to be due to adverse T-cell-mediated immune reactions against specific body proteins (Goodman, 2007). T cells may also be triggered by

exposure to metals that might be encountered repeatedly via cutaneous, respiratory, oral, or intramuscular routes (Gamerding et al., 2003).

Metals debris and metal ions can activate the immune system by inducing a delayed type hypersensitivity reaction (Hallab et al., 2001a). The most common sensitizing orthopaedic metals are nickel, cobalt, and chromium (Hallab et al., 2001a, Minang et al., 2006, Hegewald et al., 2005, Fors et al., 2012). It is thought that the stimulated T-cells generate pro-osteoclastogenic factors that can alter bone homeostasis (Frigerio et al., 2011) and therefore contribute to osteolysis. The prevalence of metal sensitivity among the general population is approximately 10% to 15% and the prevalence of metal sensitivity among patients with well-functioning and poorly functioning implants has been reported to be ~25 and 60%, respectively, as measured by dermal patch testing. (Hallab et al., 2001a) The response of metal-specific lymphocytes has been linked to poor implant performance. Cell-mediated type-IV hypersensitivity reaction characterized by vasculitis with perivascular and intramural lymphocytic infiltration of the postcapillary venules, swelling of the vascular endothelium, recurrent localized bleeding, and necrosis has been reported following metal-on-metal hip replacements (Willert et al., 2005). Lymphocyte infiltrates have also been reported in soft-tissue masses, described as pseudo-tumours, following MOM resurfacing arthroplasty (Boardman et al., 2006, Pandit et al., 2008). Additionally, metal specific T-cells have been isolated from patients with contact dermatitis, indicating a T-cell led inflammatory reaction against a metal derived antigen (Moulon et al., 1995). For example, chromium exposure has been shown to upset the immunoregulatory balance between Th1 and Th2 cells that control different immune effect or functions through the production of distinct cytokines (Villanueva et al., 2000). In the work of these authors, the effects of cadmium, chromium, inorganic mercury, and inorganic lead exposure on the immune system were determined by measuring cytokine production of human peripheral blood mononuclear cells. Their results showed that the cytokines assayed were differentially affected by heavy metal exposure. Of particular interest, chromium significantly increased the production of IL-1 β while decreasing the production of IFN- γ , IL-6, IL-8, and IL-10.

It has been suggested that activation of T-cells following exposure to biomaterial particles is driven by macrophages and requires synergistic signals primed by both antigen presentation and costimulation (Jiranek et al., 1993, Goodman et al., 1998, Voronov et al., 1998). Bainbridge et al., (2001) examined the expression of CD80 and CD86 costimulatory molecules in U937 cells that had been exposed to TiAlV implant wear debris. This was compared to the expression of these costimulatory molecules in tissues taken from patients with aseptic loosening. They demonstrated the increased expression of costimulatory molecules in response to wear particles both at the bone implant interface and *in vitro*. These findings reinforce the hypothesis that macrophages have the potential to aid T-cell activation in response to metal or metal ions from orthopaedic implants, as well as to augment any T-cell mediated response.

Metals modulate the activities of immunocompetent cells by a variety of mechanisms. The outcome of this modulation may depend on the particular metal, its concentration and biologic availability (Lawrence and McCabe, 2002). A variety of soluble metals (Ni^{2+} , V^{3+} , Al^{3+} , Be^{2+} , Co^{2+} , Cr^{3+} , Cu^{2+} , Fe^{3+} , Mo^{5+} , Nb^{5+} , Zr^{2+}) at a range of concentrations (0.05, 0.1, 0.5, 1.0, and 5mM) were found to induce Jurkat T-lymphocyte DNA damage, apoptosis, and/or direct necrosis in a metal-, and concentration-dependent manner (Caicedo et al., 2008). A mixed population of monocytes/macrophages and lymphocytes were cultured *in vitro* with titanium, titanium alloy (Ti6Al4V), and stainless steel 316L particles by Cachinho et al., (2013) and they showed a significant decrease in TNF α and IL-6 production. As a consequence, and to complement the findings of the previous chapters, the effects of metal wear debris and cobalt ions on primary human lymphocytes were explored in the present chapter. Particularly, it was of interest to find out whether the same trends on viability, proliferation, cytokine production and apoptosis observed on U937 cells would be also observed on primary lymphocytes.

5.2 Aim

- To assess the toxicity of Co-Cr nanoparticles released from a resurfacing implant and Co ions on primary human lymphocytes.

5.3 Results

The aim of this study was to assess the toxicity of Co-Cr nanoparticles released from a resurfacing hip implant and Co ions on primary human lymphocytes. In order to achieve this, viability, proliferation, cytokine production, and apoptosis were evaluated.

5.3.1 Effects of metal debris and ions on human primary lymphocyte cell viability as measured by MTT and NR

The viability of primary human lymphocytes was tested after 24 and 120h of exposure to 5mg wear debris/ 1×10^6 cells, $0.1 \mu\text{M}$ of Co^{2+} and 5mg wear debris/ 1×10^6 cells combined with $0.1 \mu\text{M}$ of Co^{2+} . Contrary to observations in Chapter 3, a significant increase in cell number as indicated by the NR assay was measured both at 24 and 120h of exposure to wear debris when compared to controls (Figure 5.1). However, although there was an initial increase, there was no significant difference in the reduction of MTT in cells exposed to the same treatments. On the other hand, Co ions on their own did not seem to have an effect on cell number or cell metabolic activity. Together, these could suggest that it is the particles rather than low Co ion concentration that stimulate lymphocytes. These findings could also suggest that lymphocytes are more reactive to higher concentrations of Co ions or that the effects are due to the synergistic action of both Co and Cr ions.

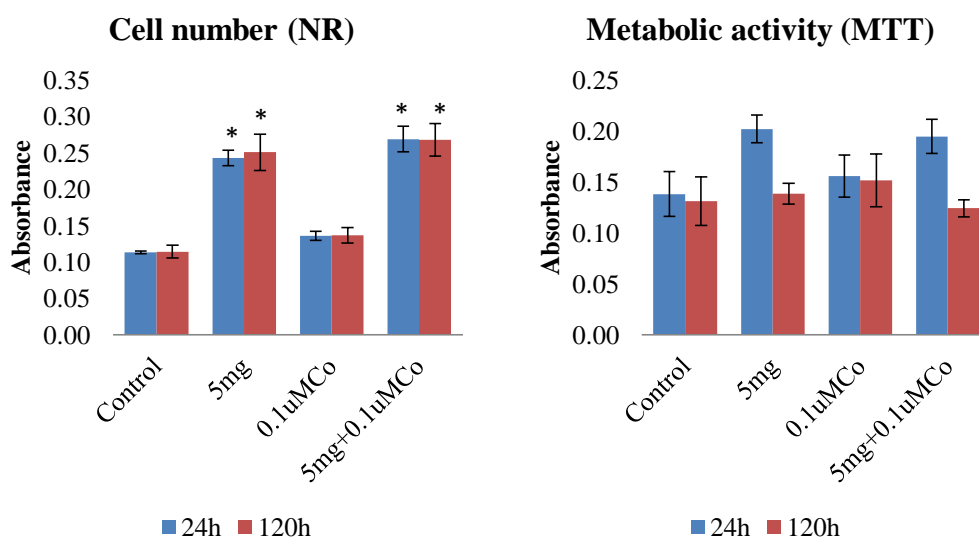


Figure 5.1. Cell number (NR) and metabolic activity (MTT) of human lymphocytes. Results are absorbance values (\pm SEM, $n=12$) where controls are untreated cells.*Significantly different from control values ($p<0.05$) by one-way ANOVA followed by Dunnett's multiple comparison test.

5.3.2 Effects of metal debris and ions on human primary lymphocyte cell proliferation assessed with BrdU

Effects on cell proliferation were assessed with the BrdU cell proliferation assay after 48 and 120h of treatment with 5mg wear debris/ 1×10^6 cells, $0.1 \mu\text{M}$ of Co^{2+} and 5mg wear debris/ 1×10^6 cells combined with $0.1 \mu\text{M}$ of Co^{2+} . There is an initial decrease in cell proliferation followed by an increase by 120h of treatment (Figure 5.2). These results could suggest an activation response to both debris and ions, where the cells overcome the initial growth arrest effect and start proliferating. However, it has been established that, in the absence of monocytes, activated T-cells produce less IL-2 and do not proliferate (Martin-Chouly et al., 2011). So, even if the cells were being activated by the debris and ions, the fact that this experiment was carried out on an enriched lymphocyte cell population might have had an effect on initial proliferation rates.

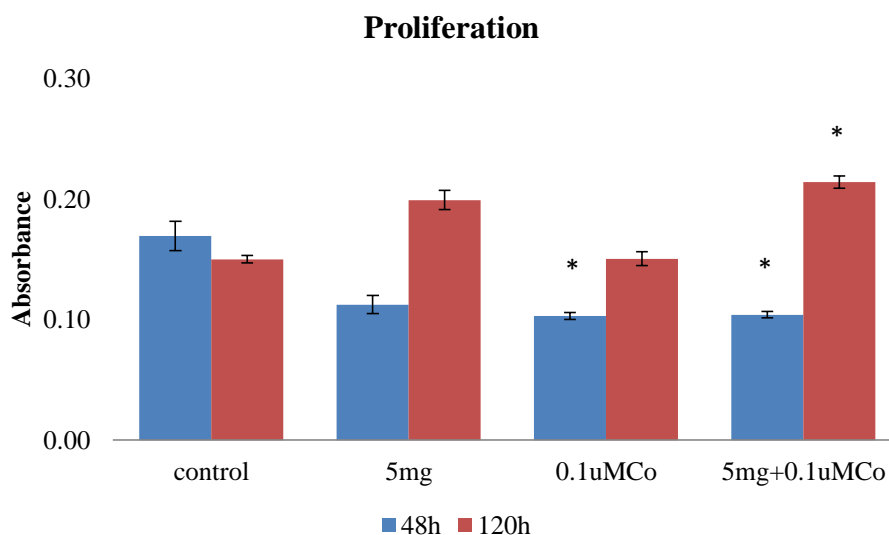


Figure 5.2. Proliferation of human lymphocytes measured by BrdU assay. Results are absorbance values (\pm SEM, n=6) where controls are untreated cells.*Significantly different from control values ($p < 0.05$) by one-way ANOVA followed by Dunnett's multiple comparison test.

5.3.3 Effects of metal debris and ions on cytokine release by human primary lymphocyte cells measured by ELISA

Interleukins such as IL-2, IL-6, IFN γ , and TNF α are regarded as indicators of the inflammation evoked by particulate metals (Cachinho et al., 2013). Levels of these four cytokines were determined in the supernatants of human primary lymphocyte cultures after 24 and 120h of treatment with cobalt ions and wear debris.

There was a general decrease in cytokine production particularly when cells were in contact with metal particles (Figure 5.3). IFN γ and IL-6 levels decreased after 24h of exposure and continued to be low for 120h. TNF α levels were mainly decreased after 120h of exposure. Interestingly, IL-2 was the only cytokine to be affected by all treatments. This could suggest a dose-dependent involvement of Co ions on the inhibition of IL-2 production. Cobalt ion treatment did not have an effect on IL-6, IFN γ , and TNF α production. These findings could be reflecting a variety of mechanisms by which metal debris and ions modulate immunocompetent cell function. As with the viability results, 0.1 μ M Co ions could be at too low a concentration and therefore did not elicit changes in the production of the mentioned

cytokines. Since the effects were observed where the metal particles were present, it might be that higher concentrations of cobalt emanating from the particles were required to cause an effect. It might also be that the significant decrease was due to either Cr ions, or the presence of both Cr and Co ions emanating from the particular debris.

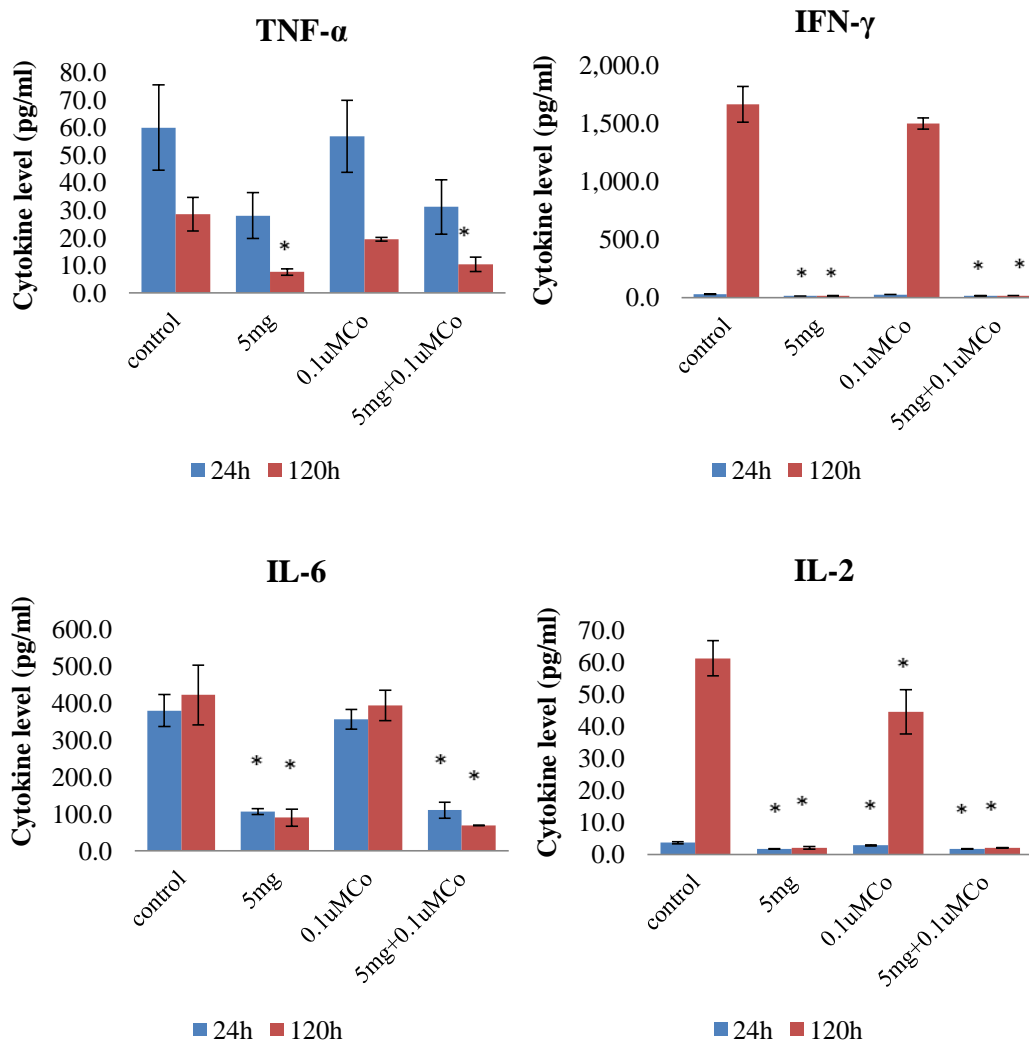


Figure 5.3. Cytokine production by human lymphocytes. Results are expressed as mean values (\pm SEM, n=4). *Significantly different from control values (p<0.05) by one-way ANOVA followed by Dunnett's multiple comparison test.

5.3.4 Effects of metal debris and ions on human primary lymphocyte cell apoptosis assessed by flow cytometry

To determine the effects of metal ions on irreversible cell damage leading to apoptosis, flow cytometry following Annexin V and 7-AAD staining at 24 and 48h of exposure was performed. Even though cytotoxic effects were not seen at the 5mg metal debris/ 1×10^6 cells dose, a lower debris concentration (2.5mg metal debris/ 1×10^6 cells) was used for apoptosis analysis in order to be able to establish a comparison with the results observed on U937 cells.

Similarly to what was observed in U937 cell, apoptosis was not observed within 24h of exposure, but was evident after 48h (Figure 5.4). This could suggest an up-regulation of the anti-apoptotic machinery in response to the metal challenge, allowing the cells to defend themselves for the first 24h of exposure. Further investigation of gene expression could help elucidate if Co and Cr can affect lymphocytes at such a molecular level. Even though a defence mechanism could have been triggered, the high metal ion levels being released from the debris could have overwhelmed the system leading to the significant increase in apoptosis where the particles were present for 48h of exposure. Additional apoptosis screening through western blot was originally planned for this experiment in order to confirm FACS results. However, the low protein concentrations obtain from the cells did not allow us to perform the assay.

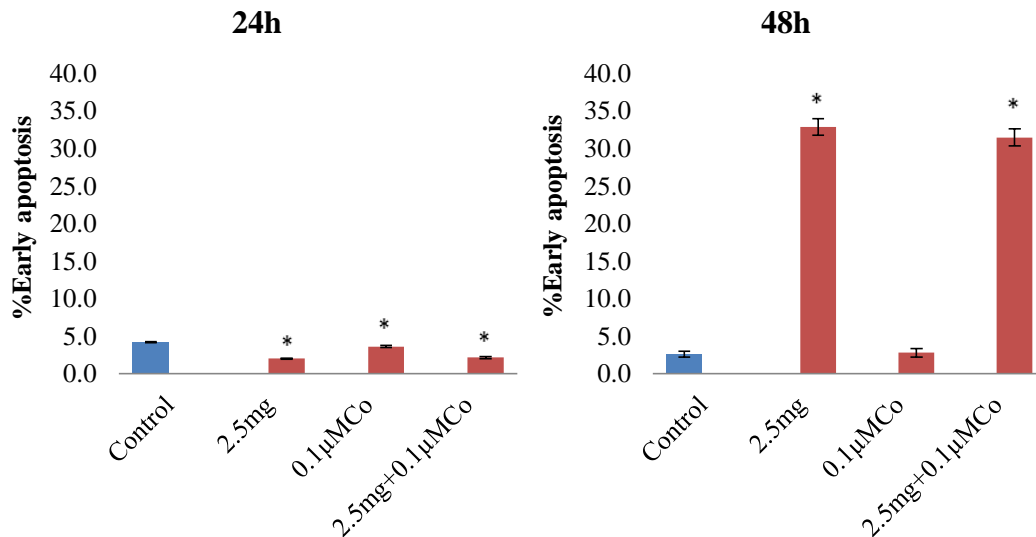


Figure 5.4. Apoptosis. Results are expressed as percentages (\pm SEM, n=12) *Significantly different from control values ($p < 0.05$) by one-way ANOVA followed by Dunnett's multiple comparison test.

5.4 Discussion

Several studies have described perivascular lymphocytes in tissue membranes around failed MOM implants apparently not associated with infection, and the authors have interpreted this inflammation as an immunologic reaction against metal ions or metal particles associated with those articulations (Bohler et al., 2002, Campbell et al., 2010, Davies et al., 2005, Korovessis et al., 2006, Willert et al., 2005). In the present chapter, primary human lymphocytes were exposed to cobalt ions and high concentrations of metal wear debris derived from a MoM hip resurfacing device in order to evaluate the cell response to these treatments and to assess whether or not Co-Cr particles and ions could activate human lymphocytes.

T-lymphocytes are normally maintained in a quiescent state while remaining capable of rapid responses and effector function (Macintyre and Rathmell). T-cell proliferation occurs as the result of a precisely orchestrated set of events involving two distinct signals, namely recognition of an antigen followed by release of costimulatory molecules such as IL-2 cytokine (Deweck et al., 1984, Habetswallner et al., 1988). After activation, T cells undergo a transient period with little cell growth and then begin to rapidly grow and divide (Macintyre and Rathmell). In this

chapter, high concentrations of metal debris caused an increase in cell number despite the initial decrease in cell proliferation suggesting that the particles could be exerting a cell activation effect, which could be taking place during the first 48h of treatment reflected by the initial lower proliferation rates (24-48h) and the rapid growth and division seen by 120h. In addition to this, a significant decrease in IL-2 production was observed after 24h of exposure to all the treatments. Since IL-2 is such an important molecule for lymphocyte activation and proliferation, its diminished production could have contributed to the decrease in proliferation observed at 48h. It has also been suggested that failure of effector T cells to up-regulate glucose metabolism appropriately results in decreased cytokine production, proliferation, and can lead to apoptosis (Gerriets and Rathmell, 2012). The fact that the levels of metabolic activity did not seem to significantly change despite the increase in cell number and proliferation at 120h, may be an indication of such failure and could also explain the marked reduction in cytokine production.

On the other hand, a state of reduced function in which a viable, antigen-specific T cell is unable to respond to an immunogenic stimulus has been referred to as anergy (Zheng et al., 2008). Anergy can be induced under a number of circumstances that can be categorized as resulting from either a normal antigenic stimulus received in the absence of costimulation or from an altered and/or chronic T-cell receptor stimulus (Wells, 2009). To the author's knowledge, anergy has not been described as part of the biological reaction to metal debris and ions. This could mainly be due to the fact that most studies have reported implant-related hypersensitivity reactions, in particular type-IV delayed-type hypersensitivity mediated by T lymphocytes. Nevertheless, results from this investigation could be suggesting an anergy-like response to high concentrations of metal debris. The significant decrease in IL-2 production and proliferation observed here are hallmarks of T-cell anergy (Chappert and Schwartz, 2010, Kuklina, 2013). Moreover, defective production of inflammatory cytokines such as IFN γ and TNF α is also a characteristic of anergy (Wells, 2009) and significant decreases in both cytokines were observed in the presence of metal debris.

As mentioned in previous chapters, metals corrode *in vivo* releasing metal ions. Such ions can potentially bind to proteins, remain in solution, or disseminate into the surrounding tissues, bloodstream, and thus reach remote organs. The present study has shown how (Chapter 4) the microenvironment conditions surrounding the debris can influence the rate of ion release. It is generally presumed that metal ions facilitate cell activation and sensitization. However, depending on the concentration of metal ions present, they may also be cytotoxic and suppressive. It has been shown that production of TNF α and IL-6 by human peripheral blood mononuclear cells exposed to Cr (1, 5, and 10 μ M) significantly decrease (Villanueva et al., 2000). In the current investigation, inhibition of cytokine production was observed in the presence of metal particles. IFN γ , TNF α , and IL-6 levels did not seem to be affected by cobalt ions alone. This seems to suggest that the toxicity of chromium may be related to the regulation of these cytokines whereas IL-2 production is more likely to be modulated by cobalt. Additionally, high concentrations (5mg debris/ 1×10^6 cells) of metal debris were not found to be cytotoxic for primary lymphocytes. Nevertheless, a marked increase in apoptosis was observed at a lower dose (2.5mg debris/ 1×10^6 cells). Considering that in previous chapters the cytotoxicity and apoptosis induction potential of the same doses of metal debris on U937 cells was established, these findings could be suggesting a dose and cell type dependent effect on cellular death pathways. Of particular interest is the fact that all treatments seem to have delayed apoptosis on lymphocytes at 24h. Akbar et al., (2011), exposed resting and activated lymphocytes to a range of cobalt and chromium ions. They found that exposure to Cr $^{6+}$ (10 and 100 μ M), and Co $^{2+}$ (100 μ M) significantly decreased cell viability and increased apoptosis in both resting and activated lymphocytes at 24 and 48h of exposure. However, in this study metal ions were assessed independently. The effects observed in the current chapter may be the result of the concerted action of the particles and both Co and Cr ions. A more detailed analysis would help understand what the tipping point is. The author suggests exposing the primary lymphocytes to a range of concentrations of debris and testing for apoptosis at several and more frequent time points, accompanied by gene expression analysis. Unfortunately, both money and time constraints prevented this being included in the present study.

Released metal ions can activate the immune system by forming metal-protein complexes that are considered to be candidate antigens for eliciting hypersensitivity responses (Korovessis et al., 2006). Upon recognition by lymphocytes, the metal-protein complexes induce the production of proinflammatory cytokines and chemokines by various cell types due to triggering of innate immune responses (Martin, 2004). According to this, it is thought that high local metal ion and nanoparticles concentrations facilitate a T-lymphocyte mediated inflammatory response resulting in the destruction seen around the prostheses (Davies et al., 2005; Willert et al., 2005; Boardman et al., 2006; Counsell et al., 2008; Kwon et al., 2009). Three mechanisms have been proposed by which metal-protein complexes can activate lymphocytes: 1. antigen-independent, 2. antigen-dependent, and 3. superantigen-like, which is a synergistic combination of the first two mechanisms (Hallab et al., 2001b). Metals may act with serum proteins to crosslink lymphocyte receptors (e.g., BV17 of CDR1 T cell receptor) without the presence of an antigen-presenting cell leading to a superantigen enhancement of T cell receptor-protein contact (Vollmer et al., 1997, Vollmer et al., 1999). In this circumstance, proteins or peptides that would not otherwise be antigenic are able to provoke a response (Hallab et al., 2001b). The lymphocyte reactions in the current investigation seem to be consistent with such nonspecific mitogenic activation mechanisms, which could explain the increase in cell proliferation despite the significant decrease in IL-2 production.

In summary, the present chapter has shown that high concentrations of wear debris, derived from a Co-Cr metal on metal hip resurfacing, did not induce a decrease in cell viability in terms of cell number and metabolic activity. However, such high concentrations seem to have induced apoptosis. Whatsmore, they seem to inhibit cytokine production. Although this does not appear to have an effect on T-lymphocyte proliferation *in vitro*, it could still result in disturbed immune response, which could contribute to failure MOM implanted devices. Finally, the fact that IL-2 production was affected by 0.1 μM Co (5.9ppb or 5.9 $\mu\text{g/L}$) suggests a mode of action of cobalt toxicity. This means that even ion concentrations at the guideline levels of

7ppb or 7 μ g/L (MHRA) may also contribute to the impairment of immune regulation in patients with MoM implants.

6. CORRELATION BETWEEN GENE EXPRESSION AND METAL ION LEVELS IN CLINICAL BLOOD SAMPLES

6.1 Introduction

6.1.1 RNA stability in clinical blood samples

The concern regarding circulating elevated levels of metal ions in patients with MoM implants raises the demand for *in vitro* methods to detect the effects these metals cause to patients (Seo et al., 2010). Archived frozen blood represents a robust and invaluable source of human tissue for gene expression research (Li et al., 2008). Gene expression studies of human blood samples in the context of clinical diagnosis and epidemiologic surveillance face challenges such as having the capability to produce reliable detection of transcript levels. Several factors contribute to the variability of target detection including the method of blood collection, sample handling, RNA stabilization, and RNA isolation (Thach et al., 2003). Despite the importance of biological sample processing, very little has been published on selection and validation of these procedures, particularly for human whole blood.

Gene expression analysis of human blood cells allows minimally invasive repeated measurements and has been used in clinical studies for biomarker discovery (Beekman et al., 2009, Weber et al., 2010). Several examples of successful biomarker discovery in transcriptome data derived from peripheral blood have been reported from studies in neurological disorders such as Huntington's disease (Borovecki et al., 2005), migraine and chronic migraine (Hershey et al., 2004), neurofibromatosis type I and epilepsy (Tang et al., 2005); oncology settings such as renal cell carcinoma (Twine et al., 2003, Burczynski et al., 2005); severe acute respiratory syndrome (Yu et al., 2005) and gastrointestinal disorders such as Crohn's disease and ulcerative colitis (Burczynski et al., 2006). For these studies peripheral whole blood was collected into either Vacutainer sodium citrate cell purification tubes (Twine et al., 2003, Burczynski et al., 2005) or tubes containing EDTA (Borovecki et al., 2005, Hershey et al., 2004, Tang et al., 2005, Yu et al., 2005,

Burczynski et al., 2006), and in one of them the PAXgene blood RNA kit was used (Borovecki et al., 2005). Total RNA was isolated either within 2 hours of collection or after blood sample overnight storage. However, peripheral blood gene expression profiles change significantly after collection due to RNA degradation. The extraction and purification process can introduce further degradation (Asare et al., 2008) due to the susceptibility of RNA to RNases (Fleige and Pfaffl, 2006).

Reverse transcription-quantitative polymerase chain reaction (qRT-PCR) is a sensitive method commonly used for mRNA quantification. Such quantification can be either absolute or relative (Pfaffl, 2001). Absolute quantification gives the copy number of a target mRNA. It requires the construction of a calibration curve using standards of known concentration (Ho-Pun-Cheung et al., 2009). An example of this method is the quantification of virus RNA, such as hepatitis C, in serum (Hagiwara et al., 1993). This assay is useful in evaluating the state of viral replication in hepatitis C virus infection. On the other hand, relative quantification determines the changes in mRNA levels of a target gene across multiple samples and expresses it relative to the levels of a reference (Fleige et al., 2006). It requires data normalization, which involves the examination of one or several reference genes, the expression of which is assumed to be stable between individuals, experimental conditions or physiological states (Ho-Pun-Cheung et al., 2009). This method can help determine if a given treatment had an effect on the level of expression of a gene of interest (Livak and Schmittgen, 2001). This strategy has been successfully used to investigate physiological changes in gene expression levels (Fleige et al., 2006). An application of particular interest to relative gene expression quantification is studying the effects of wear debris in the long-term outcome of total joint replacement surgery and understanding the molecular events of such effects (Epstein et al., 2005, Nilsson et al., 2012, Akbar et al., 2012, Tamaki et al., 2009).

After withdrawing blood from the body RNA is unstable. There are systematic studies reviewing the stability of a wide range of bioanalytes, including DNA, RNA, and defined proteins, in whole blood in different anti-coagulants, at varying temperatures and under differing transport conditions (Elliott et al., 2008, Peakman

and Elliott, 2008, Salway et al., 2008). These investigations show that RNA degradation can occur due to inadequate sample handling, prolonged storage, suboptimal storage conditions, or inter-laboratory shipment of samples. Moreover, RNA may be degraded through exposure to heat or UV, or cleavage by RNase enzymes (Vermeulen et al., 2011, Fleige and Pfaffl, 2006, Becker et al., 2010). This is a problem for clinical samples and their downstream applications (Opitz et al., 2010). There are studies showing the influence of RNA integrity on the performance of gene expression profiling using qRT-PCR or microarrays (Ho-Pun-Cheung et al., 2009, Becker et al., 2010). It has been shown that with increasing RNA quality the variability of qRT-PCR results decreases and the amplification of products over 400bp is dependent on high RNA quality (Fleige et al., 2006). An inhibitory effect of degraded RNA on qRT-PCR results has also been shown. Degraded or impure RNA can limit the efficiency of the reverse transcriptase reaction and reduce complementary DNA (cDNA) yield (Fleige and Pfaffl, 2006). When conducting PCR on complex biological materials such as blood, residual materials from the samples or from pre-treatment steps can inhibit and significantly reduce the efficiency of the PCR process (Perch-Nielsen et al., 2003). The presence of several factors in blood that reduce the amplification efficiency, such as heme (Akane et al., 1994) and anticoagulants like heparin (Israeli et al., 1991), may limit downstream applications. Additionally, Rossen et al. tested the influence on PCR of several compounds including detergents, lysozyme, NaOH, alcohols and EDTA used during sampling or RNA extraction and found them to have an inhibitory effect. PCR inhibitors generally act at one or more of three essential points in the reaction in the following ways: they interfere with the cell lysis necessary for extraction of RNA, they interfere by nucleic acid degradation or capture, and they inhibit polymerase activity for amplification of target cDNA (Wilson, 1997). In other words, only experiments performed with high quality starting material provide reliable results and therefore special care needs to be taken when sampling, storing and extracting RNA (Becker et al., 2010). For this purpose, time between sampling and safely storing tissue in RNase inhibitors should be minimized. The extraction and purification process must be free of protein and genomic DNA, enzymatic inhibitors for qRT-PCR reactions, substances that complex co-factors like Mg^{2+} , and free of

nucleases in order to be successfully stored (Fleige and Pfaffl, 2006). It would seem, therefore, that a rigorous assessment of RNA integrity and purity is essential before using RNA samples in downstream applications.

RNA quality refers to both its purity (absence of inhibitors) and its integrity (absence of degradation) (Ho-Pun-Cheung et al., 2009). Low-quality RNA may compromise the expression analysis results. Quantity is another factor to be considered since many molecular applications may require several micrograms of starting material (Gonzalez-Roca et al., 2010). As a consequence, verification of RNA quantity, purity, and integrity prior to usage in downstream molecular applications is the first step in obtaining reliable gene expression data to allow meaningful comparisons (Fleige and Pfaffl, 2006).

The spectrophotometer absorbance measurement methods to evaluate RNA concentration and purity are well established and widely used (Fleige et al., 2006). Absorbance at 260nm (A₂₆₀) gives an accurate measure of RNA concentration, and the A₂₆₀/A₂₈₀ and A₂₆₀/A₂₃₀ ratios are accepted indicators of purity. A₂₆₀/A₂₈₀ ratios higher than 1.8 are indicative of limited protein contaminations, whereas low A₂₆₀/A₂₃₀ ratios are indicative of residual contamination by organic compounds such as phenol, sugars, or alcohol, which could be highly detrimental to downstream applications of a RNA sample. However, these methods do not give any information on DNA contamination, degradation state, or integrity of the sample (Fleige et al., 2006, Denisov et al., 2008). Several approaches have been used to assess RNA quality. These include spectrophotometry, analysis of 18S and 28S rRNA by electrophoresis, analysis of the complete RNA pattern on electrophoresis (Fleige and Pfaffl, 2006), the 5'–3' assay (Nolan et al., 2006) and PCR amplification of different target lengths of cDNA (Bauer et al., 2003, Gong et al., 2006). The micro-fluidic capillary electrophoresis method has developed into a common tool, particularly in gene expression profiling platforms. Instruments, such as the Agilent 2100 Bioanalyzer (Agilent Technologies, Palo Alto, CA) and the Experion™ (Bio-Rad Laboratories, Hercules, CA), are becoming the standard since their use decreased the amount of RNA needed to evaluate integrity down to the nanogram scale (Fleige et

al., 2006). The Experion™ automated electrophoresis system provides a method for determining quality of RNA to be used in gene expression analysis experiments using as little as 25ng total RNA. Bio-Rad introduced the RNA Quality Indicator (RQI) in Experion software as a method to standardise and quantitate RNA integrity. Using an algorithm, RQI calculations are based on mapping an electropherogram profile of a sample's RNA into a set of degradation standards (**Error! Reference source not found..A**). The RQI method returns a number between 10 (intact RNA) and 1 (highly degraded RNA) for each eukaryotic RNA sample run. As the ribosomal RNAs degrade, there is an accumulation of low molecular weight components toward the left end of the electropherogram (**Error! Reference source not found..B**) (Denisov et al., 2008).

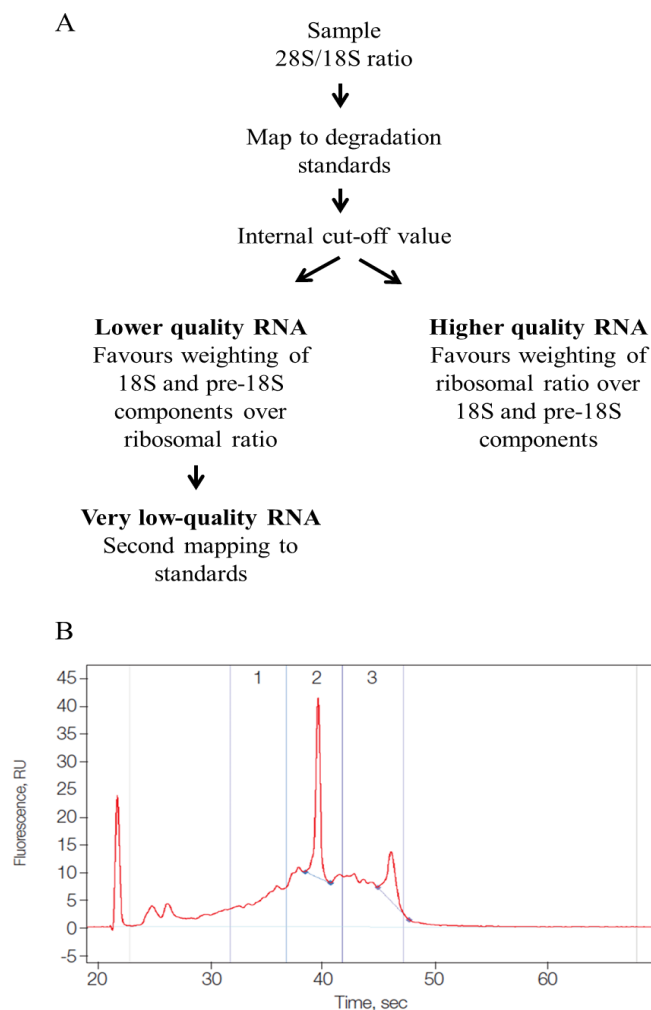


Figure 6.1. RQI calculation. A) Algorithm flow diagram. B) Three electropherogram regions used for RQI determination are indicated on an electropherogram of partially

degraded RNA: 1) pre-18S peak area, 2) 18S peak area and 3) 28S peak area (adapted from Denisov et al., 2008)

In order to circumvent the problem of RNA degradation in clinical tissue and blood samples, several commercial RNA whole blood collection tubes and stabilizing products have been developed. Such systems have the advantage of lysing whole blood at the time of collection, while simultaneously stabilizing RNA for later purification (Asare et al., 2008). Examples of such products are Paxgene™ Blood RNA System (Qiagen), Tempus™ Whole Blood RNA isolation system (Applied Biosystems) and RNAlater (Ambion and Qiagen). Paxgene™ Blood RNA System consists of a Paxgene RNA tube (PAX tube) for blood collection and a processing kit (PAX kit) for isolation of total RNA from whole blood (Thach et al., 2003). The Tempus™ Whole Blood RNA isolation system offers an alternative approach to peripheral blood RNA isolation, using a Tempus blood RNA tube with a proprietary solution to directly lyse whole blood and stabilize RNA and a processing kit (Asare et al., 2008). RNAlater is a stabilization reagent for RNA in cells and tissues increasingly being used in genomic studies and biobanking (Weber et al., 2010). This reagent does not implement collection tubes and it needs a complementary RNA extraction kit.

The Paxgene system is designed to extract $\geq 3\mu\text{g}$ of total RNA from 2.5ml of healthy human whole blood (according to the manufacturer), costing approx. £8.30 per sample. The Tempus system allows isolation of 2 to $8\mu\text{g}/\text{ml}$ of total RNA from 3ml of whole blood (according to the manufacturer), costing approx. £7.84 per sample. On the other hand, RiboPure™-Blood Kit (Ambion) is a RNA extraction kit design to work with 0.3-0.5ml of blood samples either fresh or stored in RNAlater. Yields of total RNA are typically 2 to $4\mu\text{g}$ from 0.5ml whole blood from normal healthy donors (according to the manufacturer), costing £8.30 approx per sample. Moreover, with a few additional reagents and some protocol modifications, the RiboPure™-Blood Kit can be used to isolate total RNA that includes miRNA. miRNAs are short (~22 nucleotides), single-stranded, noncoding RNAs that bind messenger RNA in a sequence-specific manner to regulate gene expression (Bartel and Chen, 2004). miRNAs play essential regulatory roles in fundamental biological processes such as differentiation, proliferation, apoptosis, and homeostasis (Williams et al., 2013). As a

consequence, miRNAs are increasingly being used as biomarkers for the diagnosis and prognosis of many diseases including cancer (Kosaka et al., 2010, Chen et al., 2008), rheumatoid arthritis and osteoarthritis (Murata et al., 2010). Being able to isolate RNA including the small RNA fraction, gives the RiboPure™-Blood Kit a key feature, which was a contributing factor to choosing this kit for the present study.

The introduction of such RNA stabilizing additives has significantly improved the quality of RNA isolated from clinical blood samples (Beekman et al., 2009). It also has the advantage of not having to extract the RNA immediately; instead, blood samples can be collected, stored at room temperature (i.e. Paxgene: 3 days, Tempus: 5 days, RNAlater: 7 days), 4°C (i.e. Paxgene: 5 days, Tempus: 7 days, RNAlater: 4 weeks) or frozen and stored for months at -80°C before extraction and analysis (Asare et al., 2008, Weber et al., 2010). This is a great advantage when dealing with samples from clinical environments where handling and storage processes may not be as rigorously controlled as they would be in a research laboratory.

Even though these commercial stabilizing systems are available, there still may be a need to perform RNA profiling experiments with legacy blood samples that were collected with common blood collection systems, such as EDTA tubes, and frozen after a variable time at ambient temperature. The main challenge of RNA extraction from frozen EDTA blood samples is to obtain sufficient RNA suitable for molecular studies. The freezing of EDTA-treated blood destroys the blood cells, exposing the RNA to enzymes causing its degradation (Beekman et al., 2009). As a result, gene expression analysis has to be performed with partially, and even extensively, degraded RNA. Little is known about the possibility of obtaining reliable qRT-PCR data from RNA samples with impaired RNA quality (Fleige et al., 2006). As a consequence, there is an ongoing debate as to how far gene expression results are affected by various degrees of degradation, and to what extent degradation of the tissue samples can occur and the RNA quality still be useful for analysis (Opitz et al., 2010).

Archived frozen blood samples represent an invaluable source for molecular studies.

Unfortunately, high quality RNA may not always be obtained from these samples. Although commercial products are now available to store blood and stabilize RNA, and protocols have been developed to overcome this difficulty, more research on the subject is needed in order to ensure the extraction of high quality RNA. As molecular assays evolve, so do the systems and protocols to obtain the starting material needed. In this case, *RNAlater* allows stabilisation of RNA for gene studies. However, it is not designed to protect protein or DNA. Qiagen has developed Allprotect™, which allow simultaneous preservation of DNA, RNA and native proteins in one tissue sample. This system allows preserving the *in vivo* profile for a variety of downstream applications. Research and development of biomolecule stabilisation procedures for clinical samples would enable archived frozen blood as a robust source for diagnostics and understanding of human pathologies and diseases.

7.1.1 Brief review of gene expression studies *in vivo* related to osteolysis and joint implant failure

Some progress has been made towards a better understanding of the major causes of implant failure, with factors such as stress shielding and poor surgical technique identified as possible contributors to early failure (Joshi et al., 2000, Wik et al., 2010). However, as has been discussed in previous chapters, there is evidence that aseptic loosening is associated with wear particles liberated from articulating prostheses (Crotti et al., 2004).

The pro-inflammatory cytokines IL-1 β , IL-8, and TNF- α play a major role in the process of bone resorption during aseptic loosening of joint prostheses (Hundric-Haspl et al., 2006). Epstein et al. (2005) examined the effects of ultra-high molecular weight polyethylene (UHMWPE) particles on TNF- α , IL-1 β , IL-6 and MCP-1 gene expression by the addition of polyethylene particles in an *in vivo* murine intramedullary rod model. They found that UHMWPE particles stimulated gene transcription of all the genes investigated in mononuclear cells when examined at 2, 4 and 10 weeks post-surgery. By using an *in vivo* animal model in which osteoclasts carrying out bone resorption were exposed to Ti particles, Nilsson et al. (2012)

analysed the gene expression of inflammatory markers. After exposure to Ti particles for 1 day, there was up-regulation in peri-implant tissue of Prostaglandin E Synthase (PGES) (8-fold), inducible Nitric Oxide Synthase (NOS2) (4-fold), TNF- α (2-fold), IL- β (3-fold), chemoattractant CCL2 (3-fold), and IL-6 (67-fold). After two more days of Ti particle exposure, the expression of CCL2 continued to increase and was up-regulated 5-fold, TGF β 2-fold, and the earlier 67 fold increase of IL-6 declined to a 7-fold up-regulation. To investigate the acute inflammatory responses to CoCr wear debris from a MoM hip resurfacing implant, Akbar et al. (2012) used an *in vivo* rodent air-pouch model. Their assessment of inflammatory gene transcripts from air-pouch tissue showed that CoCr wear debris increased the expression IL-1 β , TGF- β , CXCL2, and CCL2. These studies illustrate how wear particles produced at the articulation site induce the modulation of molecules that contribute to osteolysis and the subsequent aseptic loosening. They also seem to suggest that the presence of wear particles is what initially triggers the response, which is then exacerbated to different extents by the nature of the particles.

In addition to the proinflammatory cytokines mentioned above, Toll-like receptors (TLR), which are transmembrane proteins found in various cells, have been suggested to play a role in periprosthetic tissues and arthritic synovium (Pearl et al., 2011). In humans, the TLR family consists of 10 functional members (TLR1-TLR10) (Barreiro et al., 2009). Each member of the TLR family is activated by a different stimulus and subsequently activates a response to that type of pathogen (Pearl et al., 2011). Becker et al. (2005) proposed that cells may recognize particles through pattern recognition via TLR2 and TLR4; and later on (Hao et al., 2010) suggested mechanisms by which heat-shock protein 60 (Hsp60) positively modulates inflammatory cytokines via TLR4 signal transduction pathway on mononuclear cells in response to wear debris particles. Additionally, Tamaki et al. (2009) found increased levels of TLR 2, 4, 5, and 9 in both aseptic and septic periprosthetic tissues obtained at revision surgery. When some of the TLRs are stimulated, they interact with adapter proteins, including myeloid differentiation factor 88 (MyD88), which couples the TLR to downstream signalling kinases (Beutler, 2004). Pearl et al. (2011) challenged a murine macrophage cell line with PMMA particles and compared the

expression of TNF- α in the presence and absence of a small peptide inhibitor of MyD88. They showed that the presence of the inhibitor significantly diminished the production of TNF- α , demonstrating that the inflammatory response to PMMA particles is partly dependent on TLR signalling. Moreover, Potnis et al. (2013) exposed human monocytes (THP-1) to Co-alloy particles at increasing particle:cell ratios for 24h. They observed that particles caused up-regulation of IL-8 and that the addition of blocking antibodies against TLR4 or gene silencing of MyD88 markedly inhibited IL-8 release. Since a key element in the initiation of the innate immune response against pathogens is the recognition of components commonly found on the pathogen, referred to as pathogen-associated molecular patterns (PAMP) (Werling and Jungi, 2003), all these studies seem to suggest that wear particles could have a PAMP-like behaviour and bind to TLRs being expressed by macrophages, which then initiates signalling pathways leading to the stimulation of the immune response.

Receptor activator of nuclear factor- κ B ligand (RANKL), its receptor, receptor activator of nuclear factor- κ B (RANK), and its soluble inhibitor osteoprotegerin (OPG) are recognized as key regulators of osteoclast formation that regulate bone resorption in both health and disease (Crotti et al., 2004). Several studies have demonstrated the expression of mRNA encoding RANKL, OPG and RANK in peri-implant tissues associated with osteolytic zones. Haynes et al. (2001) showed a significant correlation between the ratio of RANKL:OPG mRNA in cells isolated from joint tissues involved in focal bone erosion in active rheumatoid arthritis, and the ability of these cells to form osteoclasts in culture. By investigating the expression of RANK, RANKL and OPG in the peri-implant tissues of patients with osteolysis compared with levels in synovial tissues from osteoarthritic and healthy subjects, (Crotti et al.) (2004) showed that significantly higher levels of RANKL, relative to OPG, are expressed in peri-implant tissues of patients with prosthetic loosening and that these levels of RANKL may significantly contribute to osteoclast-mediated peri-implant osteolysis. (Holding et al.) (2006) obtained tissue from zones of peri-prosthetic osteolysis from 11 patients undergoing revision of total hip prostheses and found a strong statistical correlation ($p < 0.02$) between volume of bone loss, polyethylene wear debris, and RANK, RANKL and TNF α expression.

Using quantitative real-time PCR analysis of peri-prosthetic soft tissue from osteolysis patients, Koulouvaris et al. (2008) detected elevated levels of expression of alternative macrophage activation markers: CHIT1, CCL18, IL8, MIP1 α , and markers of osteoclast precursor cell differentiation and multinucleation (Cathepsin K, TRAP, DC-STAMP) relative to osteoarthritis controls. Expression levels of TNF- α , IL-6, and RANKL were unchanged, while OPG was reduced in osteolysis patients. Mandelin et al. (2003) studied 11 patients with aseptic loosening who were in pain and whose radiographs showed the presence of periprosthetic osteolysis and found that RANKL and RANK were up-regulated at the mRNA and cellular (protein) level in stroma around loose implants. To provoke inflammatory osteolysis, Mao et al. (2012) injected Ti particles into established air pouches for female BALB/C mice. All of the air pouches were harvested 14 days after the surgical procedure and were processed for molecular and histological analysis. The results demonstrated that Ti injection elevated the expression of RANKL, OPG, VEGF, and tumour necrosis factor receptor-associated factor 6 (TRAF6) at both the gene and protein levels. Chen et al. (2012) used a murine osteolysis model to examine the hypothesis that administration of a matrix metalloproteinase-9 inhibitor reduces the expression of RANK and RANKL and, thereby, suppresses Ti debris-induced inflammatory osteolysis. They found that the down-regulation of RANK/RANKL significantly inhibits debris-induced inflammatory osteolysis.

It has also been postulated that patient-related factors could cause variability in the host response to particulate wear debris (von Knoch et al., 2004, Zhang et al., 2008). Nich et al. (2001) evaluated the influence of oestrogen deficiency on experimental particle-induced osteolysis using a murine model. After polyethylene implantation, the RANKL/OPG mRNA ratio significantly increased in all mice groups, but remained unchanged in mice that had been subjected to ovariectomy. These findings suggest a protective effect of oestrogen deprivation in the osteolytic response to polyethylene particles.

It is clear that a range of studies have been carried out in order to understand how wear debris affects the levels of expression of genes involved in osteolysis in tissues surrounding the joint implant. However, there are not enough studies relating such results with peripheral blood gene expression and ion levels in patients with either failed or well-functioning joint replacements. If a correlation between gene expression levels in peripheral blood and stages of osteolysis could be established, a minimally invasive method of early detection of osteolysis could potentially be developed.

6.2 Aims

- To establish a storing protocol for clinical blood samples collected with common collection systems such as EDTA tubes, that allows extraction of RNA suitable for molecular applications.
- To determine whether gene expression levels of RANK, RANKL and OPG are related to whole blood metal ion levels of patients with metal-on-metal hip implants.

6.3 Results

6.3.1 Whole blood sample storage and RNA isolation from samples with the RiboPure Blood kit

Whole blood samples were withdrawn with EDTA collection tubes from patients with metal on metal hip implants at the Southern General Hospital in Glasgow, UK, with appropriate consent obtained. This study was approved by the NHS Research Ethics Committee (ref: 04/S0702/60) and by the University Ethics Committee. Samples were kept at 4°C until delivery to the research laboratory, which generally took place within 4 to 5h from collection.

As a starting point, the possibility of extracting qRT-PCR quality RNA from archived whole blood samples stored in EDTA collection tubes at -80°C was investigated. For this purpose, RNA was extracted from archived whole blood samples, that had been stored at -80°C, and its integrity determined.

To study the ability of *RNAlater* to preserve RNA in freshly obtained blood, 500µl aliquots of sample were taken into 2ml microcentrifuge tubes with and without 1.3ml of *RNAlater* (Life technologies; Paisley, UK). RNA was extracted immediately upon arrival at the laboratory from some of the aliquots and the remaining ones were stored at -80°C overnight before RNA extraction.

The RiboPure Blood Kit contains reagents and materials for isolation of high quality total RNA from EDTA-anticoagulated whole blood.

RNA was extracted from three archived whole blood samples that had been stored at -80°C for 1, 6 and 12 months. When the Experion RNA quality analysis was performed, the RNA samples mapped to more degraded standards, which meant that more emphasis was placed on the pre-18S and 18S regions of the electropherograms for generating the RQI values. As a result, low RQI numbers were obtained with these archived samples (**Error! Reference source not found.**), which indicates that the RNA is mostly degraded and may not be suitable for molecular analysis.

Archived samples	
Storage at -80°C with no RNA stabiliser (months)	RQI (1=poor, 10=high)
1	3.2
6	3
12	2.9

Table 6.1. RNA quality indicator (RQI) numbers obtained with archived samples stored with no RNA stabiliser.

Sample	RNAlater	RQI (1=poor, 10=high)	Yield (μg)
Archived	No	3.03 \pm 0.09	1.15 \pm 0.17
Fresh	Yes	8.13 \pm 0.53	5.64 \pm 0.48
Fresh	No	6.70 \pm 1.38	4.90 \pm 1.26
Fresh blood, stored at -80°C overnight	Yes	8.28 \pm 0.40	4.93 \pm 0.66
Fresh blood, stored at -80°C overnight	No	3.07 \pm 0.23 [†]	3.87 \pm 0.15

Table 6.2. RNA quality indicator (RQI) numbers. Results are mean values (\pm SEM, $n \geq 3$). RQI values from 7 upwards indicate that the RNA is suitable for molecular applications. [†]Significant difference in RQI values between samples stored overnight at -80°C in the presence and absence of RNAlater by two-sample t-Test ($p < 0.05$).

In order to confirm the role of the RNAlater to reduce RNA degradation, RNA was extracted from samples upon receipt and after being stored at -80°C overnight in the presence and absence of RNAlater. The results from this experiment are summarised in **Error! Reference source not found.** In terms of fresh whole blood samples, no significant difference was observed in RNA integrity between the presence and absence of RNAlater. However, after samples had been stored overnight at -80°C, the quality of RNA significantly decreased in the absence of the RNA stabiliser. Additionally, there was no significant difference in RNA yield in the presence and absence of RNAlater. These results highlight the fact that yield measurements do not give any information about the integrity of the RNA as well as the importance of RNA stabilisation even when performing the extraction upon receipt of samples.

6.3.2 RNA stability during freeze/thaw cycles

In order to simulate the processes of freezing and thawing of archived blood samples during research, aliquots of whole blood, in the presence and absence of RNAlater, were frozen for 15min at -80°C and thawed at room temperature for 15min. After 0,

3, 6, and 10 such freeze/thaw cycles, RNA was extracted and quality determined. There was no significant difference in RQI values from samples stored with *RNAlater* at 3 freeze/thaw cycles when compared to 0 freeze/thaw cycles. Results indicate that *RNAlater* can protect RNA from degradation for up to 3 freeze/thaw cycles (Table 6.3, Figure 6.2). It is important to note that there was also no significant difference in RNA yield across all samples. This indicates that it is insufficient to perform only spectrophotometer analysis for yield when requiring to establish integrity of RNA for molecular experiments.

Freeze/thaw cycles	<i>RNAlater</i>	RQI (1=poor, 10=high)	Yield (μg)
0	Yes	8.13 \pm 0.53	5.64 \pm 0.48
	No	6.70 \pm 1.38	4.90 \pm 1.26
3	Yes	7.98 \pm 0.57	4.82 \pm 0.24
	No	3.33 \pm 0.11 [†]	4.53 \pm 0.62
6	Yes	3.57 \pm 0.81 [*]	6.11 \pm 1.64
	No	2.10 \pm 0.06	4.38 \pm 1.04
10	Yes	3.03 \pm 0.13 [*]	5.78 \pm 1.94
	No	2.40 \pm 0.15	4.74 \pm 0.82

Table 6.3. RNA quality indicator (RQI) numbers. Results are mean RQI values (\pm SEM, $n \geq 3$). RQI values from 7 upwards are considered indicative of high quality RNA suitable for molecular applications. ^{*}Significant difference in RQI values of samples stored with *RNAlater* when compared to 0 freeze/thaw cycles by ANOVA followed by Dunnet's comparison test ($p < 0.05$). [†]Significant difference in RQI values between samples at 3 freeze/thaw cycles in the presence and absence of *RNAlater* by two-sample t-Test ($p < 0.05$).

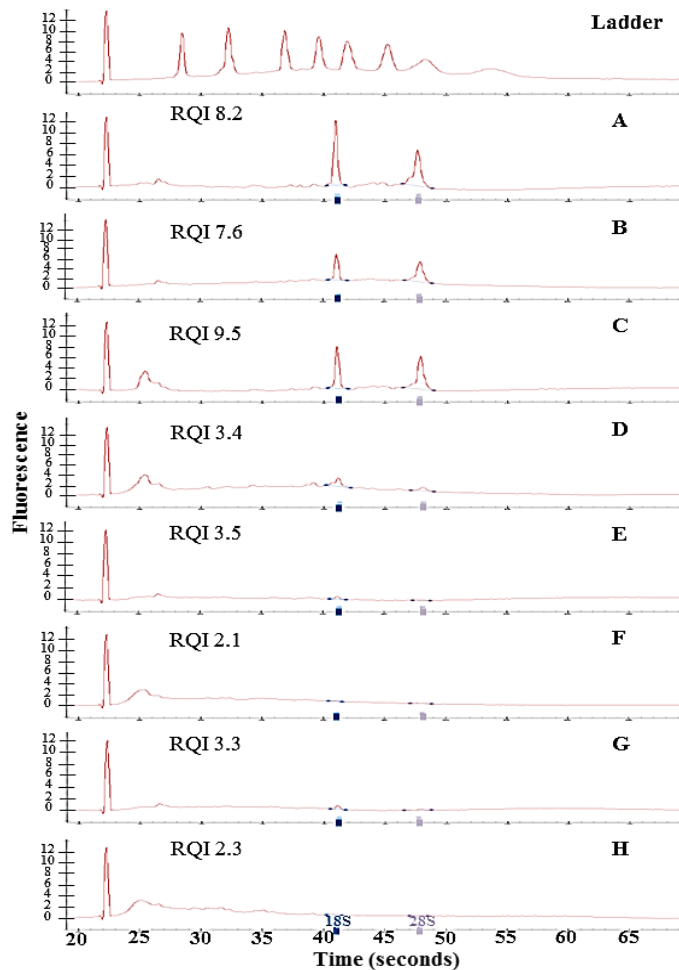


Figure 6.2. Electropherograms from freeze/thaw cycles. Ladder, RNA standard. **A**, 0 freeze/thaw cycles in presence of RNAlater. **B**, 0 freeze/thaw cycles in absence of RNAlater. **C**, 3 freeze/thaw cycles in presence of RNAlater. **D**, 3 freeze/thaw cycles in absence of RNAlater. **E**, 6 freeze/thaw cycles in presence of RNAlater. **F**, 6 freeze/thaw cycles in absence of RNAlater. **G**, 10 freeze/thaw cycles in presence of RNAlater. **H**, 10 freeze/thaw cycles in absence of RNAlater. Electropherograms representative of $n \geq 3$.

6.3.3 Whole blood metal ion levels

ICP-MS was performed in order to measure metal ion levels in the clinical blood samples chosen for the gene expression analysis. The already established protocol for this technique in the laboratory was followed, which selects Rh as the internal standard. However, Figure 6.3 shows poor recovery of Rh in these samples, and that recovery fluctuated outside the acceptable range limits for internal standard recovery.

As a result, the recovery of three internal standards (Rh, Sc, In) was evaluated in whole blood samples. Figure 6.4 shows that Sc is the internal standard that fluctuates the least and remains within the 90-110% acceptable recovery range. Based on this, Sc was selected as the internal standard for the ICP-MS analysis of blood samples.

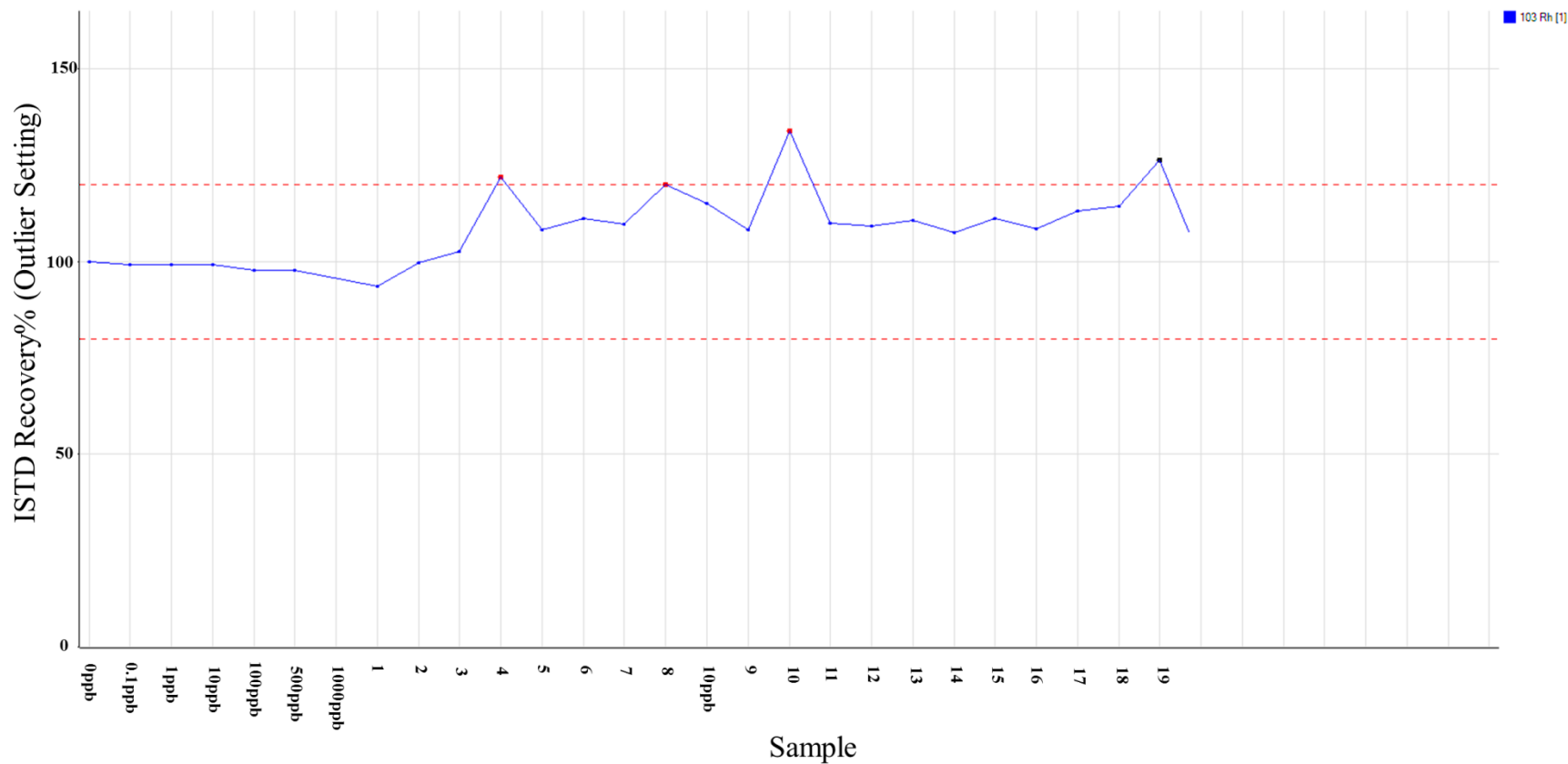


Figure 6.3. ICP-MS Internal standard (ISTD) recovery. Red dotted line marks acceptable range limits (90-110%) for internal standard recovery. Red dots represent the samples that are outside the range (outlier setting) Rh: Rhodium. Standards: 0, 0.1, 1, 10, 100, 500, and 1000ppb (0, 0.1, 1, 10, 100, 500, and 1000µg/l).

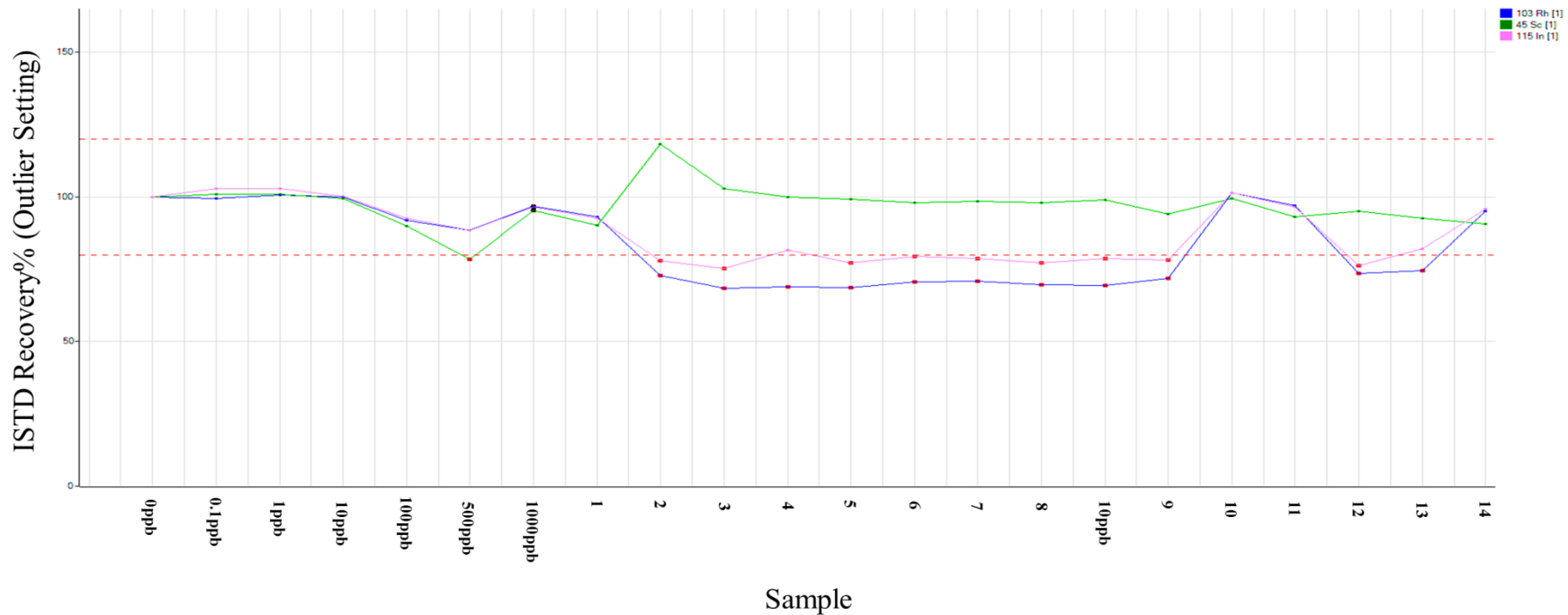


Figure 6.4. ICP-MS internal standard recovery of the candidates Sc, Rh, In. Red dotted line marks acceptable range limits (90-110%) for internal standard recovery. Red dots represent the samples that are outside the range (outlier setting). Sc: Scandium. Rh: Rhodium. In: Indium. Standards: 0, 0.1, 1, 10, 100, 500, and 1000ppb (0, 0.1, 1, 10, 100, 500, and 1000 μ g/l).

The concentration of Co and Cr ion levels in whole blood samples from six different patients with metal-on-metal hip implants was determined with ICP-MS. The detection limits for Cr and Co were 0.084µg/l and 0.051µg/l, respectively. Table 6.4 summarises the metal ion levels measured in whole blood. There was no apparent relation between the period of time the patient had had the implant for, the type of implant and the whole blood metal concentration. In general, higher levels of cobalt than chromium were detected. Only patient 2 had levels of Cr and Co ions which were above the recommended guideline of 7µg/l for Cr plus Co ions (MDA/2010/069).

Patient	Metal level (µg/l)		Period of time with the implant
	Whole blood		
	Cr	Co	
1	Below detection limit (<0.084)		1 year
2	2.134	6.720	1 year
3	0.843	0.876	2 years
4	0.897	1.087	2 years
5	0.709	0.917	2 years, resurfacing
6	0.508	0.148	2 years, resurfacing

Table 6.4. Metal ion levels in whole blood from patients with metal-on-metal hip implants.

6.3.4 Effects of RNA integrity on qRT-PCR results

As mentioned in Chapter 4, in order to control for experimental variations in the amount of RNA used in each real time PCR and batch-to-batch variations in PCR reagents, measurement of reference genes has been used for the normalization of target gene expression data.

For the present study, TNF receptor-associated protein 1 (TRAP1), Folylpolylglutamate synthase (FPGS), 2,4-dienoyl CoA reductase 1, mitochondrial (DECR1) and peptidylprolyl isomerase B (PPIB) were selected as potential reference genes due to the fact that they have been identified as stably expressed genes in whole blood of humans of both genders with multiple disease conditions and ages 2 to 78. They have been suggested to be appropriate normalization genes for

microarray and RT-PCR whole blood studies of human physiology, metabolism and disease (Stamova et al., 2009).

RNA degradation can affect the quantification of gene expression changes that could result in either underestimating or overestimating such changes misleading the analysis and interpretation of results (Fleige and Pfaffl, 2006). For this reason, the influence of RNA quality on qRT-PCR results was explored by carrying out qRT-PCR reactions with intact RNA (RQI=8.9), partially degraded RNA (RQI=5.8) and degraded RNA (RQI=2.9). The effect of RQI on qRT-PCR performance was investigated by correlating the RQI values with the C_q of the PCR runs for the potential reference genes.

The results summarised in Table 6.5 show that RNA quality had an impact on the quantification cycle (C_q) for each gene. Each gene had different C_q values for the varying RQIs. C_q is a relative measure of the concentration of target in the PCR reaction. The C_q value increases with a decreasing amount of target template (Ruijter et al., 2013). However, factors such as impaired quality of RNA can cause template-independent changes to the C_q value (Fleige et al., 2006, Fleige and Pfaffl, 2006). For example, the C_q for FPGS at RQI 8.9 is 29.97, however at RQI 5.8 the C_q is 31.67. Results from this trial illustrate how gene analysis results could vary depending on the integrity of the RNA and have a direct impact on comparisons to be made, since the effects on gene expression exerted by a treatment are based on the comparison of C_q values for reference and target genes (Pfaffl, 2001).

Gene	RQI (1=poor, 10=high)	Mean Cq (\pm SEM)
PPIB	8.9	26.37 \pm 0.09
	5.8	31.20 \pm 0.41
	2.9	27.09 \pm 0.08
DECR1	8.9	26.75 \pm 0.32
	5.8	29.35 \pm 0.10
	2.9	28.02 \pm 0.19
FPGS	8.9	29.97 \pm 0.44
	5.8	31.67 \pm 0.12
	2.9	32.61 \pm 0.09
TRAP1	8.9	30.99 \pm 0.24
	5.8	32.44 \pm 0.09
	2.9	33.13 \pm 0.10

Table 6.5. Effect of RNA quality on reference gene Cqs. PPIB, peptidylprolyl isomerase B (cyclophilin B). DECR1, 2,4-dienoyl CoA reductase 1, mitochondrial. FPGS, folylpolyglutamate synthase. TRAP1, TNF receptor-associated protein 1. Results are expressed as mean Ct values (\pm SEM, n=3).

6.3.5 Whole blood gene expression analysis

RANK, RANKL, and OPG were selected as target genes due to their role in controlling the balance between bone formation and bone resorption. For this purpose, TaqMan validated gene expression probes were selected (Table 2.8, Section 2.2.6). TaqMan chemistry uses the 5'-3' exonuclease activity of Taq DNA polymerase, which degrades a non-extendable fluorescent DNA probe following hybridization and extension in the PCR (VanGuilder et al., 2008). Sequence-specific TaqMan probes are labeled with both a fluorescent reporter and a quencher, which are maintained in close proximity until hybridization to the target occurs. In conventional TaqMan technology, the reporter fluorophore and fluorescent quencher are bound to the 5' and 3' ends of the probe sequence, and fluorescence-resonance energy transfer (FRET) from the reporter to the quencher achieves suppression of reporter molecule fluorescence (Reynisson et al., 2006). Following annealing of the forward and reverse primers to the target sequence, the TaqMan probe is designed to anneal between these primer sites and is hydrolyzed by the 5'-3' exonuclease activity of the Taq polymerase. If no product is present, the probe does not bind and is not degraded; hence the reporter remains quenched. Probe hydrolysis results in de-suppression of the reporter and a subsequent cumulative increase in fluorescence

proportional to the amount of transcript present. This oligonucleotide primer/probe approach increases accuracy and specificity of PCR product detection due to the requirement for precise, gene-specific matching of three independent nucleotide sequences (Wang and Brown, 1999, VanGuilder et al., 2008). As a consequence, the melting curve analysis performed with SYBR Green probes is not required (VanGuilder et al., 2008)

RANK, RANKL, and OPG gene expression levels were investigated in whole blood samples patients with metal-on-metal hip implants. As shown in Section 7.3.4, RNA integrity is an essential step for molecular downstream applications. Before performing qRT-PCR, RNA integrity in all whole blood samples was assessed. Although several whole blood samples were available for this study, the RNA integrity from a number of them was impaired, which was probably due to the fact that such samples had taken longer to be delivered and consequently they had started to deteriorate before the stabilisation step. Therefore such samples were not suitable for gene expression analysis. As a result, six samples that had RQI values higher than 7 (Table 6.6) were selected for the present study. Additionally, whole blood samples of three healthy volunteers were included as controls. These control samples were kept separate.

Sample	RQI	Purity (A260/280)
Controls	7.87±0.22	1.98±0.03
1	8.2	1.86
2	9.6	1.97
3	9.3	2.00
4	8.5	2.04
5	8.8	1.96
6	7.2	1.92

Table 6.6. RQI values of whole blood samples from patients and controls (healthy volunteers). Control values are expressed as mean ± SEM (n=3).

As mentioned in Chapter 4, the empirical determination of suitable reference gene for a set of experimental conditions is essential for data normalization. In order to determine the most appropriate reference gene for patients' whole blood samples, four candidate genes (TRAP1, FPGS, DECR1, and PPIB), that have been shown to

be stable in whole blood samples, were chosen from the literature (Stamova et al., 2009) and evaluated for their stability under these experimental conditions.

In the current study, C_q values from all patients and controls were analysed by RefFinder, which as described in Chapter 4, is an online tool that integrates the four most commonly used approaches to compare and rank the tested candidate reference genes (Xie et al., 2012). Results are summarised in Table 6.7 and Figure 6.5.

Ranking Order (Better--Good--Average)				
Method	1	2	3	4
Delta CT	PPIB	DECR1	FPGS	TRAP1
BestKeeper	PPIB	TRAP1	DECR1	FPGS
Normfinder	PPIB	DECR1	TRAP1	FPGS
Genorm	DECR1-PPIB		FPGS	TRAP1
Recommended comprehensive ranking	PPIB	DECR1	TRAP1	FPGS

Table 6.7. RefFinder ranking order of the four candidate reference genes.

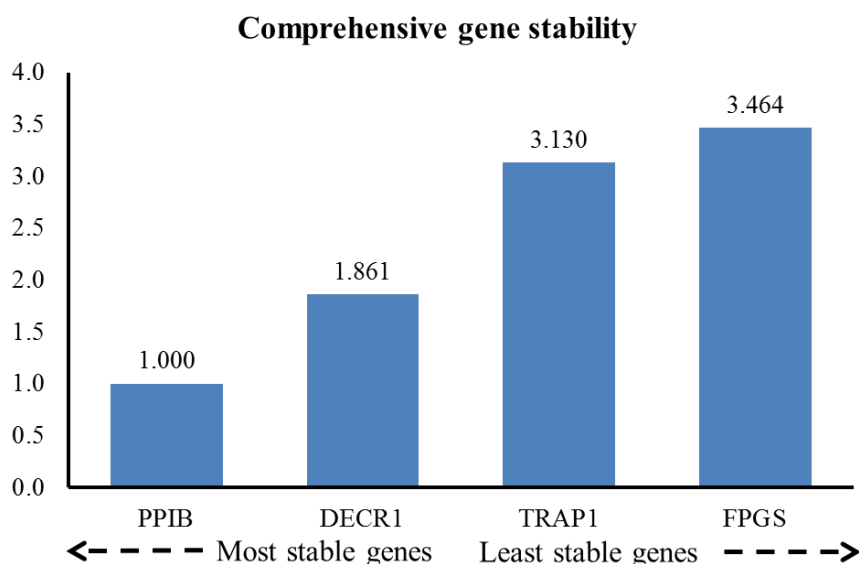


Figure 6.5. RefFinder results. Comprehensive gene stability integrates the four commonly used approaches to compare and rank the tested candidate reference genes calculating the geometric mean of their weights for the overall final ranking.

According to this, PPIB would be the most appropriate reference gene for these samples. Following the selection of the reference gene, PCR reactions for the target genes were carried out. Negative PCR controls (H_2O and RT-) for each of the assays

showed no amplicons. Comparison of the expression of each gene between control (healthy volunteers) and treatment (patient) was then determined with the $2^{-\Delta\Delta C_t}$ method (Livak and Schmittgen, 2001) where C_t refers to quantification cycle values (C_q). Fold variation results are summarised in

Sample	RANK	RANKL	OPG
Controls	1.000±0.148	1.000±0.192	1.000±0.102
1	0.517±0.041	0.564±0.108	0.705±0.001
2	0.850±0.101	1.533±0.129	0.046±0.003
3	10.115±0.272	1.636±0.278	0.050±0.003
4	1.484±0.375	6.278±0.338	0.088±0.003
5	3.610±0.281	2.573±0.193	0.094±0.004
6	5.042±0.265	2.766±0.272	0.104±0.002

Table 6.8 6.8 and Figure 6.6.

Sample	RANK	RANKL	OPG
Controls	1.000±0.148	1.000±0.192	1.000±0.102
1	0.517±0.041	0.564±0.108	0.705±0.001
2	0.850±0.101	1.533±0.129	0.046±0.003
3	10.115±0.272	1.636±0.278	0.050±0.003
4	1.484±0.375	6.278±0.338	0.088±0.003
5	3.610±0.281	2.573±0.193	0.094±0.004
6	5.042±0.265	2.766±0.272	0.104±0.002

Table 6.8. Fold variations of target genes. The sample column refers to the patient number. Three qRT-PCR reactions were performed per sample (i.e. one biological sample with 3 technical replicates per gene assayed, n=3). Gene fold variations are expressed as mean values of the technical replicates (\pm SD, n=3).

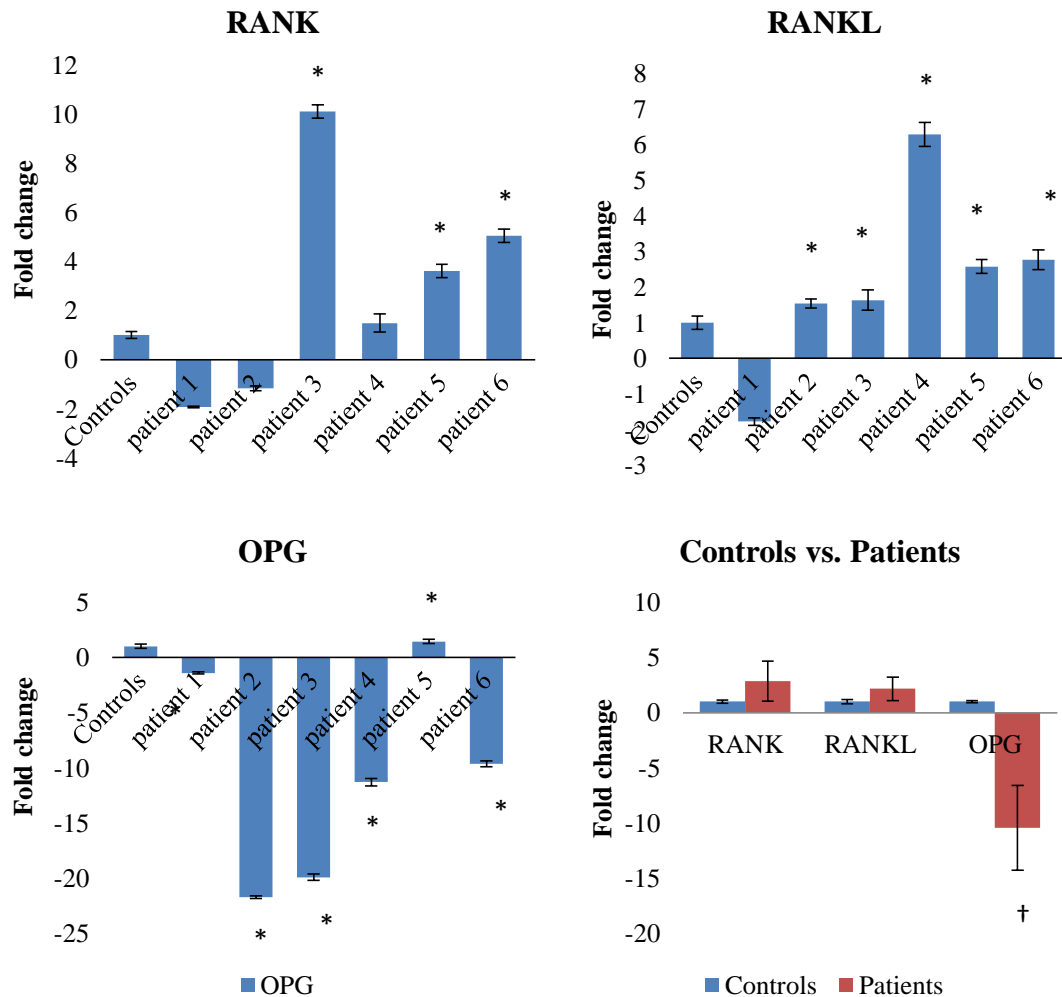


Figure 6.6. Fold variations of target genes. Results are mean values \pm SD (n=3, one biological sample with 3 technical replicates per gene assayed) expressed as the negative inverted. *Significantly different from control values by ANOVA analysis followed by Dunnet's comparison test ($p < 0.05$). †Significant difference between control samples and patient samples as a group ($p < 0.05$) by 2 sample t-Test.

Results show biological variation in gene expression fold change between individuals. All patients had a statistically significant down-regulation of OPG when compared to controls. Patients 3, 4, 5 and 6, which are the patients that have had the implant longer than 1 year, showed significant change in the expression of all three genes when compared to controls. Additionally, when patient samples as a group were compared to control samples, OPG showed significant down-regulation. It has been suggested that the RANKL/OPG ratio is raised significantly in patients with severe osteolysis and that this imbalance is involved in bone resorption mechanisms

(Perez-Sayans et al., 2010). Table 6.9 summarises RANKL/OPG ratios calculated for each patient. Since OPG was generally down-regulated, patients had higher ratios when compared to controls, which suggests an imbalance in the bone turnover system favouring bone resorption. However, when ratios were plotted against metal ion levels, a clear trend could not be established (Figure 6.7).

Sample	RANKL/OPG ratio	Cr ($\mu\text{g/l}$)	Co ($\mu\text{g/l}$)	Co+Cr ($\mu\text{g/l}$)
Controls	1.000	0.595	0.992	1.587
patient 1	0.800	0.001	0.419	0.42
patient 2	33.300	2.134	6.72	8.854
patient 3	32.572	0.843	0.876	1.719
patient 4	71.000	0.897	1.087	1.984
patient 5	1.793	0.709	0.917	1.626
patient 6	26.686	0.508	0.148	0.656

Table 6.9. RANKL/OPG ratios. RANKL/OPG ratios were calculated for each patient and controls.

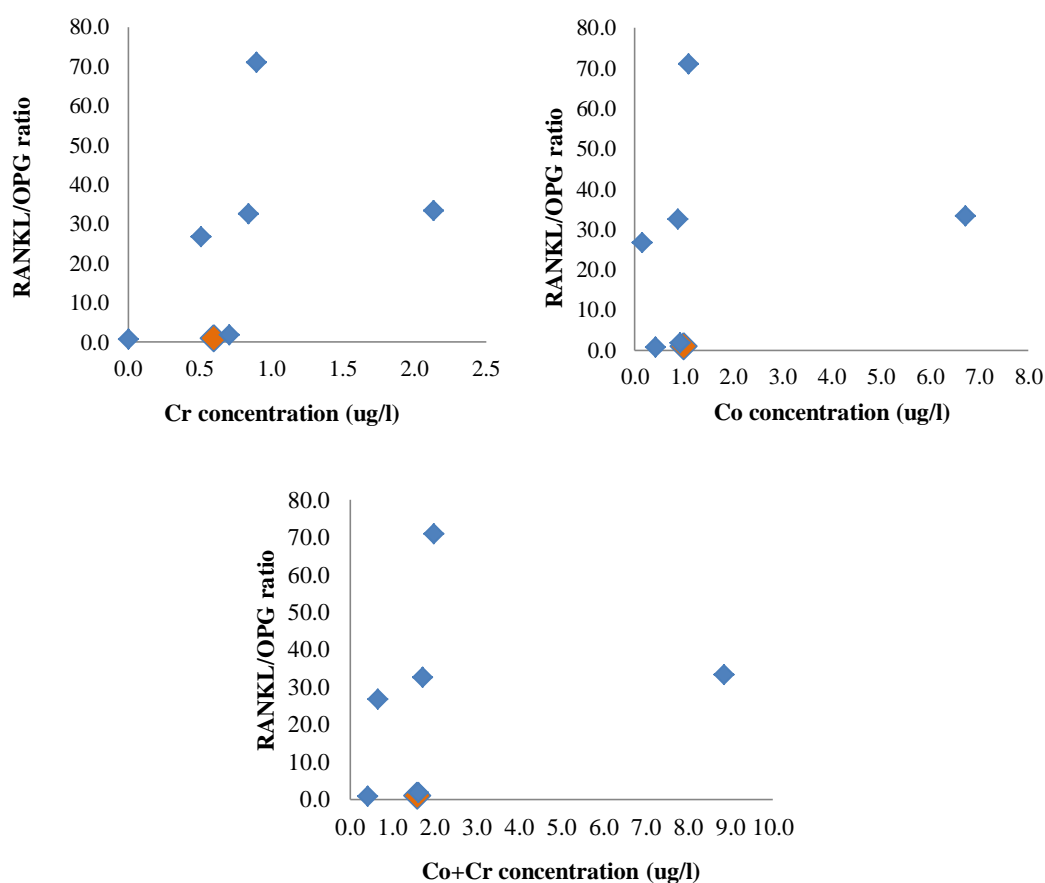


Figure 6.7. Scatter plots of RANKL/OPG ratios. RANKL/OPG ratios were plotted against Cr, Co, and Cr+Co ion levels. Orange diamond represents the controls.

6.4 Discussion

In this study, yield and quality of total RNA obtained from whole blood archived samples stored at -80°C , and fresh whole blood samples in the presence and absence of *RNAlater*, were compared in order to establish an appropriate method for storage and RNA isolation for gene expression analysis from frozen whole blood samples. In addition to this, the RNA stability of clinical blood samples in the presence and absence of *RNAlater* after freeze/thaw cycles was also tested in order to mimic the processes that such samples may undergo during research.

Archived frozen blood samples represent a great source of material for research. It has been demonstrated in this chapter that archived samples stored at -80°C in the absence of RNA stabilising agents are likely to be unsuitable for molecular analysis as RNA isolated from them is degraded. On the other hand, results suggest that *RNAlater* provides protection to RNA. For up to three freeze/thaw cycles before RNA extraction samples still yield RNA in quantity and quality required for molecular studies. This could mean that, depending on the application, blood samples might not need to be split into aliquots as long as they are treated with *RNAlater*. In the case of samples in the absence of *RNAlater*, freezing and freeze/thaw cycles caused rapid RNA degradation. This finding has important implications for the convenient collection of blood samples, and maximizing the biomarker information that can be collected from them.

The RiboPure Blood extraction kit performed as expected. An often underestimated critical issue underlying the reliability of gene expression results is the quality of the RNA samples. RNA analysis by spectrophotometer does not give complete information about the quality of the RNA being quantified, which is why RNA integrity was verified with the Experion automated electrophoresis system. In addition to this, the Minimum Information for Publication of Quantitative Real-Time PCR Experiments (MIQE) guidelines provides specifications for the minimum information that must be reported for a qPCR experiment to ensure its relevance, accuracy, correct interpretation, and repeatability (The MIQE Guidelines: Minimum

Information for Publication of Quantitative Real-Time PCR Experiments). RNA integrity assessment is one of the parameters that these guidelines consider essential. Variation between RNA isolation results could be due to external variables such as the extraction method itself, the intrinsic characteristics of each patient's blood sample and/or the time between collection of the blood from the patient and the addition of *RNAlater*. After several repetitions, a protocol for the storage of clinical blood samples that allows the extraction of high quality RNA was established. This protocol requires the addition of *RNAlater* to the clinical samples as soon as they arrive at the laboratory, and thereafter storage at -80°C.

qRT-PCR is increasingly used to quantify gene expression changes. Relative quantification determines the changes in mRNA levels of a gene across multiple samples and expresses it relative to the levels of an internal control RNA (reference gene). An essential requirement for a successful quantitative mRNA analysis using qRT-PCR is the usage of intact RNA. A significant negative relationship between the RQI and Ct has been reported previously (Fleige et al., 2006) as well as the direct influence of RNA integrity on the absolute gene expression results (Imbeaud et al., 2005). Archived frozen blood samples from the same patient at different time points, would contribute greatly in assessing changes in expression of genes of interest and small RNA biomarkers through time. In order to clarify the effects that impaired quality of RNA would have in qRT-PCR analysis performed with such archived samples, reactions were carried out with RNA of varying integrity. Results in this study are in agreement with previous reports: as RNA degrades quantitative expression levels determined by qRT-PCR change. As a result, the archive samples could not be used for the present study and only clinical whole blood samples that had been stabilised with *RNAlater* and that had an RQI ≥ 7 , were selected for the gene expression analysis.

It has been mentioned in previous chapters that osteolysis is one of the foremost problems limiting the survival of current hip arthroplasty procedures (Holding et al., 2006). It is induced by the wear particles and corrosion products which incite an inflammatory response resulting in bone resorption, eventual loosening and failure of

the prosthesis. Host factors are presumed to play a role in this process which involves a variety of cytokines and mediators (Agarwal, 2004). In normal bone, there is a fine balance between bone formation mediated by osteoblasts and bone resorption mediated by osteoclasts. RANK, RANKL, and OPG have been identified as key intermediates in maintaining such balance (Kwan Tat et al., 2008). RANK is a transmembrane protein expressed in the osteoclasts, which are activated when RANK binds with RANKL, and it is expressed on the surface of preosteoblastic/stromal cells (Khosla, 2001). OPG, a protein that inhibits the development of osteoclasts, acts as a decoy receptor by sequestering RANKL and inhibiting RANK, which blocks osteoblastic activation and induces apoptosis (Hofbauer et al., 2001) (Figure 6.8).

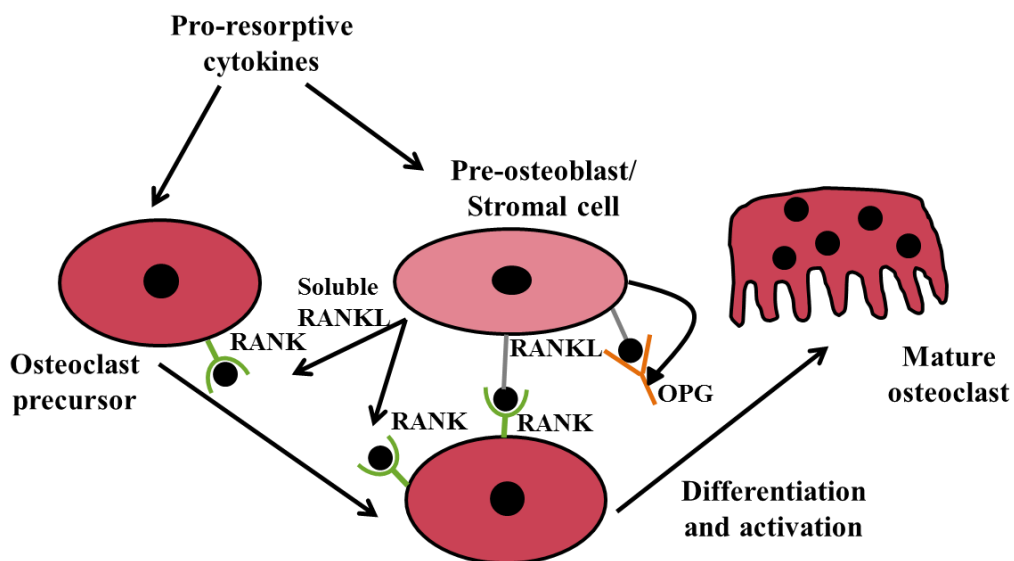


Figure 6.8 OPG/RANK/RANKL molecular and cellular mechanisms of action (adapted from (Khosla, 2001)). OPG: Tumor necrosis factor receptor superfamily, member 11b. RANK: Tumor necrosis factor receptor superfamily, member 11a, NF κ B activator. RANKL: Tumor necrosis factor (ligand) superfamily, member 11.

This chapter has shown gene expression changes of RANK, RANKL, and OPG in patients with metal-on-metal hip implants, and correlates gene expression with the metal ion levels at the time of the analysis. In order to achieve this, an adequate reference gene had to be determined. For this purpose, four candidate genes were tested. PPIB was shown to be the most stable throughout the samples and was selected as the most appropriate reference gene for this study. Delta-delta ($\Delta\Delta$) C_T

analysis ($(\Delta\Delta)C_q$) found that five out of six MoM patients had a decrease in OPG/RANKL ratio compared to controls, which suggests an unbalance in the bone remodelling process. Ideally, gene expression analysis should be carried out at different time points for each individual as since there is intrinsic variability between individuals, analysis of pre-surgery gene expression would give a clear base line and a point of reference for the follow-up of each patient. The initial idea of this study was to include gene expression analysis of archived whole blood samples, which would have given several time points for each individual allowing us to establish direct comparisons within the same patient. However, it was demonstrated in Chapter 6 that such archived blood samples are not suitable for qRT-PCR analysis due to extensive RNA degradation. Although this current study identifies changes in gene expression in MoM patients compared to controls, the lack of pre-surgery data makes it impossible to determine whether the metal-on-metal implant was the cause of such changes. Access to sufficient numbers of blood samples from MoM patients was also a limiting factor as this part of the research took place after the withdrawal of the DePuy ASR™ and fewer MoM implants had been inserted following that date.

Circulating physiological levels of cobalt and chromium are normally $<0.25\mu\text{g/l}$ (Andrews et al., 2011). However, much of the research cited in Chapter 1 evaluating metal ion measurements in patients with metal-on-metal total hip and metal-on-metal resurfacing implant systems, found Co and Cr levels in whole blood of control subjects (no implant) ranging from $0.1\text{-}1.88\mu\text{g/l}$ to $0.05\text{-}1.14\mu\text{g/l}$, respectively. In addition, current recommendations state that surgeons may be compelled to revise well-functioning MoM implants based solely on a metal ion level of greater than $7\mu\text{g/l}$ (Griffin et al., 2012). The concentration of metal ions in whole blood is regarded as the most accurate representation of systemic exposure to metal (Langton et al., 2008). In this study, whole blood ion levels from patients were analysed by ICP-MS. Although the ion levels detected for one of the patients are higher than the normal, they are only just above the $7\mu\text{g/l}$ threshold recommended for Co + Cr in the circulation (MDA/2010/069). All the other patients had ion levels within the normal ranges mentioned above. Unfortunately, there are insufficient samples to obtain a correlation between these ion levels and the changes observed in gene expression.

As mentioned above, bone remodelling is tightly controlled by OPG and RANKL. The ratio of RANKL/OPG is considered to reflect environmental signals. A low ratio of RANKL/OPG is indicative of promoting bone formation while a high ratio favours bone resorption (Kwan Tat et al., 2008). (Wang et al., 2010) showed that patients with a loosened THA MoP had higher RANKL expression on osteoblastic stromal cells in the periprosthetic bone marrow than patients with stable THA. They also reported that loosened THA patients also had higher RANKL levels and higher RANKL/OPG ratios in the synovial fluid than primary THA patients. Their study suggests that UHMWPE particles may induce the over-expression of RANKL and that periprosthetic osteolysis may be mediated by the increase in of RANKL/OPG ratios in the periprosthetic microenvironment. (Zijlstra et al., 2012) determined the effects of Co and Cr ions on the expression of bone turnover regulatory proteins RANKL and OPG on human osteoblast-like cells. They found that the RANKL/OPG ratio increased after 72h of exposure to 10µg/l Co, 1µg/l Cr and higher, and at 1µg/l Co+Cr and higher, indicating net bone loss. These findings are interesting since they seem to suggest that even in well-functioning metal-on-metal implants with systemic cobalt and chromium levels around 1µg/l, local peri-prosthetic osteolytic reactions may take place. In the current study there was no evidence of a clear correlation between RANKL/OPG ratios and whole blood metal ion levels. However, four patients (patients 2, 3, 4 and 6) had a greatly higher ratio when compared to controls. These findings suggest that metal ions released from the metal-on-metal articulation could be triggering an inflammatory response leading to the recruitment of activated osteoclasts, which may result in bone resorption in the long term. However, such imbalance has also been encountered in patients with malignant and lytic bone diseases where RANKL is up-regulated as well as in osteoblastic disorders where OPG is up-regulated (Pilichou et al., 2008). Significantly increased RANKL/OPG ratio has been reported in bone metastases and in tumour associated with severe osteolysis when compared to controls (Grimaud et al., 2003). Moreover, factors such as age, gender, body mass index, and bone mineral density may affect RANKL and OPG serum levels (Wagner and Fahrleitner-Pammer, 2010).

It has been established that osteolysis is a particle-induced biologic process at the metal–bone or cement–bone interface of prosthetic implants (Agarwal, 2004). Higher rates of wear have been linked to this mode of implant failure and have been shown to result in raised systemic levels of Cr and cobalt Co ions (Davda et al., 2011, Kwon et al., 2010). However, in this investigation it has not been possible to establish a clear correlation between whole blood ion levels and gene expression. This could be as a result of the small number of patients analysed (n=6), the fact that these patients did not have markedly elevated blood metal ion levels, or that at the levels measured, Co and Cr ions have no direct effect on the target genes. Nevertheless, abnormalities of the RANKL/OPG system have been detected in various metabolic bone diseases that are characterized by both locally or systemically enhanced osteoclast activity and bone resorption (Hofbauer et al., 2001). In conclusion, in the current study significant increases of RANKL and significant decreases of OPG expression have been shown. These findings suggest an enhanced ability of preosteoblastic cells to support osteoclast development, which would lead to an imbalance between bone formation and resorption and rapid bone loss. All these together, suggest that bone metabolism in these patients is unbalanced and tilted towards osteoclastogenesis. The question of whether such unbalance is due to a pre-existing health condition or the presence of wear metal debris and metal ions derived from the implant remains.

This study has, however, provided proof-of-concept for the analysis of gene expression in such samples. During the experimental approach the following parameters and protocols were set up, and these will greatly facilitate further studies on the expression of pro-inflammatory/osteolytic genes in MoM patient blood and tissues in the future:

- Establishment of stabilisation and storage procedures of clinical whole blood samples for molecular applications
- Identification of stable candidate reference genes for gene expression analysis in whole blood samples from patients with MoM replacements
- Identification of TaqMan® gene expression assays for reference and target genes suitable for clinical whole blood samples
- Refinement of ICP-MS protocol for processing and analysing whole blood

7. SUMMARY AND FUTURE WORK

7.1 Summary of thesis results

The total number of joint replacement procedures recorded by the National Joint Registry of England, Wales and Northern Ireland (NJR) exceeded 1.2 million records between 1 April 2003 and 31 March 2012. The total number of hip procedures entered into the NJR during 2011 was 80311, an increase of 5% compared with 2010 as reported in the NJR 8th Annual Report. Of these, 71675 were primary and 8639 were revision procedures. There was an increase of 787 revision surgeries compared with 2010 and the main indications for the procedure are summarised in Table 7.1 (National Joint Registry, 2012).

Indications for surgery	Number	Percentage (%)
Aseptic loosening	3627	42%
Pain	2091	24%
Osteolysis	1116	13%
Dislocation/subluxation	1156	13%
Infection	1076	12%
Wear of acetabular component	1033	12%
Adverse soft tissue reaction	947	11%
Peri-prosthetic fracture	727	8%

Table 7.1. Indications for hip revision procedures in 2011 (National Joint Registry, 2012).

In addition to the above, revision rates were considerably higher for metal-on-metal bearings compared to metal-on-polyethylene and ceramic-on-ceramic (National Joint Registry, 2012).

Bearing	Revision rates after primary hip replacement (%)						
	Year 1	Year 2	Year 3	Year 4	Year 5	Year 6	Year 7
THA							
MoM	1.61	3.45	6.14	9.20	12.92	18.24	23.80
MoP	2.99	4.41	5.64	6.62	8.11	9.69	10.72
CoC	1.53	2.38	2.92	3.55	4.20	4.86	5.51
Resurfacing (MoM)	1.26	2.20	3.16	3.73	4.56	5.33	6.35

Table 7.2. Revision rates after primary hip replacement (%) for up to 7 years. Data collected by the NJR from 1 April 2003 to 31 December 2011 (National Joint Registry, 2012).

The current investigation has been focused on the toxicity, immunological, and gene expression effects of cobalt ions and wear debris produced by a metal-on-metal hip resurfacing device. A vast literature on the effects of different kinds of debris as well as ions exists with many groups engaged in discussion of mechanisms involved. However, to the author's knowledge, there has not been an extensive study where effects of combined debris and ions have been assessed nor the effects of debris on cells pre-treated with metal ions. The intention behind the cobalt pre-treatment was to explore the scenario of patients subject to revision surgery. What impact does this pre-exposure to circulating metal ions have on the patients and their responses to the new implant? In this context we examined only the effect of pre-exposure to cobalt ions on U937 cells and human primary lymphocytes due to their increased mobility compared to Cr ions (Afolaranmi et al., 2012) and therefore their potential to reach remote organs in greater concentrations. Results from this study showed that metal debris tends to be more toxic and has a greater influence on gene expression in the presence of Co ion pre-treatment. This could potentially mean that patients that receive a second implant may be at higher risk of an adverse tissue response.

In the following sections of this chapter the main findings of this work and their implications for patients exposed to metallic wear debris from Co-Cr alloy and Co/Cr metal ions are summarised.

7.1.1 Effects of cobalt ions and wear metal debris derived from a hip resurfacing on U937 cells *in vitro*

U937 cells were exposed to metal wear debris and Co ions, individually and in combination, for 24, 48 and 120h. Cells were treated with the Co ion concentration that has been advised as the recommended maximum circulating blood level for patients with MoM implants. If either cobalt or chromium ion levels in whole blood are elevated above 0.1µM, the guidance states that then a second blood sample should be analysed for metal ions three months after the first in order to establish whether the elevation is still observed, and to identify patients who require closer surveillance and possible revision of their implant. The metal debris concentrations

to be used in the experiments were calculated taking into account the volume of debris generated by an active person during 25 years. These were extrapolated to the *in vitro* situation and an exposure of 0.05, 0.1 and 0.2mg/1x10⁶cells carried out. Higher concentrations (5mg/1x10⁶cells) were also implemented to simulate the scenario of metallosis in the patient.

Low concentrations of debris (0.05, 0.1, and 0.2mg/1x10⁶cells) did not seem to have an effect on the viability of U937 cells. However, a significant increase in cellular MTT reduction was observed mainly in the presence of Co pre-treatment and Co ion exposure. The higher metal particle concentration (5mg/1x10⁶cells) caused significant decrease in cell viability. As with the lower concentrations, effects were observed mostly in the presence of Co pre-treatment. Morphology changes were not evident under any of the treatments. Nevertheless, when treated with 5mg wear debris/1x10⁶cells for 120h, a significant decrease in cell number was observed as expected from the NR viability results. No significant difference was observed in cell proliferation.

Levels of IL-6, TNF- α , and IFN- γ were determined for all treatments at each cell culture end point. Cytokine production by resting U937 cells did not seem to be affected by the treatments. On the other hand, activated cells showed significant decrease in IL-6 and TNF- α production in the presence of metal debris. Overall, this study showed that high concentrations of metal debris were more toxic for resting cells in the presence of Co pre-treatment.

7.1.2 Correlation between gene expression, apoptosis, and metal ion levels on U937 cells *in vitro*

This study demonstrated that Co and Cr ions are released from metal debris into culture medium, which illustrates the corrosion process that a metal device and metal particles undergo in biological environments. It also showed the ability of the cells to take up such ions, suggesting that the released metal ions play an important part in adverse tissue responses *in vivo*.

The ability of metal debris (2.5mg wear debris/1x10⁶cells) and Co ions to induce apoptosis was detected by flow cytometry and western blot analysis. Results obtained from both techniques showed that the presence of metal particles induced apoptosis by 48h of exposure. The expression of five genes of major toxicological relevance involved in key cellular and immunological processes was measured in the cells post exposure to the metal ions and debris. The effects on gene expression of NOS2, LTA, BAG1, GADD45A, and FOS were studied. After incorporating primer efficiency into the calculations, up-regulation of LTA and FOS was significant in the presence of the metal debris alone. NOS2 and BAG1 were up-regulated in the presence of Co ions and the combination of Co ions and debris. Interestingly, there was up-regulation of all five genes in cells pre-treated with Co and then exposed to the combinations of Co ions and debris.

In line with results from the previous chapter, this study showed that Co-Cr wear debris was more effective as an inducer of changes in gene expression when cells were pre-treated with Co ions. Moreover, it suggested that the toxicity of Co ions could be related to both nitric oxide metabolic processes and apoptosis.

7.1.3 Effects of cobalt ions and wear metal debris derived from a hip resurfacing on freshly isolated human lymphocytes *in vitro*

Primary human lymphocytes were isolated from buffy coats of healthy donors. Cells were treated with wear debris and Co ions, individually and in combination, for 24, 48 and 120h. Resting lymphocytes were exposed to 5mg wear debris/1x10⁶cells for viability, proliferation and cytokine production analysis, and to 2.5mg wear debris/1x10⁶cells for apoptosis analysis.

There was a significant increase in cell number where metal particles were present even though no significant change was found in reduction of MTT. Additionally, an initial decrease followed by an increase in cell proliferation was observed. IL-2, IL-6, IFN γ , and TNF α production levels were measured by ELISA, and IL-6, IFN γ , and TNF α levels significantly decreased in the presence of metal particles. Of particular

interest is the finding that IL-2 production levels were significantly decreased by both debris and Co ions. Flow cytometry analysis showed that the cells initially protected themselves against the apoptotic response to the metal challenge, but by 48h the presence of wear debris seems to have exhausted the protective systems, and this was reflected in the significant increase of apoptosis.

Metal debris and ions affect different cell types in diverse ways at the cellular and molecular level. It has been shown in this investigation that the same concentration of metal particles found to be cytotoxic for U937 cells were not toxic to primary human lymphocytes. Nevertheless, this investigation showed that chronic exposure to metal debris induces lymphocyte proliferation, which could indicate that activation of resting lymphocytes occurs in patients with CoCr MoM hip implants in response to the metal wear debris. Although cytokine production by lymphocytes was affected mainly by metal debris, this investigation revealed that cobalt toxicity could be related to IL-2 production modulation.

7.1.4 Correlation between gene expression and metal ions levels in clinical blood samples

When this project was initiated it was thought that archived whole blood samples from patients with MoM implants would have been a valuable resource for molecular studies and correlating metal ion levels to gene expression changes. To determine whether this was the case, experiments were conducted to establish whether or not RNA, in sufficient quantities and of a quality suitable for molecular analysis, could be isolated from such archived samples. For this purpose, RNA from samples that had been stored at -80°C, for 3, 6, and 12 months, was isolated and yield, quality and purity measured. These values were compared to values obtained from fresh whole blood. Poor RNA yield and quality were obtained from the archived frozen blood, which demonstrated that they may not be suitable for gene expression analysis.

In order to establish a storage protocol that would allow the isolation of RNA suitable for molecular applications, a trial was performed in which fresh whole blood

samples were stored in the presence and absence of an RNA stabiliser reagent (RNA_{later}, Ambion). Samples were subjected to freeze and thaw cycles to simulate the situation where samples are stored at -80°C and allowed to thaw at room temperature. RNA was isolated after a number of freeze/thaw cycles and yield, quality and purity analysed. This limited trial suggested that RNA_{later} provides some protection to RNA even after several freeze/thaw cycles before RNA extraction. In addition, this process yielded RNA in quantities and qualities required for molecular studies. As a result, a protocol for storing fresh whole blood samples upon arrival at the laboratory was established for use in future experiments. Disappointingly, these findings showed that the plethora of stored samples could not be used to examine gene expression in patient blood in response to insertion of a MoM implant.

Co and Cr ion concentrations were measured in whole blood samples from patients with MOM hip replacements in order to correlate metal ion levels with changes in gene expression.. Most patients studied had circulating Co and Cr levels which were below the established guideline limit of 7µg/l (7ppb) (MDA/2010/033).

There is substantial literature to show that the RANK/RANKL/OPG system plays a major role in regulating bone turnover (Haynes, 2004, Khosla, 2001, Perez-Sayans et al., 2010, Crotti et al., 2002). It is reasonable to think that osteolysis happening at the implant site could be due to the misbalance of this system. For this reason, these three genes were chosen for this trial. All 6 patients showed altered gene expression when compared to controls, which could indicate a response to the presence of the MOM implant. It was interesting to see that patients with hip resurfacing implants had the same trend in the levels of gene expression. However, due to the small number of patients analysed, it is difficult to establish a correlation between metal ion levels and gene expression changes. Despite the limitations, this study has provided proof of concept for the molecular analysis of these samples. If a correlation between metal ion levels and gene expression could be established, it would enhance the understanding of the processes involved in loosening of MOM

hip replacements. This sort of approach is unlikely to yield a system to monitor such loosening, however, as it is, at present, too expensive for routine use.

7.2 Main findings

The main findings of this thesis are:

- High concentrations of wear debris were more toxic in resting U937, in terms of cell number, than in activated cells.
- Cytokine production by U937 cells is affected by both metal debris and metal ions
- Metal debris induces apoptosis in both U937 cells and primary human lymphocytes
- Co-Cr wear debris was more toxic as well as more effective as an inducer of changes in gene expression when cells were pre-treated with Co ions
- Ions released from wear metal debris play an important role in the cellular response at the peri-implant tissues
- The toxicity of Co ions in macrophages could be related to nitric oxide metabolic processes and apoptosis and to IL-2 production modulation in lymphocytes.
- Chronic exposure to metal debris induces primary human lymphocyte cell proliferation
- Cytokine production by primary human lymphocytes is affected mainly by metal debris
- RNA is not stable in human blood stored frozen using routine anticoagulation protocols
- Expression of genes related to key cellular and immunological processes may be altered in response to both particulate and soluble metal wear debris

7.3 Limitations of these studies

Although the current thesis has shown that metal ions and debris released from MoM hip implants can elicit an adverse response, there are a number of limitations within each of the individual studies. To start with, the *in vitro* data from Chapters 3, 4, and

5 may not be reflective of the *in vivo* situation where the adverse tissue response is the result of the concerted action of different cell types. Additionally, the isolated *in vitro* environment of the immune response, as in chapters 3, 4, and 5, is not reflective of the immune response *in vivo*. Buffy coat donors for primary lymphocytes isolation were anonymous, which means that it was not possible to determine whether there was any pre-existing condition, such as smoking, previous exposure to metal or indeed whether they had a metal orthopaedic implant, that could potentially influence cell responsiveness to metal.

Furthermore, the concentrations at which metal debris had a toxic effect on U937 cells were quite high. The data showed that high concentrations induce toxic effects *in vitro*, whereas there was little effect observed following exposure to the lower concentrations. As described in chapter 3, amounts of wear debris ranging from 67mg (Matziolis et al., 2003) to 48.1g (Kempf and Semlitsch, 1990) have been reported in peri-implant tissues with metallosis recovered during revision surgery. However, the exact amount of debris to which cells would be exposed to *in vivo* is not known and it could vary substantially from patient to patient. On the other hand, the approximate wear debris amount produced by a very active person was calculated to be to $\sim 0.2\text{mg}/1 \times 10^6$ cells, assuming that the prosthesis is *in situ* for 25 years. Such a length of time represents a chronic exposure to debris and ions. Cells were exposed to the treatments for up to 5 days in the experiments reported here and, this may not be reflective of the *in vivo* situation.

Unlike U937 cells, primary lymphocytes are not an immortalised cell line; they have a limited life-span making the time frame available to experiment on them a lot shorter. For this reason, Co pre-treatment could not be performed on these cells and it remains unclear what effects prolonged exposure to metal ions would cause on primary lymphocytes. Activated U937 cells presented a challenge for the apoptosis and gene expression analysis. Since they have a lower proliferation rate, by the end of the 5 days of exposure to the treatments, it was difficult to isolate sufficient amounts of RNA to carry out RT-qPCR analysis. This was particularly the case where the metal particles were present. As a result, the effects of metal debris on

gene expression in activated U937 cells could not be performed. Additionally, after 24 and 48h of culture insufficient amounts of protein could be obtained for the western blot analysis with either activated U937 cells or primary lymphocytes. At this point, increasing the initial cell densities for both activated U937 cells and primary lymphocytes was considered. However, the quantity of CoCr wear debris that we had available would have not been enough to cover the high concentration treatments (5mg debris/ 1×10^6 cells). Moreover, work carried out with fresh lymphocytes was limited by the cost of the buffy coat. An alternative for future work could be to assess apoptosis with other methods such as the comet assay, which gives information about the extent of damage and heterogeneity of DNA, or caspase activity assays (Martinez et al., 2010).

There were also some limitations regarding the experiments with whole blood samples. Samples were taken from patients in the morning at the hospital with EDTA collection tubes. These tubes would then be stored at 4°C until sent to the laboratory in the afternoon. However, there was no consistency in terms of either collection or delivery times. Relying on the delivery of the samples meant having no control over the initial handling and the stabilisation would have to take place upon arrival to the laboratory. It is uncertain to what extent these variables could compromise the results on gene expression analysis. Since the archived samples were not suitable for molecular studies, the number of patients included in Chapter 6 was very small. Additionally, the cost of the reagents needed for this study did not allow analysis of a greater number of samples. As a result, a clear correlation between ion levels and changes in gene expression could not be established. Furthermore, this part of the study was being carried out after withdrawal of the DePuy ASR™ MoM device, and corresponded with a decline in the implantation of MoM devices in general (Figure 7.1) (National Joint Registry, 2012). Consequently, it was not feasible to obtain more whole blood samples from patients at that time. It has been reported that genomic DNA is more stable than RNA in whole blood samples and can be used for molecular applications without the need of sample stabilisation (Peakman and Elliott, 2008, Chaisomchit et al., 2005, Halsall et al., 2008, Vaught, 2006, Lahiri and Schnabel, 1993, Freeman et al., 2003). Retrospectively and in light of these

challenges and results, the author would have probably focused on studying the potential epigenetic effects of long term exposure to metal debris and ions and if there is a correlation between such effects and whole blood metal ion levels.

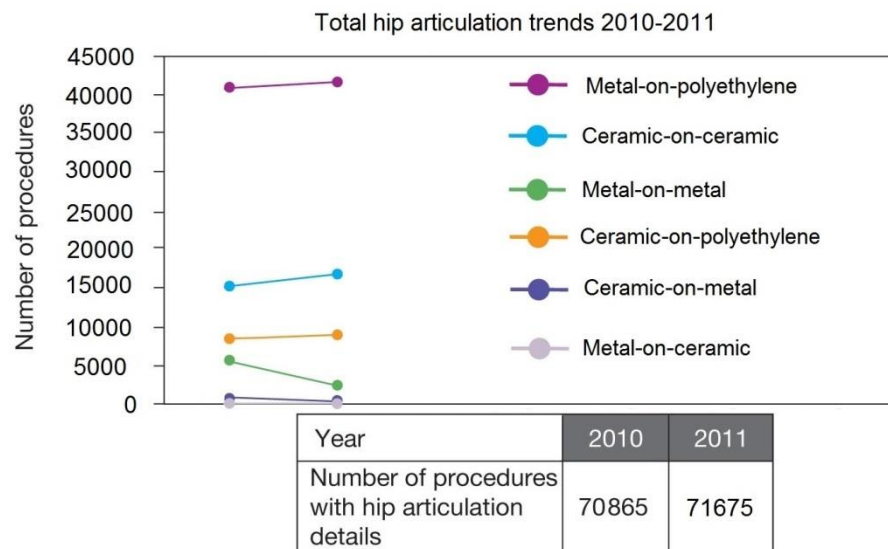


Figure 7.1. Total hip articulation trends 2010/2011. Metal-on-metal hip bearings implantation decreased compared to other bearings (National Joint Registry, 2012).

7.4 Future work

7.4.1 Inflammatory response triggering mechanisms

Although there has been widespread research on the various functions of different cytokines, questions concerning how inflammatory responses are triggered by wear particles remain largely unanswered. In the current investigation, it has been demonstrated that CoCr particles and ions can affect cells from the immune system such as macrophages and lymphocytes. However, the mechanisms by which their response is triggered remain to be elucidated. Specific organelles could play an important role in the cellular response triggered by wear particles. A growing body of evidence has suggested a role for endoplasmic reticulum (ER) stress in initiating inflammation, which is now thought to be fundamental to the pathogenesis of inflammatory diseases (Zhang and Kaufman, 2008, Hansson and Libby, 2006). There is evidence suggesting that metal particles can cause increasing ER stress in various types of cells (Tsai et al., 2011, Zhang et al., 2012a). This brings up the possibility

that wear particles, produced around the prosthesis, have the potential to stimulate ER stress and thus may play a role in particle-induced osteolysis.

ER stress is characterised by the activation of a set of signalling pathways termed the Unfolded Protein Response (UPR) (Ron and Walter, 2007). Determination of increased expression levels of the proteins C/EBP homologous protein (CHOP), glucose-regulated-protein-78 (GRP78), and X-box binding protein 1 (XBP1) has been used as ER stress detection method (Matsuo et al., 2013, Marhfour et al., 2012, Samali et al., 2010). Moreover, 4-phenylbutyric acid (4-PBA) has been used in several studies as an ER stress blocker (Zhang et al., 2012a, Zheng et al., 2012, Hosoi et al., 2008, Rahman et al., 2009, Malo et al., 2013). It would be beneficial to determine whether the effects caused by CoCr wear particles and ions are mediated by ER stress. This scenario could be explored by examining the expression of ER stress markers in macrophages treated with CoCr particles and ions as well as testing the effect of an ER stress blocker on the expression of inflammatory cytokines in such macrophages. This would bring new insights in the mechanisms of particle induced osteolysis, which could potentially lead to therapeutic approaches.

7.4.2 Revision surgery patients

Willert et al., (2005) studied a group of patients who had a total hip replacement with a second-generation metal-on-metal articulation and had persistent or early recurrence of preoperative symptoms. After revision surgery, hip and thigh pain persisted in the patients who had received a second metal-on-metal articulation. In twelve patients, an alumina ceramic-on-polyethylene bearing was used to replace the metal-on-metal articulation. In two patients, a metal-on-cross-linked polyethylene combination was inserted. At the time of follow-up, one to seven years after revision, patients without an all-metal articulation reported total relief of pain. This finding suggests that an immunological response persisted after the first revision and that the patients had been sensitized to the components of the all-metal articulation. The current study has found that CoCr wear metal debris was more toxic in the presence of Co ion pre-treatment. It would be of interest to investigate the biological responses

to metal wear debris of primary cells isolated from revision surgery patients at different follow-ups. For this purpose, at least three donors would be needed and 60ml buffy coat samples from each donor at each follow up would be ideal. This volume would allow the isolation of enough primary lymphocytes to carry out exposure experiments (including replicates) to particulate and soluble metal debris. At the beginning of the current chapter, the rates of revision surgery up to 2011 were summarised in Table 7.2. It is the author's opinion that based on these rates, it could be feasible to generate a research proposal. As a result, a new prospective on cellular and immune response to metal particles as well as a better understanding of the consequences to the patient of receiving a second metal-on-metal articulation would be achieved.

7.4.3 Metal-on-Metal Implants: Epigenetic effects

Chronic environmental exposure to some metal compounds, including arsenic, nickel, chromium and cadmium, has been known to induce cancers and other diseases in exposed individuals (Martinez-Zamudio and Ha, 2011). While it has been shown that these metals disturb a vast array of cellular processes, such as redox state and various intracellular stress-signalling pathways, their ability to induce acute and/or chronic pathologies remains poorly understood. Sources of potential environmental exposure to these metals include occupational exposure and environmental contamination from industrial production (Martinez-Zamudio and Ha, 2011). Additionally, with all the evidence on particles and ions derived from metal orthopaedic implants, such replacements should be considered as an additional source of exposure.

Emerging epidemiological studies show that the carcinogenic potential of some toxic metals may involve epigenetic changes, including silencing of DNA repair and tumor-suppressor genes (Martinez-Zamudio and Ha, 2011). The combinations of mechanisms, which confer long-term programming to genes and could bring about a change in gene function without changing gene sequence are termed epigenetic (Szyf, 2007). The three principal molecular mechanisms mediating epigenetic

regulation of gene expression are: (1) DNA methylation; (2) histone modifications; and (3) expression of noncoding RNAs. These processes can be influenced by a variety of environmental factors, and their deregulations are implicated in many disease states (Baccarelli and Bollati, 2009, Hou et al., 2012).

Oxidative stress may lead to an increased level of unrepaired cellular DNA damage, which is considered a risk for tumour initiation (Waris and Ahsan, 2006, Hegde et al., 2008). Mismatch repair (MMR) enzymes act as proofreading complexes that maintain genomic integrity and MMR-deficient cells show an increased mutation rate (Boiteux et al., 2002). One important gene in the MMR complex is the MutL homolog 1 (MLH1) gene. MLH1 is inactivated by hypermethylation, and a promoter methylation-dependent downregulation of the corresponding gene expression in some cancer tissues has been found (Esteller, 2002). Barreto et al. (2007) demonstrated that GADD45A has a key role in active DNA demethylation by showing that GADD45A overexpression activates methylation-silenced reporter plasmids and promotes global DNA demethylation. In the current investigation expression of GADD45A was up-regulated in Co pre-treated cells exposed to both particles and ions. The author suggests studying hMLH1 expression levels in ion and particle treated cells as well as assessing its methylation status. As artificial articulations are being implanted in younger people epigenetic studies could help assess how long term exposure to metal debris and ions could bring about epigenetic changes altering gene expression which may have significant health-related consequences for these patients.

7.4.4 Implications of this research to the health and quality of life of patients with MOM

The current thesis has shown that CoCr wear debris was more toxic as well as a more effective inducer of changes in gene expression when cells were pre-treated with 0.1 μM Co (5.9 $\mu\text{g}/\text{l}$ or 5ppb). At present the MHRA has set a metal ion concentration safety threshold of 7 $\mu\text{g}/\text{l}$ (7ppb or 0.12 μM) within the whole blood of patients following hip arthroplasty. Therefore, the author believes that the MHRA safety level

may not be adequate for revision surgery patients or patients receiving a second MoM device. Since high metal ion levels have been related to adverse tissue responses, the circulatory metal ion concentrations should be regularly analysed following MoM hip arthroplasty as an indicator for implant performance particularly in revision surgery patients.

As mentioned in Chapter 1, CoCr alloy is not only used in hip devices but also in other joint devices such as knee and ankle. All of these represent a risk for generation of CoCr wear debris as well as the release of Co and Cr ions. Therefore the concern of medical device induced exposure to Co and Cr ions should not be limited to MoM hip replacements. Ti alloys and stainless steel alloys are also commonly used in orthopaedic devices. Ti alloys are generally used in plates, screws and non-bearing surfaces of total joint replacement components and stainless steel alloys are usually wires, pins, screws and plates (Long, 2008, Navarro et al., 2008). Ti ions have been related to hypersensitisation reactions in dental implants and it has been shown that Ti ions accumulate in tissues surrounding dental and orthopaedic implants, as well as in regional lymph nodes and pulmonary tissue (Sicilia et al., 2008, Kohilas et al., 1999). Similarly Ti wear debris has been reported to significantly increase RANK and RANKL gene expression leading to osteolysis (Geng et al., 2011, Geng et al., 2010, Mao et al., 2012). Elevated serum Cr levels and focal osteolysis were shown in a study on patients treated with a modular stainless steel femoral intramedullary nail (Jones et al., 2001). Kim et al. (2005) found high serum levels of Ni and Cr after posterior spinal arthrodesis using stainless steel implants. Moreover, Savarino et al. (2000) found increased levels of chromium and nickel, as well as a positive correlation between such levels and sister chromatid exchanges, in patients with fixation devices. All these investigations demonstrate that concerns about potential metal wear debris toxicity and ion exposure should not be restricted to CoCr alloy. The author believes that the monitoring of whole blood metal ion levels should include a broader range of metal device implants.

It has been shown at the beginning of the current Chapter that revision rates are higher for metal-on-metal bearings and resurfacings compared to other articulating

surfaces, which has led to an increase in ceramic-on-ceramic bearing surfaces being used particularly in younger patients. Ceramics are mainly used in total hip replacement in the alumina-on-alumina combination (Lusty et al., 2007). The theoretical advantages of alumina ceramic are related to the high scratch resistance and wettability of the material, both of which reduce wear production wear (Toni et al., 2006). The linear wear rate of alumina ceramic articulating against alumina ceramic has been reported to be 4000 times lower than that of metal articulating against polyethylene (Hamadouche et al., 2002). Bohler et al. (2000) showed that the concentrations of wear particles in the periprosthetic tissues around failed alumina-on-alumina bearings were lower were than those previously observed around metal-on-polyethylene articulations. Due to the low volume of wear particles produced, the subsequent biologic reaction to ceramic wear debris has been assumed to be moderate. However, long term effects of particulate and soluble debris released from these devices remain to be elucidated. Aluminium (Al) ions could potentially be released from both the ceramic surfaces and the ceramic wear debris. Once in the blood stream, Al binds to transferrin entering the cellular environment via specific transferrin receptors (Perez et al., 2005). Al has been implicated as a deleterious factor in osseous, neurological and haematological diseases (Perez et al., 2001). The author believes that since the use of CoC hip replacements in younger patients is increasing, studies on the short and long term effects of Al ion levels derived from ceramics should be performed. Additionally, measurement of circulatory Al ion levels in patients with CoC should be implemented as part of their follow ups.

The potential dangers to patient health of CoCr alloy wear debris generation and release of Co and Cr ions into the circulation have been identified and patient health has benefited. However, until the regulations for thoroughly testing the safety of medical devices such as hip replacements and other orthopaedic implants is more stringent there is a very real possibility that 20 years from now we will be reading articles on the award of compensation for the next generation of articulations.

APPENDIX

Appendix 1. Sodium Phosphate buffer (NaPi) composition

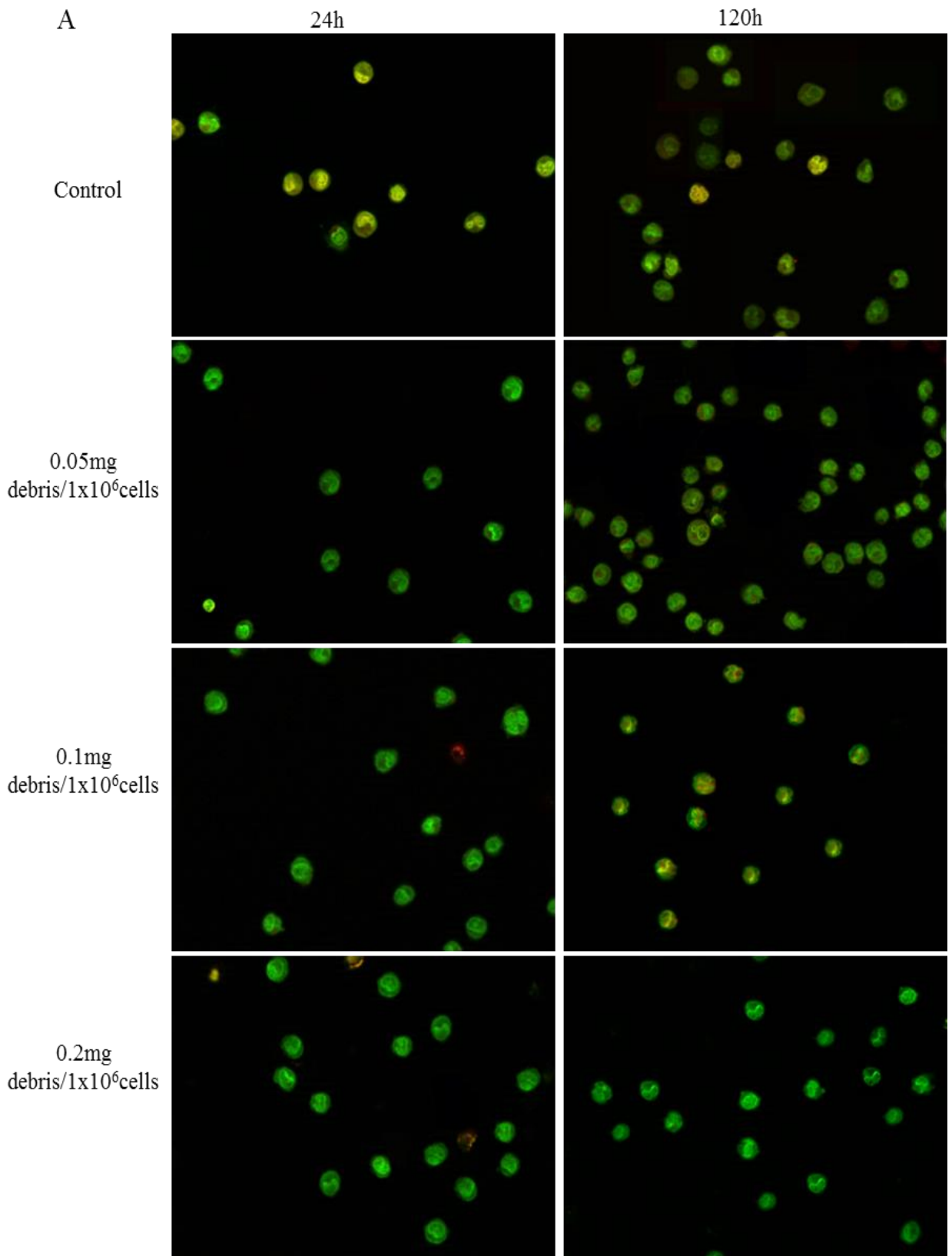
Sodium Phosphate buffer (NaPi) pH 7.6: 87ml of 0.2M Na₂HPO₄+ 13ml of 0.2M NaH₂PO₄ diluted to 200ml with dH₂O.

0.2M Na ₂ HPO ₄	14.2g Na ₂ HPO ₄ (Sigma-Aldrich; Dorset, UK) in 500ml dH ₂ O
0.2M NaH ₂ PO ₄	2.4g NaH ₂ PO ₄ (Sigma-Aldrich; Dorset, UK) in 100ml dH ₂ O

Appendix 2. Fluorescence microscopy images of resting and activated U937 cells exposed to varying concentrations of metal wear debris.

2.1. Fluorescence microscopy images (40X) following PI (Dead cells, red)/AO (Live cells, green) staining of resting U937 and Co pre-treated resting U937 cells exposed to 0.05mg/1x10⁶cells, 0.1mg/1x10⁶cells, and 0.2mg/1x10⁶cells wear debris for 24 and 120h.

A: Resting U937 cells exposed to 0.05mg/1x10⁶cells, 0.1mg/1x10⁶cells and 0.2mg/1x10⁶cells wear debris. B: Resting U937 cells exposed to 0.05mg/1x10⁶cells, 0.1mg/1x10⁶cells and 0.2mg/1x10⁶cells wear debris in combination with 0.1µM Co. C: Co pre-treated resting U937 cells exposed to 0.05mg/1x10⁶cells, 0.1mg/1x10⁶cells and 0.2mg/1x10⁶cells wear debris. D: Co pre-treated resting U937 cells exposed to 0.05mg/1x10⁶cells, 0.1mg/1x10⁶cells and 0.2mg/1x10⁶cells wear debris in combination with 0.1µM Co. Images are representative of 5 independent images from each sample at each end point.

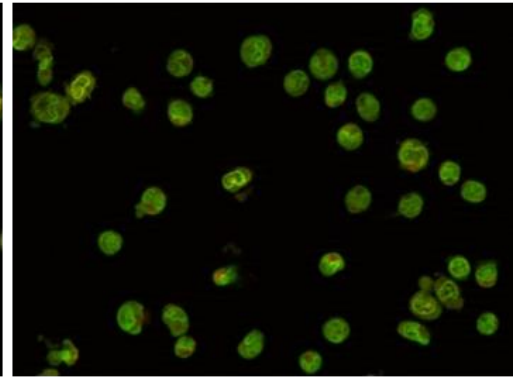
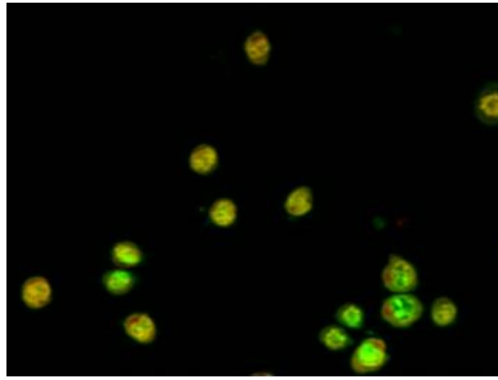


B

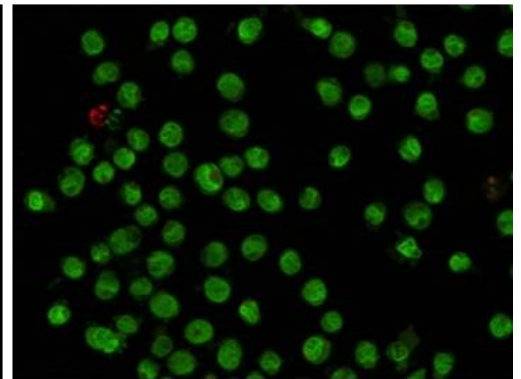
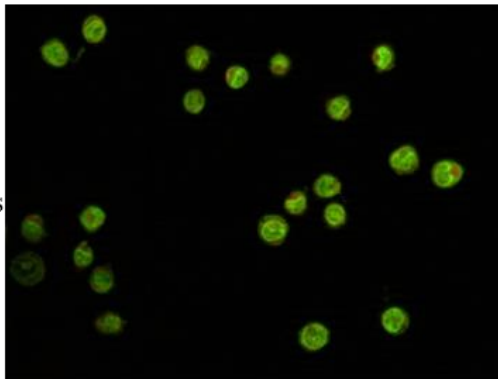
24h

120h

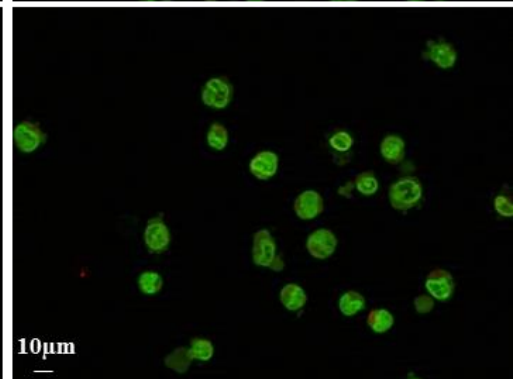
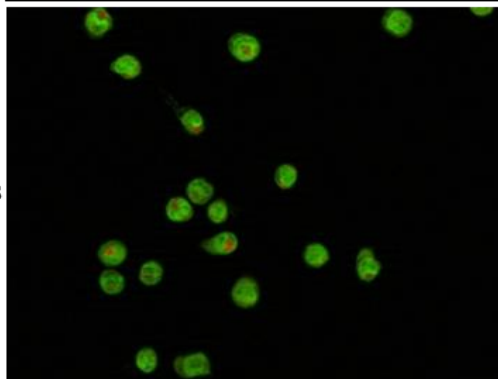
0.05mg
debris/ 1×10^6 cells
+ 0.1 μ M Co



0.1mg
debris/ 1×10^6 cells
+ 0.1 μ M Co



0.2mg
debris/ 1×10^6 cells
+ 0.1 μ M Co

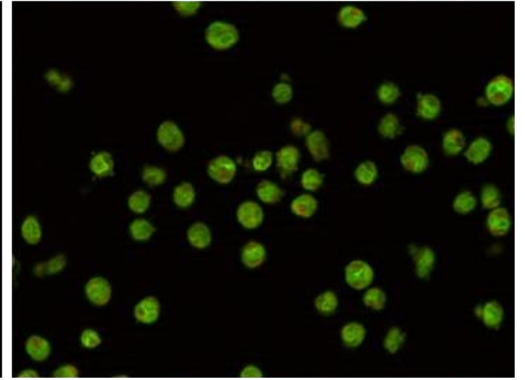
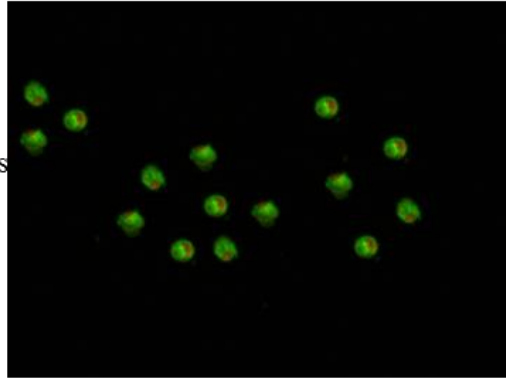


C

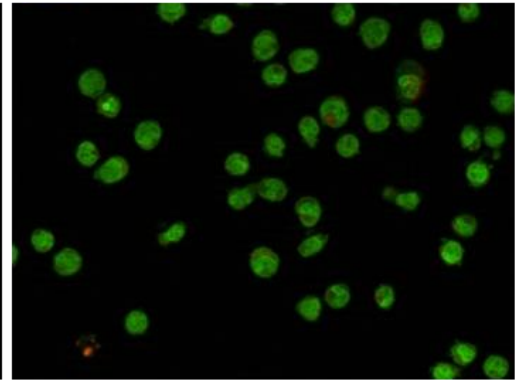
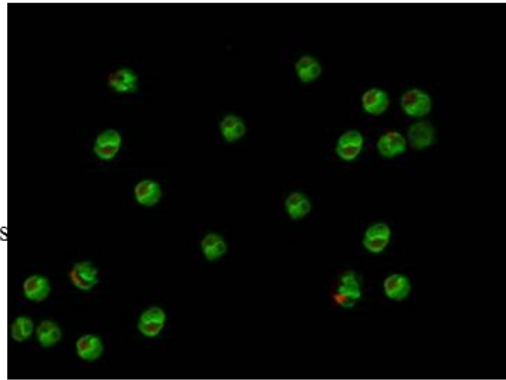
24h

120h

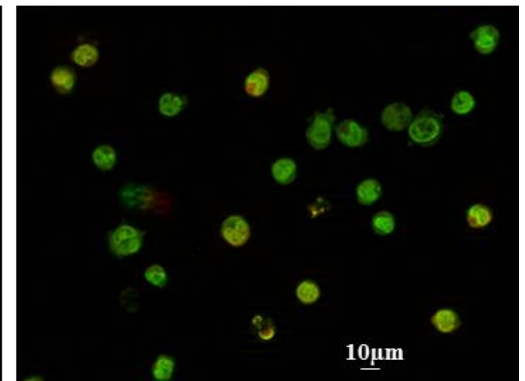
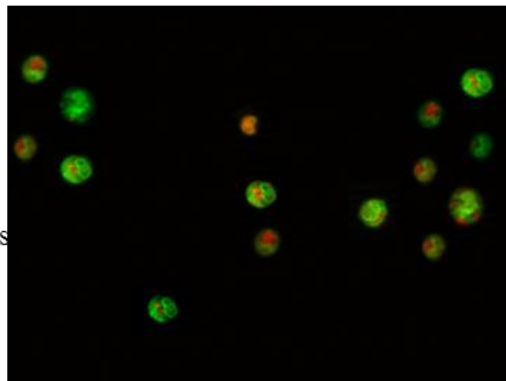
Co pre-treated
0.05mg
debris/ 1×10^6 cells

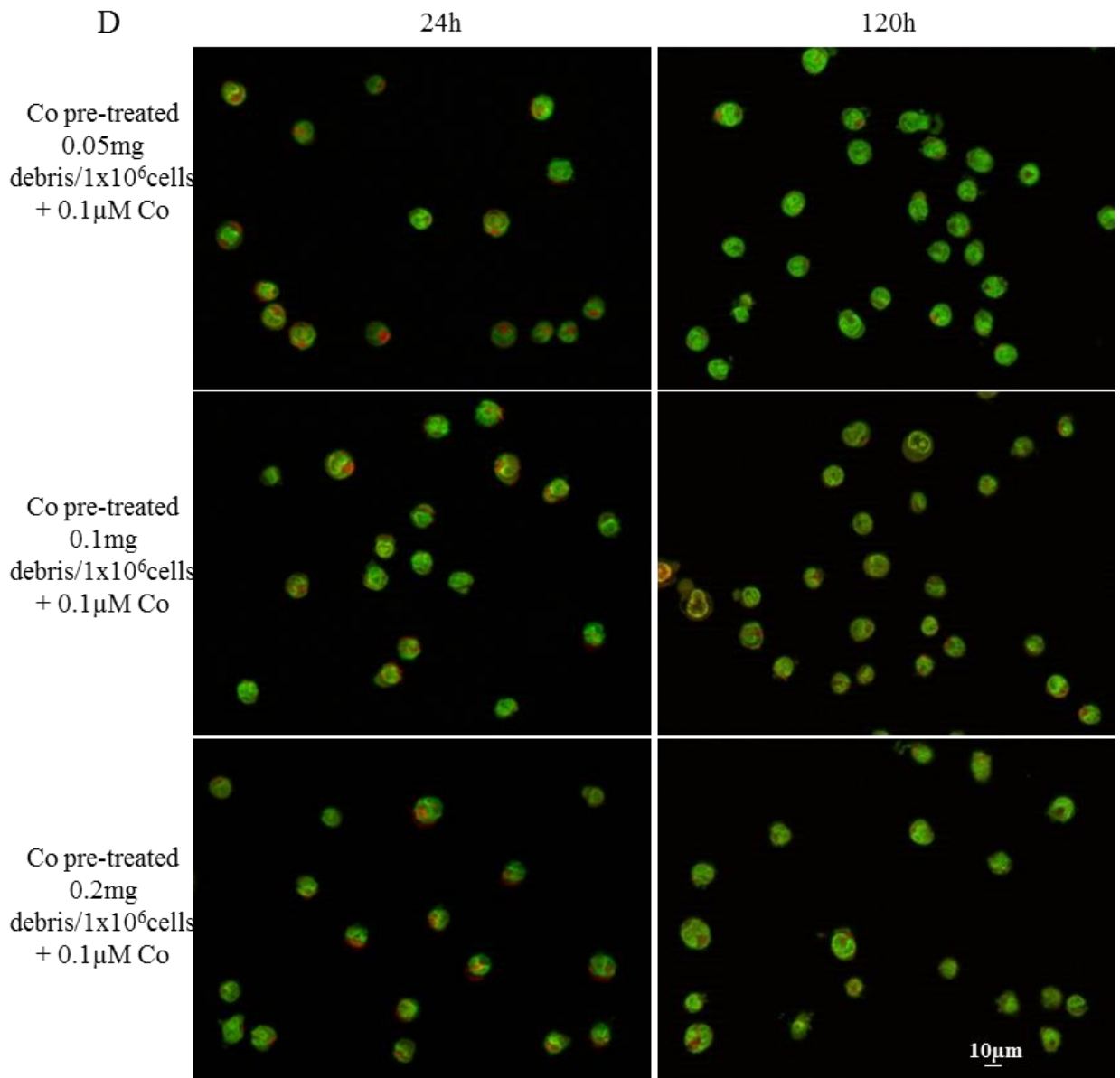


Co pre-treated
0.1mg
debris/ 1×10^6 cells



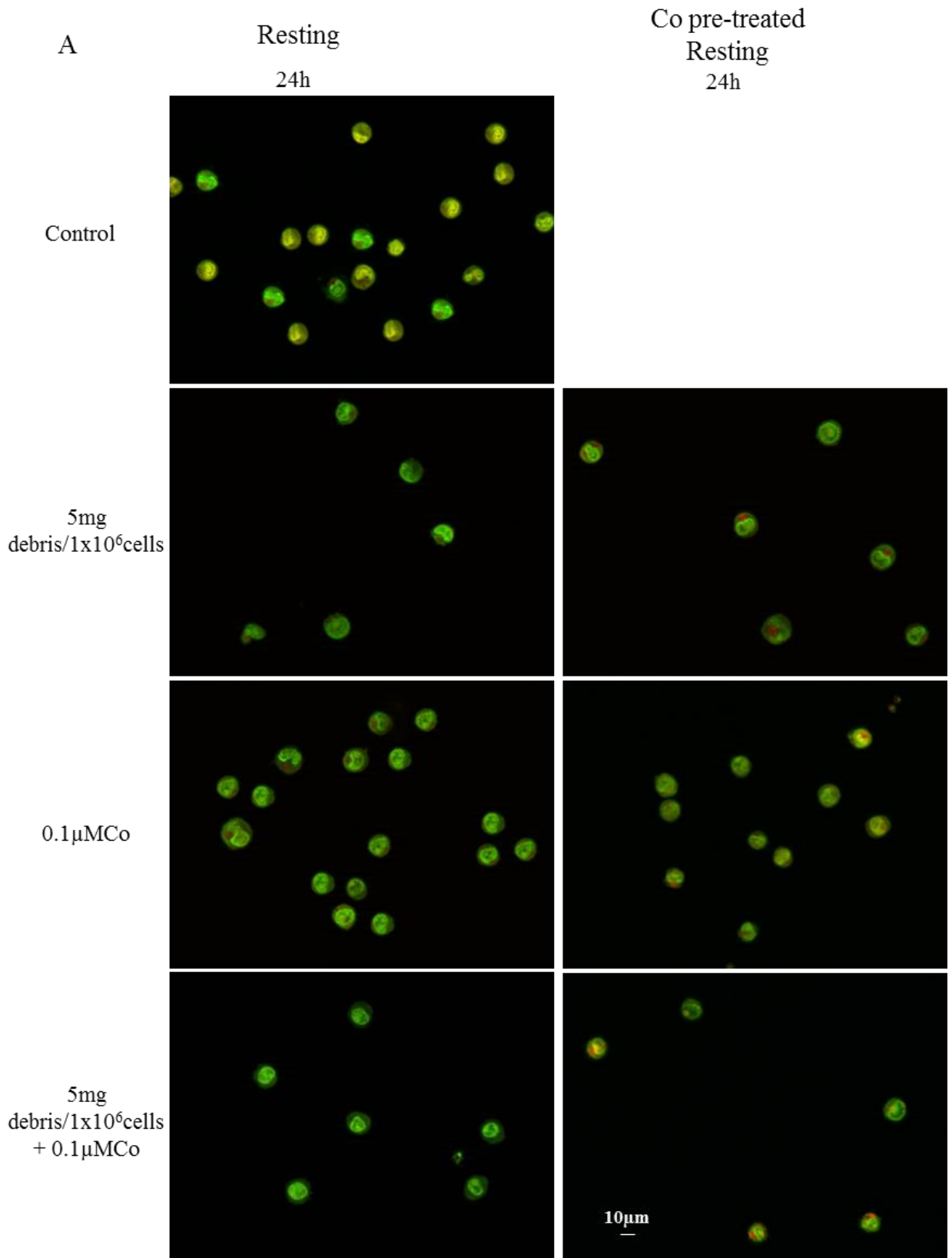
Co pre-treated
0.2mg
debris/ 1×10^6 cells

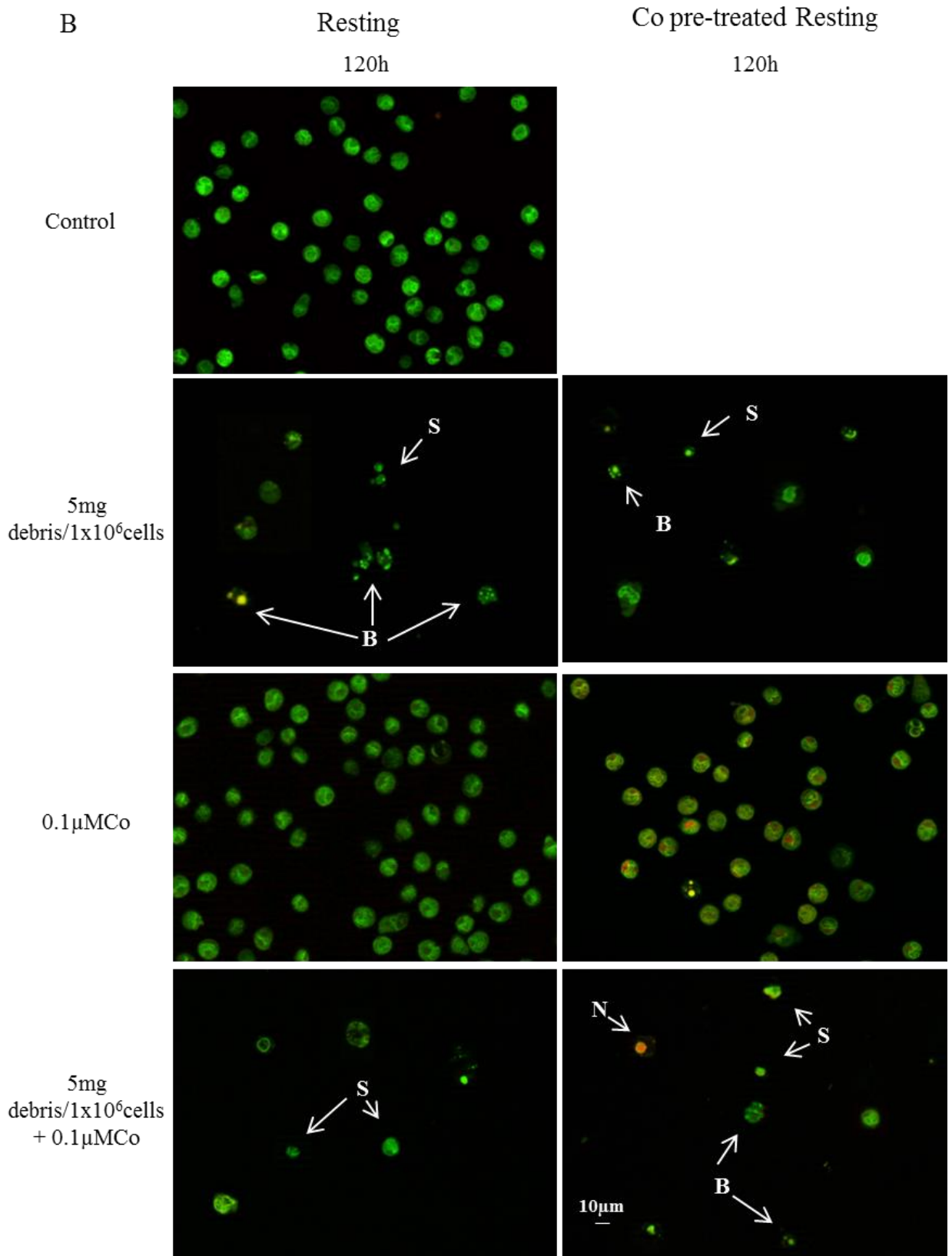




2.2 Fluorescence microscopy images (40X) following PI (Dead cells, red)/AO (Live cells, green) staining of resting U937 and Co pre-treated resting U937 cells exposed to 5mg debris/1x10⁶cells, 0.1μM Co and 5mg debris/1x10⁶cells + 0.1μM Co.

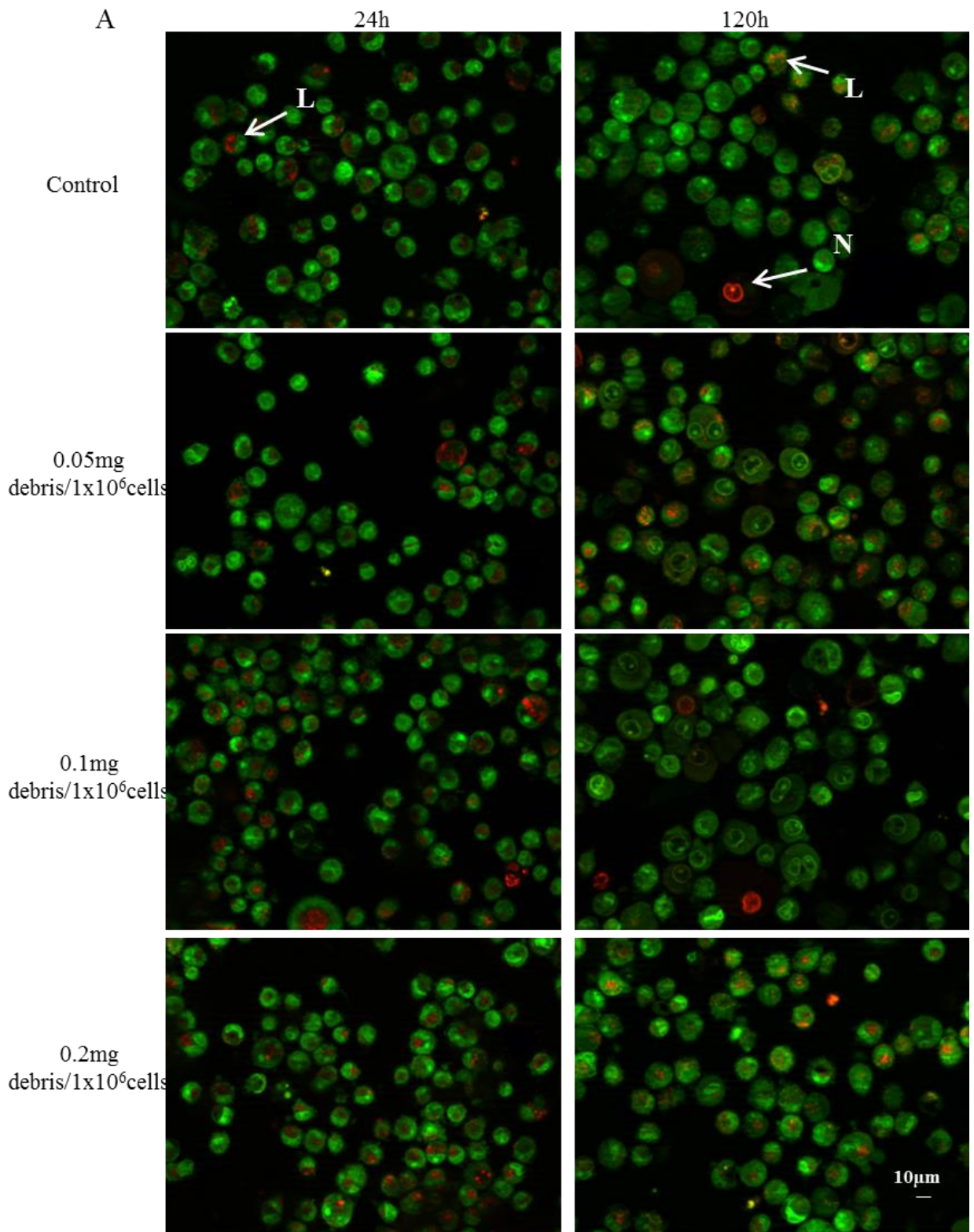
A: 24h of exposure. B: 120h of exposure. Images are representative of 5 independent images from each sample at each end point. “B” indicates cell blebbing, “S” indicates cell shrinkage and “N” indicates necrotic.

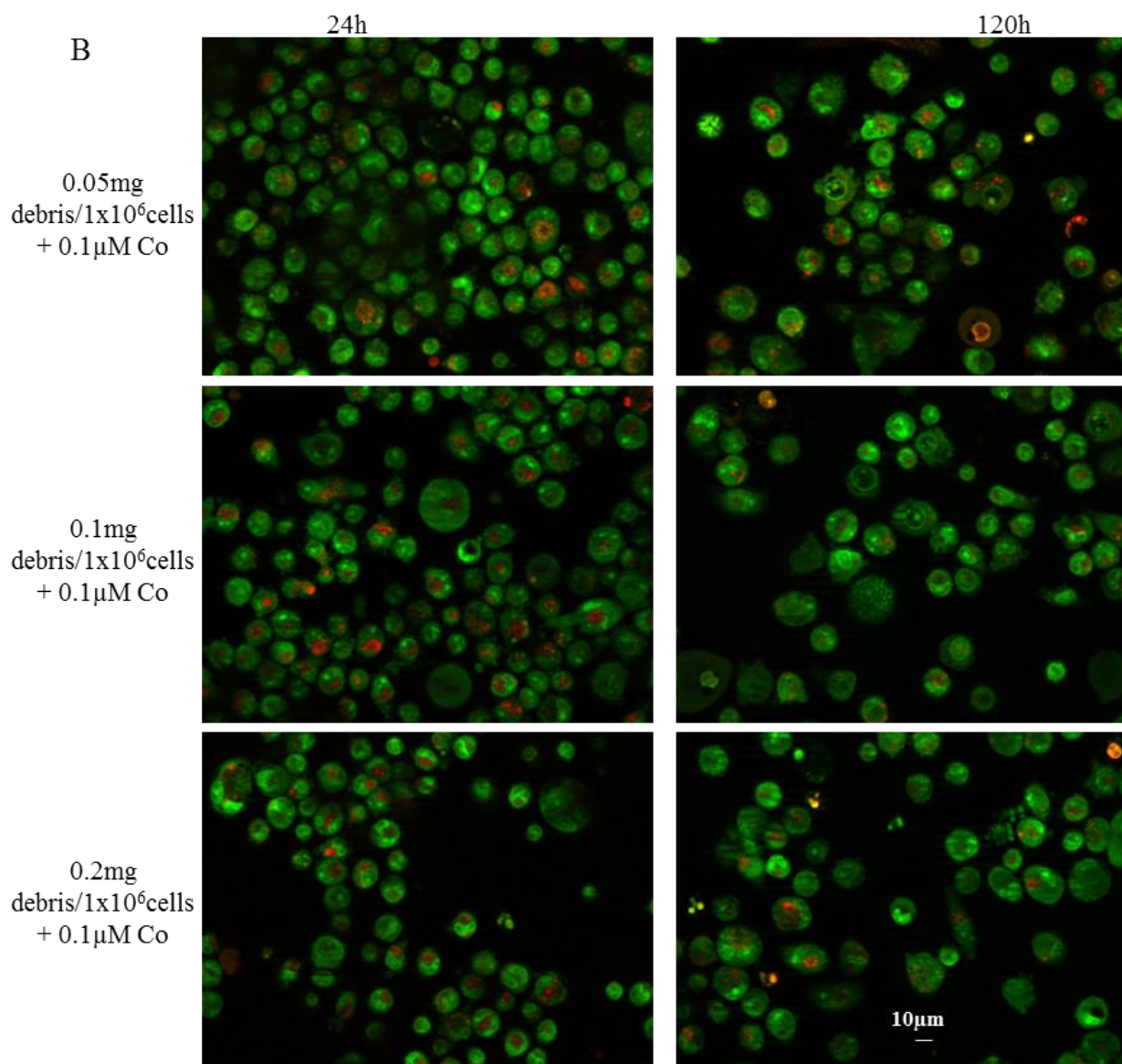


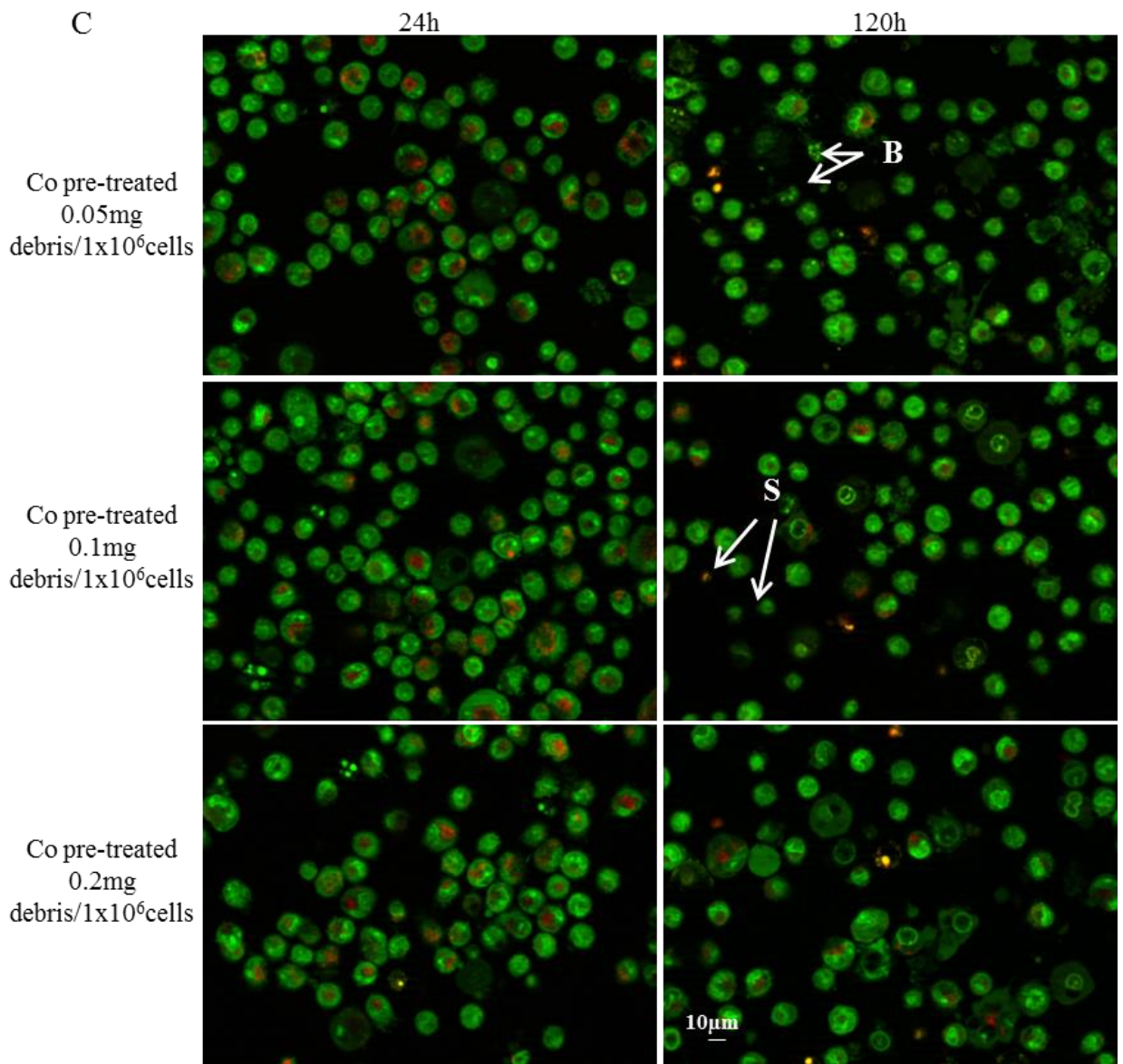


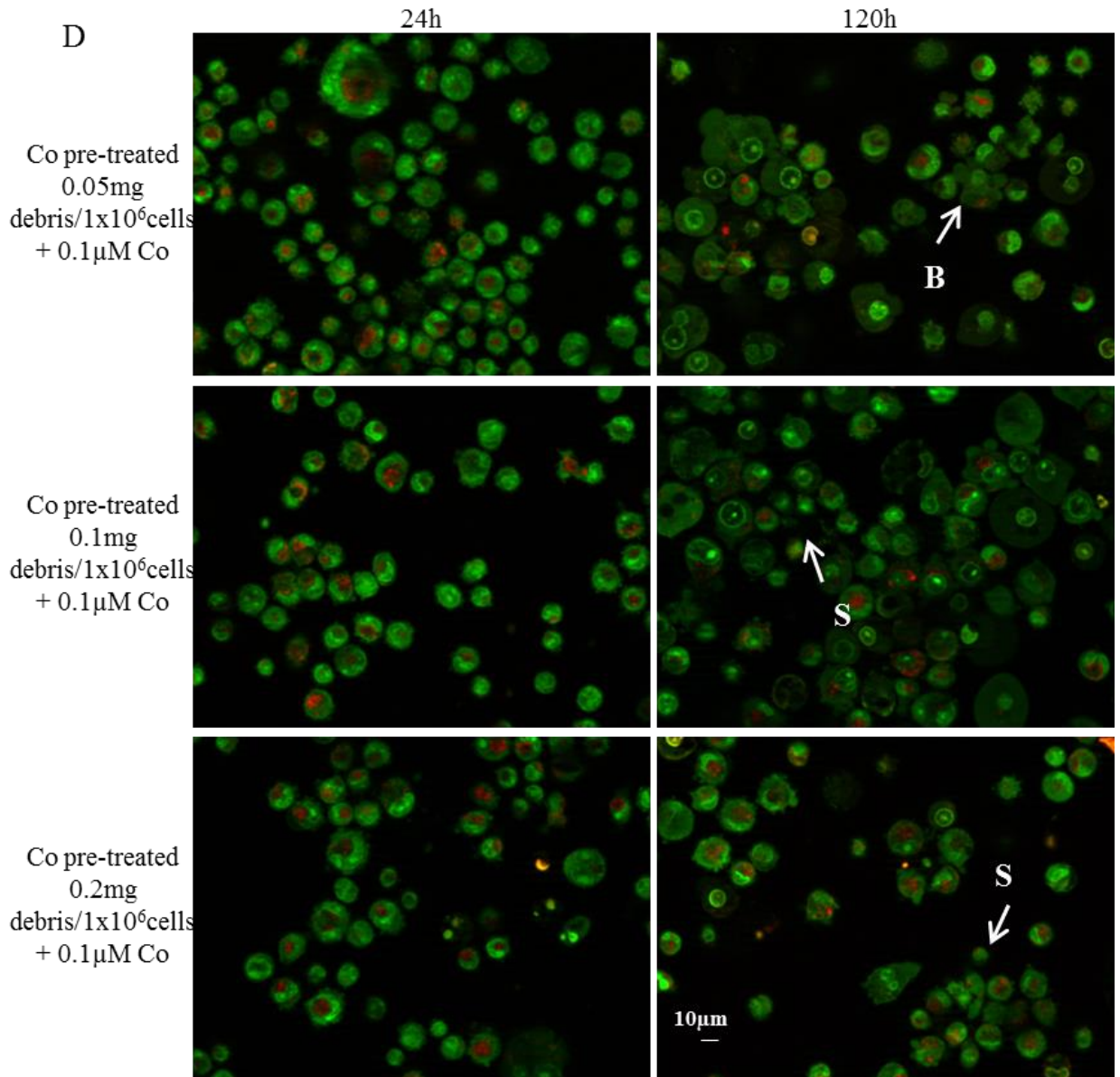
2.3 Fluorescence microscopy images (40X) following PI (Dead cells, red)/AO (Live cells, green) staining of activated U937 and Co pre-treated activated U937 cells exposed to 0.05mg/1x10⁶cells, 0.1mg/1x10⁶cells and 0.2mg/1x10⁶cells wear debris for 24, 48 and 120h.

A: Activated U937 cells exposed to 0.05mg/1x10⁶cells, 0.1mg/1x10⁶cells and 0.2mg/1x10⁶cells wear debris. B: Activated U937 cells exposed to 0.05mg/1x10⁶cells, 0.1mg/1x10⁶cells and 0.2mg/1x10⁶cells wear debris in combination with 0.1μM Co. C: Co pre-treated activated U937 cells exposed to 0.05mg/1x10⁶cells, 0.1mg/1x10⁶cells and 0.2mg/1x10⁶cells wear debris. D: Co pre-treated activated U937 cells exposed to 0.05mg/1x10⁶cells, 0.1mg/1x10⁶cells and 0.2mg/1x10⁶cells wear debris in combination with 0.1μM Co. “L” indicates lysosomes, “B” indicates cell blebbing, “S” indicates cell shrinkage and “N” indicates necrotic.



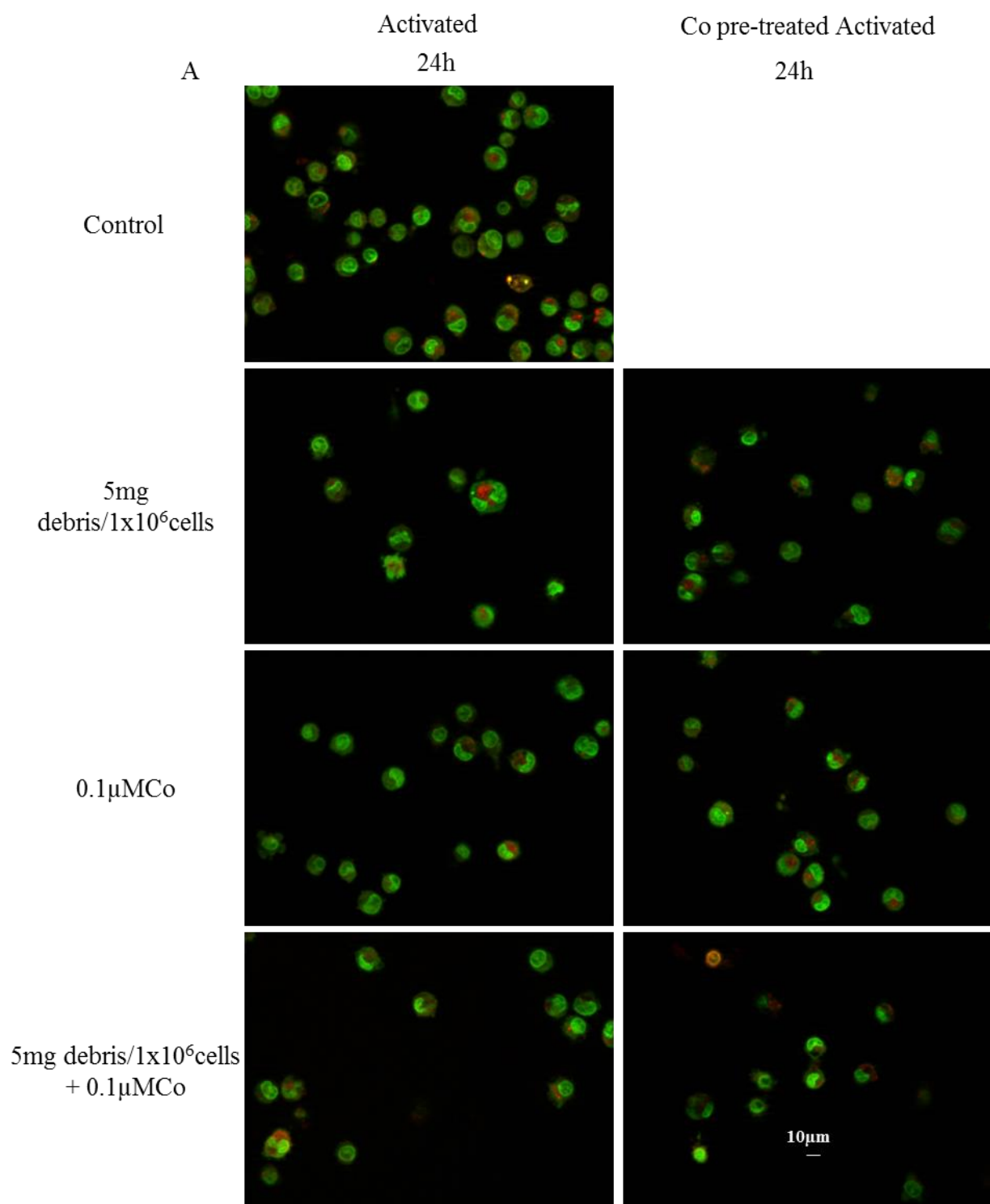


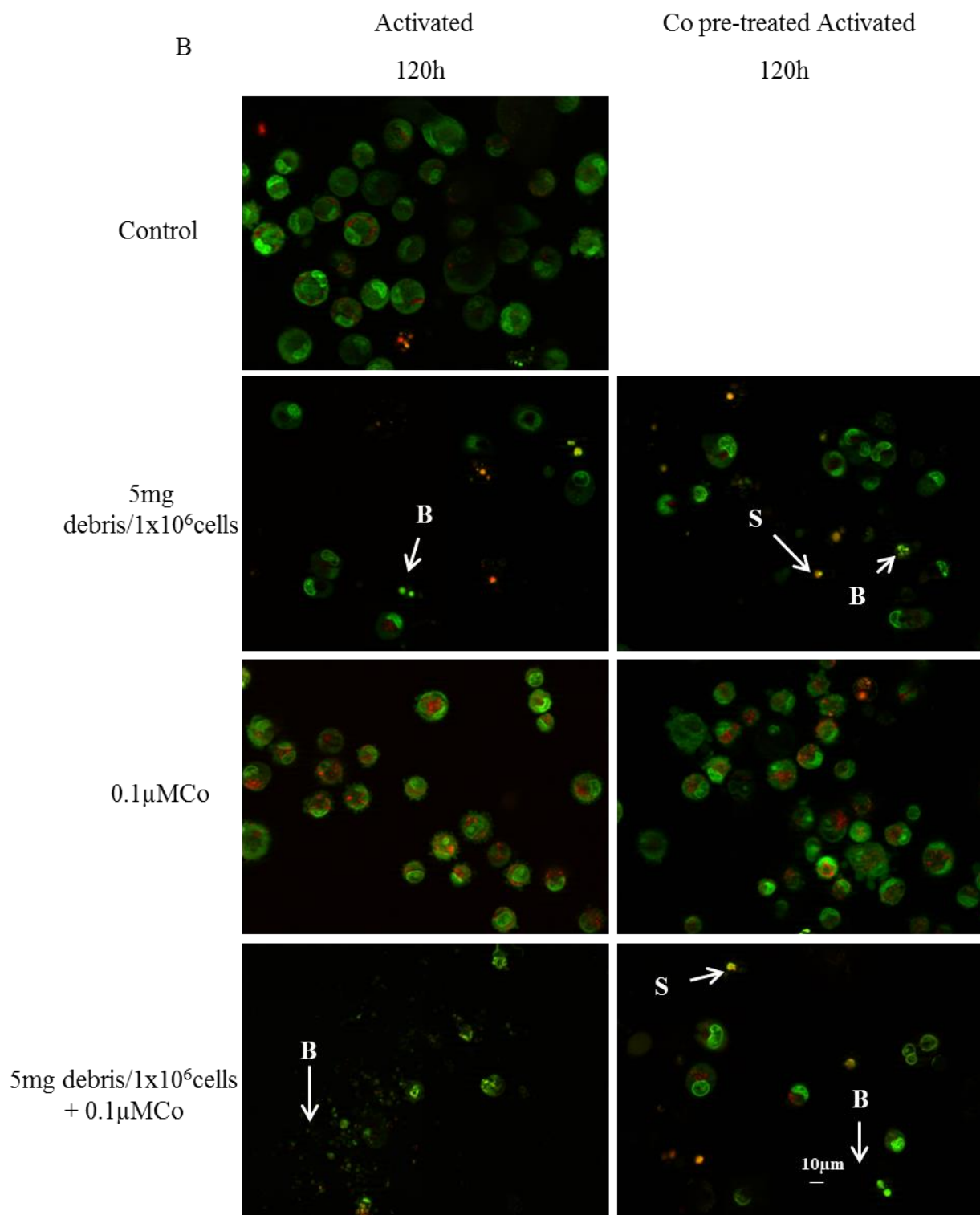




2.4 Fluorescence microscopy images (40X) of activated U937 and Co pre-treated activated U937 cells exposed to 5mg debris/ 1×10^6 cells, 0.1 μ M Co and 5mg debris/ 1×10^6 cells + 0.1 μ M Co.

A: 24h of exposure. B: 120h of exposure. "B" indicates cell blebbing, "S" indicates cell shrinkage.





Appendix 3. MIQE check list

The MIQE checklist for authors, reviewers and editors is presented in Table A.1.

Table A.1. MIQE checklist							
Item To Check	Importance	Checklist	Comments	Item To Check	Importance	Checklist	Comments
EXPERIMENTAL DESIGN				qPCR OLIGONUCLEOTIDES			
Definition of experimental and control groups	E	✓		Primer sequences	E	✓	
Number within each group	E	✓		RTPrimerDB Identification Number	D	✓	
Assay carried out by core lab or investigator's lab?	D	✓		Probe sequences	D**	✓	
Acknowledgement of authors' contributions	D	✓		Location and identity of any modifications	E	N/A	
SAMPLE				Manufacturer of oligonucleotides			
Description	E	✓		Purification method	D	✓	
Volume/mass of sample processed	D	✓		qPCR PROTOCOL			
Microdissection or macrodissection	E	N/A		Complete reaction conditions	E	✓	
Processing procedure	E	✓		Reaction volume and amount of cDNA/DNA	E	✓	
If frozen - how and how quickly?	E	✓		Primer, (probe), Mg ⁺⁺ and dNTP concentrations	E	✓	
If fixed - with what, how quickly?	E	N/A		Polymerase identity and concentration	E	✓	
Sample storage conditions and duration (especially for FFPE samples)	E	✓		Buffer/kit identity and manufacturer	E	✓	
NUCLEIC ACID EXTRACTION				Exact chemical constitution of the buffer			
Procedure and/or instrumentation	E	✓		Additives (SYBR Green I, DMSO, etc.)	E	✓	
Name of kit and details of any modifications	E	✓		Manufacturer of plates/tubes and catalog number	D	✓	
Source of additional reagents used	D	✓		Complete thermocycling parameters	E	✓	
Details of DNase or RNase treatment	E	✓		Reaction setup (manual/robotic)	D	✓	

Table A.1. MIQE checklist							
Item To Check	Importance	Checklist	Comments	Item To Check	Importance	Checklist	Comments
Contamination assessment (DNA or RNA)	E	✓		Manufacturer of qPCR instrument	E	✓	
Nucleic acid quantification	E	✓		qPCR VALIDATION			
Instrument and method	E	✓		Evidence of optimisation (from gradients)	D	✓	
Purity (A260/A280)	D	✓		Specificity (gel, sequence, melt, or digest)	E	✓	
Yield	D	✓		For SYBR Green I, Cq of the NTC	E	✓	
RNA integrity method/instrument	E	✓		Standard curves with slope and y-intercept	E	✓	
RIN/RQI or Cq of 3' and 5' transcripts	E	✓		PCR efficiency calculated from slope	E	✓	
Electrophoresis traces	D	-		Confidence interval for PCR efficiency or standard error	D	✓	
Inhibition testing (Cq dilutions, spike or other)	E	✓		r ² of standard curve	E	✓	
REVERSE TRANSCRIPTION				Linear dynamic range	E	✓	
Complete reaction conditions	E	✓		Cq variation at lower limit	E	-	
Amount of RNA and reaction volume	E	✓		Confidence intervals throughout range	D	-	
Priming oligonucleotide (if using GSP) and concentration	E	N/A		Evidence for limit of detection	E	-	
Reverse transcriptase and concentration	E	✓		If multiplex, efficiency and LOD of each assay.	E	N/A	
Temperature and time	E	✓		DATA ANALYSIS			
Manufacturer of reagents and catalogue numbers	D	✓		qPCR analysis program (source, version)	E	✓	
Cqs with and without RT	D*	✓		Cq method determination	E	✓	
Storage conditions of cDNA	D	✓		Outlier identification and disposition	E	-	

Table A.1. MIQE checklist							
Item To Check	Importance	Checklist	Comments	Item To Check	Importance	Checklist	Comments
qPCR TARGET INFORMATION				Results of NTCs	E	✓	
If multiplex, efficiency and LOD of each assay.	E	N/A		Justification of number and choice of reference genes	E	✓	
Sequence accession number	E	✓		Description of normalisation method	E	✓	
Location of amplicon	D	✓		Number and concordance of biological replicates	D	✓	
Amplicon length	E	✓		Number and stage (RT or qPCR) of technical replicates	E	✓	
<i>In silico</i> specificity screen (BLAST, etc)	E	✓		Repeatability (intra-assay variation)	E	✓	
Pseudogenes, retropseudogenes or other homologs?	D	✓		Reproducibility (inter-assay variation, %CV)	D	-	
Sequence alignment	D	✓		Power analysis	D	-	
Secondary structure analysis of amplicon	D	✓		Statistical methods for result significance	E	✓	
Location of each primer by exon or intron (if applicable)	E	✓		Software (source, version)	E	✓	
What splice variants are targeted?	E	✓		Cq or raw data submission using RDML	D	N/A	

Table A.1. MIQE checklist. *Assessing the absence of DNA using a no RT assay is essential when first extracting RNA. Once the sample has been validated as RDNA-free, inclusion of a no-RT control is desirable, but no longer essential. All essential information (E) must be submitted with the manuscript. Desirable information (D) should be submitted if available. **Disclosure of the probe sequence is highly desirable and strongly encouraged. However, since not all commercial pre-designed assay vendors provide this information, it cannot be an essential requirement. Use of such assays is advised against (Bustin et al., 2009).

PUBLICATIONS

Posters

- **O.M. Posada**, R.J.Tate, M.H. Grant. “RNA Stability in Frozen/Thawed Clinical Samples”. PgBiomed, Glasgow, UK, August 2011
- **O.M. Posada, R.J.Tate**, M.H. Grant. “RNA Stability in Clinical Blood Samples”. The British Toxicology Society Meeting, Nottingham, UK, September 2011.
- **O.M. Posada**, R.J.Tate, M.H. Grant. “Effects of Co-Cr metal wear debris and Co ions generated from metal-on-metal hip implants on human monocyte-like U937 cells” Presented at the STIG meeting, Edinburgh University, Edinburgh, UK, June 2012.
- **O.M. Posada**, R.J.Tate, M.H. Grant. “Co-Cr wear particles and cobalt ions stimulate the expression of human general toxicology related genes on monocyte like U937 cells”. Presented at The British Toxicology Society Annual Congress, Solihull, UK, April 2013.
- **O.M. Posada**, D. Gilmour, R.J.Tate, M.H. Grant. “Co-Cr wear products derived from metal-on-metal articulations induce apoptosis in human monocyte-like U937 cells” Presented at Eurotox Congress, Interlaken, Switzerland, September 2013.

Oral presentations

- “RNA Stability in Clinical Blood Samples”. STIG meeting, University of Dundee, Dundee, UK, November 2011.
- “Effects of Co-Cr metal wear debris generated from metal-on-metal hip implants and Co ions on human monocyte-like U937 cells”. GLORI meeting, Southern Hospital, Glasgow, UK, October 2011.

REFERENCES

- ADEREM, A. & ULEVITCH, R. J. 2000. Toll-like receptors in the induction of the innate immune response. *Nature*, 406, 782-787.
- AFFATATO, S., SPINELLI, M., ZAVALLONI, M., TRAINA, F., CARMIGNATO, S. & TONI, A. 2010. Ceramic-On-Metal for Total Hip Replacement: Mixing and Matching Can Lead to High Wear. *Artificial Organs*, 34, 319-323.
- AFOLARANMI, G. A., AKBAR, M., BREWER, J. & GRANT, M. H. 2012. Distribution of metal released from cobalt-chromium alloy orthopaedic wear particles implanted into air pouches in mice. *Journal of Biomedical Materials Research Part A*, 100A, 1529-1538.
- AFOLARANMI, G. A., TETTEY, J., MEEK, R. M. D. & GRANT, M. H. 2008. Release of chromium from orthopaedic arthroplasties. *The open orthopaedics journal*, 2, 10-8.
- AGARWAL, S. 2004. Osteolysis - basic science, incidence and diagnosis. *Current Orthopaedics*, 18, 220-231.
- AKANE, A., MATSUBARA, K., NAKAMURA, H., TAKAHASHI, S. & KIMURA, K. 1994. IDENTIFICATION OF THE HEME COMPOUND COPURIFIED WITH DEOXYRIBONUCLEIC-ACID (DNA) FROM BLOODSTAINS, A MAJOR INHIBITOR OF POLYMERASE CHAIN-REACTION (PCR) AMPLIFICATION. *Journal of Forensic Sciences*, 39, 362-372.
- AKBAR, M., BREWER, J. M. & GRANT, M. H. 2011. Effect of chromium and cobalt ions on primary human lymphocytes in vitro. *Journal of Immunotoxicology*, 8, 140-149.
- AKBAR, M., FRASER, A. R., GRAHAM, G. J., BREWER, J. M. & GRANT, M. H. 2012. Acute inflammatory response to cobalt chromium orthopaedic wear debris in a rodent air-pouch model. *Journal of the Royal Society Interface*, 9, 2109-2119.
- AKDIS, C. A. 2006. Allergy and hypersensitivity mechanisms of allergic disease - Editorial overview. *Current Opinion in Immunology*, 18, 718-726.
- AKITA, K., OKAMURA, H., YOSHIDA, K., MORIMOTO, H., OGAWA-IYEHARA, H. & HANEJI, T. 2007. Cobalt chloride induces apoptosis and zinc chloride suppresses cobalt-induced apoptosis by Bcl-2 expression in human submandibular gland HSG cells. *International Journal of Oncology*, 31, 923-929.
- ALGAN, S. M., PURDON, M. & HOROWITZ, S. M. 1996. Role of tumor necrosis factor alpha in particulate-induced bone resorption. *Journal of Orthopaedic Research*, 14.
- ALLOUNI, Z. E., HOL, P. J., CAUQUI, M. A., GJERDET, N. R. & CIMPAN, M. R. 2012. Role of physicochemical characteristics in the uptake of TiO₂ nanoparticles by fibroblasts. *Toxicology in Vitro*, 26, 469-479.
- AMSTUTZ, H. C. & LE DUFF, M. J. 2006. Background of metal-on-metal resurfacing. *Proceedings of the Institution of Mechanical Engineers Part H-Journal of Engineering in Medicine*, 220, 85-94.
- ANDERSEN, C. L., JENSEN, J. L. & ORNTOFT, T. F. 2004. Normalization of real-time quantitative reverse transcription-PCR data: A model-based variance

- estimation approach to identify genes suited for normalization, applied to bladder and colon cancer data sets. *Cancer Research*, 64, 5245-5250.
- ANDERSON, J. M. 2009. In Vitro and In Vivo Monocyte, Macrophage, Foreign Body Giant Cell, and Lymphocyte Interactions with Biomaterials. *Biological Interactions on Materials Surfaces: Understanding and Controlling Protein, Cell, and Tissue Responses*, 225-244.
- ANDERSON, J. M., RODRIGUEZ, A. & CHANG, D. T. 2008. Foreign body reaction to biomaterials. *Seminars in Immunology*, 20, 86-100.
- ANDREWS, R. E., SHAH, K. M., WILKINSON, J. M. & GARTLAND, A. 2011. Effects of cobalt and chromium ions at clinically equivalent concentrations after metal-on-metal hip replacement on human osteoblasts and osteoclasts: Implications for skeletal health. *Bone*, 49, 717-723.
- ANTONIOU, J., MARTINEAU, P. A., FILION, K. B., HAIDER, S., ZUKOR, D. J., HUK, O. L., PILOTE, L. & EISENBERG, M. J. 2004. In hospital cost of total hip arthroplasty in Canada and the United States. *Journal of Bone and Joint Surgery-American Volume*, 86A, 2435-2439.
- ANTONIOU, J., ZUKOR, D. J., MWALE, F., MINARIK, W., PETIT, A. & HUK, O. L. 2008. Metal ion levels in the blood of patients after hip resurfacing: A comparison between twenty-eight and thirty-six-millimeter-head metal-on-metal prostheses. *Journal of Bone and Joint Surgery-American Volume*, 90A, 142-148.
- ANTUNES, F., CADENAS, E. & BRUNK, U. T. 2001. Apoptosis induced by exposure to a low steady-state concentration of H₂O₂ is a consequence of lysosomal rupture. *Biochemical Journal*, 356, 549-555.
- ANTUNES, R. A. & LOPES DE OLIVEIRA, M. C. 2012. Corrosion fatigue of biomedical metallic alloys: Mechanisms and mitigation. *Acta Biomaterialia*, 8, 937-962.
- ARAYA, J., MARUYAMA, M., INOUE, A., FUJITA, T., KAWAHARA, J., SASSA, K., HAYASHI, R., KAWAGISHI, Y., YAMASHITA, N., SUGIYAMA, E. & KOBAYASHI, M. 2002. Inhibition of proteasome activity is involved in cobalt-induced apoptosis of human alveolar macrophages. *American Journal of Physiology-Lung Cellular and Molecular Physiology*, 283, L849-L858.
- ARCHIBECK, M. J., JACOBS, J. J., ROEBUCK, K. A. & GLANT, T. T. 2001. The basic science of periprosthetic osteolysis. *Instructional course lectures*, 50, 185-95.
- ARORA, A., SONG, Y., CHUN, L., HUIE, P., TRINDADE, M., SMITH, R. L. & GOODMAN, S. 2003. The role of the TH1 and TH2 immune responses in loosening and osteolysis of cemented total hip replacements. *Journal of Biomedical Materials Research Part A*, 64A, 693-697.
- ASARE, A. L., KOLCHINSKY, S. A., GAO, Z., WANG, R., RADDASSI, K., BOURCIER, K. & SEYFERT-MARGOLIS, V. 2008. Differential gene expression profiles are dependent upon method of peripheral blood collection and RNA isolation. *Bmc Genomics*, 9.
- ASPENBERG, P., AGHOLME, F., MAGNUSSON, P. & FAHLGREN, A. 2011. Targeting RANKL for reduction of bone loss around unstable implants: OPG-Fc compared to alendronate in a model for mechanically induced loosening. *Bone*, 48, 225-230.

- ATKINS, R. M., LANGKAMER, V. G., PERRY, M. J., ELSON, C. J. & COLLINS, C. M. P. 1997. Bone-membrane interface in aseptic loosening of total joint arthroplasties. *Journal of Arthroplasty*, 12, 461-464.
- AU, A., HA, J., HERNANDEZ, M., POLOTSKY, A., HUNGERFORD, D. S. & FRONDOZA, C. G. 2006. Nickel and vanadium metal ions induce apoptosis of T-lymphocyte Jurkat cells. *Journal of Biomedical Materials Research Part A*, 79A, 512-521.
- AUSTRALIAN ORTHOPAEDIC ASSOCIATION NATIONAL JOINT REPLACEMENT REGISTRY, A. 2011. Hip and Knee Arthroplasty Annual Report 2011 <http://www.surfacehippy.info/pdf/australian-nat-reg-2011.pdf>.
- AVEIC, S., PIGAZZI, M. & BASSO, G. 2011. BAG1: The Guardian of Anti-Apoptotic Proteins in Acute Myeloid Leukemia. *Plos One*, 6.
- BACCARELLI, A. & BOLLATI, V. 2009. Epigenetics and environmental chemicals. *Current Opinion in Pediatrics*, 21, 243-251.
- BAEK, Y.-S., HAAS, S., HACKSTEIN, H., BEIN, G., HERNANDEZ-SANTANA, M., LEHRACH, H., SAUER, S. & SEITZ, H. 2009. Identification of novel transcriptional regulators involved in macrophage differentiation and activation in U937 cells. *Bmc Immunology*, 10.
- BAGCHI, D., STOHS, S. J., DOWNS, B. W., BAGCHI, M. & PREUSS, H. G. 2002. Cytotoxicity and oxidative mechanisms of different forms of chromium. *Toxicology*, 180, 5-22.
- BAINBRIDGE, J. A., REVELL, P. A. & AL-SAFFAR, N. 2001. Costimulatory molecule expression following exposure to orthopaedic implants wear debris. *Journal of Biomedical Materials Research*, 54, 328-334.
- BANK, H. L. 1987. ASSESSMENT OF ISLET CELL VIABILITY USING FLUORESCENT DYES. *Diabetologia*, 30, 812-816.
- BANK, H. L. 1988. RAPID ASSESSMENT OF ISLET VIABILITY WITH ACRIDINE-ORANGE AND PROPIDIUM IODIDE. *In Vitro Cellular & Developmental Biology*, 24, 266-273.
- BANKS, T. A., RICKERT, S. & WARE, C. F. 2006. Restoring immune defenses via lymphotoxin signaling - Lessons from cytomegalovirus. *Immunologic Research*, 34, 243-253.
- BARREIRO, L. B., BEN-ALI, M., QUACH, H., LAVAL, G., PATIN, E., PICKRELL, J. K., BOUCHIER, C., TICHIT, M., NEYROLLES, O., GICQUEL, B., KIDD, J. R., KIDD, K. K., ALCAIS, A., RAGIMBEAU, J., PELLEGRINI, S., ABEL, L., CASANOVA, J.-L. & QUINTANA-MURCI, L. 2009. Evolutionary Dynamics of Human Toll-Like Receptors and Their Different Contributions to Host Defense. *Plos Genetics*, 5.
- BARRETO, G., SCHAEFER, A., MARHOLD, J., STACH, D., SWAMINATHAN, S. K., HANDA, V., DOEDERLEIN, G., MALTRY, N., WU, W., LYKO, F. & NIEHRS, C. 2007. Gadd45a promotes epigenetic gene activation by repair-mediated DNA demethylation. *Nature*, 445, 671-675.
- BARTEL, D. P. & CHEN, C. Z. 2004. Micromanagers of gene expression: the potentially widespread influence of metazoan microRNAs. *Nature Reviews Genetics*, 5, 396-400.
- BAS, A., FORSBERG, G., HAMMARSTROM, S. & HAMMARSTROM, M. L. 2004. Utility of the housekeeping genes 18S rRNA, beta-actin and glyceraldehyde-3-phosphate-dehydrogenase for normalization in real-time

- quantitative reverse transcriptase-polymerase chain reaction analysis of gene expression in human T lymphocytes. *Scandinavian Journal of Immunology*, 59, 566-573.
- BASTONINI, E., VERDONE, L., MORRONE, S., SANTONI, A., SETTIMO, G., MARSILI, G., LA FORTEZZA, M., DI MAURO, E. & CASERTA, M. 2011. Transcriptional modulation of a human monocytic cell line exposed to PM10 from an urban area. *Environmental Research*, 111, 765-774.
- BAUER, M., POLZIN, S. & PATZELT, D. 2003. Quantification of RNA degradation by semi-quantitative duplex and competitive RT-PCR: a possible indicator of the age of bloodstains? *Forensic Science International*, 138, 94-103.
- BECKER, C., HAMMERLE-FICKINGER, A., RIEDMAIER, I. & PFAFFL, M. W. 2010. mRNA and microRNA quality control for RT-qPCR analysis. *Methods*, 50, 237-243.
- BECKER, S., DAILEY, L., SOUKUP, J. M., SILBAJORIS, R. & DEVLIN, R. B. 2005. TLR-2 is involved in airway epithelial cell response to air pollution particles. *Toxicology and Applied Pharmacology*, 203, 45-52.
- BEEKMAN, J. M., REISCHL, J., HENDERSON, D., BAUER, D., TERNES, R., PENA, C., LATHIA, C. & HEUBACH, J. F. 2009. Recovery of microarray-quality RNA from frozen EDTA blood samples. *Journal of pharmacological and toxicological methods*, 59, 44-9.
- BEMEUR, C., STE-MARIE, L., DESJARDINS, P., HAZELL, A. S., VACHON, L., BUTTERWORTH, R. & MONTGOMERY, J. 2004. Decreased beta-actin mRNA expression in hyperglycemic focal cerebral ischemia in the rat. *Neuroscience Letters*, 357, 211-214.
- BEUTLER, B. 2004. Inferences, questions and possibilities in toll-like receptor signalling. *Nature*, 430, 257-263.
- BHAMRA, M. S. & CASE, C. P. 2006. Biological effects of metal-on-metal hip replacements. *Proceedings of the Institution of Mechanical Engineers Part H-Journal of Engineering in Medicine*, 220, 379-384.
- BHATTACHARYYA, M. H. 2009. Cadmium osteotoxicity in experimental animals: Mechanisms and relationship to human exposures. *Toxicology and Applied Pharmacology*, 238, 258-265.
- BIEDERMANN, K. A. & LANDOLPH, J. R. 1990. ROLE OF VALENCE STATE AND SOLUBILITY OF CHROMIUM COMPOUNDS ON INDUCTION OF CYTOTOXICITY, MUTAGENESIS, AND ANCHORAGE INDEPENDENCE IN DIPLOID HUMAN FIBROBLASTS. *Cancer Research*, 50, 7835-7842.
- BISSELING, P., ZEILSTRA, D. J., HOL, A. M. & VAN SUSANTE, J. L. C. 2011. Metal ion levels in patients with a lumbar metal-on-metal total disc replacement SHOULD WE BE CONCERNED? *Journal of Bone and Joint Surgery-British Volume*, 93B, 949-954.
- BLEACKLEY, M. R. & MACGILLIVRAY, R. T. A. 2011. Transition metal homeostasis: from yeast to human disease. *Biometals*, 24, 785-809.
- BLOTTIERE, H. M., DACULSI, G., ANEGON, I., POUZAT, J. A., NELSON, P. N. & PASSUTI, N. 1995. UTILIZATION OF ACTIVATED U937 MONOCYTIC CELLS AS A MODEL TO EVALUATE

- BIOCOMPATIBILITY AND BIODEGRADATION OF SYNTHETIC CALCIUM-PHOSPHATE. *Biomaterials*, 16, 497-503.
- BOADI, W. Y., HARRIS, S., ANDERSON, J. B. & ADUNYAH, S. E. 2013. Lipid peroxides and glutathione status in human progenitor mononuclear (U937) cells following exposure to low doses of nickel and copper. *Drug and chemical toxicology*, 39, 155-62.
- BOARDMAN, D. R., MIDDLETON, F. R. & KAVANAGH, T. G. 2006. A benign psoas mass following metal-on-metal resurfacing of the hip. *Journal of Bone and Joint Surgery-British Volume*, 88B, 402-404.
- BOHLER, M., KANZ, F., SCHWARZ, B., STEFFAN, I., WALTER, A., PLENK, H. & KNAHR, K. 2002. Adverse tissue reactions to wear particles from Co-alloy articulations, increased by alumina-blasting particle contamination from cementless Ti-based total hip implants - A report of seven revisions with early failure. *Journal of Bone and Joint Surgery-British Volume*, 84B, 128-136.
- BOHLER, M., MOCHIDA, Y., BAUER, T. W., PLENK, H. & SALZER, M. 2000. Wear debris from two different alumina-on-alumina total hip arthroplasties. *Journal of Bone and Joint Surgery-British Volume*, 82B, 901-909.
- BOITEUX, S., GELLON, L. & GUIBOURT, N. 2002. Repair of 8-oxoguanine in *Saccharomyces cerevisiae*: Interplay of DNA repair and replication mechanisms. *Free Radical Biology and Medicine*, 32, 1244-1253.
- BOROVECKI, F., LOVRECIC, L., ZHOU, J., JEONG, H., THEN, F., ROSAS, H. D., HERSCH, S. M., HOGARTH, P., BOUZOU, B., JENSEN, R. V. & KRAINIC, D. 2005. Genome-wide expression profiling of human blood reveals biomarkers for Huntington's disease. *Proceedings of the National Academy of Sciences of the United States of America*, 102, 11023-11028.
- BORRUTO, A. 2010. A new material for hip prosthesis without considerable debris release. *Medical Engineering & Physics*, 32, 908-913.
- BOUKES, G. J. & VAN DE VENTER, M. 2012. Rooperol as an antioxidant and its role in the innate immune system: An in vitro study. *Journal of Ethnopharmacology*, 144, 692-699.
- BRODBECK, W. G., MACEWAN, M., COLTON, E., MEYERSON, H. & ANDERSON, J. M. 2005. Lymphocytes and the foreign body response: Lymphocyte enhancement of macrophage adhesion and fusion. *Journal of Biomedical Materials Research Part A*, 74A, 222-229.
- BROWN, C., FISHER, J. & INGHAM, E. 2006. Biological effects of clinically relevant wear particles from metal-on-metal hip prostheses. *Proceedings of the Institution of Mechanical Engineers Part H-Journal of Engineering in Medicine*, 220, 355-369.
- BROWN, D. M., DICKSON, C., DUNCAN, P., AL-ATTILI, F. & STONE, V. 2010. Interaction between nanoparticles and cytokine proteins: impact on protein and particle functionality. *Nanotechnology*, 21.
- BRUDER, S. P., FINK, D. J. & CAPLAN, A. I. 1994. MESENCHYMAL STEM-CELLS IN IN BONE-DEVELOPMENT, BONE REPAIR, AND SKELETAL REGENERATION THERAPY. *Journal of Cellular Biochemistry*, 56, 283-294.
- BURCZYNSKI, M. E., PETERSON, R. L., TWINE, N. C., ZUBEREK, K. A., BRODEUR, B. J., CASCIOTTI, L., MAGANTI, V., REDDY, P. S.,

- STRAHS, A., IMMERMANN, F., SPINELLI, W., SCHWERTSCHLAG, U., SLAGER, A. M., COTREAU, M. M. & DORNER, A. J. 2006. Molecular classification of Crohn's disease and ulcerative colitis patients using transcriptional profiles in peripheral blood mononuclear cells. *Journal of Molecular Diagnostics*, 8, 51-61.
- BURCZYNSKI, M. E., TWINE, N. C., DUKART, G., MARSHALL, B., HIDALGO, M., STADLER, W. M., LOGAN, T., DUTCHER, J., HUDES, G., TREPICCHIO, W. L., STRAHS, A., IMMERMANN, F., SLONIM, D. K. & DORNER, A. J. 2005. Transcriptional profiles in peripheral blood mononuclear cells prognostic of clinical outcomes in patients with advanced renal cell carcinoma. *Clinical Cancer Research*, 11, 1181-1189.
- BUSTIN, S. A., BEAULIEU, J.-F., HUGGETT, J., JAGGI, R., KIBENGE, F. S. B., OLSVIK, P. A., PENNING, L. C. & TOEGEL, S. 2010. MIQE precis: Practical implementation of minimum standard guidelines for fluorescence-based quantitative real-time PCR experiments. *Bmc Molecular Biology*, 11.
- BUSTIN, S. A., BENES, V., GARSON, J. A., HELLEMANS, J., HUGGETT, J., KUBISTA, M., MUELLER, R., NOLAN, T., PFAFFL, M. W., SHIPLEY, G. L., VANDESOMPELE, J. & WITWER, C. T. 2009. The MIQE Guidelines: Minimum Information for Publication of Quantitative Real-Time PCR Experiments. *Clinical Chemistry*, 55, 611-622.
- CACHINHO, S. C. P., PU, F. R. & HUNT, J. A. 2013. Cytokine secretion from human peripheral blood mononuclear cells cultured in vitro with metal particles. *Journal of Biomedical Materials Research Part A*, 101A, 1201-1209.
- CADOSCH, D., CHAN, E., GAUTSCHI, O. P. & FILGUEIRA, L. 2009. Metal is not inert: Role of metal ions released by biocorrosion in aseptic loosening-Current concepts. *Journal of Biomedical Materials Research Part A*, 91A, 1252-1262.
- CAICEDO, M., JACOBS, J. J., REDDY, A. & HALLAB, N. J. 2008. Analysis of metal ion-induced DNA damage, apoptosis, and necrosis in human (Jurkat) T-cells demonstrates Ni²⁺, and V³⁺ are more toxic than other metals: Al³⁺, Be²⁺, Co²⁺, Cr³⁺, Cu²⁺, Fe³⁺, Mo⁵⁺, Nb⁵⁺, Zr²⁺. *Journal of Biomedical Materials Research Part A*, 86A, 905-913.
- CAMPBELL, P., EBRAMZADEH, E., NELSON, S., TAKAMURA, K., DE SMET, K. & AMSTUTZ, H. C. 2010. Histological Features of Pseudotumor-like Tissues From Metal-on-Metal Hips. *Clinical Orthopaedics and Related Research*, 468, 2321-2327.
- CANADIAN JOINT REPLACEMENT REGISTRY, C. 2013. Title Hip and Knee Replacements in Canada: Canadian Joint Replacement Registry 2013 Annual Report. https://secure.cihi.ca/free_products/CJRR_2013_Annual_Report_EN.pdf.
- CANONICO, P. G. & BIRD, J. W. C. 1969. USE OF ACRIDINE ORANGE AS A LYSOSOMAL MARKER IN RAT SKELETAL MUSCLE. *Journal of Cell Biology*, 43, 367-&.
- CARDOSO, L., HERMAN, B. C., VERBORGT, O., LAUDIER, D., MAJESKA, R. J. & SCHAFFLER, M. B. 2009. Osteocyte Apoptosis Controls Activation of Intracortical Resorption in Response to Bone Fatigue. *Journal of Bone and Mineral Research*, 24, 597-605.

- CARON, E., LIAUTARD, J. P. & KOHLER, S. 1994. DIFFERENTIATED U937 CELLS EXHIBIT INCREASED BACTERICIDAL ACTIVITY UPON LPS ACTIVATION AND DISCRIMINATE BETWEEN VIRULENT AND AVIRULENT LISTERIA AND BRUCELLA SPECIES. *Journal of Leukocyte Biology*, 56, 174-181.
- CASE, C. P., LANGKAMER, V. G., JAMES, C., PALMER, M. R., KEMP, A. J., HEAP, P. F. & SOLOMON, L. 1994. WIDESPREAD DISSEMINATION OF METAL DEBRIS FROM IMPLANTS. *Journal of Bone and Joint Surgery-British Volume*, 76B.
- CATALANI, S., RIZZETTI, M. C., PADOVANI, A. & APOSTOLI, P. 2012. Neurotoxicity of cobalt. *Human & Experimental Toxicology*, 31, 421-437.
- CATELAS, I., PETIT, A., VALI, H., FRAGISKATOS, C., MEILLEUR, R., ZUKOR, D. J., ANTONIOU, J. & HUK, O. L. 2005. Quantitative analysis of macrophage apoptosis vs. necrosis induced by cobalt and chromium ions in vitro. *Biomaterials*, 26, 2441-2453.
- CATELAS, I., PETIT, A., ZUKOR, D. J., ANTONIOU, J. & HUK, O. L. 2003. TNF-alpha secretion and macrophage mortality induced by cobalt and chromium ions in vitro-Qualitative analysis of apoptosis. *Biomaterials*, 24, 383-391.
- CATELAS, I., PETIT, A., ZUKOR, D. J. & HUK, O. L. 2001. Cytotoxic and apoptotic effects of cobalt and chromium ions on J774 macrophages - Implication of caspase-3 in the apoptotic pathway. *Journal of Materials Science-Materials in Medicine*, 12, 949-953.
- CATELAS, I., WIMMER, M. & UTZSCHNEIDER, S. 2011. Polyethylene and metal wear particles: characteristics and biological effects. *Seminars in Immunopathology*, 33, 257-271.
- CATELAS, I. & WIMMER, M. A. 2011. New Insights into Wear and Biological Effects of Metal-on-Metal Bearings. *Journal of Bone and Joint Surgery-American Volume*, 93A, 76-83.
- CDC, C. F. D. C. A. P. 2010. National Hospital Discharge Survey: 2007 Summary. <http://www.cdc.gov/nchs/data/nhsr/nhsr029.pdf>.
- CHABOT, S., CHARLET, D., WILSON, T. L. & YONG, V. W. 2001. Cytokine production consequent to T cell-microglia interaction: the PMA/IFN gamma-treated U937 cells display similarities to human microglia. *Journal of Neuroscience Methods*, 105.
- CHAISSOMCHIT, S., WICHAJARN, R., JANEJAI, N. & CHAREONSIRIWATANA, W. 2005. Stability of genomic DNA in dried blood spots stored on filter paper. *Southeast Asian Journal of Tropical Medicine and Public Health*, 36, 270-273.
- CHAMBELLAN, A., LEAHY, R., XU, W., CRUICKSHANK, P. J., JANOCHA, A., SZABO, K., CANNADY, S. B., COMHAIR, S. A. A. & ERZURUM, S. C. 2009. Pivotal role of c-Fos in nitric oxide synthase 2 expression in airway epithelial cells. *Nitric Oxide-Biology and Chemistry*, 20, 143-149.
- CHANG, D. T., COLTON, E., MATSUDA, T. & ANDERSON, J. M. 2009. Lymphocyte adhesion and interactions with biomaterial adherent macrophages and foreign body giant cells. *Journal of Biomedical Materials Research Part A*, 91A, 1210-1220.

- CHANG, J. D., LEE, S. S., HUR, M., SEO, E. M., CHUNG, Y. K. & LEE, C. J. 2005. Revision total hip arthroplasty in hip joints with metallosis - A single-center experience with 31 cases. *Journal of Arthroplasty*, 20.
- CHAPPERT, P. & SCHWARTZ, R. H. 2010. Induction of T cell anergy: integration of environmental cues and infectious tolerance. *Current Opinion in Immunology*, 22, 552-559.
- CHAUHAN, V., BREZNAN, D., GOEGAN, P., NADEAU, D., KARTHIKEYAN, S., BROOK, J. R. & VINCENT, R. 2004. Effects of ambient air particles on nitric oxide production in macrophage cell lines. *Cell Biology and Toxicology*, 20, 221-239.
- CHEN, D. S., ZHANG, X. L., GUO, Y. Y., SHI, S. F., MAO, X., PAN, X. Y. & CHENG, T. 2012. MMP-9 inhibition suppresses wear debris-induced inflammatory osteolysis through downregulation of RANK/RANKL in a murine osteolysis model. *International Journal of Molecular Medicine*, 30, 1417-1423.
- CHEN, F., VALLYATHAN, V., CASTRANOVA, V. & SHI, L. 2001. Cell apoptosis induced by carcinogenic metals. *Molecular and Cellular Biochemistry*, 222, 183-188.
- CHEN, J., BARDES, E. E., ARONOW, B. J. & JEGGA, A. G. 2009. ToppGene Suite for gene list enrichment analysis and candidate gene prioritization. *Nucleic Acids Research*, 37, W305-W311.
- CHEN, J., BRUNS, A. H., DONNELLY, H. K. & WUNDERINK, R. G. 2010. Comparative in vitro stimulation with lipopolysaccharide to study TNF alpha gene expression in fresh whole blood, fresh and frozen peripheral blood mononuclear cells. *Journal of Immunological Methods*, 357, 33-37.
- CHEN, K., GUNTER, K. & MAINES, M. D. 2000. Neurons overexpressing heme oxygenase-1 resist oxidative stress-mediated cell death. *Journal of Neurochemistry*, 75, 304-313.
- CHEN, X., BA, Y., MA, L., CAI, X., YIN, Y., WANG, K., GUO, J., ZHANG, Y., CHEN, J., GUO, X., LI, Q., LI, X., WANG, W., ZHANG, Y., WANG, J., JIANG, X., XIANG, Y., XU, C., ZHENG, P., ZHANG, J., LI, R., ZHANG, H., SHANG, X., GONG, T., NING, G., WANG, J., ZEN, K., ZHANG, J. & ZHANG, C.-Y. 2008. Characterization of microRNAs in serum: a novel class of biomarkers for diagnosis of cancer and other diseases. *Cell Research*, 18, 997-1006.
- CHEN, X., ZHU, G., JIN, T., GU, S., XIAO, H. & QIU, J. 2011. Cadmium induces differentiation of RAW264.7 cells into osteoclasts in the presence of RANKL. *Food and Chemical Toxicology*, 49, 2392-2397.
- CHIANG, E. Y., KOLUMAM, G. A., YU, X., FRANCESCO, M., IVELJA, S., PENG, I., GRIBLING, P., SHU, J., LEE, W. P., REFINO, C. J., BALAZS, M., PALER-MARTINEZ, A., NGUYEN, A., YOUNG, J., BARCK, K. H., CARANO, R. A. D., FERRANDO, R., DIEHL, L., CHATTERJEA, D. & GROGAN, J. L. 2009. Targeted depletion of lymphotoxin-alpha-expressing T(H)1 and T(H)17 cells inhibits autoimmune disease. *Nature Medicine*, 15, 766-U10.
- CIAPETTI, G., GRANCHI, D., SAVARINO, L., CENNI, E., MAGRINI, E., BALDINI, N. & GIUNTI, A. 2002. In vitro testing of the potential for

- orthopedic bone cements to cause apoptosis of osteoblast-like cells. *Biomaterials*, 23, 617-627.
- CLARKE, M. T., LEE, P. T. H., ARORA, A. & VILLAR, R. N. 2003. Levels of metal ions after small- and large-diameter metal-on-metal hip arthroplasty. *Journal of Bone and Joint Surgery-British Volume*, 85B, 913-917.
- CODD, R., DILLON, C. T., LEVINA, A. & LAY, P. A. 2001. Studies on the genotoxicity of chromium: from the test tube to the cell. *Coordination Chemistry Reviews*, 216, 537-582.
- CORTEN, K. & MACDONALD, S. J. 2010. Hip Resurfacing Data from National Joint Registries What Do They Tell Us? What Do They Not Tell Us? *Clinical Orthopaedics and Related Research*, 468, 351-357.
- CROTTI, T. N., SMITH, M. D., FINDLAY, D. M., ZREIQAT, H., AHERN, M. J., WEEDON, H., HATZINIKOLOUS, G., CAPONE, M., HOLDING, C. & HAYNES, D. R. 2004. Factors regulating osteoclast formation in human tissues adjacent to peri-implant bone loss: expression of receptor activator NF kappa B, RANK ligand and osteoprotegerin. *Biomaterials*, 25, 565-573.
- CROTTI, T. N., SMITH, M. D., WEEDON, H., AHERN, M. J., FINDLAY, D. M., KRAAN, M., TAK, P. P. & HAYNES, D. R. 2002. Receptor activator NF-kappa B ligand (RANKL) expression in synovial tissue from patients with rheumatoid arthritis, spondyloarthropathy, osteoarthritis, and from normal patients: semiquantitative and quantitative analysis. *Annals of the Rheumatic Diseases*, 61, 1047-1054.
- CUTRESS, R. I., TOWNSEND, P. A., BRIMMELL, M., BATEMAN, A. C., HAGUE, A. & PACKHAM, G. 2002. BAG-I expression and function in human cancer. *British Journal of Cancer*, 87, 834-839.
- DADDA, F., BORLERI, D., MIGLIORI, M., MOSCONI, G., MEDOLAGO, G., VIROTTA, G., COLOMBO, F. & SEGHIZZI, P. 1994. CARDIAC-FUNCTION STUDY IN HARD METAL WORKERS. *Science of the Total Environment*, 150, 179-186.
- DAIGNEAULT, M., PRESTON, J. A., MARRIOTT, H. M., WHYTE, M. K. B. & DOCKRELL, D. H. 2010. The Identification of Markers of Macrophage Differentiation in PMA-Stimulated THP-1 Cells and Monocyte-Derived Macrophages. *Plos One*, 5.
- DANIEL, J., ZIAEE, H., PRADHAN, C., PYNSENT, P. B. & MCMINN, D. J. W. 2007a. Blood and urine metal ion levels in young and active patients after Birmingham hip resurfacing arthroplasty - Four-year results of a prospective longitudinal study. *Journal of Bone and Joint Surgery-British Volume*, 89B, 169-173.
- DANIEL, J., ZIAEE, H., PYNSENT, P. B. & MCMINN, D. J. W. 2007b. The validity of serum levels as a surrogate measure of systemic exposure to metal ions in hip replacement. *Journal of Bone and Joint Surgery-British Volume*, 89B, 736-741.
- DAVDA, K., LALI, F. V., SAMPSON, B., SKINNER, J. A. & HART, A. J. 2011. An analysis of metal ion levels in the joint fluid of symptomatic patients with metal-on-metal hip replacements. *Journal of Bone and Joint Surgery-British Volume*, 93B, 738-745.
- DAVIES, A. P., WILLERT, H. G., CAMPBELL, P. A., LEARMONTH, I. D. & CASE, C. P. 2005. An unusual lymphocytic perivascular infiltration in tissues

- around contemporary metal-on-metal joint replacements. *Journal of Bone and Joint Surgery-American Volume*, 87A, 18-27.
- DAY, C. S., LEE, A. H. & AHMED, I. 2013. Acute carpal tunnel secondary to metallosis after total wrist arthroplasty. *Journal of Hand Surgery-European Volume*, 38E, 80-81.
- DE BOECK, M., KIRSCH-VOLDERS, M. & LISON, D. 2003. Cobalt and antimony: genotoxicity and carcinogenicity. *Mutation Research-Fundamental and Molecular Mechanisms of Mutagenesis*, 533.
- DE FLORA, S. 2000. Threshold mechanisms and site specificity in chromium(VI) carcinogenesis. *Carcinogenesis*, 21, 533-541.
- DE HAAN, R., PATTYN, C., GILL, H. S., MURRAY, D. W., CAMPBELL, P. A. & DE SMET, K. 2008. Correlation between inclination of the acetabular component and metal ion levels in metal-on-metal hip resurfacing replacement. *Journal of Bone and Joint Surgery-British Volume*, 90B, 1291-1297.
- DEARNLEY, P. A. 1999. A review of metallic, ceramic and surface-treated metals used for bearing surfaces in human joint replacements. *Proceedings of the Institution of Mechanical Engineers Part H-Journal of Engineering in Medicine*, 213, 107-135.
- DEL AGUILA, E. M., DUTRA, M. B., SILVA, J. T. & PASCHOALIN, V. M. F. 2005. Comparing protocols for preparation of DNA-free total yeast RNA suitable for RT-PCR. *Bmc Molecular Biology*, 6.
- DEMURCIA, G. & DEMURCIA, J. M. 1994. POLY(ADP-RIBOSE) POLYMERASE - A MOLECULAR NICK-SENSOR. *Trends in Biochemical Sciences*, 19, 172-176.
- DENAMUR, S., TYTECA, D., MARCHAND-BRYNAERT, J., VAN BAMBEKE, F., TULKENS, P. M., COURTOY, P. J. & MINGEOT-LECLERCQ, M.-P. 2011. Role of oxidative stress in lysosomal membrane permeabilization and apoptosis induced by gentamicin, an aminoglycoside antibiotic. *Free Radical Biology and Medicine*, 51, 1656-1665.
- DENISOV, V., STRONG, W., WALDER, M., GRINGRICH, J. & WINTZ, H. 2008. Development and Validation of RQI: an RNA quality indicator for the Experion™ Automated Electrophoresis System. *Bio-Rad Bulletin*
- DEPREZ, R. H. L., FIJNVANDRAAT, A. C., RUIJTER, J. M. & MOORMAN, A. F. M. 2002. Sensitivity and accuracy of quantitative real-time polymerase chain reaction using SYBR green I depends on cDNA synthesis conditions. *Analytical Biochemistry*, 307, 63-69.
- DESROCHERS, J., AMREIN, M. W. & MATYAS, J. R. 2013. Microscale surface friction of articular cartilage in early osteoarthritis. *Journal of the mechanical behavior of biomedical materials*, 25, 11-22.
- DETOGNI, P., GOELLNER, J., RUDDLE, N. H., STREETER, P. R., FICK, A., MARIATHASAN, S., SMITH, S. C., CARLSON, R., SHORNICK, L. P., STRAUSSCHOENBERGER, J., RUSSELL, J. H., KARR, R. & CHAPLIN, D. D. 1994. ABNORMAL-DEVELOPMENT OF PERIPHERAL LYMPHOID ORGANS IN MICE DEFICIENT IN LYMPHOTOXIN. *Science*, 264, 703-707.
- DEWECK, A. L., KRISTENSEN, F., JONCOURT, F., BETTENS, F., WALKER, C. & WANG, Y. 1984. ANALYSIS OF LYMPHOCYTE-PROLIFERATION

- BY CYTOFLUOROMETRIC TECHNIQUES IN AGING AND VARIOUS CLINICAL CONDITIONS. *Asian Pacific Journal of Allergy and Immunology*, 2, 253-261.
- DHEDA, K., HUGGETT, J. F., BUSTIN, S. A., JOHNSON, M. A., ROOK, G. & ZUMLA, A. 2004. Validation of housekeeping genes for normalizing RNA expression in real-time PCR. *Biotechniques*, 37, 112-+.
- DILLON, C. T., LAY, P. A., BONIN, A. M., CHOLEWA, M. & LEGGE, G. J. F. 2000. Permeability, cytotoxicity, and genotoxicity of Cr(III) complexes and some Cr(V) analogues in V79 Chinese hamster lung cells. *Chemical Research in Toxicology*, 13, 742-748.
- DING, J., LIN, L., HANG, W. & YAN, X. M. 2009. Beryllium uptake and related biological effects studied in THP-1 differentiated macrophages. *Metallomics*, 1, 471-478.
- DOMINGOS, R. F., TUFENKJI, N. & WILKINSON, K. J. 2009. Aggregation of Titanium Dioxide Nanoparticles: Role of a Fulvic Acid. *Environmental Science & Technology*, 43, 1282-1286.
- DORRESTEIJN, M. J. D., VAN DER HOEVEN, J.G.PICKKERS, P. 2006. Lipopolysaccharide stimulated whole blood cytokine production does not predict the inflammatory response in human endotoxemia. *Innate Immunity*, 16, 248-253.
- DUNSTAN, E., SANGHRAJKA, A. P., TILLEY, S., UNWIN, P., BLUNN, G., CANNON, S. R. & BRIGGS, T. W. R. 2005. Metal ion levels after metal-on-metal proximal femoral replacements - A 30-year follow-up. *Journal of Bone and Joint Surgery-British Volume*, 87B, 628-631.
- EBREO, D., KHAN, A., EL-MELIGY, M., ARMSTRONG, C. & PETER, V. 2011. Metal ion levels decrease after revision for metallosis arising from large-diameter metal-on-metal hip arthroplasty. *Acta Orthopaedica Belgica*, 77, 777-781.
- ECKHARDT, W., BELLMANN, K. & KOLB, H. 1999. Regulation of inducible nitric oxide synthase expression in beta cells by environmental factors: heavy metals. *Biochemical Journal*, 338, 695-700.
- EDGAR, R. C. 2004. MUSCLE: multiple sequence alignment with high accuracy and high throughput. *Nucleic Acids Research*, 32, 1792-1797.
- ELLIOTT, P., PEAKMAN, T. C. & BIOBANK, U. K. 2008. The UK Biobank sample handling and storage protocol for the collection, processing and archiving of human blood and urine. *International Journal of Epidemiology*, 37, 234-244.
- EPSTEIN, N. J., BRAGG, W. E., MA, T., SPANOGLA, J., SMITH, R. L. & GOODMAN, S. B. 2005. UHMWPE wear debris upregulates mononuclear cell proinflammatory gene expression in a novel murine model of intramedullary particle disease. *Acta Orthopaedica*, 76, 412-420.
- ESTELLER, M. 2002. CpG island hypermethylation and tumor suppressor genes: a booming present, a brighter future. *Oncogene*, 21, 5427-5440.
- FIELD, R. E. & RAJAKULENDRAN, K. 2011. The Labro-Acetabular Complex. *Journal of Bone and Joint Surgery-American Volume*, 93A, 22-27.
- FIORITO, S., MAGRINI, L. & GOALARD, C. 2003. Pro-inflammatory and anti-inflammatory circulating cytokines and periprosthetic osteolysis. *Journal of Bone and Joint Surgery-British Volume*, 85B, 1202-1206.

- FLEIGE, S. & PFAFFL, M. W. 2006. RNA integrity and the effect on the real-time qRT-PCR performance. *Molecular Aspects of Medicine*, 27, 126-139.
- FLEIGE, S., WALF, V., HUCH, S., PRGOMET, C., SEHM, J. & PFAFFL, M. W. 2006. Comparison of relative mRNA quantification models and the impact of RNA integrity in quantitative real-time RT-PCR. *Biotechnology Letters*, 28, 1601-1613.
- FORBES, J. R. & GROS, P. 2003. Iron, manganese, and cobalt transport by Nramp1 (Slc11a1) and Nramp2 (Slc11a2) expressed at the plasma membrane. *Blood*, 102, 1884-1892.
- FORDHAM, R., SKINNER, J., WANG, X., NOLAN, J. & EXETER PRIMARY OUTCOME STUDY, G. 2012. The economic benefit of hip replacement: a 5-year follow-up of costs and outcomes in the Exeter Primary Outcomes Study. *Bmj Open*, 2.
- FORNSAGLIO, J. L., O'BRIEN, T. J. & PATIERNO, S. R. 2005. Differential impact of ionic and coordinate covalent chromium (Cr)-DNA binding on DNA replication. *Molecular and Cellular Biochemistry*, 279, 149-155.
- FORS, R., STENBERG, B., STENLUND, H. & PERSSON, M. 2012. Nickel allergy in relation to piercing and orthodontic appliances - a population study. *Contact Dermatitis*, 67, 342-350.
- FRANZ, S., RAMMELT, S., SCHARNWEBER, D. & SIMON, J. C. 2011. Immune responses to implants - A review of the implications for the design of immunomodulatory biomaterials. *Biomaterials*, 32, 6692-6709.
- FREEMAN, B., SMITH, N., CURTIS, C., HUCKETT, L., MILL, J. & CRAIG, I. W. 2003. DNA from buccal swabs recruited by mail: Evaluation of storage effects on long-term stability and suitability for multiplex polymerase chain reaction genotyping. *Behavior Genetics*, 33, 67-72.
- FRIESENBICHLER, J., MAURER-ERTL, W., SADOGLI, P., LOVSE, T., WINDHAGER, R. & LEITHNER, A. 2012. Serum metal ion levels after rotating-hinge knee arthroplasty: comparison between a standard device and a megaprosthesis. *International Orthopaedics*, 36, 539-544.
- FRIGERIO, E., PIGATTO, P. D., GUZZI, G. & ALTOMARE, G. 2011. Metal sensitivity in patients with orthopaedic implants: a prospective study. *Contact Dermatitis*, 64, 273-279.
- FRITZSCHE, J., BORISCH, C. & SCHAEFER, C. 2012. Case Report: High Chromium and Cobalt Levels in a Pregnant Patient with Bilateral Metal-on-Metal Hip Arthroplasties. *Clinical Orthopaedics and Related Research*, 470, 2325-2331.
- FUJIYOSHI, K. & HUNT, J. A. 2006. The effect of particulate material on the regulation of chemokine receptor expression in leukocytes. *Biomaterials*, 27, 3888-3896.
- GALLO, J., GOODMAN, S. B., KONTTINEN, Y. T. & RASKA, M. 2013. Particle disease: Biologic mechanisms of periprosthetic osteolysis in total hip arthroplasty. *Innate Immunity*, 19, 213-224.
- GAMBI, N., TRAMONTANO, F. & QUESADA, P. 2008. Poly(ADPR)potymerase inhibition and apoptosis induction in cDDP-treated human carcinoma cell lines. *Biochemical Pharmacology*, 75, 2356-2363.
- GAMERDINGER, K., MOULON, C., KARP, D. R., VAN BERGEN, J., KONING, F., WILD, D., PFLUGFELDER, U. & WELTZIEN, H. U. 2003. A new type

- of metal recognition by human T cells: Contact residues for peptide-independent bridging of T cell receptor and major histocompatibility complex by nickel. *Journal of Experimental Medicine*, 197, 1345-1353.
- GARCIA, A., SERRANO, A., ABRIL, E., JIMENEZ, P., REAL, L. M., CANTON, J., GARRIDO, F. & RUIZ-CABELLO, F. 1999. Differential effect on U937 cell differentiation by targeting transcriptional factors implicated in tissue- or stage-specific induced integrin expression. *Experimental Hematology*, 27, 353-364.
- GARRIGUES, G. E., CHO, D. R., RUBASH, H. E., GOLDRING, S. R., HERNDON, J. H. & SHANBHAG, A. S. 2005. Gene expression clustering using self-organizing maps: analysis of the macrophage response to particulate biomaterials. *Biomaterials*, 26.
- GEBOREK, P., SAXNE, T., PETTERSSON, H. & WOLLHEIM, F. A. 1989. SYNOVIAL-FLUID ACIDOSIS CORRELATES WITH RADIOLOGICAL JOINT DESTRUCTION IN RHEUMATOID-ARTHRITIS KNEE JOINTS. *Journal of Rheumatology*, 16, 468-472.
- GEISSMANN, F., MANZ, M. G., JUNG, S., SIEWEKE, M. H., MERAD, M. & LEY, K. 2010. Development of Monocytes, Macrophages, and Dendritic Cells. *Science*, 327, 656-661.
- GENG, D., XU, Y., YANG, H., WANG, J., ZHU, X., ZHU, G. & WANG, X. 2010. Protection against titanium particle induced osteolysis by cannabinoid receptor 2 selective antagonist. *Biomaterials*, 31, 1996-2000.
- GENG, D. C., MAO, H. Q., WANG, J. H., ZHU, X. S., HUANG, C., CHEN, L., YANG, H. L. & XU, Y. Z. 2011. Protective effects of COX-2 inhibitor on titanium-particle-induced inflammatory osteolysis via the down-regulation of RANK/RANKL. *Acta Biomaterialia*, 7, 3216-3221.
- GERMAIN, M. A., HATTON, A., WILLIAMS, S., MATTHEWS, J. B., STONE, M. H., FISHER, J. & INGHAM, E. 2003. Comparison of the cytotoxicity of clinically relevant cobalt-chromium and alumina ceramic wear particles in vitro. *Biomaterials*, 24, 469-479.
- GERRIETS, V. A. & RATHMELL, J. C. 2012. Metabolic pathways in T cell fate and function. *Trends in Immunology*, 33, 168-173.
- GILBERT, C. J., CHEUNG, A., BUTANY, J., ZYWIEL, M. G., SYED, K., MCDONALD, M., WONG, F. & OVERGAARD, C. 2013. Hip Pain and Heart Failure: The Missing Link. *Canadian Journal of Cardiology*, 29.
- GILL, H. S., GRAMMATOPOULOS, G., ADSHEAD, S., TSIALOGIANNIS, E. & TSIRIDIS, E. 2012a. Molecular and immune toxicity of CoCr nanoparticles in MoM hip arthroplasty. *Trends in Molecular Medicine*, 18, 145-155.
- GILL, I. P. S., WEBB, J., SLOAN, K. & BEAVER, R. J. 2012b. Corrosion at the neck-stem junction as a cause of metal ion release and pseudotumour formation. *Journal of Bone and Joint Surgery-British Volume*, 94B, 895-900.
- GLANT, T. T. & JACOBS, J. J. 1994. RESPONSE OF 3 MURINE MACROPHAGE POPULATIONS TO PARTICULATE DEBRIS - BONE-RESORPTION IN ORGAN-CULTURES. *Journal of Orthopaedic Research*, 12, 720-731.
- GOMEZ, P. F. & MORCUENDE, J. A. 2005. Early attempts at hip arthroplasty--1700s to 1950s. *The Iowa orthopaedic journal*, 25, 25-9.

- GONG, X., TAO, R. & LI, Z. 2006. Quantification of RNA damage by reverse transcription polymerase chain reactions. *Analytical Biochemistry*, 357, 58-67.
- GONZALEZ-ROCA, E., GARCIA-ALBENIZ, X., RODRIGUEZ-MULERO, S., GOMIS, R. R., KORNACKER, K. & AUER, H. 2010. Accurate Expression Profiling of Very Small Cell Populations. *Plos One*, 5.
- GOODMAN, S. B. 2007. Wear particles, periprosthetic osteolysis and the immune system. *Biomaterials*, 28, 5044-5048.
- GOODMAN, S. B., HUIE, P., SONG, Y., SCHURMAN, D., MALONEY, W., WOOLSON, S. & SIBLEY, R. 1998. Cellular profile and cytokine production at prosthetic interfaces - Study of tissues retrieved from revised hip and knee replacements. *Journal of Bone and Joint Surgery-British Volume*, 80B, 531-539.
- GOODMAN, S. B. & MA, T. 2010. Cellular chemotaxis induced by wear particles from joint replacements. *Biomaterials*, 31, 5045-5050.
- GORDON, A., GREENFIELD, E. M., EASTELL, R., KISS-TOTH, E. & WILKINSON, J. M. 2010. Individual Susceptibility to Periprosthetic Osteolysis Is Associated with Altered Patterns of Innate Immune Gene Expression in Response to Pro-Inflammatory Stimuli. *Journal of Orthopaedic Research*, 28, 1127-1135.
- GORDON, S. & MARTINEZ, F. O. 2010. Alternative Activation of Macrophages: Mechanism and Functions. *Immunity*, 32, 593-604.
- GORDON, S. & TAYLOR, P. R. 2005. Monocyte and macrophage heterogeneity. *Nature Reviews Immunology*, 5, 953-964.
- GRANCHI, D., CENNI, E., CIAPETTI, G., SAVARINO, L., STEA, S., GAMBERINI, S., GORI, A. & PIZZOFERRATO, A. 1998. Cell death induced by metal ions: necrosis or apoptosis? *Journal of Materials Science-Materials in Medicine*, 9, 31-37.
- GRAY, S. J. & STERLING, K. 1950. THE TAGGING OF RED CELLS AND PLASMA PROTEINS WITH RADIOACTIVE CHROMIUM. *Journal of Clinical Investigation*, 29, 1604-1613.
- GRIFFIN, K. P., WARD, D. T., LIU, W., STEWART, G., MORRIS, I. D. & SMITH, C. P. 2005. Differential expression of divalent metal transporter DMT1 (Slc11a2) in the spermatogenic epithelium of the developing and adult rat testis. *American Journal of Physiology-Cell Physiology*, 288, C176-C184.
- GRIFFIN, W. L., FEHRING, T. K., KUDRNA, J. C., SCHMIDT, R. H., CHRISTIE, M. J., ODUM, S. M. & DENNOS, A. C. 2012. Are metal ion levels a useful trigger for surgical intervention? *The Journal of arthroplasty*, 27, 32-6.
- GRIMAUD, E., SOUBIGOU, L., COUILLAUD, S., COIPEAU, P., MOREAU, A., PASSUTI, N., GOUIN, F., REDINI, F. & HEYMANN, D. 2003. Receptor activator of nuclear factor kappa B ligand (RANKL)/osteoprotegerin (OPG) ratio is increased in severe osteolysis. *American Journal of Pathology*, 163, 2021-2031.
- GRUBL, A., MARKER, M., BRODNER, W., GIUREA, A., HEINZE, G., MEISINGER, V., ZEHETGRUBER, H. & KOTZ, R. 2007. Long-term follow-up of metal-on-metal total hip replacement. *Journal of Orthopaedic Research*, 25, 841-848.

- HABETSWALLNER, D., PELOSI, E., BULGARINI, D., CAMAGNA, A., SAMOGGIA, P., MONTESORO, E., GIANNELLA, G., LAZZARO, D., ISACCHI, G., TESTA, U. & PESCHLE, C. 1988. ACTIVATION AND PROLIFERATION OF NORMAL RESTING HUMAN LYMPHOCYTES-T IN SERUM-FREE CULTURE - ROLE OF IL-4 AND IL-6. *Immunology*, 65, 357-364.
- HAGIWARA, H., HAYASHI, N., MITA, E., NAITO, M., KASAHARA, A., FUSAMOTO, H. & KAMADA, T. 1993. QUANTITATION OF HEPATITIS-C VIRUS-RNA IN SERUM OF ASYMPTOMATIC BLOOD-DONORS AND PATIENTS WITH TYPE-C CHRONIC LIVER-DISEASE. *Hepatology*, 17, 545-550.
- HALEEM-SMITH, H., ARGINTAR, E., BUSH, C., HAMPTON, D., POSTMA, W. F., CHEN, F. H., RIMINGTON, T., LAMB, J. & TUAN, R. S. 2012. Biological responses of human mesenchymal stem cells to titanium wear debris particles. *Journal of Orthopaedic Research*, 30, 853-863.
- HALLAB, N., MERRITT, K. & JACOBS, J. J. 2001a. Metal sensitivity in patients with orthopaedic implants. *Journal of Bone and Joint Surgery-American Volume*, 83A, 428-436.
- HALLAB, N. J., ANDERSON, S., STAFFORD, T., GLANT, T. & JACOBS, J. J. 2005. Lymphocyte responses in patients with total hip arthroplasty. *Journal of Orthopaedic Research*, 23, 384-391.
- HALLAB, N. J. & JACOBS, J. J. 2009. Biologic effects of implant debris. *Bulletin of the NYU hospital for joint diseases*, 67, 182-8.
- HALLAB, N. J., MIKECZ, K., VERMES, C., SKIPOR, A. & JACOBS, J. J. 2001b. Differential lymphocyte reactivity to serum-derived metal-protein complexes produced from cobalt-based and titanium-based implant alloy degradation. *Journal of Biomedical Materials Research*, 56, 427-436.
- HALLAB, N. J., VERMES, C., MESSINA, C., ROEBUCK, K. A., GLANT, T. T. & JACOBS, J. J. 2002. Concentration- and composition-dependent effects of metal ions on human MG-63 osteoblasts. *Journal of Biomedical Materials Research*, 60, 420-433.
- HALSALL, A., RAVETTO, P., REYES, Y., THELWELL, N., DAVIDSON, A., GAUT, R. & LITTLE, S. 2008. The quality of DNA extracted from liquid or dried blood is not adversely affected by storage at 4 degrees C for up to 24 h. *International Journal of Epidemiology*, 37, 7-10.
- HAMADOUCHE, M., BOUTIN, P., DAUSSANGE, J., BOLANDER, M. E. & SEDEL, L. 2002. Alumina-on-alumina total hip arthroplasty - A minimum 18.5-year follow-up study. *Journal of Bone and Joint Surgery-American Volume*, 84A, 69-77.
- HANAWA, T. 2004. Metal ion release from metal implants. *Materials Science & Engineering C-Biomimetic and Supramolecular Systems*, 24, 745-752.
- HANAWA, T., HIROMOTO, S. & ASAMI, K. 2001. Characterization of the surface oxide film of a Co-Cr-Mo alloy after being located in quasi-biological environments using XPS. *Applied Surface Science*, 183, 68-75.
- HANSSON, G. K. & LIBBY, P. 2006. The immune response in atherosclerosis: a double-edged sword. *Nature Reviews Immunology*, 6, 508-519.
- HAO, H. N., ZHENG, B. R., NASSER, S., REN, W. P., LATTEIER, M., WOOLEY, P. & MORAWA, L. 2010. The roles of monocytic heat shock protein 60 and

- Toll-like receptors in the regional inflammation response to wear debris particles. *Journal of Biomedical Materials Research Part A*, 92A, 1373-1381.
- HARRIS, W. H. 1994. OSTEOLYSIS AND PARTICLE DISEASE IN HIP-REPLACEMENT - A REVIEW. *Acta Orthopaedica Scandinavica*, 65, 113-123.
- HARRIS, W. H. 2009. The First 50 Years of Total Hip Arthroplasty: Lessons Learned. *Clinical Orthopaedics and Related Research*, 467, 28-31.
- HART, A. J., HESTER, T., SINCLAIR, K., POWELL, J. J., GOODSHIP, A. E., PELE, L., FERSHT, N. L. & SKINNER, J. 2006. The association between metal ions from hip resurfacing and reduced T-cell counts. *Journal of Bone and Joint Surgery-British Volume*, 88B.
- HART, A. J., QUINN, P. D., SAMPSON, B., SANDISON, A., ATKINSON, K. D., SKINNER, J. A., POWELL, J. J. & MOSSELMANS, J. F. W. 2010. The chemical form of metallic debris in tissues surrounding metal-on-metal hips with unexplained failure. *Acta Biomaterialia*, 6, 4439-4446.
- HART, A. J., SABAH, S., HENCKEL, J., LEWIS, A., COBB, J., SAMPSON, B., MITCHELL, A. & SKINNER, J. A. 2009. The painful metal-on-metal hip resurfacing. *Journal of Bone and Joint Surgery-British Volume*, 91B, 738-744.
- HART, A. J., SABAH, S. A., BANDI, A. S., MAGGIORE, P., TARASSOLI, P., SAMPSON, B. & SKINNER, J. A. 2011. Sensitivity and specificity of blood cobalt and chromium metal ions for predicting failure of metal-on-metal hip replacement. *Journal of Bone and Joint Surgery-British Volume*, 93B, 1308-1313.
- HASEGAWA, M., YOSHIDA, K., WAKABAYASHI, H. & SUDO, A. 2012. Cobalt and Chromium Ion Release After Large-Diameter Metal-on-Metal Total Hip Arthroplasty. *Journal of Arthroplasty*, 27, 990-996.
- HAYNES, D. R. 2004. Bone lysis and inflammation. *Inflammation Research*, 53, 596-600.
- HAYNES, D. R., CROTTI, T. N., LORIC, M., BAIN, G. I., ATKINS, G. J. & FINDLAY, D. M. 2001. Osteoprotegerin and receptor activator of nuclear factor kappaB ligand (RANKL) regulate osteoclast formation by cells in the human rheumatoid arthritic joint. *Rheumatology*, 40, 623-630.
- HEGDE, M. L., HAZRA, T. K. & MITRA, S. 2008. Early steps in the DNA base excision/single-strand interruption repair pathway in mammalian cells. *Cell Research*, 18, 27-47.
- HEGEWALD, J., UTER, W., PFAHLBERG, A., GEIER, J., SCHNUCH, A. & IVDK 2005. A multifactorial analysis of concurrent patch-test reactions to nickel, cobalt, and chromate. *Allergy*, 60, 372-378.
- HERMIDA, J. C., BERGULA, A., CHEN, P., COLWELL, C. W. & D'LIMA, D. D. 2003. Comparison of the wear rates of twenty-eight and thirty-two-millimeter femoral heads on cross-linked polyethylene acetabular cups in a wear simulator. *Journal of Bone and Joint Surgery-American Volume*, 85A, 2325-2331.
- HERSHEY, A. D., TANG, Y., POWERS, S. W., KABBOUCHE, M. A., GILBERT, D. L., GLAUSER, T. A. & SHARP, F. R. 2004. Genomic abnormalities in patients with migraine and chronic migraine: Preliminary blood gene expression suggests platelet abnormalities. *Headache*, 44, 994-1004.

- HEWISON, M., BRENNAN, A., SINGHRANGER, R., WALTERS, J. C., KATZ, D. R. & ORIORDAN, J. L. H. 1992. THE COMPARATIVE ROLE OF 1,25-DIHYDROXYCHOLECALCIFEROL AND PHORBOL ESTERS IN THE DIFFERENTIATION OF THE U937 CELL-LINE. *Immunology*, 77, 304-311.
- HO-PUN-CHEUNG, A., BASCOUL-MOLLEVI, C., ASSENAT, E., BOISSIERE-MICHOT, F., BIBEAU, F., CELLIER, D., YCHOU, M. & LOPEZ-CRAPEZ, E. 2009. Reverse transcription-quantitative polymerase chain reaction: description of a RIN-based algorithm for accurate data normalization. *Bmc Molecular Biology*, 10.
- HOFBAUER, L. C., NEUBAUER, A. & HEUFELDER, A. E. 2001. Receptor activator of nuclear factor-kappa B ligand and osteoprotegerin - Potential implications for the pathogenesis and treatment of malignant bone diseases. *Cancer*, 92, 460-470.
- HOLDING, C. A., FINDLAY, D. M., STAMENKOV, R., NEALE, S. D., LUCAS, H., DHARMAPATNI, A., CALLARY, S. A., SHRESTHA, K. R., ATKINS, G. J., HOWIE, D. W. & HAYNES, D. R. 2006. The correlation of RANK, RANKL and TNF alpha expression with bone loss volume and polyethylene wear debris around hip implants. *Biomaterials*, 27, 5212-5219.
- HOLLANDER, M. C., ALAMO, I., JACKMAN, J., WANG, M. G., MCBRIDE, O. W. & FORNACE, A. J. 1993. ANALYSIS OF THE MAMMALIAN GADD45 GENE AND ITS RESPONSE TO DNA-DAMAGE. *Journal of Biological Chemistry*, 268, 24385-24393.
- HORNUNG, V., BAUERNFEIND, F., HALLE, A., SAMSTAD, E. O., KONO, H., ROCK, K. L., FITZGERALD, K. A. & LATZ, E. 2008. Silica crystals and aluminum salts activate the NALP3 inflammasome through phagosomal destabilization. *Nature Immunology*, 9, 847-856.
- HOSOI, T., SASAKI, M., MIYAHARA, T., HASHIMOTO, C., MATSUO, S., YOSHII, M. & OZAWA, K. 2008. Endoplasmic Reticulum Stress Induces Leptin Resistance. *Molecular Pharmacology*, 74, 1610-1619.
- HOU, L., ZHANG, X., WANG, D. & BACCARELLI, A. 2012. Environmental chemical exposures and human epigenetics. *International Journal of Epidemiology*, 41, 79-105.
- HOUGEE, S., SANDERS, A., FABER, J., GRAUS, Y. M. F., VAN DEN BERG, W. B., GARSSSEN, J., SMIT, H. F. & HOIJER, M. A. 2005. Decreased pro-inflammatory cytokine production by LPS-stimulated PBMC upon in vitro incubation with the flavonoids apigenin, luteolin or chrysin, due to selective elimination of monocytes/macrophages. *Biochemical Pharmacology*, 69, 241-248.
- HOWLING, G. I., SAKODA, H., ANTONARULRAJAH, A., MARRS, H., STEWART, T. D., APPLEYARD, S., RAND, B., FISHER, J. & INGHAM, E. 2003. Biological response to wear debris generated in carbon based composites as potential bearing surfaces for artificial hip joints. *Journal of Biomedical Materials Research Part B-Applied Biomaterials*, 67B, 758-764.
- HU, X. & IVASHKIV, L. B. 2009. Cross-regulation of Signaling Pathways by Interferon-gamma: Implications for Immune Responses and Autoimmune Diseases. *Immunity*, 31, 539-550.

- HUANG, Z. X. L., FAILLA, M. L. & REEVES, P. G. 2001. Differentiation of human U937 promonocytic cells is impaired by moderate copper deficiency. *Experimental Biology and Medicine*, 226, 222-228.
- HUGGETT, J., DHEDA, K., BUSTIN, S. & ZUMLA, A. 2005. Real-time RT-PCR normalisation; strategies and considerations. *Genes and Immunity*, 6, 279-284.
- HUK, O. L., CATELAS, I., MWALE, F., ANTONIOU, J., ZUKOR, D. J. & PETIT, A. 2004. Induction of apoptosis and necrosis by metal ions in vitro. *Journal of Arthroplasty*, 19, 84-87.
- HUK, O. L., ZUKOR, D. J., RALSTON, W., LISBONA, A. & PETIT, A. 2001. Apoptosis in interface membranes of aseptically loose total hip arthroplasty. *Journal of Materials Science-Materials in Medicine*, 12, 653-658.
- HUME, D. A. 2006. The mononuclear phagocyte system. *Current Opinion in Immunology*, 18, 49-53.
- HUNDRIC-HASPL, Z., PECINA, M., HASPL, M., TOMICIC, M. & JUKIC, I. 2006. Plasma cytokines as markers of aseptic prosthesis loosening. *Clinical orthopaedics and related research*, 453, 299-304.
- HUO, M. H., DUMONT, G. D., KNIGHT, J. R. & MONT, M. A. 2011. What's New in Total Hip Arthroplasty. *Journal of Bone and Joint Surgery-American Volume*, 93A, 1944-1950.
- Iavicoli, I., GIANLUCA, F., ALESSANDRELLI, M., RAFAELLA, C., DE SANTIS, V., SALVATORI, S., ALIMONTI, A. & CARELLI, G. 2006. The release of metals from metal-on-metal surface arthroplasty of the hip. *Journal of Trace Elements in Medicine and Biology*, 20, 25-31.
- IMBEAUD, S., GRAUDENS, E., BOULANGER, V., BARLET, X., ZABORSKI, P., EVENO, E., MUELLER, O., SCHROEDER, A. & AUFRAY, C. 2005. Towards standardization of RNA quality assessment using user-independent classifiers of microcapillary electrophoresis traces. *Nucleic Acids Research*, 33, 12.
- INGHAM, E., GREEN, T. R., STONE, M. H., KOWALSKI, R., WATKINS, N. & FISHER, J. 2000. Production of TNF-alpha and bone resorbing activity by macrophages in response to different types of bone cement particles. *Biomaterials*, 21, 1005-1013.
- IWAMA, K., NAKAJO, S., AIUCHI, T. & NAKAYA, K. 2001. Apoptosis induced by arsenic trioxide in leukemia U937 cells is dependent on activation of p38, inactivation of ERK and the Ca²⁺-dependent production of superoxide. *International Journal of Cancer*, 92, 518-526.
- IZRAELI, S., PFLEIDERER, C. & LION, T. 1991. DETECTION OF GENE-EXPRESSION BY PCR AMPLIFICATION OF RNA DERIVED FROM FROZEN HEPARINIZED WHOLE-BLOOD. *Nucleic Acids Research*, 19, 6051-6051.
- JACOB, F., GUERTLER, R., NAIM, S., NIXDORF, S., FEDIER, A., HACKER, N. F. & HEINZELMANN-SCHWARZ, V. 2013. Careful Selection of Reference Genes Is Required for Reliable Performance of RT-qPCR in Human Normal and Cancer Cell Lines. *Plos One*, 8.
- JAKOBSEN, S. S., LARSEN, A., STOLTENBERG, M., BRUUN, J. M. & SOBALLE, K. 2007. Effects of as-cast and wrought cobalt-chrome-molybdenum and titanium-aluminium-vanadium alloys on cytokine gene

- expression and protein secretion in J774A.1 macrophages. *European Cells & Materials*, 14, 45-54.
- JIANG, Y., ZHANG, K., DIE, J., SHI, Z., ZHAO, H. & WANG, K. 2011. A Systematic Review of Modern Metal-on-Metal Total Hip Resurfacing vs Standard Total Hip Arthroplasty in Active Young Patients. *Journal of Arthroplasty*, 26, 419-426.
- JIRANEK, W. A., MACHADO, M., JASTY, M., JEVSEVAR, D., WOLFE, H. J., GOLDRING, S. R., GOLDBERG, M. J. & HARRIS, W. H. 1993. PRODUCTION OF CYTOKINES AROUND LOOSENEED CEMENTED ACETABULAR COMPONENTS - ANALYSIS WITH IMMUNOHISTOCHEMICAL TECHNIQUES AND IN-SITU HYBRIDIZATION. *Journal of Bone and Joint Surgery-American Volume*, 75A, 863-879.
- JONES, D. M., MARSH, J. L., NEPOLA, J. V., JACOBS, J. J., SKIPOR, A. K., URBAN, R. M., GILBERT, J. L. & BUCKWALTER, J. A. 2001. Focal osteolysis at the junctions of a modular stainless-steel femoral intramedullary nail. *Journal of Bone and Joint Surgery-American Volume*, 83A, 537-548.
- JONES, L. C., TUCCI, M. & FRONDOZA, C. 2006. Macrophages and fibroblasts respond differently to PMMA particles and mechanical strain. *Biomedical Sciences Instrumentation, Vol 42*, 42, 223-230.
- JOSHI, M. G., ADVANI, S. G., MILLER, F. & SANTARE, M. H. 2000. Analysis of a femoral hip prosthesis designed to reduce stress shielding. *Journal of Biomechanics*, 33, 1655-1662.
- JOYCE, T. J., LANGTON, D. J. & NARGOL, A. V. F. 2011. A study of the wear of explanted metal-on-metal resurfacing hip prostheses. *Tribology International*, 44, 517-522.
- KAGI, D., HO, A., ODERMATT, B., ZAKARIAN, A., OHASHI, P. S. & MAK, T. W. 1999. TNF receptor 1-dependent beta cell toxicity as an effector pathway in autoimmune diabetes. *Journal of Immunology*, 162, 4598-4605.
- KANAJI, A., CAICEDO, M. S., VIRDI, A. S., SUMNER, D. R., HALLAB, N. J. & SENA, K. 2009. Co-Cr-Mo alloy particles induce tumor necrosis factor alpha production in MLO-Y4 osteocytes: A role for osteocytes in particle-induced inflammation. *Bone*, 45, 528-533.
- KARAS, S. 2012. Outcomes of birmingham hip resurfacing: a systematic review. *Asian journal of sports medicine*, 3, 1-7.
- KASTEN, U., HARTWIG, A. & BEYERSMANN, D. 1992. MECHANISMS OF COBALT(II) UPTAKE INTO V79-CHINESE HAMSTER-CELLS. *Archives of Toxicology*, 66, 592-597.
- KEEGAN, G. M., LEARMONTH, I. D. & CASE, C. P. 2007. Orthopaedic metals and their potential toxicity in the arthroplasty patient - Review of current knowledge and future strategies. *Journal of Bone and Joint Surgery-British Volume*, 89B, 567-573.
- KEMPF, I. & SEMLITSCH, M. 1990. MASSIVE WEAR OF A STEEL BALL HEAD BY CERAMIC FRAGMENTS IN THE POLYETHYLENE ACETABULAR CUP AFTER REVISION OF A TOTAL HIP-PROSTHESIS WITH FRACTURED CERAMIC BALL. *Archives of Orthopaedic and Trauma Surgery*, 109, 284-287.

- KHAN, R. J. K., WIMHURST, J., FOROUGH, S. & TOMS, A. 2009. The natural history of metallosis from catastrophic failure of a polyethylene liner in a total hip. *The Journal of arthroplasty*, 24, 1144.e1-4.
- KHOSLA, S. 2001. Minireview: The OPG/RANKL/RANK system. *Endocrinology*, 142, 5050-5055.
- KIM, P. R., BEAULE, P. E., DUNBAR, M., LEE, J. K. L., BIRKETT, N., TURNER, M. C., YENUGADHATI, N., ARMSTRONG, V. & KREWSKI, D. 2011. Cobalt and Chromium Levels in Blood and Urine Following Hip Resurfacing Arthroplasty with the Conserve Plus Implant. *Journal of Bone and Joint Surgery-American Volume*, 93A, 107-117.
- KIM, S. H., JOHNSON, V. J. & SHARMA, R. P. 2002. Mercury inhibits nitric oxide production but activates proinflammatory cytokine expression in murine macrophage: differential modulation of NF-kappa B and p38 MAPK signaling pathways. *Nitric Oxide-Biology and Chemistry*, 7, 67-74.
- KIM, Y. J., KASSAB, F., BERVEN, S. H., ZURAKOWSKI, D., HRESKO, M. T., EMANS, J. B. & KASSER, J. R. 2005. Serum levels of nickel and chromium after instrumented posterior spinal arthrodesis. *Spine*, 30, 923-926.
- KIRKEGAARD, T., ROTH, A. G., PETERSEN, N. H. T., MAHALKA, A. K., OLSEN, O. D., MOILANEN, I., ZYLICZ, A., KNUDSEN, J., SANDHOFF, K., ARENZ, C., KINNUNEN, P. K. J., NYLANDSTED, J. & JAATTELA, M. 2010. Hsp70 stabilizes lysosomes and reverts Niemann-Pick disease-associated lysosomal pathology. *Nature*, 463, 549-U171.
- KNIGHT, S. R., AUJLA, R. & BISWAS, S. P. 2011. Total Hip Arthroplasty - over 100 years of operative history *Orthopedic Reviews* 3:e16, 72-74.
- KOCBACH, A., TODANDSDAL, A. I., LAG, M., REFSNES, A. & SCHWARZE, P. E. 2008. Differential binding of cytokines to environmentally relevant particles: A possible source for misinterpretation of in vitro results? *Toxicology Letters*, 176, 131-137.
- KOEDRITH, P. & SEO, Y. R. 2011. Advances in Carcinogenic Metal Toxicity and Potential Molecular Markers. *International Journal of Molecular Sciences*, 12, 9576-9595.
- KOHILAS, K., LYONS, M., LOFTHOUSE, R., FRONDOZA, C. G., JINNAH, R. & HUNGERFORD, D. S. 1999. Effect of prosthetic titanium wear debris on mitogen-induced monocyte and lymphoid activation. *Journal of Biomedical Materials Research*, 47, 95-103.
- KOLUNDZIC, R., TRKULJA, V. & ORLIC, D. 2012. History and factors of survival of total hip arthroplasty. *Medicinski Glasnik*, 9, 136-142.
- KONDO, M., INAMURA, H., MATSUMURA, K.-I. & MATSUOKA, M. 2012. Cadmium activates extracellular signal-regulated kinase 5 in HK-2 human renal proximal tubular cells. *Biochemical and Biophysical Research Communications*, 421, 490-493.
- KOROVESIS, P., PETSINIS, G., REPANTI, M. & REPANTIS, T. 2006. Metallosis after contemporary metal-on-metal total hip arthroplasty - Five to nine-year follow-up. *Journal of Bone and Joint Surgery-American Volume*, 88A, 1183-1191.
- KOSAKA, N., IGUCHI, H. & OCHIYA, T. 2010. Circulating microRNA in body fluid: a new potential biomarker for cancer diagnosis and prognosis. *Cancer Science*, 101, 2087-2092.

- KOULOVARIS, P., LY, K., IVASHKIV, L. B., BOSTROM, M. P., NESTOR, B. J., SCULCO, T. P. & PURDUE, P. E. 2008. Expression profiling reveals alternative macrophage activation and impaired osteogenesis in periprosthetic osteolysis. *Journal of Orthopaedic Research*, 26, 106-116.
- KRANZ, I., GONZALEZ, J. B., DORFEL, I., GEMEINERT, M., GRIEPENTROG, M., KLAFFKE, D., KNABE, C., OSTERLE, W. & GROSS, U. 2009. Biological response to micron- and nanometer-sized particles known as potential wear products from artificial hip joints: Part II: Reaction of murine macrophages to corundum particles of different size distributions. *Journal of Biomedical Materials Research Part A*, 89A, 390-401.
- KRAVENSKAYA, Y. V. & FEDIRKO, N. V. 2011. Mechanisms Underlying Interaction of Zinc, Lead, and Cobalt with Nonspecific Permeability Pores in the Mitochondrial Membranes. *Neurophysiology*, 43, 163-172.
- KROLL, A., PILLUKAT, M. H., HAHN, D. & SCHNEKENBURGER, J. 2012. Interference of engineered nanoparticles with in vitro toxicity assays. *Archives of Toxicology*, 86, 1123-1136.
- KUKLINA, E. M. 2013. Molecular mechanisms of T-cell anergy. *Biochemistry-Moscow*, 78, 144-156.
- KURTZ, S., ONG, K., LAU, E., MOWAT, F. & HALPERN, M. 2007. Projections of primary and revision hip and knee arthroplasty in the United States from 2005 to 2030. *Journal of Bone and Joint Surgery-American Volume*, 89A, 780-785.
- KWAN TAT, S., PELLETIER, J. P., LAJEUNESSE, D., FAHMI, H., LAVIGNE, M. & MARTEL-PELLETIER, J. 2008. The differential expression of osteoprotegerin (OPG) and receptor activator of nuclear factor kappaB ligand (RANKL) in human osteoarthritic subchondral bone osteoblasts is an indicator of the metabolic state of these disease cells. *Clinical and experimental rheumatology*, 26, 295-304.
- KWON, Y. M., GLYN-JONES, S., SIMPSON, D. J., KAMALI, A., MCLARDY-SMITH, P., GILL, H. S. & MURRAY, D. W. 2010. Analysis of wear of retrieved metal-on-metal hip resurfacing implants revised due to pseudotumours. *Journal of Bone and Joint Surgery-British Volume*, 92B, 356-361.
- KWON, Y. M., OSTLERE, S. J., MCLARDY-SMITH, P., ATHANASOU, N. A., GILL, H. S. & MURRAY, D. W. 2011. "Asymptomatic" Pseudotumors After Metal-on-Metal Hip Resurfacing Arthroplasty. *Journal of Arthroplasty*, 26, 511-518.
- LAHIRI, D. K. & SCHNABEL, B. 1993. DNA ISOLATION BY A RAPID METHOD FROM HUMAN BLOOD-SAMPLES - EFFECTS OF MGCL₂, EDTA, STORAGE TIME, AND TEMPERATURE ON DNA YIELD AND QUALITY. *Biochemical Genetics*, 31, 321-328.
- LANDGRAEBER, S., VON KNOCH, M., LOER, F., BRANKAMP, J., TSOKOS, M., GRABELLUS, F., SCHMID, K. W. & TOTSCH, M. 2009. Association between Apoptosis and CD4(+)/CD8(+) T-Lymphocyte Ratio in Aseptic Loosening after Total Hip Replacement. *International Journal of Biological Sciences*, 5, 182-191.
- LANDGRAEBER, S., VON KNOCH, M., LOER, F., WEGNER, A., TSOKOS, M., HUSSMANN, B. & TOTSCH, M. 2008. Extrinsic and intrinsic pathways of

- apoptosis in aseptic loosening after total hip replacement. *Biomaterials*, 29, 3444-3450.
- LANGTON, D. J., JAMESON, S. S., JOYCE, T. J., HALLAB, N. J., NATU, S. & NARGOL, A. V. F. 2010. Early failure of metal-on-metal bearings in hip resurfacing and large-diameter total hip replacement A CONSEQUENCE OF EXCESS WEAR. *Journal of Bone and Joint Surgery-British Volume*, 92B, 38-46.
- LANGTON, D. J., JAMESON, S. S., JOYCE, T. J., WEBB, J. & NARGOL, A. V. F. 2008. The effect of component size and orientation on the concentrations of metal ions after resurfacing arthroplasty of the hip. *Journal of Bone and Joint Surgery-British Volume*, 90B, 1143-1151.
- LANGTON, D. J., JOYCE, T. J., JAMESON, S. S., LORD, J., VAN ORSOUW, M., HOLLAND, J. P., NARGOL, A. V. F. & DE SMET, K. A. 2011. Adverse reaction to metal debris following hip resurfacing THE INFLUENCE OF COMPONENT TYPE, ORIENTATION AND VOLUMETRIC WEAR. *Journal of Bone and Joint Surgery-British Volume*, 93B, 164-171.
- LARRICK, J. W., FISCHER, D. G., ANDERSON, S. J. & KOREN, H. S. 1980. CHARACTERIZATION OF A HUMAN MACROPHAGE-LIKE CELL-LINE STIMULATED INVITRO - A MODEL OF MACROPHAGE FUNCTIONS. *Journal of Immunology*, 125, 6-12.
- LAVIGNE, M., BELZILE, E. L., ROY, A., MORIN, F., AMZICA, T. & VENDITTOLI, P. A. 2011. Comparison of Whole-Blood Metal Ion Levels in Four Types of Metal-on-Metal Large-Diameter Femoral Head Total Hip Arthroplasty: The Potential Influence of the Adapter Sleeve. *Journal of Bone and Joint Surgery-American Volume*, 93A, 128-136.
- LAWRENCE, D. A. & MCCABE, M. J. 2002. Immunomodulation by metals. *International Immunopharmacology*, 2, 293-302.
- LAZENNEC, J. Y., BOYER, P., POUPON, J., ROUSSEAU, M. A., ROY, C., RAVAUD, P. & CATONNE, Y. 2009. Outcome and serum ion determination up to 11 years after implantation of a cemented metal-on-metal hip prosthesis. *Acta Orthopaedica*, 80, 168-173.
- LEARMONTH, I. D., YOUNG, C. & RORABECK, C. 2007. The operation of the century: total hip replacement. *Lancet*, 370, 1508-1519.
- LEE, P. D., SLADEK, R., GREENWOOD, C. M. T. & HUDSON, T. J. 2002. Control genes and variability: Absence of ubiquitous reference transcripts in diverse mammalian expression studies. *Genome Research*, 12, 292-297.
- LESLIE, I., WILLIAMS, S., BROWN, C., ISAAC, G., JIN, Z. M., INGHAM, E. & FISHER, J. 2008. Effect of bearing size on the long-term wear, wear debris, and ion levels of large diameter metal-on-metal hip replacements - An in vitro study. *Journal of Biomedical Materials Research Part B-Applied Biomaterials*, 87B, 163-172.
- LESSIG, J., NEU, B., GLANDER, H.-J., ARNHOLD, J. & REIBETANZ, U. 2011. Phagocytotic Competence of Differentiated U937 Cells for Colloidal Drug Delivery Systems in Immune Cells. *Inflammation*, 34, 99-110.
- LHOTKA, C., SZEKERES, T., STEFFAN, I., ZHUBER, K. & ZWEYMULLER, K. 2003. Four-year study of cobalt and chromium blood levels in patients managed with two different metal-on-metal total hip replacements. *Journal of Orthopaedic Research*, 21, 189-195.

- LI, M., KONDO, T., ZHAO, Q. L., LI, F. J., TANABE, K., ARAI, Y., ZHOU, Z. C. & KASUYA, M. 2000. Apoptosis induced by cadmium in human lymphoma U937 cells through Ca²⁺-calpain and caspase-mitochondria dependent pathways. *Journal of Biological Chemistry*, 275, 39702-39709.
- LIAO, Y.-F., HUNG, H.-C., HSU, P.-C., KAO, M.-C., HOUR, T.-C., TSAY, G. J. & LIU, G.-Y. 2008. Ornithine decarboxylase interferes with macrophage-like differentiation and matrix metalloproteinase-9 expression by tumor necrosis factor alpha via NF-kappa B. *Leukemia Research*, 32, 1124-1140.
- LIEW, Y. Y., DOCTER, E., RAY, D. W., HUTCHINSON, I. & BROGAN, I. J. 2002. Effect of rapamycin and prednisolone in differentiated THP-1 and U937 cells. *Transplantation Proceedings*, 34, 2872-2873.
- LIU, F. C., QIN, J., WU, H. S., WU, Y. L. & ZHU, Y. L. 2011. Co and Cr accumulation in hair after metal-on-metal hip resurfacing arthroplasty. *Anz Journal of Surgery*, 81, 436-439.
- LIU, W. H. & SAINT, D. A. 2002. A new quantitative method of real time reverse transcription polymerase chain reaction assay based on simulation of polymerase chain reaction kinetics. *Analytical Biochemistry*, 302, 52-59.
- LIVAK, K. J. & SCHMITTGEN, T. D. 2001. Analysis of relative gene expression data using real-time quantitative PCR and the 2(T)(-Delta Delta C) method. *Methods*, 25, 402-408.
- LOHMANN, C. H., SCHWARTZ, Z., KOSTER, G., JAHN, U., BUCHHORN, G. H., MACDOUGALL, M. J., CASASOLA, D., LIU, Y., SYLVIA, V. L., DEAN, D. D. & BOYAN, B. D. 2000. Phagocytosis of wear debris by osteoblasts affects differentiation and local factor production in a manner dependent on particle composition. *Biomaterials*, 21, 551-561.
- LONG, P. H. 2008. Medical Devices in Orthopedic Applications. *Toxicologic Pathology*, 36, 85-91.
- LOPES, L., GODOY, L. M. F., DE OLIVEIRA, C. C., GABARDO, J., SCHADECK, R. J. G. & BUCHI, D. D. 2006. Phagocytosis, endosomal/lysosomal system and other cellular aspects of macrophage activation by Canova medication. *Micron*, 37, 277-287.
- LOWRY, O. H., ROSEBROUGH, N. J., FARR, A. L. & RANDALL, R. J. 1951. PROTEIN MEASUREMENT WITH THE FOLIN PHENOL REAGENT. *Journal of Biological Chemistry*, 193, 265-275.
- LUCARELLI, M., GATTI, A. M., SAVARINO, G., QUATTRONI, P., MARTINELLI, L., MONARI, E. & BORASCHI, D. 2004. Innate defence functions of macrophages can be biased by nano-sized ceramic and metallic particles. *European Cytokine Network*, 15, 339-346.
- LUCKHEERAM, R. V., ZHOU, R., VERMA, A. D. & XIA, B. 2012. CD4(+)T Cells: Differentiation and Functions. *Clinical & Developmental Immunology*.
- LUO, L., PETIT, A., ANTONIOU, J., ZUKOR, D. J., HUK, O. L., LIU, R. C. W., WINNIK, F. M. & MWALE, F. 2005. Effect of cobalt and chromium ions on MMP-1 TIMP-1, and TNF-alpha gene expression in human U937 macrophages: A role for tyrosine kinases. *Biomaterials*, 26, 5587-5593.
- LUSTY, P. J., TAI, C. C., SEW-HOY, R. P., WALTER, W. L., WALTER, W. K. & ZICAT, B. A. 2007. Third-generation alumina-on-alumina ceramic bearings in cementless total hip arthroplasty. *Journal of Bone and Joint Surgery-American Volume*, 89A, 2676-2683.

- LUTTIKHUIZEN, D. T., HARMSSEN, M. C. & VAN LUYN, M. J. A. 2006. Cellular and molecular dynamics in the foreign body reaction. *Tissue Engineering*, 12, 1955-1970.
- LUU-THE, V., PAQUET, N., CALVO, E. & CUMPS, J. 2005. Improved real-time RT-PCR method for high-throughput measurements using second derivative calculation and double correction. *Biotechniques*, 38, 287-293.
- MACDONALD, S. J. 2004. Can a safe level for metal ions in patients with metal-on-metal total hip arthroplasties be determined? *Journal of Arthroplasty*, 19, 71-77.
- MACINTYRE, A. & RATHMELL, J. Activated lymphocytes as a metabolic model for carcinogenesis. *Cancer & Metabolism C7 - 5*, 1, 1-12.
- MAEZAWA, K., NOZAWA, M., MATSUDA, K., SUGIMOTO, M., SHITOTO, K. & KUROSAWA, H. 2009. Serum Chromium Levels Before and After Revision Surgery for Loosened Metal-On-Metal Total Hip Arthroplasty. *Journal of Arthroplasty*, 24, 549-553.
- MAHENDRA, G., PANDIT, H., KLISKEY, K., MURRAY, D., GILL, H. S. & ATHANASOU, N. 2009. Necrotic and inflammatory changes in metal-on-metal resurfacing hip arthroplasties Relation to implant failure and pseudotumor formation. *Acta Orthopaedica*, 80, 653-659.
- MALCHAU, H., HERBERTS, P., EISLER, T., GARELLICK, G. & SODERMAN, P. 2002. The Swedish total hip replacement register. *Journal of Bone and Joint Surgery-American Volume*, 84A, 2-20.
- MALO, A., KRUEGER, B., GOEKE, B. & KUBISCH, C. H. 2013. 4-Phenylbutyric Acid Reduces Endoplasmic Reticulum Stress, Trypsin Activation, and Acinar Cell Apoptosis While Increasing Secretion in Rat Pancreatic Acini. *Pancreas*, 42, 92-101.
- MALVIYA, A., RAMASKANDHAN, J. R., BOWMAN, R., KOMETA, S., HASHMI, M., LINGARD, E. & HOLLAND, J. P. 2011. What advantage is there to be gained using large modular metal-on-metal bearings in routine primary hip replacement? A PRELIMINARY REPORT OF A PROSPECTIVE RANDOMISED CONTROLLED TRIAL. *Journal of Bone and Joint Surgery-British Volume*, 93B, 1602-1609.
- MANDELIN, J., LI, T. F., LIJESTROM, M., KROON, M. E., HANEMAAIJER, R., SANTAVIRTA, S. & KONTTINEN, Y. T. 2003. Imbalance of RANKL/RANK/OPG system in interface tissue in loosening of total hip replacement. *Journal of Bone and Joint Surgery-British Volume*, 85B, 1196-1201.
- MANSSON, B., GEBOREK, P., SAXNE, T. & BJORNSSON, S. 1990. CYTIDINE DEAMINASE ACTIVITY IN SYNOVIAL-FLUID OF PATIENTS WITH RHEUMATOID-ARTHRITIS - RELATION TO LACTOFERRIN, ACIDOSIS, AND CARTILAGE PROTEOGLYCAN RELEASE. *Annals of the Rheumatic Diseases*, 49, 594-597.
- MANTOVANI, A., SICA, A., SOZZANI, S., ALLAVENA, P., VECCHI, A. & LOCATI, M. 2004. The chemokine system in diverse forms of macrophage activation and polarization. *Trends in Immunology*, 25, 677-686.
- MANTOVANI, A., SOZZANI, S., LOCATI, M., ALLAVENA, P. & SICA, A. 2002. Macrophage polarization: tumor-associated macrophages as a paradigm

- for polarized M2 mononuclear phagocytes. *Trends in Immunology*, 23, 549-555.
- MAO, X., PAN, X. Y., ZHAO, S., PENG, X. C., CHENG, T. & ZHANG, X. L. 2012. Protection Against Titanium Particle-Induced Inflammatory Osteolysis by the Proteasome Inhibitor Bortezomib In Vivo. *Inflammation*, 35, 1378-1391.
- MARHFOUR, I., LOPEZ, X. M., LEFKADITIS, D., SALMON, I., ALLAGNAT, F., RICHARDSON, S. J., MORGAN, N. G. & EIZIRIK, D. L. 2012. Expression of endoplasmic reticulum stress markers in the islets of patients with type 1 diabetes. *Diabetologia*, 55, 2417-2420.
- MARKS-KONCZALIK, J., CHU, S. C. & MOSS, J. 1998. Cytokine-mediated transcriptional induction of the human inducible nitric oxide synthase gene requires both activator protein 1 and nuclear factor kappa B-binding sites. *Journal of Biological Chemistry*, 273, 22201-22208.
- MARTIN, S. F. 2004. T lymphocyte-mediated immune responses to chemical haptens and metal ions: Implications for allergic and autoimmune disease. *International Archives of Allergy and Immunology*, 134, 186-198.
- MARTIN-CHOULY, C., MORZADEC, C., BONVALET, M., GALIBERT, M.-D., FARDEL, O. & VERNHET, L. 2011. Inorganic arsenic alters expression of immune and stress response genes in activated primary human T lymphocytes. *Molecular Immunology*, 48, 956-965.
- MARTIN-ROMERO, C., SANTOS-ALVAREZ, J., GOBERNA, R. & SANCHEZ-MARGALET, V. 2000. Human leptin enhances activation and proliferation of human circulating T lymphocytes. *Cellular Immunology*, 199, 15-24.
- MARTINEZ, F. O., HELMING, L. & GORDON, S. 2009. Alternative Activation of Macrophages: An Immunologic Functional Perspective. *Annual Review of Immunology*, 27, 451-483.
- MARTINEZ, M. M., REIF, R. D. & PAPPAS, D. 2010. Detection of apoptosis: A review of conventional and novel techniques. *Analytical Methods*, 2, 996-1004.
- MARTINEZ-ZAMUDIO, R. & HA, H. C. 2011. Environmental epigenetics in metal exposure. *Epigenetics*, 6, 820-827.
- MARTINI, F., NATH, J. & BARTHOLOMEW, E. 2011. *Fundamentals of Anatomy & Physiology* Pearson.
- MATSUO, K., GRAY, M. J., YANG, D. Y., SRIVASTAVA, S. A., TRIPATHI, P. B., SONODA, L. A., YOO, E.-J., DUBEAU, L., LEE, A. S. & LIN, Y. G. 2013. The endoplasmic reticulum stress marker, glucose-regulated protein-78 (GRP78) in visceral adipocytes predicts endometrial cancer progression and patient survival. *Gynecologic Oncology*, 128, 552-559.
- MATSUSAKI, T., KAWANABE, K., ISE, K., NAKAYAMA, T., TOGUCHIDA, J. & NAKAMURA, T. 2007. Gene expression profile of macrophage-like U937 cells in response to polyethylene particles - A novel cell-particle culture system. *Journal of Arthroplasty*, 22, 960-965.
- MATTHEWS, J. B., GREEN, T. R., STONE, M. H., WROBLEWSKI, B. M., FISHER, J. & INGHAM, E. 2000. Comparison of the response of primary murine peritoneal macrophages and the U937 human histiocytic cell line to challenge with in vitro generated clinically relevant UHMWPE particles. *Bio-Medical Materials and Engineering*, 10, 229-240.

- MATTHEWS, J. B., GREEN, T. R., STONE, M. H., WROBLEWSKI, B. M., FISHER, J. & INGHAM, E. 2001. Comparison of the response of three human monocytic cell lines to challenge with polyethylene particles of known size and dose. *Journal of Materials Science-Materials in Medicine*, 12, 249-258.
- MATTHIES, A. K., SKINNER, J. A., OSMANI, H., HENCKEL, J. & HART, A. J. 2012. Pseudotumors Are Common in Well-positioned Low-wearing Metal-on-Metal Hips. *Clinical Orthopaedics and Related Research*, 470, 1895-1906.
- MATZIOLIS, G., PERKA, C. & DISCH, A. 2003. Massive metallosis after revision of a fractured ceramic head onto a metal head. *Archives of Orthopaedic and Trauma Surgery*, 123, 48-50.
- MCKAY, G. C., MACNAIR, R., MACDONALD, C. & GRANT, M. H. 1996. Interactions of orthopaedic metals with an immortalized rat osteoblast cell line. *Biomaterials*, 17, 1339-1344.
- MDA/2010/033, M. A. H. P. R. A. Medical Device Alert. Ref: MDA/2010/033. Issues: 22 April 2010. <http://www.mhra.gov.uk/home/groups/dtsbs/documents/medicaldevicealert/con079162.pdf>.
- MDA/2010/069, M. A. H. P. R. A. Medical Device Alert. Ref: MDA/2010/069. Issues: 7 September 2010. <http://www.mhra.gov.uk/home/groups/dtsbs/documents/medicaldevicealert/con093791.pdf>.
- MEDLEY, J. B., CHAN, F. W., KRYGIER, J. J. & BOBYN, J. D. 1996. Comparison of alloys and designs in a hip simulator study of metal on metal implants. *Clinical Orthopaedics and Related Research*, S148-S159.
- MENGIARDI, B., PFIRRMANN, C. W. A. & HODLER, J. 2007. Hip pain in adults: MR imaging appearance of common causes. *European Radiology*, 17, 1746-1762.
- MERKEL, K. D., ERDMANN, J. M., MCHUGH, K. P., ABU-AMER, Y., ROSS, F. P. & TEITELBAUM, S. L. 1999. Tumor necrosis factor-alpha mediates orthopedic implant osteolysis. *American Journal of Pathology*, 154, 203-210.
- MERRITT, K. & BROWN, S. A. 1995. RELEASE OF HEXAVALENT CHROMIUM FROM CORROSION OF STAINLESS-STEEL AND COBALT-CHROMIUM ALLOYS. *Journal of Biomedical Materials Research*, 29, 627-633.
- MHRA Medical Device Alert. Ref: MDA/2010/033. Issues: 22 April 2010.
- MILLER, A. C., BROOKS, K., SMITH, J. & PAGE, N. 2004. Effect of the militarily-relevant heavy metals, depleted uranium and heavy metal tungsten-alloy on gene expression in human liver carcinoma cells (HepG2). *Molecular and Cellular Biochemistry*, 255, 247-256.
- MINANG, J. T., ARESTROM, I., TROYE-BLOMBERG, M., LUNDEBERG, L. & AHLBORG, N. 2006. Nickel, cobalt, chromium, palladium and gold induce a mixed Th1- and Th2-type cytokine response in vitro in subjects with contact allergy to the respective metals. *Clinical and Experimental Immunology*, 146, 417-426.

- MORITA, M., HASHIMOTO, T., YAMAUCHI, K., SUTO, Y., HOMMA, T. & KIMURA, Y. 2007. Evaluation of biocompatibility for titanium-nickel shape memory alloy in vivo and in vitro environments. *Materials Transactions*, 48.
- MORLOCK, M., DELLING, G., RÜTHER, W., HAHN, M. & BISHOP, N. 2006. In-vivo wear of hip surface replacements—a comparison of retrievals and simulator results. *Journal of Biomechanics*, 39, S121.
- MORONI, A., NOCCO, E., HOQUE, M., DIREMIGIO, E., BUFFOLI, D., CANTU, F., CATALANI, S. & APOSTOLI, P. 2012. Cushion bearings versus large diameter head metal-on-metal bearings in total hip arthroplasty: a short-term metal ion study. *Archives of Orthopaedic and Trauma Surgery*, 132, 123-129.
- MORONI, A., SAVARINO, L., HOQUE, M., CADOSSO, M. & BALDINI, N. 2011. Do Ion Levels In Hip Resurfacing Differ From Metal-on-metal THA at Midterm? *Clinical Orthopaedics and Related Research*, 469, 180-187.
- MOSKALEV, A. A., SMIT-MCBRIDE, Z., SHAPOSHNIKOV, M. V., PLYUSNINA, E. N., ZHAVORONKOV, A., BUDOVSKY, A., TACUTU, R. & FRAIFELD, V. E. 2012. Gadd45 proteins: Relevance to aging, longevity and age-related pathologies. *Ageing Research Reviews*, 11, 51-66.
- MOSMANN, T. 1983. RAPID COLORIMETRIC ASSAY FOR CELLULAR GROWTH AND SURVIVAL - APPLICATION TO PROLIFERATION AND CYTO-TOXICITY ASSAYS. *Journal of Immunological Methods*, 65, 55-63.
- MOSSER, D. M. 2003. The many faces of macrophage activation. *Journal of Leukocyte Biology*, 73, 209-212.
- MOSTARDI, R. A., KOVACIK, M. W., RAMSIER, R. D., BENDER, E. T., FINEFROCK, J. M., BEAR, T. F. & ASKEW, M. J. 2010. A comparison of the effects of prosthetic and commercially pure metals on retrieved human fibroblasts: The role of surface elemental composition. *Acta Biomaterialia*, 6, 702-707.
- MOU, Y. H., YANG, J. Y., CUI, N., WANG, J. M., HOU, Y., SONG, S. & WU, C. F. 2012. Effects of cobalt chloride on nitric oxide and cytokines/chemokines production in microglia. *International Immunopharmacology*, 13, 120-125.
- MOULON, C., VOLLMER, J. & WELTZIEN, H. U. 1995. Characterization of processing requirements acid metal cross-reactivities in T cell clones from patients with allergic contact dermatitis to nickel. *European Journal of Immunology*, 25, 3308-3315.
- MOUNTZIARIS, P. M. & MIKOS, A. G. 2008. Modulation of the inflammatory response for enhanced bone tissue regeneration. *Tissue Engineering Part B-Reviews*, 14, 179-186.
- MUDTER, J. & NEURATH, M. F. 2007. Apoptosis of T cells and the control of inflammatory bowel disease: therapeutic implications. *Gut*, 56, 293-303.
- MURATA, K., YOSHITOMI, H., TANIDA, S., ISHIKAWA, M., NISHITANI, K., ITO, H. & NAKAMURA, T. 2010. Plasma and synovial fluid microRNAs as potential biomarkers of rheumatoid arthritis and osteoarthritis. *Arthritis Research & Therapy*, 12.
- NAAL, F. D., PILZ, R., MUNZINGER, U., HERSCHE, O. & LEUNIG, M. 2011. High Revision Rate at 5 Years after Hip Resurfacing with the Durom Implant. *Clinical Orthopaedics and Related Research*, 469, 2598-2604.

- NATIONAL JOINT REGISTRY, N. 2012. National Joint Registry for England and Wales 9th Annual Report. www.njrcentre.org.uk.
- NAVARRO, M., MICHIARDI, A., CASTANO, O. & PLANELL, J. A. 2008. Biomaterials in orthopaedics. *Journal of the Royal Society Interface*, 5, 1137-1158.
- NAVARRO-ZARZA, J. E., VILLASENOR-OVIES, P., VARGAS, A., CANOSO, J. J., CHIAPAS-GASCA, K., HERNANDEZ-DIAZ, C., SAAVEDRA, M. A. & KALISH, R. A. 2012. Clinical anatomy of the pelvis and hip. *Reumatologia clinica*, 8 Suppl 2, 33-8.
- NICH, C., LANGLOIS, J., MARCHADIER, A., VIDAL, C., COHEN-SOLAL, M., PETITE, H. & HAMADOUCHE, M. 2011. Oestrogen deficiency modulates particle-induced osteolysis. *Arthritis research & therapy*, 13, R100.
- NICHOLSON, D. W., ALI, A., THORNBERRY, N. A., VAILLANCOURT, J. P., DING, C. K., GALLANT, M., GAREAU, Y., GRIFFIN, P. R., LABELLE, M., LAZEBNIK, Y. A., MUNDAY, N. A., RAJU, S. M., SMULSON, M. E., YAMIN, T. T., YU, V. L. & MILLER, D. K. 1995. IDENTIFICATION AND INHIBITION OF THE ICE/CED-3 PROTEASE NECESSARY FOR MAMMALIAN APOPTOSIS. *Nature*, 376, 37-43.
- NICKENS, K. P., PATIERNO, S. R. & CERYAK, S. 2010. Chromium genotoxicity: A double-edged sword. *Chemico-Biological Interactions*, 188, 276-288.
- NILSSON, A., NORSGARD, M., ANDERSSON, G. & FAHLGREN, A. 2012. Fluid pressure induces osteoclast differentiation comparably to titanium particles but through a molecular pathway only partly involving TNF α . *Journal of Cellular Biochemistry*, 113, 1224-1234.
- NOLAN, T., HANDS, R. E. & BUSTIN, S. A. 2006. Quantification of mRNA using real-time RT-PCR. *Nature Protocols*, 1, 1559-1582.
- NOVOSELOVA, E. G., GLUSHKOVA, O. V., CHERENKOV, D. A., PARFENYUK, S. B., NOVOSELOVA, T. V., LUNIN, S. M., KHRENOV, M. O., GUZHOVA, I. V., MARGULIS, B. A. & FESENKO, E. E. 2006. Production of heat shock proteins, cytokines, and nitric oxide in toxic stress. *Biochemistry-Moscow*, 71, 376-383.
- NUNLEY, R. M., DELLA VALLE, C. J. & BARRACK, R. L. 2009. Is Patient Selection Important for Hip Resurfacing? *Clinical Orthopaedics and Related Research*, 467, 56-65.
- O'BRIEN, S. T., BURNELL, C. D., HEDDEN, D. R. & BRANDT, J.-M. 2013. Abrasive wear and metallosis associated with cross-linked polyethylene in total hip arthroplasty. *The Journal of arthroplasty*, 28, 197.e17-21.
- OISHI, Y., WATANABE, Y., SHINODA, S., NAKA, M., OZAWA, Y., MATSUYAMA, T., MOROZUMI, K. & FUKU, Y. 2012. The IL6 gene polymorphism -634C > G and IL17F gene polymorphism 7488T > C influence bone mineral density in young and elderly Japanese women. *Gene*, 504, 75-83.
- OKAMOTO, S. & ELTIS, L. D. 2011. The biological occurrence and trafficking of cobalt. *Metallomics*, 3, 963-970.
- OKAZAKI, Y. & GOTOH, E. 2005. Comparison of metal release from various metallic biomaterials in vitro. *Biomaterials*, 26, 11-21.

- OKOKO, T. & ORUAMBO, I. F. 2008. Garcinia kola extract reduced lipopolysaccharide activation of macrophages using U937 cells as a model. *African Journal of Biotechnology*, 7, 792-795.
- OLDENBURG, M., WEGNER, R. & BAUR, X. 2009. Severe Cobalt Intoxication Due to Prosthesis Wear in Repeated Total Hip Arthroplasty. *The Journal of arthroplasty*, 24, 825.e15-20.
- OLLIVERE, B., DARRAH, C., BARKER, T., NOLAN, J. & PORTEOUS, M. J. 2009. Early clinical failure of the Birmingham metal-on-metal hip resurfacing is associated with metallosis and soft-tissue necrosis. *Journal of Bone and Joint Surgery-British Volume*, 91B, 1025-1030.
- OLSSON, G. M., RUNGBY, J., RUNDQUIST, I. & BRUNK, U. T. 1989. EVALUATION OF LYSOSOMAL STABILITY IN LIVING CULTURED MACROPHAGES BY CYTOFLUOROMETRY - EFFECT OF SILVER LACTATE AND HYPOTONIC CONDITIONS. *Virchows Archiv B-Cell Pathology Including Molecular Pathology*, 56, 263-269.
- OPITZ, L., SALINAS-RIESTER, G., GRADE, M., JUNG, K., JO, P., EMONS, G., GHADIMI, B. M., BEISSBARTH, T. & GAEDCKE, J. 2010. Impact of RNA degradation on gene expression profiling. *Bmc Medical Genomics*, 3.
- OPYDO-CHANEK, M., STOJAK, M., MAZUR, L. & NIEMEYER, U. 2010. Changes in the size of U937 cells following exposure to new generation oxazaphosphorines *ACTA BIOLOGICA CRACOVIENSIA Series Zoologia*, 52, 25-29.
- PANDIT, H., GLYN-JONES, S., MCLARDY-SMITH, P., GUNDLE, R., WHITWELL, D., GIBBONS, C. L. M., OSTLERE, S., ATHANASOU, N., GILL, H. S. & MURRAY, D. W. 2008. Pseudotumours associated with metal-on-metal hip resurfacings. *Journal of Bone and Joint Surgery-British Volume*, 90B, 847-851.
- PAP, G., MACHNER, A., RINNERT, T., HORLER, D., GAY, R. E., SCHWARZBERG, H., NEUMANN, W., MICHEL, B. A., GAY, S. & PAP, T. 2001. Development and characteristics of a synovial-like interface membrane around cemented tibial hemiarthroplasties in a novel rat model of aseptic prosthesis loosening. *Arthritis and Rheumatism*, 44, 956-963.
- PAPAGEORGIOU, I., BROWN, C., SCHINS, R., SINGH, S., NEWSON, R., DAVIS, S., FISHER, J., INGHAM, E. & CASE, C. P. 2007a. The effect of nano- and micron-sized particles of cobalt-chromium alloy on human fibroblasts in vitro. *Biomaterials*, 28, 2946-2958.
- PAPAGEORGIOU, I., YIN, Z. R., LADON, D., BAIRD, D., LEWIS, A. C., SOOD, A., NEWSON, R., LEARMONTH, I. D. & CASE, C. P. 2007b. Genotoxic effects of particles of surgical cobalt chrome alloy on human cells of different age in vitro. *Mutation Research-Fundamental and Molecular Mechanisms of Mutagenesis*, 619, 45-58.
- PARK, J. D., CHERRINGTON, N. J. & KLAASSEN, C. D. 2002. Intestinal absorption of cadmium is associated with divalent metal transporter 1 in rats. *Toxicological Sciences*, 68, 288-294.
- PARK, S.-Y., BAE, D.-J., KIM, M.-J., PIAO, M. L. & KIM, I.-S. 2012. Extracellular Low pH Modulates Phosphatidylserine-dependent Phagocytosis in Macrophages by Increasing Stabilin-1 Expression. *Journal of Biological Chemistry*, 287, 11261-11271.

- PEAKMAN, T. C. & ELLIOTT, P. 2008. The UK Biobank sample handling and storage validation studies. *International Journal of Epidemiology*, 37, 2-6.
- PEARL, J. I., MA, T., IRANI, A. R., HUANG, Z. N., ROBINSON, W. H., SMITH, R. L. & GOODMAN, S. B. 2011. Role of the Toll-like receptor pathway in the recognition of orthopedic implant wear-debris particles. *Biomaterials*, 32, 5535-5542.
- PENNY, J. O., VARMARKEN, J. E., OVESEN, O., NIELSEN, C. & OVERGAARD, S. 2013. Metal ion levels and lymphocyte counts: ASR hip resurfacing prosthesis vs. standard THA 2-year results from a randomized study. *Acta Orthopaedica*, 84, 130-137.
- PERCH-NIELSEN, I. R., BANG, D. D., POULSEN, C. R., EL-ALI, J. & WOLFF, A. 2003. Removal of PCR inhibitors using dielectrophoresis as a selective filter in a microsystem. *Lab on a Chip*, 3, 212-216.
- PEREZ, G., GARBOSSA, G., DI RISIO, C., VITTORI, D. & NESSE, A. 2001. Disturbance of cellular iron uptake and utilisation by aluminium. *Journal of Inorganic Biochemistry*, 87, 21-27.
- PEREZ, G., PREGI, N., VITTORI, D., DI RISIO, C., GARBOSSA, G. & NESSE, A. 2005. Aluminum exposure affects transferrin-dependent and -independent iron uptake by K562 cells. *Biochimica Et Biophysica Acta-Molecular Cell Research*, 1745, 124-130.
- PEREZ-SAYANS, M., MANUEL SOMOZA-MARIN, J., BARROS-ANGUEIRA, F., GANDARA REY, J. M. & GARCIA-GARCIA, A. 2010. RANK/RANKL/OPG role in distraction osteogenesis. *Oral Surgery Oral Medicine Oral Pathology Oral Radiology and Endodontology*, 109, 679-686.
- PETIT, A., MWALE, F., TKACZYK, C., ANTONIOU, J., ZUKOR, D. J. & HUK, O. L. 2005. Induction of protein oxidation by cobalt and chromium ions in human U937 macrophages. *Biomaterials*, 26, 4416-4422.
- PETIT, A., MWALE, F., TKACZYK, C., ANTONIOU, J., ZUKOR, D. J. & HUK, O. L. 2006a. Cobalt and chromium ions induce nitration of proteins in human U937 macrophages in vitro. *Journal of Biomedical Materials Research Part A*, 79A, 599-605.
- PETIT, A., MWALE, F., TKACZYK, C., ANTONIOU, J., ZUKOR, D. J. & HUK, O. L. 2006b. Cobalt and chromium ions induce nitration of proteins in human U937 macrophages in vitro. *Journal of Biomedical Materials Research Part A*, 79A.
- PETIT, A., MWALE, F., ZUKOR, D. J., CATELAS, I., ANTONIOU, J. & HUK, O. L. 2004a. Effect of cobalt and chromium ions on bcl-2, bax, caspase-3, and caspase-8 expression in human U937 macrophages. *Biomaterials*, 25.
- PETIT, A., MWALE, F., ZUKOR, D. J., CATELAS, I., ANTONIOU, J. & HUK, O. L. 2004b. Effect of cobalt and chromium ions on bcl-2, bax, caspase-3, and caspase-8 expression in human U937 macrophages. *Biomaterials*, 25, 2013-2018.
- PFAFFL, M. W. 2001. A new mathematical model for relative quantification in real-time RT-PCR. *Nucleic Acids Research*, 29.
- PFAFFL, M. W., TICHOPAD, A., PRGOMET, C. & NEUVIANS, T. P. 2004. Determination of stable housekeeping genes, differentially regulated target genes and sample integrity: BestKeeper - Excel-based tool using pair-wise correlations. *Biotechnology Letters*, 26, 509-515.

- PILICHOU, A., PAPASSOTIRIOU, I., MICHALAKAKOU, K., FESSATOU, S., FANDRIDIS, E., PAPACHRISTOU, G. & TERPOS, E. 2008. High levels of synovial fluid osteoprotegenin (OPG) and increased serum ratio of receptor activator of nuclear factor-kappa B ligand (RANKL) to OPG correlate with disease severity in patients with primary knee osteoarthritis. *Clinical Biochemistry*, 41, 746-749.
- PORAT, M., PARVIZI, J., SHARKEY, P. F., BEREND, K. R., LOMBARDI, A. V., JR. & BARRACK, R. L. 2012. Causes of Failure of Ceramic-on-Ceramic and Metal-on-Metal Hip Arthroplasties. *Clinical Orthopaedics and Related Research*, 470, 382-387.
- POSADAS, S. J. & PICHLER, W. J. 2007. Delayed drug hypersensitivity reactions - new concepts. *Clinical and Experimental Allergy*, 37, 989-999.
- POTNIS, P. A., DUTTA, D. K. & WOOD, S. C. 2013. Toll-like receptor 4 signaling pathway mediates proinflammatory immune response to cobalt-alloy particles *Cellular Immunology*, 282, 53-65.
- QUEALLY, J. M., DEVITT, B. M., BUTLER, J. S., MALIZIA, A. P., MURRAY, D., DORAN, P. P. & O'BYRNE, J. M. 2009. Cobalt Ions Induce Chemokine Secretion in Primary Human Osteoblasts. *Journal of Orthopaedic Research*, 27, 855-864.
- QUESADA, M. J., MARKER, D. R. & MONT, M. A. 2008. Metal-on-Metal Hip Resurfacing. *Journal of Arthroplasty*, 23, 69-73.
- RAGHUNATHAN, V. K., GRANT, M. H. & ELLIS, E. M. 2010. Changes in protein expression associated with chronic in vitro exposure of hexavalent chromium to osteoblasts and monocytes: A proteomic approach. *Journal of Biomedical Materials Research Part A*, 92A, 615-625.
- RAHMAN, S. M., QADRI, I., JANSSEN, R. C. & FRIEDMAN, J. E. 2009. Fenofibrate and PBA prevent fatty acid-induced loss of adiponectin receptor and pAMPK in human hepatoma cells and in hepatitis C virus-induced steatosis. *Journal of Lipid Research*, 50, 2193-2202.
- RAJA, N. S., SANKARANARAYANAN, K., DHATHATHREYAN, A. & NAIR, B. U. 2011. Interaction of chromium(III) complexes with model lipid bilayers: Implications on cellular uptake. *Biochimica Et Biophysica Acta-Biomembranes*, 1808, 332-340.
- RAJAMAKI, K., NORDSTROM, T., NURMI, K., AKERMAN, K. E. O., KOVANEN, P. T., OORNI, K. & EKLUND, K. K. 2013. Extracellular Acidosis Is a Novel Danger Signal Alerting Innate Immunity via the NLRP3 Inflammasome. *Journal of Biological Chemistry*, 288, 13410-13419.
- RANDACCIO, L., GEREMIA, S., DEMITRI, N. & WUERGES, J. 2010. Vitamin B-12: Unique Metalorganic Compounds and the Most Complex Vitamins. *Molecules*, 15, 3228-3259.
- RAO, A. J., GIBON, E., MA, T., YAO, Z., SMITH, R. L. & GOODMAN, S. B. 2012. Revision joint replacement, wear particles, and macrophage polarization. *Acta Biomaterialia*, 8, 2815-2823.
- RASQUINHA, V. J., RANAWAT, C. S., WEISKOPF, J., RODRIGUEZ, J. A., SKIPOR, A. K. & JACOBS, J. J. 2006. Serum metal levels and bearing surfaces in total hip arthroplasty. *Journal of Arthroplasty*, 21, 47-52.

- REGUNATHAN, A., CERNY, E. A., VILLARREAL, J. & BHATTACHARYYA, M. H. 2002. Role of fos and src in cadmium-induced decreases in bone mineral content in mice. *Toxicology and Applied Pharmacology*, 185, 25-40.
- REILLY, S. S., RAMP, W. K., ZANE, S. F. & HUDSON, M. C. 1997. Internalization of Staphylococcus aureus by embryonic chicken osteoblasts in vivo. *Journal of Bone and Mineral Research*, 12, S231-S231.
- REMOUCHAMPS, C., BOUTAFFALA, L., GANEFF, C. & DEJARDIN, E. 2011. Biology and signal transduction pathways of the Lymphotoxin-alpha beta/LT beta R system. *Cytokine & Growth Factor Reviews*, 22, 301-310.
- REPETTO, G., DEL PESO, A. & ZURITA, J. L. 2008. Neutral red uptake assay for the estimation of cell viability/cytotoxicity. *Nature Protocols*, 3, 1125-1131.
- RIES, M. D., SCOTT, M. L. & JANI, S. 2001. Relationship between gravimetric wear and particle generation in hip simulators: Conventional compared with cross-linked polyethylene. *Journal of Bone and Joint Surgery-American Volume*, 83A, 116-122.
- RIRIE, K. M., RASMUSSEN, R. P. & WITWER, C. T. 1997. Product differentiation by analysis of DNA melting curves during the polymerase chain reaction. *Analytical Biochemistry*, 245, 154-160.
- ROMESBURG, J. W., WASSERMAN, P. L. & SCHOPPE, C. H. 2010. Metallosis and Metal-Induced Synovitis Following Total Knee Arthroplasty: Review of Radiographic and CT Findings. *Journal of radiology case reports*, 4, 7-17.
- RON, D. & WALTER, P. 2007. Signal integration in the endoplasmic reticulum unfolded protein response. *Nature Reviews Molecular Cell Biology*, 8, 519-529.
- ROSENBERG, O., GAWLIK, J., MAMALIS, A. G., VOZNY, V., SOKHAN, C. & KIM, D. J. 2006. Trends and developments in the manufacturing of hip joints: an overview. *International Journal of Advanced Manufacturing Technology*, 27, 537-542.
- ROSSEN, L., NORSEKOV, P., HOLMSTROM, K. & RASMUSSEN, O. F. 1992. INHIBITION OF PCR BY COMPONENTS OF FOOD SAMPLES, MICROBIAL DIAGNOSTIC ASSAYS AND DNA-EXTRACTION SOLUTIONS. *International Journal of Food Microbiology*, 17, 37-45.
- ROTHFUSS, A. & SPEIT, G. 2002. Overexpression of heme oxygenase-1 (HO-1) in V79 cells results in increased resistance to hyperbaric oxygen (HBO)-induced DNA damage. *Environmental and Molecular Mutagenesis*, 40, 258-265.
- RUIJTER, J. M., PFAFFL, M. W., ZHAO, S., SPIESS, A. N., BOGGY, G., BLOM, J., RUTLEDGE, R. G., SISTI, D., LIEVENS, A., DE PRETER, K., DERVEAUX, S., HELLEMANS, J. & VANDESOMPELE, J. 2013. Evaluation of qPCR curve analysis methods for reliable biomarker discovery: Bias, resolution, precision, and implications. *Methods*, 59, 32-46.
- RUIJTER, J. M., RAMAKERS, C., HOOGAARS, W. M. H., KARLEN, Y., BAKKER, O., VAN DEN HOFF, M. J. B. & MOORMAN, A. F. M. 2009. Amplification efficiency: linking baseline and bias in the analysis of quantitative PCR data. *Nucleic Acids Research*, 37.
- SAAD, B., CIARDELLI, G., MATTER, S., WELTI, M., UHLSCHMID, G. K., NEUENSCHWANDER, P. & SUTER, U. W. 1998. Degradable and highly porous polyesterurethane foam as biomaterial: Effects and phagocytosis of

- degradation products in osteoblasts. *Journal of Biomedical Materials Research*, 39, 594-602.
- SABBATINI, M., PIFFANELLI, V., BOCCAFOSCHI, F., GATTI, S., RENO, F., BOSETTI, M., LEIGHEB, M., MASSE, A. & MARIO, C. 2010. Different apoptosis modalities in periprosthetic membranes. *Journal of Biomedical Materials Research Part A*, 92A, 175-184.
- SAJJADI, H., MODARESSI, A., MAGRI, P., DOMAŃSKA, U., SINDT, M., MIELOSZYNSKI, J.-L., MUTELET, F. & ROGALSKI, M. 2013. Aggregation of nanoparticles in aqueous solutions of ionic liquids. *Journal of Molecular Liquids*, 186, 1-6.
- SALWAY, F., DAY, P. J. R., OLLIER, W. E. R. & PEAKMAN, T. C. 2008. Levels of 5' RNA tags in plasma and buffy coat from EDTA blood increase with time. *International Journal of Epidemiology*, 37, 11-15.
- SAMALI, A., FITZGERALD, U., DEEGAN, S. & GUPTA, S. 2010. Methods for monitoring endoplasmic reticulum stress and the unfolded protein response. *International journal of cell biology* 2010, 11.
- SANDERS, C., DONOVAN, J. L. & DIEPPE, P. A. 2004. Unmet need for joint replacement: a qualitative investigation of barriers to treatment among individuals with severe pain and disability of the hip and knee. *Rheumatology*, 43, 353-357.
- SANDHU, K. S. & ACHARYA, K. K. 2005. ExPrimer: to design primers from exon-exon junctions. *Bioinformatics*, 21, 2091-2092.
- SARGEANT, A. & GOSWAMI, T. 2007. Hip implants - Paper VI - Ion concentrations. *Materials & Design*, 28, 155-171.
- SARIN, A., CONANCIBOTTI, M. & HENKART, P. A. 1995. CYTOTOXIC EFFECT OF TNF AND LYMPHOTOXIN ON T-LYMPHOBLASTS. *Journal of Immunology*, 155, 3716-3718.
- SAVARINO, L., GRANCHI, D., CIAPETTI, G., CENNI, E., PANTOLI, A. N., ROTINI, R., VERONESI, C. A., BALDINI, N. & GIUNTI, A. 2002. Ion release in patients with metal-on-metal hip bearings in total joint replacement: A comparison with metal-on-polyethylene bearings. *Journal of Biomedical Materials Research*, 63, 467-474.
- SAVARINO, L., STEA, S., GRANCHI, D., VISENTIN, M., CIAPETTI, G., DONATI, M. E., ROLLO, G., ZINGHI, G., PIZZOFERRATO, A., MONTANARO, L. & TONI, A. 2000. Sister chromatid exchanges and ion release in patients wearing fracture fixation devices. *Journal of Biomedical Materials Research*, 50, 21-26.
- SCHEFE, J. H., LEHMANN, K. E., BUSCHMANN, I. R., UNGER, T. & FUNKE-KAISER, H. 2006. Quantitative real-time RT-PCR data analysis: current concepts and the novel "gene expression's C-T difference" formula. *Journal of Molecular Medicine-Jmm*, 84, 901-910.
- SCHMALZRIED, T. P., SZUSZCZEWICZ, E. S., NORTHFIELD, M. R., AKIZUKI, K. H., FRANKEL, R. E., BELCHER, G. & AMSTUTZ, H. C. 1998. Quantitative assessment of walking activity after total hip or knee replacement. *Journal of Bone and Joint Surgery-American Volume*, 80A, 54-59.
- SCHMID, H., COHEN, C. D., HENGER, A., IRRGANG, S., SCHLONDORFF, D. & KRETZLER, M. 2003. Validation of endogenous controls for gene

- expression analysis in microdissected human renal biopsies. *Kidney International*, 64, 356-360.
- SCHNEIDER, K., POTTER, K. G. & WARE, C. F. 2004. Lymphotoxin and LIGHT signaling pathways and target genes. *Immunological Reviews*, 202, 49-66.
- SCHRODER, K., HERTZOG, P. J., RAVASI, T. & HUME, D. A. 2004. Interferon-gamma: an overview of signals, mechanisms and functions. *Journal of Leukocyte Biology*, 75, 163-189.
- SCHWAB, L. P., XING, Z., HASTY, K. A. & SMITH, R. A. 2006. Titanium particles and surface-bound LPS activate different pathways in IC-21 macrophages. *Journal of Biomedical Materials Research Part B-Applied Biomaterials*, 79B, 66-73.
- SEGHIZZI, P., DADDA, F., BORLERI, D., BARBIC, F. & MOSCONI, G. 1994. COBALT MYOCARDIOPATHY - A CRITICAL-REVIEW OF LITERATURE. *Science of the Total Environment*, 150, 105-109.
- SEHATZADEH, S., KAULBACK, K. & LEVIN, L. 2012. Metal-on-Metal Hip Resurfacing Arthroplasty: An Analysis of Safety and Revision Rates. *Ontario health technology assessment series*, 12, 1-63.
- SETHI, R. K., NEAVYN, M. J., RUBASH, H. E. & SHANBHAG, A. S. 2003. Macrophage response to cross-linked and conventional UHMWPE. *Biomaterials*, 24, 2561-2573.
- SHANBHAG, A. S., JACOBS, J. J., BLACK, J., GALANTE, J. O. & GLANT, T. T. 1994. MACROPHAGE/PARTICLE INTERACTIONS - EFFECT OF SIZE, COMPOSITION AND SURFACE-AREA. *Journal of Biomedical Materials Research*, 28, 81-90.
- SHARDLOW, D. L., STONE, M. H., INGHAM, E. & FISHER, J. 2003. Cement particles containing radio-opacifiers stimulate pro-osteolytic cytokine production from a human monocytic cell line. *Journal of Bone and Joint Surgery-British Volume*, 85B.
- SHELTON, L. R. 2013. A closer look at osteoarthritis. *The Nurse practitioner*, 38, 30-6.
- SHIMMIN, A., BEAULE, P. E. & CAMPBELL, P. 2008. Metal-on-metal hip resurfacing arthroplasty. *Journal of Bone and Joint Surgery-American Volume*, 90A, 637-654.
- SHIN, D. Y., KIM, G. Y., LI, W., CHOI, B. T., KIM, N. D., KANG, H. S. & CHOI, Y. H. 2009. Implication of intracellular ROS formation, caspase-3 activation and Egr-1 induction in platycodon D-induced apoptosis of U937 human leukemia cells. *Biomedicine & Pharmacotherapy*, 63, 86-94.
- SHRIVASTAVA, H. Y., RAVIKUMAR, T., SHANMUGASUNDARAM, N., BABU, M. & NAIR, B. U. 2005. Cytotoxicity studies of chromium(III) complexes on human dermal fibroblasts. *Free Radical Biology and Medicine*, 38, 58-69.
- SIAFAKAS, A. R. & RICHARDSON, D. R. 2009. Growth arrest and DNA damage-45 alpha (GADD45 alpha). *International Journal of Biochemistry & Cell Biology*, 41, 986-989.
- SICILIA, A., CUESTA, S., COMA, G., ARREGUI, I., GUIASOLA, C., RUIZ, E. & MAESTRO, A. 2008. Titanium allergy in dental implant patients: a clinical study on 1500 consecutive patients. *Clinical Oral Implants Research*, 19, 823-835.

- SILVER, N., BEST, S., JIANG, J. & THEIN, S. L. 2006. Selection of housekeeping genes for gene expression studies in human reticulocytes using real-time PCR. *Bmc Molecular Biology*, 7.
- SIMONSEN, L. O., HARBAK, H. & BENNEKOU, P. 2012. Cobalt metabolism and toxicology-A brief update. *The Science of the total environment*, 432, 210-5.
- SINGH, R. & DAHOTRE, N. B. 2007. Corrosion degradation and prevention by surface modification of biometallic materials. *Journal of Materials Science-Materials in Medicine*, 18.
- SIOPACK, J. S. & JERGESEN, H. E. 1995. TOTAL HIP-ARTHROPLASTY. *Western Journal of Medicine*, 162, 243-249.
- SIVERLING, S., FELIX, I., CHOW, S. B., NIEDBALA, E. & SU, E. 2012. Hip resurfacing: not your average hip replacement. *Current Reviews in Musculoskeletal Medicine*, 5, 32-38.
- SON, Y.-O., LEE, J.-C., HITRON, J. A., PAN, J., ZHANG, Z. & SHI, X. 2010. Cadmium Induces Intracellular Ca²⁺- and H₂O₂-Dependent Apoptosis through JNK- and p53-Mediated Pathways in Skin Epidermal Cell line. *Toxicological Sciences*, 113, 127-137.
- SONG, J. S., SIM, S. Y., HONG, D. P., RHEE, S. D., SONG, C. W., HAN, S. S. & YANG, S. D. 2001. Lead treatment in vitro at early developmental stage of bone marrow-derived macrophages enhances NO production through IL-1 beta and IL-6 but not TNF-alpha. *Toxicology*, 162, 61-68.
- SPITTLER, A., OEHLER, R., GOETZINGER, P., HOLZER, S., REISSNER, C. M., LEUTMEZER, F., RATH, V., WRBA, F., FUEGGER, R., BOLTZNITULESCU, G. & ROTH, E. 1997. Low glutamine concentrations induce phenotypical and functional differentiation of U937 myelomonocytic cells. *Journal of Nutrition*, 127, 2151-2157.
- SPOREER, S. M. & CHALMERS, P. N. 2012. Cutaneous Manifestation of Metallosis in a Metal-on-Metal Total Hip Arthroplasty After Acetabular Liner Dissociation. *The Journal of arthroplasty*, 27, 1580.e13-6.
- STAMOVA, B. S., APPERSON, M., WALKER, W. L., TIAN, Y. F., XU, H. C., ADAMCZY, P., ZHAN, X. H., LIU, D. Z., ANDER, B. P., LIAO, I. H., GREGG, J. P., TURNER, R. J., JICKLING, G., LIT, L. & SHARP, F. R. 2009. Identification and validation of suitable endogenous reference genes for gene expression studies in human peripheral blood. *Bmc Medical Genomics*, 2, 13.
- STEA, S., VISENTIN, M., GRANCHI, D., CENNI, E., CIAPETTI, G., SUDANESE, A. & TONI, A. 2000a. Apoptosis in peri-implant tissue. *Biomaterials*, 21, 1393-1398.
- STEA, S., VISENTIN, M., GRANCHI, D., CIAPETTI, G., DONATI, M. E., SUDANESE, A., ZANOTTI, C. & TONI, A. 2000b. Cytokines and osteolysis around total hip prostheses. *Cytokine*, 12, 1575-1579.
- STEEN, K. H., STEEN, A. E. & REEH, P. W. 1995. A DOMINANT ROLE OF ACID PH IN INFLAMMATORY EXCITATION AND SENSITIZATION OF NOCICEPTORS IN RAT SKIN, IN-VITRO. *Journal of Neuroscience*, 15, 3982-3989.
- STEINEMANN, S. G. 1996. Metal implants and surface reactions. *Injury-International Journal of the Care of the Injured*, 27, 16-22.

- STOW, J. L., LOW, P. C., OFFENHAEUSER, C. & SANGERMANI, D. 2009. Cytokine secretion in macrophages and other cells: Pathways and mediators. *Immunobiology*, 214, 601-612.
- SU, E. P., CALLANDER, P. W. & SALVATI, E. A. 2003. The bubble sign - A new radiographic sign in total hip arthroplasty. *Journal of Arthroplasty*, 18, 110-112.
- SUBRAMANIAN, A., TAMAYO, P., MOOTHA, V. K., MUKHERJEE, S., EBERT, B. L., GILLETTE, M. A., PAULOVICH, A., POMEROY, S. L., GOLUB, T. R., LANDER, E. S. & MESIROV, J. P. 2005. Gene set enrichment analysis: A knowledge-based approach for interpreting genome-wide expression profiles. *Proceedings of the National Academy of Sciences of the United States of America*, 102, 15545-15550.
- SUNA, S., SAKATA, Y., SHIMIZU, M., NAKATANI, D., USAMI, M., MATSUMOTO, S., MIZUNO, H., OZAKI, K., TAKASHIMA, S., TAKEDA, H., TANAKA, T., HORI, M. & SATO, H. 2009. Lymphotoxin-alpha 3 mediates monocyte-endothelial interaction by TNFR I/NF-kappa B signaling. *Biochemical and Biophysical Research Communications*, 379, 374-378.
- SYLVIE, J., SYLVIE, T. D., PASCAL, P. M., FABIENNE, P., HASSANE, O. & GUY, C. 2010. Effect of Hydroxyapatite and beta-Tricalcium Phosphate Nanoparticles on Promonocytic U937 Cells. *Journal of Biomedical Nanotechnology*, 6, 158-165.
- SZYF, M. 2007. The dynamic epigenome and its implications in toxicology. *Toxicological Sciences*, 100, 7-23.
- TAKAYAMA, S., SATO, T., KRAJEWSKI, S., KOCHER, K., IRIE, S., MILLAN, J. A. & REED, J. C. 1995. CLONING AND FUNCTIONAL-ANALYSIS OF BAG-1 - A NOVEL BCL-2-BINDING PROTEIN WITH ANTI-CELL DEATH ACTIVITY. *Cell*, 80, 279-284.
- TAKAYANAGI, H. 2005. Mechanistic insight into osteoclast differentiation in osteoimmunology. *Journal of Molecular Medicine-Jmm*, 83, 170-179.
- TAMAKI, Y., TAKAKUBO, Y., GOTO, K., HIRAYAMA, T., SASAKI, K., KONTTINEN, Y. T., GOODMAN, S. B. & TAKAGI, M. 2009. Increased Expression of Toll-like Receptors in Aseptic Loose Periprosthetic Tissues and Septic Synovial Membranes Around Total Hip Implants. *Journal of Rheumatology*, 36, 598-608.
- TANG, S. C. 2002. BAG-1, an anti-apoptotic tumour marker. *Iubmb Life*, 53, 99-105.
- TANG, Y., GILBERT, D. L., GLAUSER, T. A., HERSHEY, A. D. & SHARP, F. R. 2005. Blood gene expression profiling of neurologic diseases - A pilot microarray study. *Archives of Neurology*, 62, 210-215.
- TANG, Y., HE, W., WEI, Y., QU, Z., ZENG, J. & QIN, C. 2013. Screening Key Genes and Pathways in Glioma Based on Gene Set Enrichment Analysis and Meta-analysis. *Journal of Molecular Neuroscience*, 50, 324-332.
- TARRANT, J. M. 2010. Blood Cytokines as Biomarkers of In Vivo Toxicity in Preclinical Safety Assessment: Considerations for Their Use. *Toxicological Sciences*, 117, 4-16.
- TERADA, S., KOMATSU, T., FUJITA, T., TERAOKAWA, A., NAGAMUNE, T., TAKAYAMA, S., REED, J. C. & SUZUKI, E. 1999. Co-expression of bcl-2

- and bag-1, apoptosis suppressing genes, prolonged viable culture period of hybridoma and enhanced antibody production. *Cytotechnology*, 31, 143-51.
- THACH, D. C., LIN, B. C., WALTER, E., KRUZELock, R., ROWLEY, R. K., TIBBETTS, C. & STENGER, D. A. 2003. Assessment of two methods for handling blood in collection tubes with RNA stabilizing agent for surveillance of gene expression profiles with high density microarrays. *Journal of Immunological Methods*, 283, 269-279.
- THELLIN, O., ZORZI, W., LAKAYE, B., DE BORMAN, B., COUMANS, B., HENNEN, G., GRISAR, T., IGOUT, A. & HEINEN, E. 1999. Housekeeping genes as internal standards: use and limits. *Journal of Biotechnology*, 75, 291-295.
- THOMAS, R. 2008. Practical Guide to ICP-MS: A Tutorial for Beginners, Second Edition. *Practical Guide to Icp-MS: a Tutorial for Beginners, Second Edition*, 1-339.
- TKACZYK, C., HUK, O. L., MWALE, F., ANTONIOU, J., ZUKOR, D. J., PETIT, A. & TABRIZIAN, M. 2009. The molecular structure of complexes formed by chromium or cobalt ions in simulated physiological fluids. *Biomaterials*, 30, 460-467.
- TKACZYK, C., HUK, O. L., MWALE, F., ANTONIOU, J., ZUKOR, D. J., PETIT, A. & TABRIZIAN, M. 2010a. Effect of chromium and cobalt ions on the expression of antioxidant enzymes in human U937 macrophage-like cells. *Journal of Biomedical Materials Research Part A*, 94A, 419-425.
- TKACZYK, C., PETIT, A., ANTONIOU, J., ZUKOR, D. J., TABRIZIAN, M. & HUK, O. L. 2010b. Significance of Elevated Blood Metal Ion Levels in Patients with Metal-on-Metal Prostheses: An Evaluation of Oxidative Stress Markers. *The open orthopaedics journal*, 4, 221-7.
- TONI, A., TRAINA, F., STEA, S., SUDANESE, A., VISENTIN, M., BORDINI, B. & SQUARZONI, S. 2006. Early diagnosis of ceramic liner fracture - Guidelines based on a twelve-year clinical experience. *Journal of Bone and Joint Surgery-American Volume*, 88A, 55-63.
- TOPOLOVEC, M., MILOSEV, I., COER, A. & BLOEBAUM, R. D. 2013. Wear debris from hip prostheses characterized by electron imaging. *Central European Journal of Medicine*, 8, 476-484.
- TOWER, S. S. 2010. Arthroprosthetic Cobaltism: Neurological and Cardiac Manifestations in Two Patients with Metal-on-Metal Arthroplasty A Case Report. *Journal of Bone and Joint Surgery-American Volume*, 92A, 2847-2851.
- TOWNSEND, P. A., CUTRESS, R. I., SHARP, A., BRIMMELL, M. & PACKHAM, G. 2003. BAG-1: a multifunctional regulator of cell growth and survival. *Biochimica Et Biophysica Acta-Reviews on Cancer*, 1603, 83-98.
- TOWNSEND, P. A., STEPHANOU, A., PACKHAM, G. & LATCHMAN, D. S. 2005. BAG-1: a multi-functional pro-survival molecule. *International Journal of Biochemistry & Cell Biology*, 37, 251-259.
- TRICARICO, C., PINZANI, P., BIANCHI, S., PAGLIERANI, M., DISTANTE, V., PAZZAGLI, M., BUSTIN, S. A. & ORLANDO, C. 2002. Quantitative real-time reverse transcription polymerase chain reaction: normalization to rRNA or single housekeeping genes is inappropriate for human tissue biopsies. *Analytical Biochemistry*, 309, 293-300.

- TSAI, Y.-Y., HUANG, Y.-H., CHAO, Y.-L., HU, K.-Y., CHIN, L.-T., CHOU, S.-H., HOUR, A.-L., YAO, Y.-D., TU, C.-S., LIANG, Y.-J., TSAI, C.-Y., WU, H.-Y., TAN, S.-W. & CHEN, H.-M. 2011. Identification of the Nanogold Particle-Induced Endoplasmic Reticulum Stress by Omic Techniques and Systems Biology Analysis. *Acs Nano*, 5, 9354-9369.
- TUAN, R. S., LEE, F. Y., KONTTINEN, Y., WILKINSON, J. M. & SMITH, R. L. 2008. What are the local and systemic biological reactions and mediators to wear debris and what host factors determine or modulate the biological response to wear particles? *The Journal of the American Academy of Orthopaedic Surgeons*, 16 Supplement 1, S42-S48.
- TURNER, B. C., KRAJEWSKI, S., KRAJEWSKA, M., TAKAYAMA, S., GUMBS, A. A., CARTER, D., REBBECK, T. R., HAFFTY, B. G. & REED, J. C. 2001. BAG-1: A novel biomarker predicting long-term survival in early-stage breast cancer. *Journal of Clinical Oncology*, 19, 992-1000.
- TWINE, N. C., STOVER, J. A., MARSHALL, B., DUKART, G., HIDALGO, M., STADLER, W., LOGAN, T., DUTCHER, J., HUDES, G., DORNER, A. J., SLONIM, D. K., TREPICCHIO, W. L. & BURCZYNSKI, M. E. 2003. Disease-associated expression profiles in peripheral blood mononuclear cells from patients with advanced renal cell carcinoma. *Cancer Research*, 63, 6069-6075.
- VALKO, M., MORRIS, H. & CRONIN, M. T.D. 2005. Metals, toxicity and oxidative stress. *Current Medicinal Chemistry*, 12.
- VALLES, G., GONZALEZ-MELENDI, P., GONZALEZ-CARRASCO, J. L., SALDANA, L., SANCHEZ-SABATE, E., MUNUERA, L. & VILABOIA, N. 2006. Differential inflammatory macrophage response to rutile and titanium particles. *Biomaterials*, 27, 5199-5211.
- VAN BRUSSEL, I., SCHRIJVERS, D. M., MARTINET, W., PINTELON, I., DESCHACHT, M., SCHNORBUSCH, K., MAES, L., BOSMANS, J. M., VRINTS, C. J., ADRIAENSEN, D., COS, P. & BULT, H. 2012. Transcript and Protein Analysis Reveals Better Survival Skills of Monocyte-Derived Dendritic Cells Compared to Monocytes during Oxidative Stress. *Plos One*, 7.
- VANDESOMPELE, J., DE PRETER, K., PATTYN, F., POPPE, B., VAN ROY, N., DE PAEPE, A. & SPELEMAN, F. 2002. Accurate normalization of real-time quantitative RT-PCR data by geometric averaging of multiple internal control genes. *Genome Biology*, 3.
- VANGUILDER, H. D., VRANA, K. E. & FREEMAN, W. M. 2008. Twenty-five years of quantitative PCR for gene expression analysis. *Biotechniques*, 44, 619-626.
- VASUDEVAN, A., DICARLO, E. F., WRIGHT, T., CHEN, D., FIGGIE, M. P., GOLDRING, S. R. & MANDL, L. A. 2012. Cellular Response to Prosthetic Wear Debris Differs in Patients With and Without Rheumatoid Arthritis. *Arthritis and Rheumatism*, 64, 1005-1014.
- VAUGHT, J. B. 2006. Blood collection, shipment, processing, and storage. *Cancer Epidemiology Biomarkers & Prevention*, 15, 1582-1584.
- VEGA-RAMOS, J. & VILLADANGOS, J. A. 2013. Consequences of direct and indirect activation of dendritic cells on antigen presentation: Functional

- implications and clinical considerations. *Molecular Immunology*, 55, 175-178.
- VERANTH, J. M., KASER, E. G., VERANTH, M. M., KOCH, M. & YOST, G. S. 2007. Cytokine responses of human lung cells (BEAS-2B) treated with micron-sized and nanoparticles of metal oxides compared to soil dusts. *Particle and fibre toxicology*, 4, 2-2.
- VERMES, C., CHANDRASEKARAN, R., JACOBS, J. J., GALANTE, J. O., ROEBUCK, K. A. & GLANT, T. T. 2001. The effects of particulate wear debris, cytokines, and growth factors on the functions of MG-63 osteoblasts. *Journal of Bone and Joint Surgery-American Volume*, 83A, 201-211.
- VERMEULEN, J., DE PRETER, K., LEFEVER, S., NUYTENS, J., DE VLOED, F., DERVEAUX, S., HELLEMANS, J., SPELEMAN, F. & VANDESOMPELE, J. 2011. Measurable impact of RNA quality on gene expression results from quantitative PCR. *Nucleic Acids Research*, 39.
- VIDAL, C. V. & MUNOZ, A. I. 2009. Effect of thermal treatment and applied potential on the electrochemical behaviour of CoCrMo biomedical alloy. *Electrochimica Acta*, 54.
- VILLANUEVA, M. B. G., KOIZUMI, S. & JONAI, H. 2000. Cytokine production by human peripheral blood mononuclear cells after exposure to heavy metals. *Journal of Health Science*, 46, 358-362.
- VIRGINIO, C., CHURCH, D., NORTH, R. A. & SURPRENANT, A. 1997. Effects of divalent cations, protons and calmidazolium at the rat P2X(7) receptor. *Neuropharmacology*, 36, 1285-1294.
- VOLLMER, J., FRITZ, M., DORMOY, A., WELTZIEN, H. U. & MOULON, C. 1997. Dominance of the BV17 element in nickel-specific human T cell receptors relates to severity of contact sensitivity. *European Journal of Immunology*, 27, 1865-1874.
- VOLLMER, J., WELTZIEN, H. U. & MOULON, C. 1999. TCR reactivity in human nickel allergy indicates contacts with complementarity-determining region 3 but excludes superantigen-like recognition. *Journal of Immunology*, 163, 2723-2731.
- VON AHSEN, N., WITWER, C. T. & SCHUTZ, E. 2001. Oligonucleotide melting temperatures under PCR conditions: Nearest-neighbor corrections for Mg²⁺, deoxynucleotide triphosphate, and dimethyl sulfoxide concentrations with comparison to alternative empirical formulas. *Clinical Chemistry*, 47, 1956-1961.
- VON KNOCH, M., JEWISON, D. E., SIBONGA, J. D., TURNER, R. T., MORREY, B. F., LOER, F., BERRY, D. J. & SCULLY, S. P. 2004. Decrease in particle-induced osteolysis in obese (ob/ob) mice. *Biomaterials*, 25, 4675-4681.
- VONGSAKUL, M., KASISITH, J., NOISUMDAENG, P. & PUTHAVATHANA, P. 2011. The difference in IL-1 beta, MIP-1 alpha, IL-8 and IL-18 production between the infection of PMA activated U937 cells with recombinant vaccinia viruses inserted 2004 H5N1 influenza HA genes and NS genes. *Asian Pacific Journal of Allergy and Immunology*, 29, 349-356.
- VORONOV, I., SANTERRE, J. P., HINEK, A., CALLAHAN, J. W., SANDHU, J. & BOYNTON, E. L. 1998. Macrophage phagocytosis of polyethylene particulate in vitro. *Journal of Biomedical Materials Research*, 39, 40-51.

- WAGNER, D. & FAHRLEITNER-PAMMER, A. 2010. Levels of osteoprotegerin (OPG) and receptor activator for nuclear factor kappa B ligand (RANKL) in serum: Are they of any help? . *Wien Med Wochenschr*, **160** 452-7
- WAN, R., MO, Y., ZHANG, X., CHIEN, S., TOLLERUD, D. J. & ZHANG, Q. 2008. Matrix metalloproteinase-2 and-9 are induced differently by metal nanoparticles in human monocytes: The role of oxidative stress and protein tyrosine kinase activation. *Toxicology and Applied Pharmacology*, 233.
- WANG, C. T., LIN, Y. T., CHIANG, B. L., LEE, S. S. & HOU, S. M. 2010. Over-expression of receptor activator of nuclear factor-kappa B ligand (RANKL), inflammatory cytokines, and chemokines in periprosthetic osteolysis of loosened total hip arthroplasty. *Biomaterials*, 31, 77-82.
- WANG, J., XIANG, G., MITCHELSON, K. & ZHOU, Y. 2011. Microarray profiling of monocytic differentiation reveals miRNA-mRNA intrinsic correlation. *Journal of cellular biochemistry*, 112.
- WANG, J. Y., WICKLUND, B. H., GUSTILO, R. B. & TSUKAYAMA, D. T. 1996. Titanium, chromium and cobalt ions modulate the release of bone-associated cytokines by human monocytes/macrophages in vitro. *Biomaterials*, 17, 2233-2240.
- WANG, M. L., TULI, R., MANNER, P. A., SHARKEY, P. F., HALL, D. J. & TUAN, R. S. 2003. Direct and indirect induction of apoptosis in human mesenchymal stem cells in response to titanium particles. *Journal of Orthopaedic Research*, 21, 697-707.
- WARD, M. B., BROWN, A. P., COX, A., CURRY, A. & DENTON, J. 2010. Microscopical analysis of synovial fluid wear debris from failing CoCr hip prostheses. Electron-Microscopy-and-Analysis-Group Conference 2009, 2010
Sep 08-11 2009 Univ Sheffield, Sheffield, ENGLAND.
- WARIS, G. & AHSAN, H. 2006. Reactive oxygen species: role in the development of cancer and various chronic conditions. *Journal of carcinogenesis*, 5, 14-14.
- WEBER, D. G., CASJENS, S., ROZYNEK, P., LEHNERT, M., ZILCH-SCHONEWEIS, S., BRYK, O., TAEGER, D., GOMOLKA, M., KREUZER, M., OTTEN, H., PESCH, B., JOHNEN, G. & BRUNING, T. 2010. Assessment of mRNA and microRNA Stabilization in Peripheral Human Blood for Multicenter Studies and Biobanks. *Biomarker insights*, 5, 95-102.
- WELLS, A. D. 2009. New Insights into the Molecular Basis of T Cell Anergy: Anergy Factors, Avoidance Sensors, and Epigenetic Imprinting. *Journal of Immunology*, 182, 7331-7341.
- WERLING, D. & JUNGI, T. W. 2003. TOLL-like receptors linking innate and adaptive immune response. *Veterinary Immunology and Immunopathology*, 91, 1-12.
- WIK, T. S., FOSS, O. A., HAVIK, S., PERSEN, L., AAMODT, A. & WITSO, E. 2010. Periprosthetic fracture caused by stress shielding after implantation of a femoral condyle endoprosthesis in a transfemoral amputee-a case report. *Acta Orthopaedica*, 81, 765-767.
- WILLERT, H. G., BUCHHORN, G. H., FAYYAZI, A., FLURY, R., WINDLER, M., KOSTER, G. & LOHMANN, C. H. 2005. Metal-on-metal bearings and hypersensitivity in patients with artificial hip joints - A clinical and

- histomorphological study. *Journal of Bone and Joint Surgery-American Volume*, 87A.
- WILLIAMS, S., LESLIE, I., ISAAC, G., JIN, Z., INGHAM, E. & FISHER, J. 2008. Tribology and wear of metal-on-metal hip prostheses: Influence of cup angle and head position. *Journal of Bone and Joint Surgery-American Volume*, 90A, 111-117.
- WILLIAMS, S., TIPPER, J. L., INGHAM, E., STONE, M. H. & FISHER, J. 2003. In vitro analysis of the wear, wear debris and biological activity of surface-engineered coatings for use in metal-on-metal total hip replacements. *Proceedings of the Institution of Mechanical Engineers. Part H, Journal of engineering in medicine*, 217, 155-63.
- WILLIAMS, Z., BEN-DOV, I. Z., ELIAS, R., MIHAILOVIC, A., BROWN, M., ROSENWAKS, Z. & TUSCHL, T. 2013. Comprehensive profiling of circulating microRNA via small RNA sequencing of cDNA libraries reveals biomarker potential and limitations. *Proceedings of the National Academy of Sciences of the United States of America*, 110, 117-122.
- WILLIS, S., DAY, C. L., HINDS, M. G. & HUANG, D. C. S. 2003. The Bcl-2-regulated apoptotic pathway. *Journal of Cell Science*, 116, 4053-4056.
- WILSON, I. G. 1997. Inhibition and facilitation of nucleic acid amplification. *Applied and Environmental Microbiology*, 63, 3741-3751.
- WITTEWER, C. T., HERRMANN, M. G., MOSS, A. A. & RASMUSSEN, R. P. 1997. Continuous fluorescence monitoring of rapid cycle DNA amplification. *Biotechniques*, 22, 130-&.
- WITZLEB, W. C., ZIEGLER, J., KRUMMENAUER, F., NEUMEISTER, V. & GUENTHER, K. P. 2006. Exposure to chromium, cobalt and molybdenum from metal-on-metal total hip replacement and hip resurfacing arthroplasty. *Acta Orthopaedica*, 77, 697-705.
- WRETENBERG, P. 2008. Good function but very high concentrations of cobalt and chromium ions in blood 37 years after metal-on-metal total hip arthroplasty. *Medical devices (Auckland, N.Z.)*, 1, 31-2.
- XIA, Z., KWON, Y.-M., MEHMOOD, S., DOWNING, C., JURKSCHAT, K. & MURRAY, D. W. 2011a. Characterization of metal-wear nanoparticles in pseudotumor following metal-on-metal hip resurfacing. *Nanomedicine-Nanotechnology Biology and Medicine*, 7, 674-681.
- XIA, Z. & TRIFFITT, J. T. 2006. A review on macrophage responses to biomaterials. *Biomedical Materials*, 1, R1-R9.
- XIA, Z. D., KWON, Y. M., MEHMOOD, S., DOWNING, C., JURKSCHAT, K. & MURRAY, D. W. 2011b. Characterization of metal-wear nanoparticles in pseudotumor following metal-on-metal hip resurfacing. *Nanomedicine-Nanotechnology Biology and Medicine*, 7, 674-681.
- XIE, F., XIAO, P., CHEN, D., XU, L. & ZHANG, B. 2012. miRDeepFinder: a miRNA analysis tool for deep sequencing of plant small RNAs. *Plant Molecular Biology*, 80, 75-84.
- XU, W. L., COMHAIR, S. A. A., ZHENG, S., CHU, S. C., MARKS-KONCZALIK, J., MOSS, J., HAQUE, S. J. & ERZURUM, S. C. 2003. STAT-1 and c-Fos interaction in nitric oxide synthase-2 gene activation. *American Journal of Physiology-Lung Cellular and Molecular Physiology*, 285, L137-L148.

- YAGIL-KELMER, E., KAZMIER, P., RAHAMAN, M. N., BAL, B. S., TESSMAN, R. K. & ESTES, D. M. 2004. Comparison of the response of primary human blood monocytes and the U937 human monocytic cell line to two different sizes of alumina ceramic particles. *Journal of Orthopaedic Research*, 22, 832-838.
- YANG, F., WU, W., CAO, L., HUANG, Y., ZHU, Z. N., TANG, T. T. & DAI, K. R. 2011. Pathways of macrophage apoptosis within the interface membrane in aseptic loosening of prostheses. *Biomaterials*, 32, 9159-9167.
- YANG, J. & BLACK, J. 1994. COMPETITIVE-BINDING OF CHROMIUM, COBALT AND NICKEL TO SERUM-PROTEINS. *Biomaterials*, 15, 262-268.
- YANG, S. Y., REN, W. P., PARK, Y. S., SIEVING, A., HSU, S., NASSER, S. & WOOLEY, P. H. 2002. Diverse cellular and apoptotic responses to variant shapes of UHMWPE particles in a murine model of inflammation. *Biomaterials*, 23, 3535-3543.
- YE, J., COULOURIS, G., ZARETSKAYA, I., CUTCUTACHE, I., ROZEN, S. & MADDEN, T. L. 2012. Primer-BLAST: A tool to design target-specific primers for polymerase chain reaction. *Bmc Bioinformatics*, 13.
- YU, S.-Y., HU, Y.-W., LIU, X.-Y., XIONG, W., ZHOU, Z.-T. & YUAN, Z.-H. 2005. Gene expression profiles in peripheral blood mononuclear cells of SARS patients. *World Journal of Gastroenterology*, 11, 5037-5043.
- ZEIDLER, P. C. & CASTRANOVA, V. 2004. Role of nitric oxide in pathological responses of the lung to exposure to environmental/occupational agents. *Redox Report*, 9, 7-18.
- ZHAN, Q. M. 2005. Gadd45a, a p53-and BRCA1-regulated stress protein, in cellular response to DNA damage. *Mutation Research-Fundamental and Molecular Mechanisms of Mutagenesis*, 569, 133-143.
- ZHANG, C., TANG, T., REN, W., ZHANG, X. & DAI, K. 2008. Influence of mouse genetic background on wear particle-induced in vivo inflammatory osteolysis. *Inflammation Research*, 57, 211-215.
- ZHANG, K., JIA, T. H., MCQUEEN, D., GONG, W. M., MARKEL, D. C., WOOLEY, P. H. & YANG, S. Y. 2009. Circulating blood monocytes traffic to and participate in the periprosthetic tissue inflammation. *Inflammation Research*, 58, 837-844.
- ZHANG, K. & KAUFMAN, R. J. 2008. From endoplasmic-reticulum stress to the inflammatory response. *Nature*, 454, 455-462.
- ZHANG, R., PIAO, M. J., KIM, K. C., KIM, A. D., CHOI, J.-Y., CHOI, J. & HYUN, J. W. 2012a. Endoplasmic reticulum stress signaling is involved in silver nanoparticles-induced apoptosis. *International Journal of Biochemistry & Cell Biology*, 44, 224-232.
- ZHANG, X. S. & REVELL, P. A. 1999. In situ localization of apoptotic changes in the interface membrane of aseptically loosened orthopaedic implants. *Journal of Materials Science-Materials in Medicine*, 10, 879-883.
- ZHANG, Y., YAN, M., YU, A. Y., MAO, H. J. & ZHANG, J. P. 2012b. Inhibitory effects of beta-tricalciumphosphate wear particles on osteocytes via apoptotic response and Akt inactivation. *Toxicology*, 297, 57-67.
- ZHANG, Y. L., YU, W. Q., JIANG, X. Q., LV, K. G., SUN, S. J. & ZHANG, F. Q. 2011. Analysis of the cytotoxicity of differentially sized titanium dioxide

- nanoparticles in murine MC3T3-E1 preosteoblasts. *Journal of Materials Science-Materials in Medicine*, 22, 1933-1945.
- ZHENG, M., KIM, S.-K., JOE, Y., BACK, S. H., CHO, H. R., KIM, H. P., IGNARRO, L. J. & CHUNG, H.-T. 2012. Sensing endoplasmic reticulum stress by protein kinase RNA-like endoplasmic reticulum kinase promotes adaptive mitochondrial DNA biogenesis and cell survival via heme oxygenase-1/carbon monoxide activity. *Faseb Journal*, 26, 2558-2568.
- ZHENG, Y., ZHA, Y. Y. & GAJEWSKI, T. F. 2008. Molecular regulation of T-cell energy. *Embo Reports*, 9, 50-55.
- ZIAEE, H., DANIEL, J., DATTA, A. K., BLUNT, S. & MCMINN, D. J. W. 2007. Transplacental transfer of cobalt and chromium in patients with metal-on-metal hip arthroplasty - A controlled study. *Journal of Bone and Joint Surgery-British Volume*, 89B, 301-305.
- ZIJLSTRA, W. P., BULSTRA, S. K., VAN RAAY, J., VAN LEEUWEN, B. M. & KUIJER, R. 2012. Cobalt and chromium ions reduce human osteoblast-like cell activity in vitro, reduce the OPG to RANKL ratio, and induce oxidative stress. *Journal of Orthopaedic Research*, 30, 740-747.
- ZIPPER, H., BRUNNER, H., BERNHAGEN, J. & VITZTHUM, F. 2004. Investigations on DNA intercalation and surface binding by SYBR Green I, its structure determination and methodological implications. *Nucleic Acids Research*, 32.
- ZOU, W. G., YAN, M. D., XU, W. J., HUO, H. R., SUN, L. Y., ZHENG, Z. C. & LIU, X. Y. 2001. Cobalt chloride induces PC12 cells apoptosis through reactive oxygen species and accompanied by AP-1 activation. *Journal of Neuroscience Research*, 64, 646-653.